Lectures on Atomic Physics

Walter R. Johnson
Department of Physics, University of Notre Dame
Notre Dame, Indiana 46556, U.S.A.

January 4, 2006

Contents

List of Tables

List of Figures

Preface

This is a set of lecture notes prepared for Physics 607, a course on Atomic Physics for second-year graduate students, given at Notre Dame during the spring semester of 1994. My aim in this course was to provide opportunities for "hands-on" practice in the calculation of atomic wave functions and energies.

The lectures started with a review of angular momentum theory including the formal rules for manipulating angular momentum operators, a discussion of orbital and spin angular momentum, Clebsch-Gordan coefficients and three-j symbols. This material should have been familiar to the students from first-year Quantum Mechanics. More advanced material on angular momentum needed in atomic structure calculations followed, including an introduction to graphical methods, irreducible tensor operators, spherical spinors and vector spherical harmonics.

The lectures on angular momentum were followed by an extended discussion of the central-field Schrödinger equation. The Schrödinger equation was reduced to a radial differential equation and analytical solutions for Coulomb wave functions were obtained. Again, this reduction should have been familiar from first-year Quantum Mechanics. This preliminary material was followed by an introduction to the finite difference methods used to solve the radial Schrödinger equation. A subroutine to find eigenfunctions and eigenvalues of the Schrödinger equation was developed. This routine was used together with parametric potentials to obtain wave functions and energies for alkali atoms. The Thomas-Fermi theory was introduced and used to obtain approximate electron screening potentials. Next, the Dirac equation was considered. The bound-state Dirac equation was reduced to radial form and Dirac-Coulomb wave functions were determined analytically. Numerical solutions to the radial Dirac equation were considered and a subroutine to obtain the eigenvalues and eigenfunctions of the radial Dirac equation was developed.

In the third part of the course, many electron wave functions were considered and the ground-state of a two-electron atom was determined variationally. This was followed by a discussion of Slater-determinant wave functions and a derivation of the Hartree-Fock equations for closed-shell atoms. Numerical methods for solving the HF equations were described. The HF equations for atoms with one-electron beyond closed shells were derived and a code was developed to solve the HF equations for the closed-shell case and for the case of a single valence electron. Finally, the Dirac-Fock equations were derived and discussed.

The final section of the material began with a discussion of second-quantization. This approach was used to study a number of structure problems in first-order perturbation theory, including excited states of two-electron atoms, excited states of atoms with one or two electrons beyond closed shells and particle-hole states. Relativistic fine-structure effects were considered using the "no-pair" Hamiltonian. A rather complete discussion of the magnetic-dipole and electric quadrupole hyperfine structure from the relativistic point of view was given, and nonrelativistic limiting forms were worked out in the Pauli approximation.

FORTRAN subroutines to solve the radial Schródinger equation and the Hartree-Fock equations were handed out to be used in connection with weekly homework assignments. Some of these assigned exercises required the student to write or use FORTRAN codes to determine atomic energy levels or wave functions. Other exercises required the student to write MAPLE routines to generate formulas for wave functions or matrix elements. Additionally, more standard "pencil and paper" exercises on Atomic Physics were assigned.

I was disappointed in not being able to cover more material in the course. At the beginning of the semester, I had envisioned being able to cover second- and higher-order MBPT methods and CI calculations and to discuss radiative transitions as well. Perhaps next year!

Finally, I owe a debt of gratitude to the students in this class for their patience and understanding while this material was being assembled, and for helping read through and point out mistakes in the text.

South Bend, May, 1994

The second time that this course was taught, the material in Chap. 5 on electromagnetic transitions was included and Chap. 6 on many-body methods was started. Again, I was dissapointed at the slow pace of the course.

South Bend, May, 1995

The third time through, additional sections of Chap. 6 were added.

South Bend, December, 2000

The fourth time that this course was taught, the section in Chap. 4 on hyperfine structure was moved to a separate chapter, Chap. 5. Material on the isotope shift was also included in Chap. 5. The material on electromagnetic transitions (now Chap. 6) remains unchanged. The chapter on many-body methods (now Chap. 7) was considerably extended and Chap. 8 on many-body methods for matrix elements was added. In order to squeeze all of this material into a one semester three credit hour course, it was necessary to skip most of the material on numerical methods. However, I am confident that the entire book could be covered in a four credit hour course.

South Bend, December, 2005

Chapter 1

Angular Momentum

Understanding the quantum mechanics of angular momentum is fundamental in theoretical studies of atomic structure and atomic transitions. Atomic energy levels are classified according to angular momentum and selection rules for radiative transitions between levels are governed by angular-momentum addition rules. Therefore, in this first chapter, we review angular-momentum commutation relations, angular-momentum eigenstates, and the rules for combining two angular-momentum eigenstates to find a third. We make use of angular-momentum diagrams as useful mnemonic aids in practical atomic structure calculations. A more detailed version of much of the material in this chapter can be found in Edmonds (1974).

1.1 Orbital Angular Momentum - Spherical Harmonics

Classically, the angular momentum of a particle is the cross product of its position vector $\mathbf{r} = (x, y, z)$ and its momentum vector $\mathbf{p} = (p_x, p_y, p_z)$:

$$\mathbf{L} = \mathbf{r} \times \mathbf{p}.$$

The quantum mechanical orbital angular momentum operator is defined in the same way with $\mathbf{p}$ replaced by the momentum operator $\mathbf{p} \rightarrow -i\hbar\boldsymbol{\nabla}$. Thus, the Cartesian components of $\mathbf{L}$ are

$$L_x = \tfrac{\hbar}{i}\Big(y\tfrac{\partial}{\partial z} - z\tfrac{\partial}{\partial y}\Big), \quad L_y = \tfrac{\hbar}{i}\Big(z\tfrac{\partial}{\partial x} - x\tfrac{\partial}{\partial z}\Big), \quad L_z = \tfrac{\hbar}{i}\Big(x\tfrac{\partial}{\partial y} - y\tfrac{\partial}{\partial x}\Big). \tag{1.1}$$

With the aid of the commutation relations between $\mathbf{p}$ and $\mathbf{r}$:

$$[p_x, x] = -i\hbar, \quad [p_y, y] = -i\hbar, \quad [p_z, z] = -i\hbar, \tag{1.2}$$

one easily establishes the following commutation relations for the Cartesian components of the quantum mechanical angular momentum operator:

$$L_xL_y - L_yL_x = i\hbar L_z, \quad L_yL_z - L_zL_y = i\hbar L_x, \quad L_zL_x - L_xL_z = i\hbar L_y. \tag{1.3}$$

Since the components of $\mathbf{L}$ do not commute with each other, it is not possible to find simultaneous eigenstates of any two of these three operators. The operator $L^2 = L_x^2 + L_y^2 + L_z^2$, however, commutes with each component of $\mathbf{L}$. It is, therefore, possible to find a simultaneous eigenstate of L^2 and any one component of $\mathbf{L}$. It is conventional to seek eigenstates of L^2 and L_z.

1.1.1 Quantum Mechanics of Angular Momentum

Many of the important quantum mechanical properties of the angular momentum operator are consequences of the commutation relations (1.3) alone. To study these properties, we introduce three abstract operators J_x, J_y, and J_z satisfying the commutation relations,

$$J_xJ_y - J_yJ_x = iJ_z\,, \quad J_yJ_z - J_zJ_y = iJ_x\,, \quad J_zJ_x - J_xJ_z = iJ_y\,. \tag{1.4}$$

The unit of angular momentum in Eq.(1.4) is chosen to be $\hbar$, so the factor of $\hbar$ on the right-hand side of Eq.(1.3) does not appear in Eq.(1.4). The sum of the squares of the three operators $J^2 = J_x^2 + J_y^2 + J_z^2$ can be shown to commute with each of the three components. In particular,

$$[J^2, J_z] = 0\,. \tag{1.5}$$

The operators $J_+ = J_x + iJ_y$ and $J_- = J_x - iJ_y$ also commute with the angular momentum squared:

$$[J^2, J_\pm] = 0\,. \tag{1.6}$$

Moreover, J_+ and J_- satisfy the following commutation relations with J_z:

$$[J_z, J_\pm] = \pm J_\pm\,. \tag{1.7}$$

One can express J^2 in terms of J_+, J_- and J_z through the relations

$$J^2 = J_+J_- + J_z^2 - J_z\,, \tag{1.8}$$

$$J^2 = J_-J_+ + J_z^2 + J_z\,. \tag{1.9}$$

We introduce simultaneous eigenstates $|\lambda, m\rangle$ of the two commuting operators J^2 and J_z:

$$J^2|\lambda, m\rangle = \lambda\,|\lambda, m\rangle\,, \tag{1.10}$$

$$J_z|\lambda, m\rangle = m\,|\lambda, m\rangle\,, \tag{1.11}$$

and we note that the states $J_\pm|\lambda, m\rangle$ are also eigenstates of J^2 with eigenvalue λ. Moreover, with the aid of Eq.(1.7), one can establish that $J_+|\lambda, m\rangle$ and $J_-|\lambda, m\rangle$ are eigenstates of J_z with eigenvalues $m \pm 1$, respectively:

$$J_zJ_+|\lambda, m\rangle = (m+1)\,J_+|\lambda, m\rangle, \tag{1.12}$$

$$J_zJ_-|\lambda, m\rangle = (m-1)\,J_-|\lambda, m\rangle. \tag{1.13}$$

Since J_+ raises the eigenvalue m by one unit, and J_- lowers it by one unit, these operators are referred to as raising and lowering operators, respectively. Furthermore, since $J_x^2 + J_y^2$ is a positive definite hermitian operator, it follows that

$$\lambda \geq m^2.$$

By repeated application of J_- to eigenstates of J_z, one can obtain states of arbitrarily small eigenvalue m, violating this bound, unless for some state $|\lambda, m_1\rangle$,

$$J_-|\lambda, m_1\rangle = 0.$$

Similarly, repeated application of J_+ leads to arbitrarily large values of m, unless for some state $|\lambda, m_2\rangle$

$$J_+|\lambda, m_2\rangle = 0.$$

Since m^2 is bounded, we infer the existence of the two states $|\lambda, m_1\rangle$ and $|\lambda, m_2\rangle$. Starting from the state $|\lambda, m_1\rangle$ and applying the operator J_+ repeatedly, one must eventually reach the state $|\lambda, m_2\rangle$; otherwise the value of m would increase indefinitely. It follows that

$$m_2 - m_1 = k, \tag{1.14}$$

where $k \geq 0$ is the number of times that J_+ must be applied to the state $|\lambda, m_1\rangle$ in order to reach the state $|\lambda, m_2\rangle$. One finds from Eqs.(1.8,1.9) that

$$\begin{aligned} \lambda|\lambda, m_1\rangle &= (m_1^2 - m_1)|\lambda, m_1\rangle, \\ \lambda|\lambda, m_2\rangle &= (m_2^2 + m_2)|\lambda, m_2\rangle, \end{aligned}$$

leading to the identities

$$\lambda = m_1^2 - m_1 = m_2^2 + m_2, \tag{1.15}$$

which can be rewritten

$$(m_2 - m_1 + 1)(m_2 + m_1) = 0. \tag{1.16}$$

Since the first term on the left of Eq.(1.16) is positive definite, it follows that $m_1 = -m_2$. The upper bound m_2 can be rewritten in terms of the integer k in Eq.(1.14) as

$$m_2 = k/2 = j.$$

The value of j is either integer or half integer, depending on whether k is even or odd:

$$j = 0, \frac{1}{2}, 1, \frac{3}{2}, \cdots .$$

It follows from Eq.(1.15) that the eigenvalue of J^2 is

$$\lambda = j(j+1). \tag{1.17}$$

The number of possible m eigenvalues for a given value of j is $k + 1 = 2j + 1$. The possible values of m are

$$m = j, j-1, j-2, \cdots, -j.$$

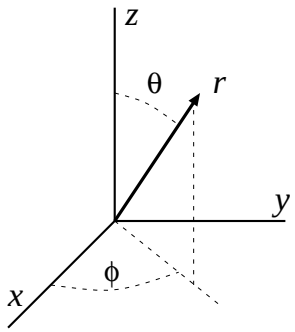

Figure 1.1: Transformation from rectangular to spherical coordinates.

Since $J_- = J_+^\dagger$, it follows that

$$J_+|\lambda, m\rangle = \eta|\lambda, m+1\rangle, \quad \langle\lambda, m|J_- = \eta^*\langle\lambda, m+1|.$$

Evaluating the expectation of $J^2 = J_-J_+ + J_z^2 + J_z$ in the state $|\lambda, m\rangle$, one finds

$$|\eta|^2 = j(j+1) - m(m+1).$$

Choosing the phase of η to be real and positive, leads to the relations

$$J_+|\lambda, m\rangle = \sqrt{(j+m+1)(j-m)}\,|\lambda, m+1\rangle, \tag{1.18}$$

$$J_-|\lambda, m\rangle = \sqrt{(j-m+1)(j+m)}\,|\lambda, m-1\rangle. \tag{1.19}$$

1.1.2 Spherical Coordinates - Spherical Harmonics

Let us apply the general results derived in Section 1.1.1 to the orbital angular momentum operator **L**. For this purpose, it is most convenient to transform Eqs.(1.1) to spherical coordinates (Fig. 1.1):

$$x = r\sin\theta\cos\phi, \qquad y = r\sin\theta\sin\phi, \qquad z = r\cos\theta,$$
$$r = \sqrt{x^2+y^2+z^2}, \quad \theta = \arccos z/r, \quad \phi = \arctan y/x.$$

In spherical coordinates, the components of **L** are

$$L_x = i\hbar\left(\sin\phi\frac{\partial}{\partial\theta} + \cos\phi\cot\theta\frac{\partial}{\partial\phi}\right), \tag{1.20}$$

$$L_y = i\hbar\left(-\cos\phi\frac{\partial}{\partial\theta} + \sin\phi\cot\theta\frac{\partial}{\partial\phi}\right), \tag{1.21}$$

$$L_z = -i\hbar\frac{\partial}{\partial\phi}, \tag{1.22}$$

and the square of the angular momentum is

$$L^2 = -\hbar^2\left(\frac{1}{\sin\theta}\frac{\partial}{\partial\theta}\sin\theta\frac{\partial}{\partial\theta} + \frac{1}{\sin^2\theta}\frac{\partial^2}{\partial\phi^2}\right). \tag{1.23}$$

Combining the equations for L_x and L_y, we obtain the following expressions for the orbital angular momentum raising and lowering operators:

$$L_\pm = \hbar e^{\pm i\phi}\left(\pm\frac{\partial}{\partial\theta} + i\cot\theta\frac{\partial}{\partial\phi}\right). \tag{1.24}$$

The simultaneous eigenfunctions of L^2 and L_z are called spherical harmonics. They are designated by $Y_{lm}(\theta,\phi)$. We decompose $Y_{lm}(\theta,\phi)$ into a product of a function of θ and a function of ϕ:

$$Y_{lm}(\theta,\phi) = \Theta_{l,m}(\theta)\Phi_m(\phi)\,.$$

The eigenvalue equation $L_zY_{l,m}(\theta,\phi) = \hbar mY_{l,m}(\theta,\phi)$ leads to the equation

$$-i\frac{d\Phi_m(\phi)}{d\phi} = m\Phi_m(\phi)\,, \tag{1.25}$$

for $\Phi_m(\phi)$. The single valued solution to this equation, normalized so that

$$\int_0^{2\pi}|\Phi_m(\phi)|^2 d\phi = 1\,, \tag{1.26}$$

is

$$\Phi_m(\phi) = \frac{1}{\sqrt{2\pi}}e^{im\phi}, \tag{1.27}$$

where m is an integer. The eigenvalue equation $L^2Y_{l,m}(\theta,\phi) = \hbar^2 l(l+1)Y_{l,m}(\theta,\phi)$ leads to the differential equation

$$\left(\frac{1}{\sin\theta}\frac{d}{d\theta}\sin\theta\frac{d}{d\theta} - \frac{m^2}{\sin^2\theta} + l(l+1)\right)\Theta_{l,m}(\theta) = 0\,, \tag{1.28}$$

for the function $\Theta_{l,m}(\theta)$. The orbital angular momentum quantum number l must be an integer since m is an integer.

One can generate solutions to Eq.(1.28) by recurrence, starting with the solution for $m = -l$ and stepping forward in m using the raising operator L_+, or starting with the solution for $m = l$ and stepping backward using the lowering operator L_-. The function $\Theta_{l,-l}(\theta)$ satisfies the differential equation

$$L_+\Theta_{l,-l}(\theta)\Phi_{-l}(\phi) = \hbar\Phi_{-l+1}(\phi)\left(-\frac{d}{d\theta} + l\cot\theta\right)\Theta_{l,-l}(\theta) = 0\,,$$

which can be easily solved to give $\Theta_{l,-l}(\theta) = c\sin^l\theta$, where c is an arbitrary constant. Normalizing this solution so that

$$\int_0^\pi |\Theta_{l,-l}(\theta)|^2\sin\theta d\theta = 1, \tag{1.29}$$

one obtains

$$\Theta_{l,-l}(\theta) = \frac{1}{2^l l!}\sqrt{\frac{(2l+1)!}{2}}\sin^l\theta\,. \tag{1.30}$$

Applying L_+^{l+m} to $Y_{l,-l}(\theta,\phi)$, leads to the result

$$\Theta_{l,m}(\theta) = \frac{(-1)^{l+m}}{2^l l!}\sqrt{\frac{(2l+1)(l-m)!}{2(l+m)!}}\sin^m\theta\frac{d^{l+m}}{d\cos\theta^{l+m}}\sin^{2l}\theta\,. \tag{1.31}$$

For $m = 0$, this equation reduces to

$$\Theta_{l,0}(\theta) = \frac{(-1)^l}{2^l l!}\sqrt{\frac{2l+1}{2}}\frac{d^l}{d\cos\theta^l}\sin^{2l}\theta\,. \tag{1.32}$$

This equation may be conveniently written in terms of Legendre polynomials $P_l(\cos\theta)$ as

$$\Theta_{l,0}(\theta) = \sqrt{\frac{2l+1}{2}}P_l(\cos\theta)\,. \tag{1.33}$$

Here the Legendre polynomial $P_l(x)$ is defined by Rodrigues' formula

$$P_l(x) = \frac{1}{2^l l!}\frac{d^l}{dx^l}(x^2-1)^l\,. \tag{1.34}$$

For $m = l$, Eq.(1.31) gives

$$\Theta_{l,l}(\theta) = \frac{(-1)^l}{2^l l!}\sqrt{\frac{(2l+1)!}{2}}\sin^l\theta\,. \tag{1.35}$$

Starting with this equation and stepping backward $l - m$ times leads to an alternate expression for $\Theta_{l,m}(\theta)$:

$$\Theta_{l,m}(\theta) = \frac{(-1)^l}{2^l l!}\sqrt{\frac{(2l+1)(l+m)!}{2(l-m)!}}\sin^{-m}\theta\frac{d^{l-m}}{d\cos\theta^{l-m}}\sin^{2l}\theta\,. \tag{1.36}$$

Comparing Eq.(1.36) with Eq.(1.31), one finds

$$\Theta_{l,-m}(\theta) = (-1)^m\Theta_{l,m}(\theta)\,. \tag{1.37}$$

We can restrict our attention to $\Theta_{l,m}(\theta)$ with $m \geq 0$ and use (1.37) to obtain $\Theta_{l,m}(\theta)$ for $m < 0$. For positive values of m, Eq.(1.31) can be written

$$\Theta_{l,m}(\theta) = (-1)^m\sqrt{\frac{(2l+1)(l-m)!}{2(l+m)!}}P_l^m(\cos\theta)\,, \tag{1.38}$$

where $P_l^m(x)$ is an associated Legendre functions of the first kind, given in Abramowitz and Stegun (1964, chap. 8), with a different sign convention, defined by

$$P_l^m(x) = (1-x^2)^{m/2}\frac{d^m}{dx^m}P_l(x)\,. \tag{1.39}$$

The general orthonormality relations $\langle l,m|l',m'\rangle = \delta_{ll'}\delta_{mm'}$ for angular momentum eigenstates takes the specific form

$$\int_0^\pi \int_0^{2\pi} \sin\theta d\theta d\phi \, Y^*_{l,m}(\theta,\phi) Y_{l',m'}(\theta,\phi) = \delta_{ll'}\delta_{mm'} \,, \tag{1.40}$$

for spherical harmonics. Comparing Eq.(1.31) and Eq.(1.36) leads to the relation

$$Y_{l,-m}(\theta,\phi) = (-1)^m Y^*_{l,m}(\theta,\phi) \,. \tag{1.41}$$

The first few spherical harmonics are:

$Y_{00} = \sqrt{\frac{1}{4\pi}}$

$Y_{10} = \sqrt{\frac{3}{4\pi}}\ \cos\theta$ $\qquad$ $Y_{1,\pm1} = \mp\sqrt{\frac{3}{8\pi}}\ \sin\theta\ e^{\pm i\phi}$

$Y_{20} = \sqrt{\frac{5}{16\pi}}\ (3\cos^2\theta - 1)$ $\qquad$ $Y_{2,\pm1} = \mp\sqrt{\frac{15}{8\pi}}\ \sin\theta\cos\theta\ e^{\pm i\phi}$

$Y_{2,\pm2} = \sqrt{\frac{15}{32\pi}}\ \sin^2\theta\ e^{\pm 2i\phi}$

$Y_{30} = \sqrt{\frac{7}{16\pi}}\ \cos\theta\ (5\cos^2\theta - 3)$ $\qquad$ $Y_{3,\pm1} = \mp\sqrt{\frac{21}{64\pi}}\ \sin\theta\ (5\cos^2\theta - 1)\ e^{\pm i\phi}$

$Y_{3,\pm2} = \sqrt{\frac{105}{32\pi}}\ \cos\theta\sin^2\theta\ e^{\pm 2i\phi}$ $\qquad$ $Y_{3,\pm3} = \mp\sqrt{\frac{35}{64\pi}}\ \sin^3\theta\ e^{\pm 3i\phi}$

1.2 Spin Angular Momentum

1.2.1 Spin $1/2$ and Spinors

The internal angular momentum of a particle in quantum mechanics is called spin angular momentum and designated by $\mathbf{S}$. Cartesian components of $\mathbf{S}$ satisfy angular momentum commutation rules (1.4). The eigenvalue of S^2 is $\hbar^2 s(s+1)$ and the $2s+1$ eigenvalues of S_z are $\hbar m$ with $m = -s, -s+1, \cdots, s$. Let us consider the case $s = 1/2$ which describes the spin of the electron. We designate the eigenstates of S^2 and S_z by two-component vectors χ_μ, $\mu = \pm 1/2$:

$$\chi_{1/2} = \begin{pmatrix} 1 \\ 0 \end{pmatrix}, \quad \chi_{-1/2} = \begin{pmatrix} 0 \\ 1 \end{pmatrix}. \tag{1.42}$$

These two-component spin eigenfunctions are called spinors. The spinors χ_μ satisfy the orthonormality relations

$$\chi^\dagger_\mu \chi_\nu = \delta_{\mu\nu}. \tag{1.43}$$

The eigenvalue equations for S^2 and S_z are

$$S^2\chi_\mu = \tfrac{3}{4}\hbar^2\chi_\mu, \qquad S_z\chi_\mu = \mu\hbar\chi_\mu.$$

We represent the operators S^2 and S_z as 2×2 matrices acting in the space spanned by χ_μ:

$$S^2 = \tfrac{3}{4}\hbar^2 \begin{pmatrix} 1 & 0 \\ 0 & 1 \end{pmatrix}, \qquad S_z = \tfrac{1}{2}\hbar \begin{pmatrix} 1 & 0 \\ 0 & -1 \end{pmatrix}.$$

One can use Eqs.(1.18,1.19) to work out the elements of the matrices representing the spin raising and lowering operators $S_\pm$:

$$S_+ = \hbar \begin{pmatrix} 0 & 1 \\ 0 & 0 \end{pmatrix}, \qquad S_- = \hbar \begin{pmatrix} 0 & 0 \\ 1 & 0 \end{pmatrix}.$$

These matrices can be combined to give matrices representing $S_x = (S_+ + S_-)/2$ and $S_y = (S_+ - S_-)/2i$. The matrices representing the components of $\mathbf{S}$ are commonly written in terms of the Pauli matrices $\boldsymbol{\sigma} = (\sigma_x, \sigma_y, \sigma_z)$, which are given by

$$\sigma_x = \begin{pmatrix} 0 & 1 \\ 1 & 0 \end{pmatrix}, \quad \sigma_y = \begin{pmatrix} 0 & -i \\ i & 0 \end{pmatrix}, \quad \sigma_z = \begin{pmatrix} 1 & 0 \\ 0 & -1 \end{pmatrix}, \tag{1.44}$$

through the relation

$$\mathbf{S} = \frac{1}{2}\hbar\boldsymbol{\sigma}\,. \tag{1.45}$$

The Pauli matrices are both hermitian and unitary. Therefore,

$$\sigma_x^2 = I, \quad \sigma_y^2 = I, \quad \sigma_z^2 = I, \tag{1.46}$$

where I is the 2×2 identity matrix. Moreover, the Pauli matrices anticommute:

$$\sigma_y\sigma_x = -\sigma_x\sigma_y\,, \quad \sigma_z\sigma_y = -\sigma_y\sigma_z\,, \quad \sigma_x\sigma_z = -\sigma_z\sigma_x\,. \tag{1.47}$$

The Pauli matrices also satisfy commutation relations that follow from the general angular momentum commutation relations (1.4):

$$\sigma_x\sigma_y - \sigma_y\sigma_x = 2i\sigma_z\,, \quad \sigma_y\sigma_z - \sigma_z\sigma_y = 2i\sigma_x\,, \quad \sigma_z\sigma_x - \sigma_x\sigma_z = 2i\sigma_y\,. \tag{1.48}$$

The anticommutation relations (1.47) and commutation relations (1.48) can be combined to give

$$\sigma_x\sigma_y = i\sigma_z\,, \quad \sigma_y\sigma_z = i\sigma_x\,, \quad \sigma_z\sigma_x = i\sigma_y\,. \tag{1.49}$$

From the above equations for the Pauli matrices, one can show

$$\boldsymbol{\sigma}\cdot\boldsymbol{a}\,\boldsymbol{\sigma}\cdot\boldsymbol{b} = \boldsymbol{a}\cdot\boldsymbol{b} + \boldsymbol{i}\boldsymbol{\sigma}\cdot[\boldsymbol{a}\times\boldsymbol{b}], \tag{1.50}$$

for any two vectors $\mathbf{a}$ and $\mathbf{b}$.

In subsequent studies we will require simultaneous eigenfunctions of L^2, L_z, S^2, and S_z. These eigenfunctions are given by $Y_{lm}(\theta,\phi)\,\chi_\mu$.

1.2.2 Infinitesimal Rotations of Vector Fields

Let us consider a rotation about the z axis by a small angle $\delta\phi$. Under such a rotation, the components of a vector $\mathbf{r} = (x, y, z)$ are transformed to

$$\begin{aligned} x' &= x + \delta\phi\, y, \\ y' &= -\delta\phi\, x + y, \\ z' &= z, \end{aligned}$$

neglecting terms of second and higher order in $\delta\phi$. The difference $\delta\psi(x, y, z) = \psi(x', y', z') - \psi(x, y, z)$ between the values of a scalar function ψ evaluated in the rotated and unrotated coordinate systems is (to lowest order in $\delta\phi$),

$$\delta\psi(x, y, z) = -\delta\phi \left(x\frac{\partial}{\partial y} - y\frac{\partial}{\partial x} \right) \psi(x, y, z) = -i\delta\phi\, L_z\, \psi(x, y, z).$$

The operator L_z, in the sense of this equation, generates an infinitesimal rotation about the z axis. Similarly, L_x and L_y generate infinitesimal rotations about the x and y axes. Generally, an infinitesimal rotation about an axis in the direction $\mathbf{n}$ is generated by $\mathbf{L} \cdot \mathbf{n}$.

Now, let us consider how a vector function

$$\mathbf{A}(x, y, z) = [A_x(x, y, z), A_y(x, y, z), A_z(x, y, z)]$$

transforms under an infinitesimal rotation. The vector $\mathbf{A}$ is attached to a point in the coordinate system; it rotates with the coordinate axes on transforming from a coordinate system (x, y, z) to a coordinate system (x', y', z'). An infinitesimal rotation $\delta\phi$ about the z axis induces the following changes in the components of $\mathbf{A}$:

$$\begin{aligned} \delta A_x &= A_x(x', y', z') - \delta\phi A_y(x', y', z') - A_x(x, y, z) \\ &= -i\delta\phi \left[L_z\, A_x(x, y, z) - i A_y(x, y, z) \right], \\ \delta A_y &= A_y(x', y', z') + \delta\phi A_x(x', y', z') - A_y(x, y, z) \\ &= -i\delta\phi \left[L_z\, A_y(x, y, z) + i A_x(x, y, z) \right], \\ \delta A_z &= A_z(x', y', z') - A_z(x, y, z) \\ &= -i\delta\phi\, L_z\, A_z(x, y, z)\,. \end{aligned}$$

Let us introduce the 3×3 matrix s_z defined by

$$s_z = \begin{pmatrix} 0 & -i & 0 \\ i & 0 & 0 \\ 0 & 0 & 0 \end{pmatrix}.$$

With the aid of this matrix, one can rewrite the equations for $\delta\mathbf{A}$ in the form $\delta\mathbf{A}(x, y, z) = -i\delta\phi\, J_z \mathbf{A}(x, y, z)$, where $J_z = L_z + s_z$. If we define angular momentum to be the generator of infinitesimal rotations, then the z component

of the angular momentum of a vector field is $J_z = L_z + s_z$. Infinitesimal rotations about the x and y axes are generated by $J_x = L_x + s_x$ and $J_z = L_y + s_y$, where

$$s_x = \begin{pmatrix} 0 & 0 & 0 \\ 0 & 0 & -i \\ 0 & i & 0 \end{pmatrix}, \quad s_y = \begin{pmatrix} 0 & 0 & i \\ 0 & 0 & 0 \\ -i & 0 & 0 \end{pmatrix}.$$

The matrices $\mathbf{s} = (s_x, s_y, s_z)$ are referred to as the spin matrices. In the following paragraphs, we show that these matrices are associated with angular momentum quantum number $s = 1$.

1.2.3 Spin 1 and Vectors

The eigenstates of S^2 and S_z for particles with spin $s = 1$ are represented by three-component vectors ξ_μ, with $\mu = -1, 0, 1$. The counterparts of the three Pauli matrices for $s = 1$ are the 3×3 matrices $\mathbf{s} = (s_x, s_y, s_z)$ introduced in the previous section. The corresponding spin angular momentum operator is $\mathbf{S} = \hbar\mathbf{s}$ where

$$s_x = \begin{pmatrix} 0 & 0 & 0 \\ 0 & 0 & -i \\ 0 & i & 0 \end{pmatrix}, \quad s_y = \begin{pmatrix} 0 & 0 & i \\ 0 & 0 & 0 \\ -i & 0 & 0 \end{pmatrix}, \quad s_z = \begin{pmatrix} 0 & -i & 0 \\ i & 0 & 0 \\ 0 & 0 & 0 \end{pmatrix}. \tag{1.51}$$

The matrix $s^2 = s_x^2 + s_y^2 + s_z^2$ is

$$s^2 = \begin{pmatrix} 2 & 0 & 0 \\ 0 & 2 & 0 \\ 0 & 0 & 2 \end{pmatrix}. \tag{1.52}$$

The three matrices s_x, s_y, and s_z satisfy the commutation relations

$$s_x s_y - s_y s_x = i s_z\,, \quad s_y s_z - s_z s_y = i s_x\,, \quad s_z s_x - s_x s_z = i s_y\,. \tag{1.53}$$

It follows that $\mathbf{S} = \hbar\mathbf{s}$ satisfies the angular momentum commutation relations (1.4).

Eigenfunctions of S^2 and S_z satisfy the matrix equations $s^2\xi_\mu = 2\xi_\mu$ and $s_z\xi_\mu = \mu\xi_\mu$. The first of these equations is satisfied by an arbitrary three-component vector. Solutions to the second are found by solving the corresponding 3×3 eigenvalue problem,

$$\begin{pmatrix} 0 & -i & 0 \\ i & 0 & 0 \\ 0 & 0 & 0 \end{pmatrix} \begin{pmatrix} a \\ b \\ c \end{pmatrix} = \mu \begin{pmatrix} a \\ b \\ c \end{pmatrix}. \tag{1.54}$$

The three eigenvalues of this equation are $\mu = -1, 0, 1$ and the associated eigenvectors are

$$\xi_1 = -\tfrac{1}{\sqrt{2}} \begin{pmatrix} 1 \\ i \\ 0 \end{pmatrix}, \quad \xi_0 = \begin{pmatrix} 0 \\ 0 \\ 1 \end{pmatrix}, \quad \xi_{-1} = \tfrac{1}{\sqrt{2}} \begin{pmatrix} 1 \\ -i \\ 0 \end{pmatrix}. \tag{1.55}$$

The phases of the three eigenvectors are chosen in accordance with Eq.(1.18), which may be rewritten $s_+\xi_\mu = \sqrt{2}\xi_{\mu+1}$. The vectors ξ_μ are called spherical basis vectors. They satisfy the orthogonality relations

$$\xi_\mu^\dagger \xi_\nu = \delta_{\mu\nu}.$$

It is, of course, possible to expand an arbitrary three-component vector $\mathbf{v} = (v_x, v_y, v_z)$ in terms of spherical basis vectors:

$$\begin{aligned} \mathbf{v} &= \sum_{\mu=-1}^{1} v^\mu \xi_\mu, \quad \text{where} \\ v^\mu &= \xi_\mu^\dagger \mathbf{v}\,. \end{aligned}$$

Using these relations, one may show, for example, that the unit vector $\hat{\mathbf{r}}$ expressed in the spherical basis is

$$\hat{\mathbf{r}} = \sqrt{\frac{4\pi}{3}} \sum_{\mu=-1}^{1} Y_{1,\mu}^*(\theta,\phi)\xi_\mu\,. \tag{1.56}$$

1.3 Clebsch-Gordan Coefficients

One common problem encountered in atomic physics calculations is finding eigenstates of the sum of two angular momenta in terms of products of the individual angular momentum eigenstates. For example, as mentioned in section (1.2.1), the products $Y_{l,m}(\theta,\phi)\chi_\mu$ are eigenstates of L^2, and L_z, as well as S^2, and S_z. The question addressed in this section is how to combine product states such as these to find eigenstates of J^2 and J_z, where $\mathbf{J} = \mathbf{L} + \mathbf{S}$.

Generally, let us suppose that we have two commuting angular momentum vectors $\mathbf{J}_1$ and $\mathbf{J}_2$. Let $|j_1, m_1\rangle$ be an eigenstate of J_1^2 and J_{1z} with eigenvalues (in units of $\hbar$) $j_1(j_1+1)$, and m_1, respectively. Similarly, let $|j_2, m_2\rangle$ be an eigenstate of J_2^2 and J_{2z} with eigenvalues $j_2(j_2+1)$ and m_2. We set $\mathbf{J} = \mathbf{J_1} + \mathbf{J_2}$ and attempt to construct eigenstates of J^2 and J_z as linear combinations of the product states $|j_1, m_1\rangle\,|j_2, m_2\rangle$:

$$|j, m\rangle = \sum_{m_1, m_2} C(j_1, j_2, j; m_1, m_2, m)|j_1, m_1\rangle|j_2, m_2\rangle\,. \tag{1.57}$$

The expansion coefficients $C(j_1, j_2, j; m_1, m_2, m)$, called Clebsch-Gordan coefficients, are discussed in many standard quantum mechanics textbooks (for example, Messiah, 1961, chap. 10). One sometimes encounters notation such as $\langle j_1, m_1, j_2, m_2|j, m\rangle$ for the Clebsch-Gordan coefficient $C(j_1, j_2, j; m_1, m_2, m)$.

Since $J_z = J_{1z} + J_{2z}$, it follows from Eq.(1.57) that

$$m|j, m\rangle = \sum_{m_1, m_2} (m_1 + m_2) C(j_1, j_2, j; m_1, m_2, m)|j_1, m_1\rangle\,|j_2, m_2\rangle\,. \tag{1.58}$$

Since the states $|j_1, m_1\rangle\,|j_2, m_2\rangle$ are linearly independent, one concludes from Eq.(1.58) that

$$(m_1 + m_2 - m)C(j_1, j_2, j; m_1, m_2, m) = 0\,. \tag{1.59}$$

It follows that the only nonvanishing Clebsch-Gordan coefficients are those for which $m_1+m_2 = m$. The sum in Eq.(1.57) can be expressed, therefore, as a sum over m_2 only, the value of m_1 being determined by $m_1 = m-m_2$. Consequently, we rewrite Eq.(1.57) as

$$|j, m\rangle = \sum_{m_2} C(j_1, j_2, j; m - m_2, m_2, m)|j_1, m - m_2\rangle\,|j_2, m_2\rangle\,. \tag{1.60}$$

If we demand that all of the states in Eq.(1.60) be normalized, then it follows from the relation

$$\langle j', m'|j, m\rangle = \delta_{j'j}\delta_{m'm}\,,$$

that

$$\sum_{m_2', m_2} C(j_1, j_2, j'; m' - m_2', m_2', m')C(j_1, j_2, j; m - m_2, m_2, m)\times$$
$$\langle j_1, m' - m_2'|j_1, m - m_2\rangle\,\langle j_2, m_2'|j_2, m_2\rangle = \delta_{j'j}\delta_{m'm}.$$

From this equation, one obtains the orthogonality relation:

$$\sum_{m_1, m_2} C(j_1, j_2, j'; m_1, m_2, m')\,C(j_1, j_2, j; m_1, m_2, m) = \delta_{j'j}\delta_{m'm}\,. \tag{1.61}$$

One can make use of this equation to invert Eq.(1.60). Indeed, one finds

$$|j_1, m - m_2\rangle|j_2, m_2\rangle\, = \sum_j C(j_1, j_2, j; m - m_2, m_2, m)|j, m\rangle\,. \tag{1.62}$$

From Eq.(1.62), a second orthogonality condition can be deduced:

$$\sum_{j,m} C(j_1, j_2, j; m_1', m_2', m)\,C(j_1, j_2, j; m_1, m_2, m) = \delta_{m_1'm_1}\delta_{m_2'm_2}\,. \tag{1.63}$$

The state of largest m is the "extended state" $|j_1, j_1\rangle\,|j_2, j_2\rangle$. With the aid of the decomposition, $J^2 = J_1^2 + J_2^2 + 2J_{1z}J_{2z} + J_{1+}J_{2-} + J_{1-}J_{2+}$, one may establish that this state is an eigenstate of J^2 with eigenvalue $j = j_1 + j_2$; it is also, obviously, an eigenstate of J_z with eigenvalue $m = j_1 + j_2$. The state $J_-|j_1, j_1\rangle\,|j_2, j_2\rangle$ is also an eigenstate of J^2 with eigenvalue $j = j_1 + j_2$. It is an eigenstate of J_z but with eigenvalue $m = j_1 + j_2 - 1$. The corresponding normalized eigenstate is

$$|j_1 + j_2, j_1 + j_2 - 1\rangle = \sqrt{\frac{j_1}{j_1 + j_2}}|j_1, j_1 - 1\rangle|j_2, j_2\rangle$$
$$+\sqrt{\frac{j_2}{j_1 + j_2}}|j_1, j_1\rangle|j_2, j_2 - 1\rangle\,. \tag{1.64}$$

Table 1.1: $C(l, 1/2, j; m - m_s, m_s, m)$

	$m_s = 1/2$	$m_s = -1/2$
$j = l + 1/2$	$\sqrt{\frac{l+m+1/2}{2l+1}}$	$\sqrt{\frac{l-m+1/2}{2l+1}}$
$j = l - 1/2$	$-\sqrt{\frac{l-m+1/2}{2l+1}}$	$\sqrt{\frac{l+m+1/2}{2l+1}}$

By repeated application of J_- to the state $|j_1, j_1\rangle|j_2, j_2\rangle$, one generates, in this way, each of the $2j + 1$ eigenstates of J_z with eigenvalues $m = j_1 + j_2, j_1 + j_2 - 1, \cdots, -j_1 - j_2$. The state

$$|j_1 + j_2 - 1, j_1 + j_2 - 1\rangle = -\sqrt{\frac{j_2}{j_1 + j_2}}|j_1, j_1 - 1\rangle|j_2, j_2\rangle + \sqrt{\frac{j_1}{j_1 + j_2}}|j_1, j_1\rangle|j_2, j_2 - 1\rangle\,, \qquad (1.65)$$

is an eigenstate of J_z with eigenvalue $j_1 + j_2 - 1$, constructed to be orthogonal to (1.64). One easily establishes that this state is an eigenstate of J^2 corresponding to eigenvalue $j = j_1 + j_2 - 1$. By repeated application of J_- to this state, one generates the $2j + 1$ eigenstates of J_z corresponding to $j = j_1 + j_2 - 1$. We continue this procedure by constructing the state orthogonal to the two states $|j_1 + j_2, j_1 + j_2 - 2\rangle$ and $|j_1 + j_2 - 1, j_1 + j_2 - 2\rangle$, and then applying J_- successively to generate all possible m states for $j = j_1 + j_2 - 2$. Continuing in this way, we construct states with $j = j_1 + j_2, j_1 + j_2 - 1, j_1 + j_2 - 2, \cdots, j_{\min}$. The algorithm terminates when we have exhausted all of the $(2j_1 + 1)(2j_2 + 1)$ possible linearly independent states that can be made up from products of $|j_1, m_1\rangle$ and $|j_2, m_2\rangle$. The limiting value $j_{\min}$ is determined by the relation

$$\sum_{j=j_{\min}}^{j_1+j_2} (2j + 1) = (j_1 + j_2 + 2)(j_1 + j_2) - j_{\min}^2 + 1 = (2j_1 + 1)(2j_2 + 1)\,, \quad (1.66)$$

which leads to the $j_{\min} = |j_1 - j_2|$. The possible eigenvalues of J^2 are, therefore, given by $j(j + 1)$, with $j = j_1 + j_2, j_1 + j_2 - 1, \cdots, |j_1 - j_2|$.

Values of the Clebsch-Gordan coefficients can be determined from the construction described above; however, it is often easier to proceed in a slightly different way. Let us illustrate the alternative for the case $\mathbf{J} = \mathbf{L} + \mathbf{S}$, with $s = 1/2$. In this case, the possible values j are $j = l + 1/2$ and $j = l - 1/2$. Eigenstates of J^2 and J_z constructed by the Clebsch-Gordan expansion are also eigenstates of

$$\Lambda = 2\mathbf{L} \cdot \mathbf{S} = 2L_z S_z + L_+ S_- + L_- S_+\,.$$

Table 1.2: $C(l,1,j;m-m_s,m_s,m)$

	$m_s=1$	$m_s=0$	$m_s=-1$
$j=l+1$	$\sqrt{\frac{(l+m)(l+m+1)}{(2l+1)(2l+2)}}$	$\sqrt{\frac{(l-m+1)(l+m+1)}{(2l+1)(l+1)}}$	$\sqrt{\frac{(l-m)(l-m+1)}{(2l+1)(2l+2)}}$
$j=l$	$-\sqrt{\frac{(l+m)(l-m+1)}{2l(l+1)}}$	$\frac{m}{\sqrt{l(l+1)}}$	$\sqrt{\frac{(l-m)(l+m+1)}{2l(l+1)}}$
$j=l-1$	$\sqrt{\frac{(l-m)(l-m+1)}{2l(2l+1)}}$	$-\sqrt{\frac{(l-m)(l+m)}{l(2l+1)}}$	$\sqrt{\frac{(l+m+1)(l+m)}{2l(2l+1)}}$

The eigenvalues of Λ are $\lambda = j(j+1) - l(l+1) - 3/4$. Thus for $j = l + 1/2$, we find $\lambda = l$; for $j = l - 1/2$, we find $\lambda = -l - 1$. The eigenvalue equation for Λ,

$$\Lambda|j,m\rangle = \lambda|j,m\rangle$$

may be rewritten as a set of two homogeneous equations in two unknowns: $x = C(l,1/2,j;m-1/2,1/2,m)$ and $y = C(l,1/2,j;m+1/2,-1/2,m)$:

$$\begin{aligned} \lambda\, x &= (m-1/2)\, x + \sqrt{(l-m+1/2)(l+m+1/2)}\, y \\ \lambda\, y &= \sqrt{(l-m+1/2)(l+m+1/2)}\, x - (m+1/2)\, y\,. \end{aligned}$$

The solutions to this equation are:

$$y/x = \begin{cases} \sqrt{\frac{l+m+1/2}{l-m+1/2}} & \text{for } \lambda = l, \\ -\sqrt{\frac{l-m+1/2}{l+m+1/2}} & \text{for } \lambda = -l-1. \end{cases} \tag{1.67}$$

We normalize these solutions so that $x^2 + y^2 = 1$. The ambiguity in phase is resolved by the requirement that $y > 0$. The resulting Clebsch-Gordan coefficients are listed in Table 1.1.

This same technique can be applied in the general case. One chooses j_1 and j_2 so that $j_2 < j_1$. The eigenvalue equation for Λ reduces to a set of $2j_2+1$ equations for $2j_2+1$ unknowns x_k, the Clebsch-Gordan coefficients for fixed j and m expressed in terms of $m_2 = j_2 + 1 - k$. The $2j_2+1$ eigenvalues of Λ can be determined from the $2j_2+1$ possible values of j by $\lambda = j(j+1) - j_1(j_1+1) - j_2(j_2+1)$. One solves the resulting equations, normalizes the solutions to $\sum_k x_k^2 = 1$ and settles the phase ambiguity by requiring that the Clebsch-Gordan coefficient for $m_2 = -j_2$ is positive; e.g., $x_{2j_2+1} > 0$. As a second example of this method, we give in Table 1.2 the Clebsch-Gordan coefficients for $\mathbf{J} = \mathbf{L} + \mathbf{S}$, with $s = 1$.

A general formula for the Clebsch-Gordan coefficients is given in Wigner (1931). Another equivalent, but more convenient one, was obtained later by

Racah (1942):

$$C(j_1,j_2,j;m_1,m_2,m)=\delta_{m_1+m_2,m}\sqrt{\frac{(j_1+j_2-j)!(j+j_1-j_2)!(j+j_2-j_1)!(2j+1)}{(j+j_1+j_2+1)!}}$$

$$\sum_k \frac{(-1)^k\sqrt{(j_1+m_1)!(j_1-m_1)!(j_2+m_2)!(j_2-m_2)!(j+m)!(j-m)!}}{k!(j_1+j_2-j-k)!(j_1-m_1-k)!(j_2+m_2-k)!(j-j_2+m_1+k)!(j-j_1-m_2+k)!}\,.$$

With the aid of this formula, the following symmetry relations between Clebsch-Gordan coefficients (see Rose, 1957, chap. 3) may be established:

$$C(j_1,j_2,j;-m_1,-m_2,-m)=(-1)^{j_1+j_2-j}C(j_1,j_2,j;m_1,m_2,m)\,, \tag{1.69}$$

$$C(j_2,j_1,j;m_2,m_1,m)=(-1)^{j_1+j_2-j}C(j_1,j_2,j;m_1,m_2,m)\,, \tag{1.70}$$

$$C(j_1,j,j_2;m_1,-m,-m_2)=$$
$$(-1)^{j_1-m_1}\sqrt{\frac{2j_2+1}{2j+1}}C(j_1,j_2,j;m_1,m_2,m)\,. \tag{1.71}$$

Expressions for other permutations of the arguments can be inferred from these basic three. As an application of these symmetry relations, we combine the easily derived equation

$$C(j_1,0,j;m_1,0,m)=\delta_{j_1j}\delta_{m_1m}\,, \tag{1.72}$$

with Eq.(1.71) to give

$$C(j_1,j,0;m_1,-m,0)=\frac{(-1)^{j_1-m_1}}{\sqrt{2j+1}}\delta_{j_1j}\delta_{m_1m}\,. \tag{1.73}$$

Several other useful formulas may also be derived directly from Eq. (1.68):

$$C(j_1,j_2,j_1+j_2;m_1,m_2,m_1+m_2)=$$
$$\sqrt{\frac{(2j_1)!(2j_2)!(j_1+j_2+m_1+m_2)!(j_1+j_2-m_1-m_2)!}{(2j_1+2j_2)!(j_1-m_1)!(j_1+m_1)!(j_2-m_2)!(j_2+m_2)!}}\,, \tag{1.74}$$

$$C(j_1,j_2,j;j_1,m-j_1,m)=$$
$$\sqrt{\frac{(2j+1)(2j_1)!(j_2-j_1+j)!(j_1+j_2-m)!(j+m)!}{(j_1+j_2-j)!(j_1-j_2+j)!(j_1+j_2+j+1)!(j_2-j_1+m)!(j-m)!}}\,. \tag{1.75}$$

1.3.1 Three-j symbols

The symmetry relations between the Clebsch-Gordan coefficients are made more transparent by introducing the Wigner **three-j** symbols defined by:

$$\begin{pmatrix} j_1 & j_2 & j_3 \\ m_1 & m_2 & m_3 \end{pmatrix}=\frac{(-1)^{j_1-j_2-m_3}}{\sqrt{2j_3+1}}C(j_1,j_2,j_3;m_1,m_2,-m_3)\,. \tag{1.76}$$

The three-j symbol vanishes unless

$$m_1+m_2+m_3=0\,. \tag{1.77}$$

The three-j symbols have a high degree of symmetry under interchange of columns; they are symmetric under even permutations of the indices $(1, 2, 3)$:

$$\begin{pmatrix} j_3 & j_1 & j_2 \\ m_3 & m_1 & m_2 \end{pmatrix} = \begin{pmatrix} j_2 & j_3 & j_1 \\ m_2 & m_3 & m_1 \end{pmatrix} = \begin{pmatrix} j_1 & j_2 & j_3 \\ m_1 & m_2 & m_3 \end{pmatrix}, \quad (1.78)$$

and they change by a phase under odd permutations of $(1, 2, 3)$, e.g.:

$$\begin{pmatrix} j_2 & j_1 & j_3 \\ m_2 & m_1 & m_3 \end{pmatrix} = (-1)^{j_1+j_2+j_3} \begin{pmatrix} j_1 & j_2 & j_3 \\ m_1 & m_2 & m_3 \end{pmatrix}. \quad (1.79)$$

On changing the sign of m_1, m_2 and m_3, the three-j symbols transform according to

$$\begin{pmatrix} j_1 & j_2 & j_3 \\ -m_1 & -m_2 & -m_3 \end{pmatrix} = (-1)^{j_1+j_2+j_3} \begin{pmatrix} j_1 & j_2 & j_3 \\ m_1 & m_2 & m_3 \end{pmatrix}. \quad (1.80)$$

The orthogonality relation (1.61) may be rewritten in terms of three-j symbols as

$$\sum_{m_1,m_2} \begin{pmatrix} j_1 & j_2 & j_3' \\ m_1 & m_2 & m_3' \end{pmatrix} \begin{pmatrix} j_1 & j_2 & j_3 \\ m_1 & m_2 & m_3 \end{pmatrix} = \frac{1}{2j_3+1} \delta_{j_3' j_3} \delta_{m_3' m_3}, \quad (1.81)$$

and the orthogonality relation (1.63) can be rewritten

$$\sum_{j_3,m_3} (2j_3+1) \begin{pmatrix} j_1 & j_2 & j_3 \\ m_1 & m_2 & m_3 \end{pmatrix} \begin{pmatrix} j_1 & j_2 & j_3 \\ m_1' & m_2' & m_3 \end{pmatrix} = \delta_{m_1 m_1'} \delta_{m_2 m_2'}. \quad (1.82)$$

We refer to these equations as "orthogonality relations for three-j symbols".

The following specific results for three-j symbols are easily obtained from Eqs. (1.73-1.75) of the previous subsection:

$$\begin{pmatrix} j & j & 0 \\ m & -m & 0 \end{pmatrix} = \frac{(-1)^{j-m}}{\sqrt{2j+1}}, \quad (1.83)$$

$$\begin{pmatrix} j_1 & j_2 & j_1+j_2 \\ m_1 & m_2 & -m_1-m_2 \end{pmatrix} = (-1)^{j_1-j_2+m_1+m_2} \times \sqrt{\frac{(2j_1)!(2j_2)!(j_1+j_2+m_1+m_2)!(j_1+j_2-m_1-m_2)!}{(2j+1+2j_2+1)!(j_1-m_1)!(j_1+m_1)!(j_2-m_2)!(j_2+m_2)!}}, \quad (1.84)$$

$$\begin{pmatrix} j_1 & j_2 & j_3 \\ m_1 & -j_1-m_3 & m_3 \end{pmatrix} = (-1)^{-j_2+j_3+m_3} \times \sqrt{\frac{(2j_1)!(j_2-j_1+j_3)!(j_1+j_2+m_3)!(j_3-m_3)!}{(j_1+j_2+j_3+1)!(j_1-j_2+j_3)!(j_1+j_2-j_3)!(j_2-j_1-m_3)!(j_3+m_3)!}}. \quad (1.85)$$

From the symmetry relation (1.80), it follows that

$$\begin{pmatrix} j_1 & j_2 & j_3 \\ 0 & 0 & 0 \end{pmatrix} = 0,$$

unless $J = j_1 + j_2 + j_3$ is even. In that case, we may write

$$\begin{pmatrix} j_1 & j_2 & j_3 \\ 0 & 0 & 0 \end{pmatrix} = (-1)^{J/2} \sqrt{\frac{(J-2j_1)!(J-2j_2)!(J-2j_3)!}{(J+1)!}} \frac{(J/2)!}{(J/2-j_1)!(J/2-j_2)!(J/2-j_3)!}\,. \tag{1.86}$$

Two MAPLE programs, based on Eq. (1.68), to evaluate Clebsch-Gordan coefficients (CGC.MAP) and three-j symbols (THREEJ.MAP), are provided as part of the course material.

1.3.2 Irreducible Tensor Operators

A family of $2k+1$ operators T^k_q, with $q = -k, -k+1, \cdots, k$, satisfying the commutation relations

$$[J_z, T^k_q] = qT^k_q\,, \tag{1.87}$$

$$[J_\pm, T^k_q] = \sqrt{(k \pm q + 1)(k \mp q)}\, T^k_{q\pm 1}\,, \tag{1.88}$$

with the angular momentum operators J_z and $J_\pm = J_x \pm iJ_y$, are called irreducible tensor operators of rank k. The spherical harmonics $Y_{lm}(\theta, \phi)$ are, according to this definition, irreducible tensor operators of rank l. The operators J_μ defined by

$$J_\mu = \begin{cases} -\frac{1}{\sqrt{2}}(J_x + iJ_y), & \mu = +1, \\ J_z, & \mu = 0, \\ \frac{1}{\sqrt{2}}(J_x - iJ_y), & \mu = -1, \end{cases} \tag{1.89}$$

are also irreducible tensor operators; in this case of rank 1.

Matrix elements of irreducible tensor operators between angular momentum states are evaluated using the *Wigner-Eckart* theorem (Wigner, 1931; Eckart, 1930):

$$\langle j_1, m_1 | T^k_q | j_2, m_2 \rangle = (-1)^{j_1 - m_1} \begin{pmatrix} j_1 & k & j_2 \\ -m_1 & q & m_2 \end{pmatrix} \langle j_1 || T^k || j_2 \rangle\,. \tag{1.90}$$

In this equation, the quantity $\langle j_1 || T^k || j_2 \rangle$, called the reduced matrix element of the tensor operator T^k, is independent of the magnetic quantum numbers m_1, m_2 and q.

To prove the Wigner-Eckart theorem, we note that the matrix elements $\langle j_1 m_1 | T^k_q | j_2 m_2 \rangle$ satisfies the recurrence relations

$$\begin{aligned} \sqrt{(j_1 \mp m_1 + 1)(j_1 \pm m_1)}\, \langle j_1 m_1 \mp 1 | T^k_q | j_2 m_2 \rangle = \\ \sqrt{(j_2 \pm m_2 + 1)(j_2 \mp m_2)}\, \langle j_1 m_1 | T^k_q | j_2 m_2 \pm 1 \rangle \\ + \sqrt{(k \pm q + 1)(k \mp q)}\, \langle j_1 m_1 | T^k_{q\pm 1} | j_2 m_2 \rangle\,. \end{aligned} \tag{1.91}$$

They are, therefore, proportional to the Clebsch-Gordan coefficients $C(j_2, k, j_1; m_2, q, m_1)$, which satisfy precisely the same recurrence relations. Since

$$C(j_2, k, j_1; m_2, q, m_1) = \sqrt{2j_1 + 1}\,(-1)^{j_1 - m_1} \begin{pmatrix} j_1 & k & j_2 \\ -m_1 & q & m_2 \end{pmatrix}, \qquad (1.92)$$

the proportionality in Eq.(1.90) is established.

As a first application of the Wigner-Eckart theorem, consider the matrix element of the irreducible tensor operator J_μ:

$$\langle j_1, m_1 | J_\mu | j_2, m_2 \rangle = (-1)^{j_1 - m_1} \begin{pmatrix} j_1 & 1 & j_2 \\ -m_1 & \mu & m_2 \end{pmatrix} \langle j_1 || J || j_2 \rangle\,. \qquad (1.93)$$

The reduced matrix element $\langle j_1 || J || j_2 \rangle$ can be determined by evaluating both sides of Eq.(1.93) in the special case $\mu = 0$. We find

$$\langle j_1 || J || j_2 \rangle = \sqrt{j_1(j_1 + 1)(2j_1 + 1)}\,\delta_{j_1 j_2}\,, \qquad (1.94)$$

where we have made use of the fact that

$$\begin{pmatrix} j_1 & 1 & j_1 \\ -m_1 & 0 & m_1 \end{pmatrix} = (-1)^{j_1 - m_1} \frac{m_1}{\sqrt{j_1(j_1 + 1)(2j_1 + 1)}}\,. \qquad (1.95)$$

As a second application, we consider matrix elements of the irreducible tensor operator

$$C^k_q = \sqrt{\frac{4\pi}{2k + 1}}\, Y_{kq}(\theta, \phi)\,,$$

between orbital angular momentum eigenstates:

$$\langle l_1 m_1 | C^k_q | l_2 m_2 \rangle = (-1)^{l_1 - m_1} \begin{pmatrix} l_1 & k & l_2 \\ -m_1 & q & m_2 \end{pmatrix} \langle l_1 || C^k || l_2 \rangle\,. \qquad (1.96)$$

The left-hand side of Eq.(1.96) is (up to a factor) the integral of three spherical harmonics. It follows that

$$Y_{kq}(\Omega) Y_{l_2 m_2}(\Omega) = \sum_{l_1} \sqrt{\frac{2k + 1}{4\pi}} \times (-1)^{l_1 - m_1} \begin{pmatrix} l_1 & k & l_2 \\ -m_1 & q & m_2 \end{pmatrix} \langle l_1 || C^k || l_2 \rangle\, Y_{l_1 m_1}(\Omega)\,, \qquad (1.97)$$

where we use the symbol Ω to designate the angles θ and ϕ. With the aid of the orthogonality relation (1.81) for the three-j symbols, we invert Eq.(1.97) to find

$$\sum_{m_2 q} \begin{pmatrix} l_1 & k & l_2 \\ -m_1 & q & m_2 \end{pmatrix} Y_{kq}(\Omega)\; Y_{l_2 m_2}(\Omega) = \sqrt{\frac{2k + 1}{4\pi}}\; \frac{(-1)^{l_1 - m_1}}{2l_1 + 1}\; \langle l_1 || C^k || l_2 \rangle Y_{l_1 m_1}(\Omega)\,. \qquad (1.98)$$

Evaluating both sides of this equation at $\theta = 0$, we obtain

$$\langle l_1||C^k||l_2\rangle = (-1)^{l_1}\sqrt{(2l_1+1)(2l_2+1)}\begin{pmatrix} l_1 & k & l_2 \\ 0 & 0 & 0 \end{pmatrix}. \tag{1.99}$$

1.4 Graphical Representation - Basic rules

In subsequent chapters we will be required to carry out sums of products of three-j symbols over magnetic quantum numbers m_j. Such sums can be formulated in terms of a set of graphical rules, that allow one to carry out the required calculations efficiently. There are several ways of introducing graphical rules for angular momentum summations (Judd, 1963; Jucys et al., 1964; Varshalovich et al., 1988). Here, we follow those introduced by Lindgren and Morrison (1985).

The basic graphical element is a line segment labeled at each end by a pair of angular momentum indices jm. The segment with j_1m_1 at one end and j_2m_2 at the other end is the graphical representation of $\delta_{j_1j_2}\delta_{m_1m_2}$; thus

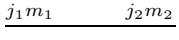

$$= \delta_{j_1j_2}\,\delta_{m_1m_2}\,. \tag{1.100}$$

A directed line segment, which is depicted by attaching an arrow to a line segment, is a second important graphical element. An arrow pointing from j_1m_1 to j_2m_2 represents the identity:

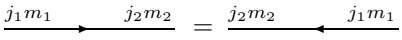

$$= (-1)^{j_2-m_2}\delta_{j_1j_2}\,\delta_{-m_1m_2}\,. \tag{1.101}$$

Reversing the direction of the arrow leads to

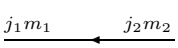

$$= (-1)^{j_2+m_2}\delta_{j_1j_2}\,\delta_{-m_1m_2}\,. \tag{1.102}$$

Connecting together two line segments at ends carrying identical values of jm is the graphical representation of a sum over the magnetic quantum number m. Therefore,

$$\sum_{m_2}$$
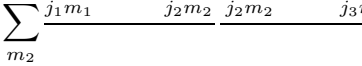

$$= \delta_{j_3j_2}$$
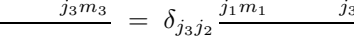

. (1.103)

It follows that two arrows directed in the same direction give an overall phase,

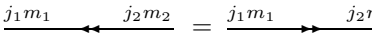

$$= (-1)^{2j_2}\delta_{j_1j_2}\delta_{m_1m_2}\,, \tag{1.104}$$

and that two arrows pointing in opposite directions cancel,

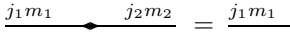

$$= \delta_{j_1j_2}\delta_{m_1m_2}\,. \tag{1.105}$$

Another important graphical element is the three-j symbol, which is represented as

$$\begin{pmatrix} j_1 & j_2 & j_3 \\ m_1 & m_2 & m_3 \end{pmatrix} = +$$
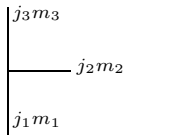

. (1.106)

The + sign designates that the lines associated with j_1m_1, j_2m_2, and j_3m_3 are oriented in such a way that a counter-clockwise rotation leads from j_1m_1 to j_2m_2 to j_3m_3. We use a $-$ sign to designate that a clockwise rotation leads from j_1m_1 to j_2m_2 to j_3m_3. Thus, we can rewrite Eq.(1.106) as

$$\begin{pmatrix} j_1 & j_2 & j_3 \\ m_1 & m_2 & m_3 \end{pmatrix} = -$$

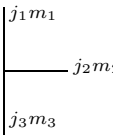

. (1.107)

The symmetry relation of Eq.(1.78) is represented by the graphical identity:

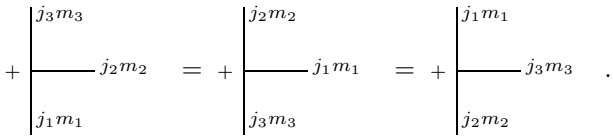

. (1.108)

The symmetry relation (1.79) leads to the graphical relation:

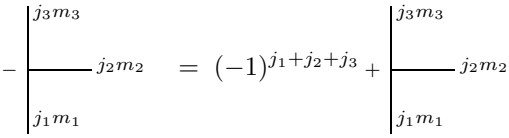

. (1.109)

One can attach directed lines and three-j symbols to form combinations such as

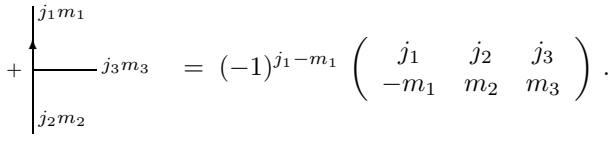

. (1.110)

Using this, the Wigner-Eckart theorem can be written

$$\langle j_1, m_1 | T^k_q | j_2, m_2 \rangle = -$$

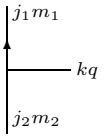

$\langle j_1 || T^k || j_2 \rangle$. (1.111)

Furthermore, with this convention, we can write

$$C(j_1, j_2, j_3; m_1, m_2, m_3) = \sqrt{2j_3 + 1} -$$

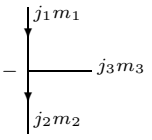

. (1.112)

Factors of $\sqrt{2j+1}$ are represented by thickening part of the corresponding line segment. Thus, we have the following representation for a Clebsch-Gordan coefficient:

$$C(j_1, j_2, j_3; m_1, m_2, m_3) = -$$

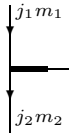

. (1.113)

The orthogonality relation for three-j symbols (1.81) can be written in graphical terms as

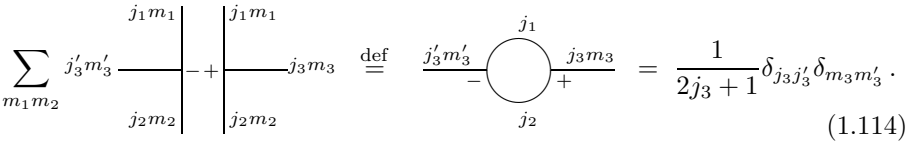

(1.114)

Another very useful graphical identity is

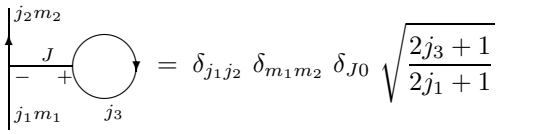

(1.115)

1.5 Spinor and Vector Spherical Harmonics

1.5.1 Spherical Spinors

We combine spherical harmonics, which are eigenstates of L^2 and L_z, and spinors, which are eigenstates of S^2 and S_z to form eigenstates of J^2 and J_z, referred to as spherical spinors. Spherical spinors are denoted by $\Omega_{jlm}(\theta,\phi)$ and are defined by the equation

$$\Omega_{jlm}(\theta,\phi) = \sum_{\mu} C(l,1/2,j;m-\mu,\mu,m) Y_{l,m-\mu}(\theta,\phi)\chi_{\mu}\,. \tag{1.116}$$

From Table 1.1, we obtain the following explicit formulas for spherical spinors having the two possible values, $j = l \pm 1/2$:

$$\Omega_{l+1/2,l,m}(\theta,\phi) = \begin{pmatrix} \sqrt{\frac{l+m+1/2}{2l+1}}\, Y_{l,m-1/2}(\theta,\phi) \\ \sqrt{\frac{l-m+1/2}{2l+1}}\, Y_{l,m+1/2}(\theta,\phi) \end{pmatrix}, \tag{1.117}$$

$$\Omega_{l-1/2,l,m}(\theta,\phi) = \begin{pmatrix} -\sqrt{\frac{l-m+1/2}{2l+1}}\, Y_{l,m-1/2}(\theta,\phi) \\ \sqrt{\frac{l+m+1/2}{2l+1}}\, Y_{l,m+1/2}(\theta,\phi) \end{pmatrix}. \tag{1.118}$$

Spherical spinors are eigenfunctions of $\boldsymbol{\sigma}\cdot\boldsymbol{L}$ and, therefore, of the operator

$$K = -1 - \boldsymbol{\sigma}\cdot\boldsymbol{L}.$$

The eigenvalue equation for K is

$$K\Omega_{jlm}(\theta,\phi) = \kappa\Omega_{jlm}(\theta,\phi)\,, \tag{1.119}$$

where the (integer) eigenvalues are $\kappa = -l-1$ for $j = l+1/2$, and $\kappa = l$ for $j = l-1/2$. These values can be summarized as $\kappa = \mp(j+1/2)$ for $j = l \pm 1/2$. The value of κ determines both j and l. Consequently, the more compact notation, $\Omega_{\kappa m} \equiv \Omega_{jlm}$ can be used.

Spherical spinors satisfy the orthogonality relations

$$\int_0^\pi \sin\theta d\theta \int_0^{2\pi} d\phi\, \Omega^\dagger_{\kappa' m'}(\theta,\phi)\Omega_{\kappa m}(\theta,\phi) = \delta_{\kappa'\kappa}\delta_{m'm}\,. \tag{1.120}$$

The parity operator P maps $\mathbf{r} \to -\mathbf{r}$. In spherical coordinates, the operator P transforms $\phi \to \phi + \pi$ and $\theta \to \pi - \theta$. Under a parity transformation,

$$PY_{lm}(\theta,\phi) = Y_{lm}(\pi-\theta,\phi+\pi) = (-1)^l Y_{lm}(\theta,\phi)\,. \tag{1.121}$$

It follows that the spherical spinors are eigenfunctions of P having eigenvalues $p = (-1)^l$. The two spinors $\Omega_{\kappa m}(\theta,\phi)$ and $\Omega_{-\kappa m}(\theta,\phi)$, corresponding to the same value of j, have values of l differing by one unit and, therefore, have opposite parity.

It is interesting to examine the behavior of spherical spinors under the operator $\boldsymbol{\sigma}\cdot\hat{\mathbf{r}}$, where $\hat{\mathbf{r}} = \mathbf{r}/r$. This operator satisfies the identity

$$\boldsymbol{\sigma}\cdot\hat{\mathbf{r}}\;\boldsymbol{\sigma}\cdot\hat{\mathbf{r}} = 1\,, \tag{1.122}$$

which follows from the commutation relations for the Pauli matrices. Furthermore, the operator $\boldsymbol{\sigma}\cdot\hat{\mathbf{r}}$ commutes with $\mathbf{J}$ and, therefore, leaves the value of j unchanged. The parity operation changes the sign of $\boldsymbol{\sigma}\cdot\hat{\mathbf{r}}$. Since the value of j remains unchanged, and since the sign of $\boldsymbol{\sigma}\cdot\hat{\mathbf{r}}$ changes under the parity transformation, it follows that

$$\boldsymbol{\sigma}\cdot\hat{\mathbf{r}}\,\Omega_{\kappa m}(\theta,\phi) = a\Omega_{-\kappa m}(\theta,\phi)\,, \tag{1.123}$$

where a is a constant. Evaluating both sides of Eq.(1.123) in a coordinate system where $\theta = 0$, one easily establishes $a = -1$. Therefore,

$$\boldsymbol{\sigma}\cdot\hat{\mathbf{r}}\,\Omega_{\kappa m}(\theta,\phi) = -\Omega_{-\kappa m}(\theta,\phi)\,. \tag{1.124}$$

Now, let us consider the operator $\boldsymbol{\sigma}\cdot\boldsymbol{p}$. Using Eq.(1.122), it follows that

$$\boldsymbol{\sigma}\cdot\mathbf{p} = \boldsymbol{\sigma}\cdot\hat{\mathbf{r}}\;\boldsymbol{\sigma}\cdot\hat{\mathbf{r}}\;\boldsymbol{\sigma}\cdot\mathbf{p} = -i\boldsymbol{\sigma}\cdot\hat{\mathbf{r}}\,\left(i\hat{\mathbf{r}}\cdot\,\mathbf{p} - \frac{\boldsymbol{\sigma}\cdot[\mathbf{r}\times\mathbf{p}]}{r}\right)\,. \tag{1.125}$$

In deriving this equation, we have made use of the identity in Eq.(1.50).

From Eq.(1.125), it follows that

$$\boldsymbol{\sigma}\cdot\mathbf{p} f(r)\Omega_{\kappa m}(\theta,\phi) = i\left(\frac{df}{dr} + \frac{\kappa+1}{r}f\right)\,\Omega_{-\kappa m}(\theta,\phi)\,. \tag{1.126}$$

This identities (1.124) and (1.126) are important in the reduction of the central-field Dirac equation to radial form.

1.5.2 Vector Spherical Harmonics

Following the procedure used to construct spherical spinors, one combines spherical harmonics with spherical basis vectors to form vector spherical harmonics $\mathbf{Y}_{JLM}(\theta,\phi)$:

$$\mathbf{Y}_{JLM}(\theta,\phi) = \sum_{\sigma} C(L,1,J;M-\sigma,\sigma,M) Y_{LM-\sigma}(\theta,\phi)\boldsymbol{\xi}_{\sigma}\,. \tag{1.127}$$

The vector spherical harmonics are eigenfunctions of J^2 and J_z. The eigenvalues of J^2 are $J(J+1)$, where J is an integer. For $J>0$, there are three corresponding values of L: $L=J\pm 1$ and $L=J$. For $J=0$, the only possible values of L are $L=0$ and $L=1$. Explicit forms for the vector spherical harmonics can be constructed with the aid of Table 1.2. Vector spherical harmonics satisfy the orthogonality relations

$$\int_0^{2\pi} d\phi \int_0^{\pi} \sin\theta d\theta\, Y^{\dagger}_{J'L'M'}(\theta,\phi)\, Y_{JLM}(\theta,\phi) = \delta_{J'J}\delta_{L'L}\delta_{M'M}\,. \tag{1.128}$$

Vector functions, such as the electromagnetic vector potential, can be expanded in terms of vector spherical harmonics. As an example of such an expansion, let us consider

$$\hat{\mathbf{r}}\, Y_{lm}(\theta,\phi) = \sum_{JLM} a_{JLM}\mathbf{Y}_{JLM}(\theta,\phi)\,. \tag{1.129}$$

With the aid of the orthogonality relation, this equation can be inverted to give

$$a_{JLM} \;=\; \int_0^{2\pi} d\phi \int_0^{\pi} \sin\theta d\theta\, \mathbf{Y}^{\dagger}_{JLM}\,\hat{\mathbf{r}}\, Y_{lm}(\theta,\phi).$$

This equation can be rewritten with the aid of (1.56) as

$$a_{JLM} = \sum_{\mu\nu} C(L,1,J;M-\mu,\mu,M)\xi^{\dagger}_{\mu}\xi_{\nu}\langle l,m|C^1_{\nu}|L,M-\nu\rangle\,. \tag{1.130}$$

Using the known expression for the matrix element of the C^1_{ν} tensor operator from Eqs.(1.96,1.99), one obtains

$$a_{JLM} \;=\; \sqrt{\frac{2L+1}{2l+1}}\, C(L,1,l;0,0,0)\,\delta_{Jl}\delta_{Mm} \tag{1.131}$$

$$\;=\; \left(\sqrt{\frac{l}{2l+1}}\delta_{Ll-1} - \sqrt{\frac{l+1}{2l+1}}\delta_{Ll+1}\right)\delta_{Jl}\delta_{Mm}\,. \tag{1.132}$$

Therefore, one may write

$$\hat{\mathbf{r}}\, Y_{JM}(\theta,\phi) = \sqrt{\frac{J}{2J+1}}Y_{JJ-1M}(\theta,\phi) - \sqrt{\frac{J+1}{2J+1}}Y_{JJ+1M}(\theta,\phi)\,. \tag{1.133}$$

This vector is in the direction $\hat{\mathbf{r}}$ and is, therefore, referred to as a longitudinal vector spherical harmonic. Following the notation of Akhiezer and Berestetskii (1953), we introduce $Y^{(-1)}_{JM}(\theta,\phi) = \hat{\mathbf{r}}\, Y_{JM}(\theta,\phi)$. The vector $Y_{JJM}(\theta,\phi)$ is orthogonal to $Y^{(-1)}_{JM}(\theta,\phi)$, and is,therefore, transverse. The combination

$$\sqrt{\frac{J+1}{2J+1}}Y_{JJ-1M}(\theta,\phi) + \sqrt{\frac{J}{2J+1}}Y_{JJ+1M}(\theta,\phi).$$

is also orthogonal to $Y^{(-1)}_{JM}(\theta,\phi)$ and gives a second transverse spherical vector. It is easily shown that the three vector spherical harmonics

$$Y^{(-1)}_{JM}(\theta,\phi) = \sqrt{\frac{J}{2J+1}}Y_{JJ-1M}(\theta,\phi) - \sqrt{\frac{J+1}{2J+1}}Y_{JJ+1M}(\theta,\phi) \tag{1.134}$$

$$Y^{(0)}_{JM}(\theta,\phi) = Y_{JJM}(\theta,\phi) \tag{1.135}$$

$$Y^{(1)}_{JM}(\theta,\phi) = \sqrt{\frac{J+1}{2J+1}}Y_{JJ-1M}(\theta,\phi) + \sqrt{\frac{J}{2J+1}}Y_{JJ+1M}(\theta,\phi) \tag{1.136}$$

satisfy the orthonormality relation:

$$\int d\Omega\, Y^{(\lambda)\dagger}_{JM}(\Omega)\, Y^{(\lambda')}_{J'M'}(\Omega) = \delta_{JJ'}\delta_{MM'}\delta_{\lambda\lambda'}\,. \tag{1.137}$$

Inverting the Eqs. (1.134-1.136), one finds

$$Y_{JJ-1M}(\theta,\phi) = \sqrt{\frac{J}{2J+1}}Y^{(-1)}_{JM}(\theta,\phi) + \sqrt{\frac{J+1}{2J+1}}Y^{(1)}_{JM}(\theta,\phi) \tag{1.138}$$

$$Y_{JJM}(\theta,\phi) = Y^{(0)}_{JM}(\theta,\phi) \tag{1.139}$$

$$Y_{JJ+1M}(\theta,\phi) = -\sqrt{\frac{J+1}{2J+1}}Y^{(-1)}_{JM}(\theta,\phi) + \sqrt{\frac{J}{2J+1}}Y^{(1)}_{JM}(\theta,\phi) \tag{1.140}$$

The following three relations may be also be proven without difficulty:

$$Y^{(-1)}_{JM}(\theta,\phi) = \hat{\mathbf{r}}\, Y_{JM}(\theta,\phi), \tag{1.141}$$

$$Y^{(0)}_{JM}(\theta,\phi) = \frac{1}{\sqrt{J(J+1)}}\,\mathbf{L}\, Y_{JM}(\theta,\phi), \tag{1.142}$$

$$Y^{(1)}_{JM}(\theta,\phi) = \frac{r}{\sqrt{J(J+1)}}\,\boldsymbol{\nabla}\, Y_{JM}(\theta,\phi)\,. \tag{1.143}$$

The first of these is just a definition; we leave the proof of the other two as exercises.

Chapter 2

Central-Field Schrödinger Equation

We begin the present discussion with a review of the Schrödinger equation for a single electron in a central potential $V(r)$. First, we decompose the Schrödinger wave function in spherical coordinates and set up the equation governing the radial wave function. Following this, we consider analytical solutions to the radial Schrödinger equation for the special case of a Coulomb potential. The analytical solutions provide a guide for our later numerical analysis. This review of basic quantum mechanics is followed by a discussion of the numerical solution to the radial Schrödinger equation.

The single-electron Schrödinger equation is used to describe the electronic states of an atom in the independent-particle approximation, a simple approximation for a many-particle system in which each electron is assumed to move independently in a potential that accounts for the nuclear field and the field of the remaining electrons. There are various methods for determining an approximate potential. Among these are the Thomas-Fermi theory and the Hartree-Fock theory, both of which will be taken up later. In the following section, we assume that an appropriate central potential has been given and we concentrate on solving the resulting single-particle Schrödinger equation.

2.1 Radial Schrödinger Equation

First, we review the separation in spherical coordinates of the Schrödinger equation for an electron moving in a central potential $V(r)$. We assume that $V(r) = V_{\rm nuc}(r) + U(r)$ is the sum of a nuclear potential

$$V_{\rm nuc}(r) = -\frac{Ze^2}{4\pi\epsilon_0}\frac{1}{r} \ ,$$

and an average potential $U(r)$ approximating the electron-electron interaction.

We let $\psi(\mathbf{r})$ designate the single-particle wave function. In the sequel, we refer to this wave function as an *orbital* to distinguish it from a many-particle wave function. The orbital $\psi(\mathbf{r})$ satisfies the Schrödinger equation

$$h\psi = E\psi \,, \tag{2.1}$$

where the Hamiltonian h is given by

$$h = \frac{p^2}{2m} + V(r) \,. \tag{2.2}$$

In Eq.(2.2), $\mathbf{p} = -i\hbar\boldsymbol{\nabla}$ is the momentum operator and m is the electron's mass. The Schrödinger equation, when expressed in spherical coordinates, (r, θ, ϕ), becomes

$$\begin{aligned} &\frac{1}{r^2}\frac{\partial}{\partial r}\left(r^2\frac{\partial\psi}{\partial r}\right) + \frac{1}{r^2\sin\theta}\frac{\partial}{\partial\theta}\left(\sin\theta\frac{\partial\psi}{\partial\theta}\right) \\ &+\frac{1}{r^2\sin^2\theta}\frac{\partial^2\psi}{\partial\phi^2} + \frac{2m}{\hbar^2}\left(E - V(r)\right)\psi = 0 \,. \end{aligned} \tag{2.3}$$

We seek a solution $\psi(r, \theta, \phi)$ that can be expressed as a product of a function P of r only, and a function Y of the angles θ and ϕ:

$$\psi(\mathbf{r}) = \frac{1}{r}P(r)\,Y(\theta, \phi) \,. \tag{2.4}$$

Substituting this *ansatz* into Eq.(2.3), we obtain the following pair of equations for the functions P and Y

$$\frac{1}{\sin\theta}\frac{\partial}{\partial\theta}\left(\sin\theta\frac{\partial Y}{\partial\theta}\right) + \frac{1}{\sin^2\theta}\frac{\partial^2 Y}{\partial\phi^2} + \lambda Y = 0 \,, \tag{2.5}$$

$$\frac{d^2P}{dr^2} + \frac{2m}{\hbar^2}\left(E - V(r) - \frac{\lambda\hbar^2}{2mr^2}\right)P = 0 \,, \tag{2.6}$$

where λ is an arbitrary separation constant.

If we set $\lambda = \ell(\ell+1)$, where $\ell = 0,\ 1,\ 2,\ \cdots$ is an integer, then the solutions to Eq.(2.5) that are finite and single valued for all angles are the spherical harmonics $Y_{\ell m}(\theta, \phi)$.

The normalization condition for the wave function $\psi(\mathbf{r})$ is

$$\int d^3r\psi^\dagger(\mathbf{r})\psi(\mathbf{r}) = 1 \,, \tag{2.7}$$

which leads to normalization condition

$$\int_0^\infty dr\, P^2(r) = 1 \,, \tag{2.8}$$

for the radial function $P(r)$.

The expectation value $\langle O \rangle$ of an operator O in the state ψ is given by

$$\langle O \rangle = \int d^3 r \psi^\dagger(\mathbf{r}) O \psi(\mathbf{r}) \,. \tag{2.9}$$

In the state described by $\psi(\mathbf{r}) = \frac{P(r)}{r} Y_{\ell m}(\theta, \phi)$, we have

$$\langle L^2 \rangle = \ell(\ell+1)\hbar^2 \,, \tag{2.10}$$
$$\langle L_z \rangle = m\hbar \,. \tag{2.11}$$

2.2 Coulomb Wave Functions

The basic equation for our subsequent numerical studies is the radial Schrödinger equation (2.6) with the separation constant $\lambda = \ell(\ell+1)$:

$$\frac{d^2 P}{dr^2} + \frac{2m}{\hbar^2}\left(E - V(r) - \frac{\ell(\ell+1)\hbar^2}{2mr^2}\right) P = 0 \,. \tag{2.12}$$

We start our discussion of this equation by considering the special case $V(r) = V_{\rm nuc}(r)$.

Atomic Units: Before we start our analysis, it is convenient to introduce atomic units in order to rid the equation of unnecessary physical constants. Atomic units are defined by requiring that the electron's mass m, the electron's charge $|e|/\sqrt{4\pi\epsilon_0}$, and Planck's constant $\hbar$, all have the value 1. The atomic unit of length is the Bohr radius, $a_0 = 4\pi\epsilon_0\hbar^2/me^2 = 0.529177\ldots$ Å, and the atomic unit of energy is $me^4/(4\pi\epsilon_0\hbar)^2 = 27.2114\ldots$ eV. Units for other quantities can be readily worked out from these basic few. For example, the atomic unit of velocity is $c\alpha$, where c is the speed of light and α is Sommerfeld's fine structure constant: $\alpha = e^2/4\pi\epsilon_0\hbar c = 1/137.0359895\ldots$.

In atomic units, Eq.(2.12) becomes

$$\frac{d^2 P}{dr^2} + 2\left(E + \frac{Z}{r} - \frac{\ell(\ell+1)}{2r^2}\right) P = 0 \,. \tag{2.13}$$

We seek solutions to the radial Schrödinger equation (2.13) that satisfy the normalization condition (2.8). Such solutions exist only for certain discrete values of the energy, $E = E_{n\ell}$, the energy eigenvalues. Our problem is to determine these energy eigenvalues and the associated eigenfunctions, $P_{n\ell}(r)$. If we have two eigenfunctions, $P_{n\ell}(r)$ and $P_{m\ell}(r)$, belonging to the same angular momentum quantum number ℓ but to distinct eigenvalues, $E_{m\ell} \neq E_{n\ell}$, then it follows from Eq.(2.13) that

$$\int_0^\infty dr P_{n\ell}(r) P_{m\ell}(r) = 0 \,. \tag{2.14}$$

Near $r = 0$, solutions to Eq.(2.13) take on one of the following limiting forms:

$$P(r) \to \begin{cases} r^{\ell+1} & \text{regular at the origin, or} \\ r^{-\ell} & \text{irregular at the origin} \end{cases} . \tag{2.15}$$

Since we seek normalizable solutions, we must require that our solutions be of the first type, regular at the origin. The desired solution grows as $r^{\ell+1}$ as r moves outward from the origin while the complementary solution decreases as $r^{-\ell}$ as r increases.

Since the potential vanishes as $r \to \infty$, it follows that

$$P(r) \to \begin{cases} e^{-\lambda r} & \text{regular at infinity, or} \\ e^{\lambda r} & \text{irregular at infinity} \end{cases} , \tag{2.16}$$

where $\lambda = \sqrt{-2E}$. Again, the normalizability constraint (2.8) forces us to seek solutions of the first type, regular at infinity. Substituting

$$P(r) = r^{\ell+1} e^{-\lambda r} F(r) \tag{2.17}$$

into Eq.(2.13), we find that $F(x)$ satisfies Kummer's equation

$$x\frac{d^2F}{dx^2} + (b - x)\frac{dF}{dx} - aF = 0 , \tag{2.18}$$

where $x = 2\lambda r$, $a = \ell+1-Z/\lambda$, and $b = 2(\ell+1)$. The solutions to Eq.(2.18) that are regular at the origin are the Confluent Hypergeometric functions (Magnus and Oberhettinger, 1949, chap. VI):

$$\begin{aligned} F(a, b, x) &= 1 + \frac{a}{b}x + \frac{a(a+1)}{b(b+1)}\frac{x^2}{2!} + \frac{a(a+1)(a+2)}{b(b+1)(b+2)}\frac{x^3}{3!} + \cdots \\ &+ \frac{a(a+1)\cdots(a+k-1)}{b(b+1)\cdots(b+k-1)}\frac{x^k}{k!} + \cdots . \end{aligned} \tag{2.19}$$

This series has the asymptotic behavior

$$F(a, b, x) \to \frac{\Gamma(b)}{\Gamma(a)}\, e^x x^{a-b}[1 + O(|x|^{-1})] , \tag{2.20}$$

for large $|x|$. The resulting radial wave function, therefore, grows exponentially unless the coefficient of the exponential in Eq.(2.20) vanishes. Since $\Gamma(b) \neq 0$, we must require $\Gamma(a) = \infty$ to obtain normalizable solutions. The function $\Gamma(a) = \infty$ when a vanishes or when a is a negative integer. Thus, normalizable wave functions are only possible when $a = -n_r$ with $n_r = 0, 1, 2, \cdots$. The quantity n_r is called the radial quantum number. With $a = -n_r$, the Confluent Hypergeometric function in Eq.(2.19) reduces to a polynomial of degree n_r. The integer n_r equals the number of nodes (zeros) of the radial wave function for $r > 0$. From $a = \ell + 1 - Z/\lambda$, it follows that

$$\lambda = \lambda_n = \frac{Z}{n_r + \ell + 1} = \frac{Z}{n} ,$$

with $n = n_r + \ell + 1$. The positive integer n is called the principal quantum number. The relation $\lambda = \sqrt{-2E}$ leads immediately to the energy eigenvalue equation

$$E = E_n = -\frac{\lambda_n^2}{2} = -\frac{Z^2}{2n^2} \, . \tag{2.21}$$

There are n distinct radial wave functions corresponding to E_n. These are the functions $P_{n\ell}(r)$ with $\ell = 0, 1, \cdots, n-1$. The radial function is, therefore, given by

$$P_{n\ell}(r) = N_{n\ell} \, (2Zr/n)^{\ell+1} e^{-Zr/n} F(-n+\ell+1, 2\ell+2, 2Zr/n) \, , \tag{2.22}$$

where $N_{n\ell}$ is a normalization constant. This constant is determined by requiring

$$N_{n\ell}^2 \int_0^\infty dr \, (2Zr/n)^{2\ell+2} e^{-2Zr/n} F^2(-n+\ell+1, 2\ell+2, 2Zr/n) = 1 \, . \tag{2.23}$$

This integral can be evaluated analytically to give

$$N_{n\ell} = \frac{1}{n(2\ell+1)!} \sqrt{\frac{Z(n+\ell)!}{(n-\ell-1)!}} \, . \tag{2.24}$$

The radial functions $P_{n\ell}(r)$ for the lowest few states are found to be:

$$P_{10}(r) = 2Z^{3/2} \, r e^{-Zr} \, , \tag{2.25}$$

$$P_{20}(r) = \frac{1}{\sqrt{2}} Z^{3/2} \, r e^{-Zr/2} \left(1 - \frac{1}{2} Zr\right) \, , \tag{2.26}$$

$$P_{21}(r) = \frac{1}{2\sqrt{6}} Z^{5/2} \, r^2 e^{-Zr/2} \, , \tag{2.27}$$

$$P_{30}(r) = \frac{2}{3\sqrt{3}} Z^{3/2} \, r e^{-Zr/3} \left(1 - \frac{2}{3} Zr + \frac{2}{27} Z^2 r^2\right) \, , \tag{2.28}$$

$$P_{31}(r) = \frac{8}{27\sqrt{6}} Z^{5/2} \, r^2 e^{-Zr/3} \left(1 - \frac{1}{6} Zr\right) \, , \tag{2.29}$$

$$P_{32}(r) = \frac{4}{81\sqrt{30}} Z^{7/2} \, r^3 e^{-Zr/3} . \tag{2.30}$$

In Fig. 2.1, we plot the Coulomb wave functions for the $n = 1$, 2 and 3 states of hydrogen, $Z = 1$. In this figure, the angular momentum states are labeled using spectroscopic notation: states with $l = 0, 1, 2, 3, 4, \cdots$ are given the labels $s, p, d, f, g, \cdots$, respectively. It should be noted that the radial functions with the lowest value of l for a given n, have no nodes for $r > 0$, corresponding to the fact that $n_r = 0$ for such states. The number of nodes is seen to increase in direct proportion to n for a fixed value of l. The outermost maximum of each wave function is seen to occur at increasing distances from the origin as n increases.

The expectation values of powers of r, given by

$$\langle r^\nu \rangle_{n\ell} = N_{n\ell}^2 \left(\frac{n}{2Z}\right)^{\nu+1} \int_0^\infty dx \, x^{2\ell+2+\nu} e^{-x} F^2(-n+\ell+1, 2\ell+2, x) \, , \tag{2.31}$$

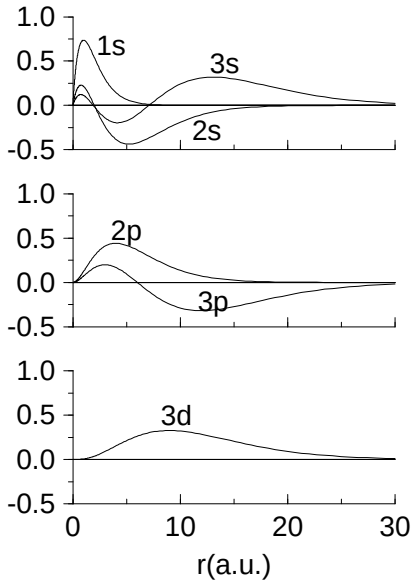

Figure 2.1: Hydrogenic Coulomb wave functions for states with $n = 1$, 2 and 3.

can be evaluated analytically. One finds:

$$\langle r^2\rangle_{n\ell} = \frac{n^2}{2Z^2}[5n^2 + 1 - 3\ell(\ell+1)]\,, \tag{2.32}$$

$$\langle r\rangle_{n\ell} = \frac{1}{2Z}[3n^2 - \ell(\ell+1)]\,, \tag{2.33}$$

$$\left\langle \frac{1}{r} \right\rangle_{n\ell} = \frac{Z}{n^2}\,, \tag{2.34}$$

$$\left\langle \frac{1}{r^2} \right\rangle_{n\ell} = \frac{Z^2}{n^3(\ell+1/2)}\,, \tag{2.35}$$

$$\left\langle \frac{1}{r^3} \right\rangle_{n\ell} = \frac{Z^3}{n^3(\ell+1)(\ell+1/2)\ell}\,, \quad \ell > 0\,, \tag{2.36}$$

$$\left\langle \frac{1}{r^4} \right\rangle_{n\ell} = \frac{Z^4[3n^2 - \ell(\ell+1)]}{2n^5(\ell+3/2)(\ell+1)(\ell+1/2)\ell(\ell-1/2)}\,, \quad \ell > 0\,. \tag{2.37}$$

These formulas follow from the expression for the expectation value of a power of r given by Bethe and Salpeter (1957):

$$\langle r^\nu\rangle = \left(\frac{n}{2Z}\right)^\nu \frac{J^{(\nu+1)}_{n+l,2l+1}}{J^{(1)}_{n+l,2l+1}}\,, \tag{2.38}$$

where, for $\sigma \geq 0$,

$$J^{(\sigma)}_{\lambda,\mu} = (-1)^{\sigma} \frac{\lambda!\,\sigma!}{(\lambda-\mu)!} \sum_{\beta=0}^{\sigma} (-1)^{\beta} \begin{pmatrix} \sigma \\ \beta \end{pmatrix} \begin{pmatrix} \lambda+\beta \\ \sigma \end{pmatrix} \begin{pmatrix} \lambda+\beta-\mu \\ \sigma \end{pmatrix}, \quad (2.39)$$

and for $\sigma = -(s+1) \leq -1$,

$$J^{(\sigma)}_{\lambda,\mu} = \frac{\lambda!}{(\lambda-\mu)!\,(s+1)!} \sum_{\gamma=0}^{s} (-1)^{s-\gamma} \frac{\begin{pmatrix} s \\ \gamma \end{pmatrix} \begin{pmatrix} \lambda-\mu+\gamma \\ s \end{pmatrix}}{\begin{pmatrix} \mu+s-\gamma \\ s+1 \end{pmatrix}}. \quad (2.40)$$

In Eqs. (2.39-2.40),

$$\begin{pmatrix} a \\ b \end{pmatrix} = \frac{a!\,(b-a)!}{b!} \quad (2.41)$$

designates the binomial coefficient.

2.3 Numerical Solution to the Radial Equation

Since analytical solutions to the radial Schrödinger equation are known for only a few central potentials, such as the Coulomb potential or the harmonic oscillator potential, it is necessary to resort to numerical methods to obtain solutions in practical cases.

We use finite difference techniques to find numerical solutions to the radial equation on a finite grid covering the region $r = 0$ to a *practical infinity*, a_∞, a point determined by requiring that $P(r)$ be negligible for $r > a_\infty$.

Near the origin, there are two solutions to the radial Schrödinger equation, the desired solution which behaves as $r^{\ell+1}$, and an irregular solution, referred to as the complementary solution, which diverges as $r^{-\ell}$ as $r \to 0$. Numerical errors near $r = 0$ introduce small admixtures of the complementary solution into the solution being sought. Integrating outward from the origin keeps such errors under control, since the complementary solution decreases in magnitude as r increases. In a similar way, in the asymptotic region, we integrate inward from a_∞ toward $r = 0$ to insure that errors from small admixtures of the complementary solution, which behaves as $e^{\lambda r}$ for large r, decrease as the integration proceeds from point to point. In summary, one expects the point-by-point numerical integration outward from $r = 0$ and inward from $r = \infty$ to yield solutions that are stable against small numerical errors.

The general procedure used to solve Eq.(2.13) is to integrate outward from the origin, using an appropriate point-by-point scheme, starting with solutions that are regular at the origin. The integration is continued to the outer *classical turning point*, the point beyond which classical motion in the potential $V(r) + \ell(\ell+1)/2r^2$ is impossible. In the region beyond the classical turning point, the equation is integrated inward, again using a point-by-point integration scheme, starting from $r = a_\infty$ with an approximate solution obtained from an asymptotic

series. Typically, we choose a_∞ so that the dimensionless quantity $\lambda r \approx 40$ for the first few steps of the inward integration. With this choice, $P(r)$ is roughly 10^{-12} of its maximum value near a_∞. The solutions from the inward and outward integrations are matched at the classical turning point. The energy is then adjusted until the derivative of $P(r)$ is continuous at the matching point.

The resulting function $P(r)$ is an eigenfunction and the corresponding energy E is its eigenvalue. To find a particular eigenfunction, we make use of the fact that different eigenfunctions have different numbers of nodes for $r > 0$. For a given value of ℓ, the lowest energy eigenfunction has no node, the next higher energy eigenfunction has one node, and so on. We first make a preliminary adjustment of the energy to obtain the desired number of nodes and then make a final fine adjustment to match the slope of the wave function at the classical turning point.

The radial wave function increases rapidly at small values of r then oscillates in the classically allowed region and gradually decreases beyond the classical turning point. To accommodate this behavior, it is convenient to adopt a nonuniform integration grid, more finely spaced at small r than at large r. Although there are many possible choices of grid, one that has proven to be both convenient and flexible is

$$\begin{array}{ll} r[i] = r_0\,(e^{t[i]} - 1)\,, & \text{where} \\ t[i] = (i-1)h\,, & i = 1, 2, \ldots, N\,. \end{array} \tag{2.42}$$

We typically choose $r_0 = 0.0005$ a.u., $h = 0.02 - 0.03$, and extend the grid to $N = 500$ points. These choices permit the radial Schrödinger equation to be integrated with high accuracy (parts in 10^{12}) for energies as low as 0.01 a.u..

We rewrite the radial Schrödinger equation as the equivalent pair of first order radial differential equations:

$$\frac{dP}{dr} = Q(r), \tag{2.43}$$

$$\frac{dQ}{dr} = -2\left(E - V(r) - \frac{\ell(\ell+1)}{2r^2}\right)P(r)\,. \tag{2.44}$$

On the uniformly-spaced t-grid, this pair of equations can be expressed as a single, two-component equation

$$\frac{dy}{dt} = f(y,t)\,, \tag{2.45}$$

where y is the array,

$$y(t) = \begin{bmatrix} P(r(t)) \\ Q(r(t)) \end{bmatrix}. \tag{2.46}$$

The two components of $f(y,t)$ are given by

$$f(y,t) = \frac{dr}{dt}\begin{bmatrix} Q(r(t)) \\ -2\left(E - V(r) - \dfrac{\ell(\ell+1)}{2r^2}\right)P(r(t)) \end{bmatrix}. \tag{2.47}$$

We can formally integrate Eq.(2.45) from one grid point, $t[n]$, to the next, $t[n+1]$, giving

$$y[n+1] = y[n] + \int_{t[n]}^{t[n+1]} f(y(t), t)\, dt\,. \tag{2.48}$$

2.3.1 Adams Method (ADAMS)

To derive the formula used in practice to carry out the numerical integration in Eq.(2.48), we introduce some notation from finite difference theory. More complete discussions of the calculus of difference operators can be found in textbooks on numerical methods such as Dahlberg and Björck (1974, chap. 7). Let the function $f(x)$ be given on a uniform grid and let $f[n] = f(x[n])$ be the value of $f(x)$ at the n^{th} grid point. We designate the backward difference operator by ∇:

$$\nabla f[n] = f[n] - f[n-1]\,. \tag{2.49}$$

Using this notation, $(1-\nabla)f_[n] = f[n-1]$. Inverting this equation, we may write,

$$\begin{array}{rcl} f[n+1] & = & (1-\nabla)^{-1} f[n], \\ f[n+2] & = & (1-\nabla)^{-2} f[n], \\ & \vdots & \end{array} \tag{2.50}$$

or more generally,

$$f[n+x] = (1-\nabla)^{-x} f[n]. \tag{2.51}$$

In these expressions, it is understood that the operators in parentheses are to be expanded in a power series in ∇, and that Eq.(2.49) is to be used iteratively to determine ∇^k .

Equation(2.51) is a general interpolation formula for equally spaced points. Expanding out a few terms, we obtain from Eq.(2.51)

$$\begin{array}{rcl} f[n+x] & = & \left(1 + \dfrac{x}{1!}\nabla + \dfrac{x(x+1)}{2!}\nabla^2 + \dfrac{x(x+1)(x+2)}{3!}\nabla^3 + \cdots\right) f[n]\,, \\ & = & \left(1 + x + \dfrac{x(x+1)}{2!} + \dfrac{x(x+1)(x+2)}{3!} + \cdots\right) f[n] \\ & - & \left(x + \dfrac{2x(x+1)}{2!} + \dfrac{3x(x+1)(x+2)}{3!} + \cdots\right) f[n-1] \\ & + & \left(\dfrac{x(x+1)}{2!} + \dfrac{3x(x+1)(x+2)}{3!} + \cdots\right) f[n-2] \\ & - & \left(\dfrac{x(x+1)(x+2)}{3!} + \cdots\right) f[n-3] + \cdots\,. \end{array} \tag{2.52}$$

Truncating this formula at the k^{th} term leads to a polynomial of degree k in x that passes through the points $f[n], f[n-1], \cdots, f[n-k]$, as x takes on the values $0, -1, -2, \cdots, -k$, respectively. We may use the interpolation formula

(2.51) to carry out the integration in Eq.(2.48), analytically leading to the result: (Adams-Bashforth)

$$\begin{aligned} y[n+1] &= y[n] - \frac{h\nabla}{(1-\nabla)\log(1-\nabla)} f[n] \,, \\ &= y[n] + h(1 + \frac{1}{2}\nabla + \frac{5}{12}\nabla^2 + \frac{9}{24}\nabla^3 + \cdots) f[n] \,. \end{aligned} \tag{2.53}$$

This equation may be rewritten, using the identity $(1-\nabla)^{-1} f[n] = f[n+1]$, as an interpolation formula: (Adams-Moulton)

$$\begin{aligned} y[n+1] &= y[n] - \frac{h\nabla}{\log(1-\nabla)} f[n+1] \,, \\ &= y[n] + h(1 - \frac{1}{2}\nabla - \frac{1}{12}\nabla^2 - \frac{1}{24}\nabla^3 + \cdots) f[n+1] \,. \end{aligned} \tag{2.54}$$

Keeping terms only to third-order and using Eqs.(2.53-2.54), we obtain the four-point (fifth-order) predict-correct formulas

$$\begin{aligned} y[n+1] &= y[n] + \frac{h}{24}(55f[n] - 59f[n-1] + 37f[n-2] - 9f[n-3]) \\ &\quad + \frac{251}{720} h^5 y^{(5)}[n] \,, \end{aligned} \tag{2.55}$$

$$\begin{aligned} y[n+1] &= y[n] + \frac{h}{24}(9f[n+1] + 19f[n] - 5f[n-1] + f[n-2]) \\ &\quad - \frac{19}{720} h^5 y^{(5)}[n] \,. \end{aligned} \tag{2.56}$$

The error terms in Eqs.(2.55-2.56) are obtained by evaluating the first neglected term in Eqs.(2.53-2.54) using the approximation

$$\nabla^k f[n] \approx h^k \left(\frac{d^k f}{dt^k} \right)[n] = h^k \left(\frac{d^{k+1} y}{dt^{k+1}} \right)[n] \,. \tag{2.57}$$

The magnitude of the error in Eq.(2.56) is smaller (by an order of magnitude) than that in Eq.(2.55), since interpolation is used in Eq.(2.56), while extrapolation is used in Eq.(2.55). Often, the less accurate extrapolation formula (2.55) is used to advance from point $t[n]$ (where $y[n]$, $f[n]$, $f[n-1]$, $f[n-2]$, and $f[n-3]$ are known) to the point $t[n+1]$. Using the predicted value of $y[n+1]$, one evaluates $f[n+1]$. The resulting value of $f[n+1]$ can then be used in the interpolation formula (2.56) to give a more accurate value for $y[n+1]$.

In our application of Adams method, we make use of the linearity of the differential equations (2.45) to avoid the extrapolation step altogether. To show how this is done, we first write the $k+1$ point Adams-Moulton interpolation formula from Eq.(2.54) in the form,

$$y[n+1] = y[n] + \frac{h}{D} \sum_{j=1}^{k+1} a[j]\, f[n-k+j] \,. \tag{2.58}$$

Table 2.1: Adams-Moulton integration coefficients

$a[1]$	$a[2]$	$a[3]$	$a[4]$	$a[5]$	$a[6]$	D	error
1	1					2	-1/12
-1	8	5				12	-1/24
1	-5	19	9			24	-19/720
-19	106	-264	646	251		720	-3/160
27	-173	482	-798	1427	475	1440	-863/60480

The coefficients $a[j]$ for 2-point to 7-point Adams-Moulton integration formulas are given in Table 2.1, along with the divisors D used in Eq.(2.58), and the coefficient of $h^{k+2}y^{(k+2)}[n]$ in the expression for the truncation error.

Setting $f(y,t) = G(t)y$, where G is a 2×2 matrix, we can take the $k+1$ term from the sum to the left-hand side of Eq.(2.58) to give

$$\left(1 - \frac{ha[k+1]}{D} G[n+1]\right) y[n+1] = y[n] + \frac{h}{D} \sum_{j=1}^{k} a[j]\, f[n-k+j]\,. \qquad (2.59)$$

From Eq.(2.47), it follows that G is an off-diagonal matrix of the form

$$G = \begin{pmatrix} 0 & b \\ c & 0 \end{pmatrix}\,, \qquad (2.60)$$

for the special case of the radial Schrödinger equation. The coefficients $b(t)$ and $c(t)$ can be read from Eq.(2.47):

$$b(t) = \tfrac{dr}{dt} \qquad c(t) = -2\tfrac{dr}{dt}\left(E - V(r) - \tfrac{\ell(\ell+1)}{2r^2}\right). \qquad (2.61)$$

The matrix

$$M[n+1] = 1 - \frac{ha[k+1]}{D}\, G[n+1]$$

on the left-hand side of Eq.(2.59) is readily inverted to give

$$M^{-1}[n+1] = \frac{1}{\Delta[n+1]} \begin{pmatrix} 1 & \lambda b[n+1] \\ \lambda c[n+1] & 1 \end{pmatrix}\,, \qquad (2.63)$$

where

$$\begin{aligned} \Delta[n+1] &= 1 - \lambda^2 b[n+1]c[n+1]\,, \\ \lambda &= \frac{ha[k+1]}{D}\,. \end{aligned}$$

Equation(2.59) is solved to give

$$y[n+1] = M^{-1}[n+1] \left(y[n] + \frac{h}{D} \sum_{j=1}^{k} a[j]\, f[n-k+j] \right)\,. \qquad (2.64)$$

This is the basic algorithm used to advance the solution to the radial Schrödinger equation from one point to the next. Using this equation, we achieve the accuracy of the predict-correct method without the necessity of separate predict and correct steps. To start the integration using Eq.(2.64), we must give initial values of the two-component function $f(t)$ at the points $1, 2, \cdots, k$. The subroutine ADAMS is designed to implement Eq.(2.64) for values of k ranging from 0 to 8.

2.3.2 Starting the Outward Integration (OUTSCH)

The k initial values of $y[j]$ required to start the outward integration using the $k+1$ point Adams method are obtained using a scheme based on Lagrangian differentiation formulas. These formulas are easily obtained from the basic finite difference expression for interpolation, Eq.(2.51). Differentiating this expression, we find

$$\left(\frac{dy}{dx}\right)[n-j] = -\log(1-\nabla)\,(1-\nabla)^j\, y[n]\,. \tag{2.65}$$

If Eq.(2.65) is expanded to k terms in a power series in ∇, and evaluated at the $k+1$ points, $j = 0, 1, 2, \cdots, k$, we obtain the $k+1$ point Lagrangian differentiation formulas. For example, with $k = 3$ and $n = 3$ we obtain the formulas:

$$\left(\frac{dy}{dt}\right)[0] = \frac{1}{6h}\left(-11y[0] + 18y[1] - 9y[2] + 2y[3]\right) - \frac{1}{4}h^3y^{(4)} \tag{2.66}$$

$$\left(\frac{dy}{dt}\right)[1] = \frac{1}{6h}\left(-2y[0] - 3y[1] + 6y[2] - y[3]\right) + \frac{1}{12}h^3y^{(4)} \tag{2.67}$$

$$\left(\frac{dy}{dt}\right)[2] = \frac{1}{6h}\left(y[0] - 6y[1] + 3y[2] + 2y[3]\right) - \frac{1}{12}h^3y^{(4)} \tag{2.68}$$

$$\left(\frac{dy}{dt}\right)[3] = \frac{1}{6h}\left(-2y[0] + 9y[1] - 18y[2] + 11y[3]\right) + \frac{1}{4}h^3y^{(4)}\,. \tag{2.69}$$

The error terms in Eqs.(2.66-2.69) are found by retaining the next higher-order differences in the expansion of Eq.(2.65) and using the approximation (2.57). Ignoring the error terms, we write the general $k+1$ point Lagrangian differentiation formula as

$$\left(\frac{dy}{dt}\right)[i] = \sum_{j=0}^{k} m[ij]\; y[j]\,, \tag{2.70}$$

where $i = 0, 1, \cdots, k$, and where the coefficients $m[ij]$ are determined from Eq.(2.65).

To find the values of $y[j]$ at the first few points along the radial grid, first we use the differentiation formulas (2.70) to eliminate the derivative terms from the differential equations at the points $j = 1, \cdots, k$, then we solve the resulting linear algebraic equations using standard methods.

Factoring $r^{\ell+1}$ from the radial wave function $P(r)$,

$$P(r) = r^{\ell+1}\, p(r)\,, \tag{2.71}$$

we may write the radial Schrödinger equation as

$$\frac{dp}{dt} = \frac{dr}{dt}\, q(t)\,, \tag{2.72}$$

$$\frac{dq}{dt} = -2\frac{dr}{dt}\left[(E - V(r))p(t) + \left(\frac{\ell+1}{r}\right) q(t)\right]\,. \tag{2.73}$$

Substituting for the derivatives from Eq.(2.70), we obtain the $2k \times 2k$ system of linear equations

$$\sum_{j=1}^{k} m[ij]\; p[j] - b[i]\; q[i] = -m[i0]\; p[0]\,, \tag{2.74}$$

$$\sum_{j=1}^{k} m[ij]\; q[j] - c[i]\; p[i] - d[i]\; q[i] = -m[i0]\; q[0]\,, \tag{2.75}$$

where

$$\begin{aligned} b(t) &= \frac{dr}{dt}\,, \\ c(t) &= -2\frac{dr}{dt}\left[E - V(r)\right]\,, \\ d(t) &= -2\frac{dr}{dt}\left(\frac{\ell+1}{r}\right)\,, \end{aligned} \tag{2.76}$$

and where $p[0]$ and $q[0]$ are the initial values of $p(t)$ and $q(t)$, respectively. If we assume that as $r \to 0$, the potential $V(r)$ is dominated by the nuclear Coulomb potential,

$$V(r) \to -\frac{Z}{r}\,, \tag{2.77}$$

then from Eq.(2.73) it follows that the initial values must be in the ratio

$$\frac{q[0]}{p[0]} = -\frac{Z}{\ell+1}\,. \tag{2.78}$$

We choose $p[0] = 1$ arbitrarily and determine $q[0]$ from Eq.(2.78).

The $2k \times 2k$ system of linear equations (2.74-2.75) are solved using standard methods to give $p[i]$ and $q[i]$ at the points $j = 1, \cdots, k$ along the radial grid. From these values we obtain

$$P[i] = r^{\ell+1}[i]\, p[i] \tag{2.79}$$

$$Q[i] = r^{\ell+1}[i]\left(q[i] + \frac{\ell+1}{r[i]}\, p[i]\right)\,. \tag{2.80}$$

These are the k initial values required to start the outward integration of the radial Schrödinger equation using the $k+1$ point Adams method. The routine OUTSCH implements the method described here to start the outward integration.

There are other ways to determine solutions to the second-order differential equations at the first k grid points. One obvious possibility is to use a power series representation for the radial wave function at small r. This method is not used since we must consider cases where the potential at small r is very different from the Coulomb potential and has no simple analytical structure. Such cases occur when we treat self-consistent fields or nuclear finite-size effects.

Another possibility is to start the outward integration using Runge-Kutta methods. Such methods require evaluation of the potential between the grid points. To obtain such values, for cases where the potential is not known analytically, requires additional interpolation. The present scheme is simple, accurate, and avoids such unnecessary interpolation.

2.3.3 Starting the Inward Integration (INSCH)

To start the inward integration using the $k+1$ point Adams method, we need k values of $P[i]$ and $Q[i]$ in the asymptotic region just preceding the practical infinity. We determine these values using an asymptotic expansion of the Schrödinger wave function. Let us suppose that the potential $V(r)$ in the asymptotic region, $r \approx a_\infty$, takes the limiting form,

$$V(r) \to -\frac{\zeta}{r}\,, \tag{2.81}$$

where ζ is the charge of the ion formed when one electron is removed. The radial Schrödinger equation in this region then becomes

$$\frac{dP}{dr} = Q(r), \tag{2.82}$$

$$\frac{dQ}{dr} = -2\left(E + \frac{\zeta}{r} - \frac{\ell(\ell+1)}{2r^2}\right)P(r)\,. \tag{2.83}$$

We seek an asymptotic expansion of $P(r)$ and $Q(r)$ of the form :

$$P(r) = r^\sigma e^{-\lambda r}\left\{a_0 + \frac{a_1}{r} + \cdots + \frac{a_k}{r^k} + \cdots\right\}\,, \tag{2.84}$$

$$Q(r) = r^\sigma e^{-\lambda r}\left\{b_0 + \frac{b_1}{r} + \cdots + \frac{b_k}{r^k} + \cdots\right\}\,. \tag{2.85}$$

Substituting the expansions (2.84-2.85) into the radial equations (2.82-2.83) and matching the coefficients of the two leading terms, we find that such an expansion is possible only if

$$\lambda = \sqrt{-2E}\,,$$

$$\sigma = \frac{\zeta}{\lambda}\,. \tag{2.86}$$

Using these values for λ and σ, the following recurrence relations for a_k and b_k are obtained by matching the coefficients of r^{-k} in Eqs.(2.82-2.83) :

$$a_k = \frac{\ell(\ell+1)-(\sigma-k)(\sigma-k+1)}{2k\lambda}\, a_{k-1}\,, \tag{2.87}$$

$$b_k = \frac{(\sigma+k)(\sigma-k+1)-\ell(\ell+1)}{2k}\, a_{k-1}\,. \tag{2.88}$$

We set $a_0 = 1$ arbitrarily, $b_0 = -\lambda$, and use Eqs.(2.87-2.88) to generate the coefficients of higher-order terms in the series. Near the practical infinity, the expansion parameter $2\lambda r$ is large (≈ 80), so relatively few terms in the expansion suffice to give highly accurate wave functions in this region. The asymptotic expansion is used to evaluate P_i and Q_i at the final k points on the radial grid. These values are used in turn to start a point-by-point inward integration to the classical turning point using the $k+1$ point Adams method. In the routine INSCH, the asymptotic series is used to obtain the values of $P(r)$ and $Q(r)$ at large r to start the inward integration using Adams method.

2.3.4 Eigenvalue Problem (MASTER)

To solve the eigenvalue problem, we:

1. Guess the energy E.
2. Use the routine OUTSCH to obtain values of the radial wave function at the first k grid points, and continue the integration to the outer classical turning point (a_c) using the routine ADAMS.
3. Use the routine INSCH to obtain the values of the wave function at the last k points on the grid, and continue the inward solution to a_c using the routine ADAMS.
4. Multiply the wave function and its derivative obtained in step 3 by a scale factor chosen to make the wave function for $r < a_c$ from step 2, and that for $r > a_c$ from step 3, continuous at $r = a_c$.

If the energy guessed in step 1 happened to be an energy eigenvalue, then not only the solution, but also its derivative, would be continuous at $r = a_c$. If it were the desired eigenvalue, then the wave function would also have the correct number of radial nodes, $n_r = n - \ell - 1$.

Generally the energy E in step 1 is just an estimate of the eigenvalue, so the numerical values determined by following steps 2 to 4 above give a wave function having an incorrect number of nodes and a discontinuous derivative at a_c. This is illustrated in Fig. 2.2. In the example shown there, we are seeking the $4p$ wave function in a Coulomb potential with $Z = 2$. The corresponding radial wave function should have $n_r = n - l - 1 = 2$ nodes. We start with the guess $E = -0.100$ a.u. for the energy and carry out steps 2 to 4 above. The resulting function, which is represented by the thin solid curve in the figure, has three nodes instead of two and has a discontinuous derivative at $a_c \approx 19$ a.u..

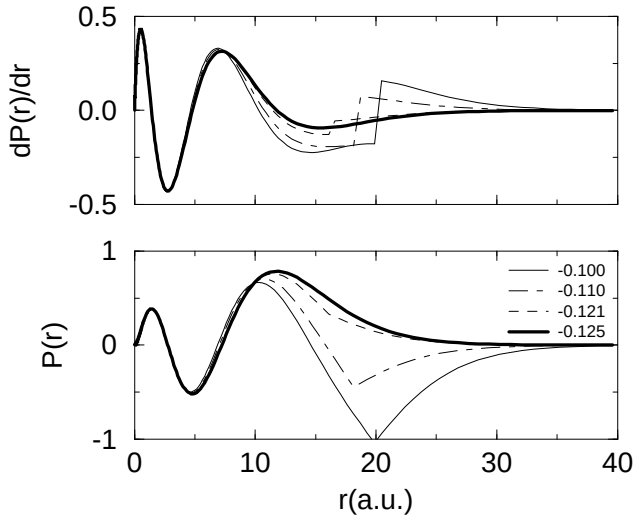

Figure 2.2: The radial wave function for a Coulomb potential with $Z = 2$ is shown at several steps in the iteration procedure leading to the $4p$ eigenstate.

The number of nodes increases with increasing energy. To reduce the number of nodes, we must, therefore, lower the energy. We do this by multiplying E (which is of course negative) by a factor of 1.1. Repeating steps 2 - 4 with $E = -0.110$ a.u., leads to the curve shown in the dot-dashed curve in the figure. The number of nodes remains $n_r = 3$, so we repeat the steps again with $E = 1.1(-0.110) = -0.121$ a.u.. At this energy, the number of nodes $n_r = 2$ is correct, as shown in the dashed curve in Fig. 2.2; however, the derivative of the wave function is still discontinuous at a_c. To achieve a wave function with a continuous derivative, we make further corrections to E using a perturbative approach.

If we let $P_1(r)$ and $Q_1(r)$ represent the radial wave function and its derivative at E_1, respectively, and let $P_2(r)$ and $Q_2(r)$ represent the same two quantities at E_2, then it follows from the radial Schrödinger equation that

$$\frac{d}{dr}(Q_2P_1 - P_2Q_1) = 2(E_1 - E_2)P_1P_2\,. \tag{2.89}$$

From this equation, we find that

$$2(E_1 - E_2)\int_{a_c}^{\infty} P_1\,P_2\,dr \;=\; -(Q_2P_1 - P_2Q_1)^+, \tag{2.90}$$

$$2(E_1 - E_2)\int_{0}^{a_c} P_1\,P_2\,dr \;=\; (Q_2P_1 - P_2Q_1)^-, \tag{2.91}$$

where the superscripts $\pm$ indicate that the quantities in parentheses are to be evaluated just above or just below a_c. These equations are combined to give

$$E_1 - E_2 = \frac{(Q_1^+ - Q_1^-)P_2(a_c) + (Q_2^- - Q_2^+)P_1(a_c)}{2\int_0^\infty P_1\, P_2\, dr}\,. \tag{2.92}$$

Suppose that the derivative Q_1 is discontinuous at a_c. If we demand that Q_2 be continuous at a_c, then the term $Q_2^- - Q_2^+$ in the numerator of (2.92) vanishes. Approximating P_2 by P_1 in this equation, we obtain

$$E_2 \approx E_1 + \frac{(Q_1^- - Q_1^+)P_1(a_c)}{2\int_0^\infty P_1^2\, dr}\,, \tag{2.93}$$

as an approximation for the eigenenergy. We use this approximation iteratively until the discontinuity in $Q(r)$ at $r = a_c$ is reduced to an insignificant level.

The program MASTER is designed to determine the wave function and the corresponding energy eigenvalue for specified values of n and ℓ by iteration. In this program, we construct an energy trap that reduces E (by a factor of 1.1) when there are too many nodes at a given step of the iteration, or increases E (by a factor of 0.9) when there are too few nodes. When the number of nodes is correct, the iteration is continued using Eq.(2.93) iteratively until the discontinuity in $Q(r)$ at $r = a_c$ is reduced to a negligible level. In the routine, we keep track of the least upper bound on the energy E_u (too many nodes) and the greatest lower bound E_l (too few nodes) as the iteration proceeds. If increasing the energy at a particular step of the iteration would lead to $E > E_u$, then we simply replace E by $(E+E_u)/2$, rather than following the above rules. Similarly, if decreasing E would lead to $E < E_l$, then we replace E by $(E + E_l)/2$.

For the example shown in the Fig. 2.2, it required 8 iterations to obtain the energy $E_{4p} = -1/8$ a.u. to 10 significant figures starting from the estimate $E = -.100$ a.u.. The resulting wave function is shown in the heavy solid line in the figure.

It is only necessary to normalize $P(r)$ and $Q(r)$ to obtain the desired radial wave function and its derivative. The normalization integral,

$$N^{-2} = \int_0^\infty P^2(r)dr\,,$$

is evaluated using the routine RINT; a routine based on the trapezoidal rule with endpoint corrections that will be discussed in the following section. As a final step in the routine MASTER, the wave function and its derivative are multiplied by N to give a properly normalized numerical solution to the radial Schrödinger equation.

2.4 Quadrature Rules (RINT)

As described earlier, our radial grid is defined by a nonlinear function $r(t)$, where t is uniformly distributed according to $t = ih,\ i = 0 \cdots n$. We require $r(0) = 0$

and choose n so large that $r(nh)$ is much larger than the atomic radius. We convert radial integrals over r into integrals over the uniform grid t.

$$\int_0^R F(r)dr = \int_0^{mh} F[r(t)]\,\frac{dr}{dt}\,dt$$

where $R = r(mh)$.

There are many methods to evaluate integrals on a uniform grid numerically, including the trapezoidal rule, Simpson's rule, and the various open-form and closed-form Newton-Cotes formulas. The trapezoidal rule

$$\int_0^{mh} f(x)dx = h\left(\frac{1}{2}f_0 + f_1 + \cdots + f_{m-1} + \frac{1}{2}f_m\right) - \frac{h^3 m}{12}f^{(2)}(\xi), \qquad (2.94)$$

has the virtue of simplicity. In the above formula, we designate $f(kh)$ by f_k. The term proportional to $f^{(2)}(\xi)$ is an estimate of the error involved in approximating the integral by the integration rule. The argument ξ of the second-derivative is some point on the interval $[0,\, mh]$. The trapezoidal rule is very efficient; with the exception of the two endpoints, only a summation is required. The principal drawback of this rule is its relatively low accuracy.

Simpson's rule

$$\int_0^{2mh} f(x)dx = \frac{h}{3}\Big(f_0 + 4\,(f_1 + f_3 \cdots + f_{2m-1}) + 2\,(f_2 + f_4 + \cdots f_{2m-2}) + f_{2m}\Big) - \frac{h^5 m}{90}f^{(4)}(\xi) \qquad (2.95)$$

is more accurate than the trapezoidal rule but is less efficient and requires that the number of integration intervals be even. Rules based on higher-order Newton-Cotes formulas, Abramowitz and Stegun (1964), are both more accurate and more complex than the trapezoidal rule or Simpson's rule.

For our purposes, we choose a trapezoidal rule modified by endpoint corrections. This type of quadrature formula maintains the simplicity of the trapezoidal rule, but can be made systematically more accurate. The structure of the modified trapezoidal rule is

$$\int_0^{mh} f(x)dx = h\Big(a_1(f_0 + f_m) + a_2(f_1 + f_{m-1}) + \cdots + a_k(f_{k-1} + f_{m-k+1}) + f_k + f_{k+1} \cdots + f_{m-k}\Big) + \epsilon_k(\xi), \qquad (2.96)$$

where $\epsilon_k(\xi)$ is an error function evaluated at some point $x = \xi$ on the integration interval. The endpoint coefficients $a_1,\, a_2,\, \cdots a_k$, are chosen to insure that the integration is exact for polynomials of degree $(0,\, 1,\, \cdots,\, k-1)$. The modified trapezoidal rule is also exact for polynomials of degree k, for odd values of k only. There is, consequently, no gain in accuracy for a rule based on an even value of k compared with one based on the next lower odd value. We therefore concentrate on rules of form (2.96) with odd values of k.

It is relatively simple to determine the weights a_i. To this end we examine the difference Δ_l between the value given by the integration rule for a polynomial $f(x) = x^l$ and the exact value of the integral $(mh)^{l+1}/(l+1)$. Let us consider the example $k = 3$.

$$\begin{aligned}
\Delta_0 &= h\,(2a_1 + 2a_2 + 2a_3 - 5) \\
\Delta_1 &= h^2 \left(a_1 + a_2 + a_3 - \frac{5}{2}\right) m \\
\Delta_2 &= h^3 \left[2a_2 + 8a_3 - 10 + \left(-2a_2 - 4a_3 + \frac{37}{6}\right) m + \left(a_1 + a_2 + a_3 - \frac{5}{2}\right) m^2\right] \\
\Delta_3 &= h^4 \left[(3a_2 + 12a_3 - 15)\, m + \left(-3a_2 - 6a_3 + \frac{37}{4}\right) m^2 \right. \\
&\qquad \left. + \left(a_1 + a_2 + a_3 - \frac{5}{2}\right) m^3\right] \qquad (2.97)
\end{aligned}$$

It can be seen that Δ_l is a polynomial of degree m^l; the lowest power of m in Δ_l is m for odd l and 1 for even l. The coefficient of m^i in Δ_l is proportional to the coefficient of m^{i-1} in Δ_{l-1}. Therefore, if Δ_{k-1} vanishes, then all $\Delta_l,\ l = 0 \cdots k-2$ automatically vanish. Thus, for odd values of k we simply require that the k coefficients of $m^l,\ l = 0 \cdots k-1$ in the expression for Δ_{k-1} vanish. This leads to a system of k equations in k unknowns. For our example $k = 3$ we have on requiring coefficients of m^l in Δ_2 to vanish

$$\begin{aligned}
a_1 + a_2 + a_3 &= \frac{5}{2} \\
2a_2 + 4a_3 &= \frac{37}{6} \\
2a_2 + 8a_3 &= 10
\end{aligned}$$

The solution to these equations is

$$(a_2,\, a_2,\, a_3) = \left(\frac{9}{24},\, \frac{28}{24},\, \frac{23}{24}\right)$$

It should ne noted that if Δ_{k-1} vanishes, Δ_k will also vanish! Values of a_l, $l = 1 \cdots k$ represented as ratios $a_l = c_l/d$ with a common denominator, are tabulated for $k = 1,\, 3,\, 5,\, 7$ in Table 2.2. It should be noted that $k = 1$ leads precisely to the trapezoidal rule.

The integration error can be estimated by expanding $f(x)$ in a power series about some point ξ in the interval $[0,\, mh]$. The function $f(x)$ is represented by a Taylor polynomial of degree k with a remainder

$$R(x) = \frac{(x-\xi)^{k+1}}{(k+1)!} f^{(k+1)}(\xi)$$

The integration error is estimated as the difference between the integral of $R(x)$ and the estimate of the integral provided by the integration rule. The error can

Table 2.2: Weights $a_i = c_i/d$ and error e_k coefficients for trapezoidal rule with endpoint corrections.

k	c_1	c_2	c_3	c_4	c_5	c_6	c_7	d	e_k
1	1							2	-0.083
3	9	28	23					24	-0.026
5	475	1902	1104	1586	1413			1440	-0.014
7	36799	176648	54851	177984	89437	130936	119585	120960	-0.009

be expressed as

$$\epsilon_k(\xi) = e_k\, mh^{k+2} f^{(k+1)}(\xi), \tag{2.98}$$

where the the coefficients e_k are tabulated in the last column of the Table 2.2. One finds that the error estimate for the case $k = 3$ is of the same order as that for Simpson's rule and that for higher values of k is proportional to mh^{k+2}.

We emphasize that the trapezoidal rule with endpoint corrections has the virtue of high accuracy together with great simplicity, or equivalently, high efficiency.

2.5 Potential Models

The potential experienced by a bound atomic electron near $r = 0$ is dominated by the nuclear Coulomb potential, so we expect

$$V(r) \approx -\frac{Z}{r},$$

for small r. At large r, on the other hand, an electron experiences a potential that is the sum of the attractive nuclear Coulomb potential and the sum of the repulsive potentials of the remaining electrons, so we expect

$$\lim_{r\to\infty} V(r) = -\frac{\zeta}{r},$$

with $\zeta = Z-N+1$ for an N electron atom with nuclear charge Z. The transition from a nuclear potential to an ionic potential is predicted by the Thomas-Fermi model, for example. However, it is possible to simply approximate the potential in the intermediate region by a smooth function of r depending on several parameters that interpolates between the two extremes. One adjusts the parameters in this potential to fit the observed energy spectrum as well as possible. We examine this approach in the following section.

Table 2.3: Comparison of $n = 3$ and $n = 4$ levels (a.u.) of sodium calculated using parametric potentials with experiment.

State	V_a	V_b	Exp.
$3s$	-0.1919	-0.1881	-0.1889
$3p$	-0.1072	-0.1124	-0.1106
$4s$	-0.0720	-0.0717	-0.0716
$3d$	-0.0575	-0.0557	-0.0559

2.5.1 Parametric Potentials

It is a simple matter to devise potentials that interpolate between the nuclear and ionic potentials. Two simple one-parameter potentials are:

$$V_a(r) = -\frac{Z}{r} + \frac{(Z-\zeta)\,r}{a^2+r^2}, \tag{2.99}$$

$$V_b(r) = -\frac{Z}{r} + \frac{Z-\zeta}{r}\,(1-e^{-r/b}). \tag{2.100}$$

The second term in each of these potentials approximates the electron-electron interaction. As an exercise, let us determine the values of the parameters a and b in Eqs.(2.99) and (2.100) that best represent the four lowest states ($3s, 3p, 4s$ and $3d$) in the sodium atom. For this purpose, we assume that the sodium spectrum can be approximated by that of a single valence electron moving in one of the above parametric potentials. We choose values of the parameters to minimize the sum of the squares of the differences between the observed levels and the corresponding numerical eigenvalues of the radial Schrödinger equation. To solve the radial Schrödinger equation, we use the routine MASTER described above. To carry out the minimization, we use the subroutine GOLDEN from the NUMERICAL RECIPES library. This routine uses the golden mean technique to find the minimum of a function of a single variable, taken to be the sum of the squares of the energy differences considered as a function of the parameter in the potential.

We find that the value $a = 0.2683$ a.u. minimizes the sum of the squares of the differences between the calculated and observed terms using the potential V_a from Eq.(2.99). Similarly, $b = 0.4072$ a.u. is the optimal value of the parameter in Eq.(2.100). In Table 2.3, we compare the observed sodium energy level with values calculated using the two potentials. It is seen that the calculated and observed levels agree to within a few percent for both potentials, although V_b leads to better agreement.

The electron-electron interaction potential for the two cases is shown in Fig. 2.3. These two potentials are completely different for $r < 1$ a.u., but agree closely for $r > 1$ a.u., where the $n = 3$ and $n = 4$ wave functions have their maxima.

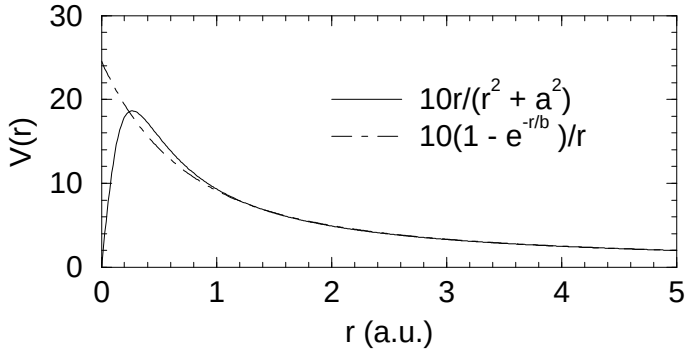

Figure 2.3: Electron interaction potentials from Eqs.(2.99) and (2.100) with parameters $a = 0.2683$ and $b = 0.4072$ chosen to fit the first four sodium energy levels.

Since the two potentials are quite different for small r, it is possible to decide which of the two is more reasonable by comparing predictions of levels that have their maximum amplitudes at small r with experiment. Therefore, we are led to compare the $1s$ energy from the two potentials with the experimentally measured $1s$ binding energy $E_{1s}^{\rm exp} = -39.4$ a.u. We find upon solving the radial Schrödinger equation that

$$E_{1s} = \begin{cases} -47.47\text{a.u.} & \text{for } V_a, \\ -40.14\text{a.u.} & \text{for } V_b. \end{cases}$$

It is seen that potential $V_b(r)$ predicts an energy that is within 2% of the experimental value, while V_a leads to a value of the $1s$ energy that disagrees with experiment by about 18%. As we will see later, theoretically determined potentials are closer to case b than to case a, as one might expect from the comparison here.

One can easily devise multi-parameter model potentials, with parameters adjusted to fit a number of levels precisely, and use the resulting wave functions to predict atomic properties. Such a procedure is a useful first step in examining the structure of an atom, but because of the *ad hoc* nature of the potentials being considered, it is difficult to assess errors in predictions made using such potentials.

2.5.2 Thomas-Fermi Potential

A simple approximation to the atomic potential was derived from a statistical model of the atom by L.H Thomas and independently by E. Fermi in 1927. This potential is known as the Thomas-Fermi potential. Although there has been a

revival of research interest in the Thomas-Fermi method in recent years, we will consider only the most elementary version of the theory here to illustrate an *ab-initio* calculation of an atomic potential.

We suppose that bound electrons in an atom behave in the same way as free electrons confined to a box of volume V. For electrons in a box, the number of states d^3N available in a momentum range d^3p is given by

$$d^3N = 2\frac{V}{(2\pi)^3}d^3p, \tag{2.101}$$

where the factor 2 accounts for the two possible electron spin states. Assuming the box to be spherically symmetric, and assuming that all states up to momentum p_f (the Fermi momentum) are filled, it follows that the particle density ρ is

$$\rho = \frac{N}{V} = \frac{1}{\pi^2}\int_0^{p_f} p^2 dp = \frac{1}{3\pi^2}\, p_f^3. \tag{2.102}$$

Similarly, the kinetic energy density is given by

$$\epsilon_k = \frac{E_k}{V} = \frac{1}{\pi^2}\int_0^{p_f} \frac{p^2}{2}\, p^2 dp = \frac{1}{10\pi^2}\, p_f^5. \tag{2.103}$$

Using Eq.(2.102), we can express the kinetic energy density in terms of the particle density through the relation

$$\epsilon_k = \frac{3}{10}(3\pi^2)^{2/3}\rho^{5/3}\,. \tag{2.104}$$

In the Thomas-Fermi theory, it is assumed that this relation between the kinetic-energy density and the particle density holds not only for particles moving freely in a box, but also for bound electrons in the nonuniform field of an atom. In the atomic case, we assume that each electron experiences a spherically symmetric field and, therefore, that $\rho = \rho(r)$ is independent of direction.

The electron density $\rho(r)$ is assumed to vanish for $r \geq R$, where R is determined by requiring

$$\int_0^R 4\pi r'^2 \rho(r')dr' \; = N, \tag{2.105}$$

where N is the number of bound electrons in the atom.

In the Thomas-Fermi theory, the electronic potential is given by the classical potential of a spherically symmetric charge distribution:

$$V_e(r) = \int_0^R \frac{1}{r_>}\, 4\pi r'^2 \rho(r')dr'\,, \tag{2.106}$$

where $r_> = \max(r, r')$. The total energy of the atom in the Thomas-Fermi theory is obtained by combining Eq.(2.104) for the kinetic energy density with the classical expressions for the electron-nucleus potential energy and the electron-electron potential energy to give the following semi-classical expression for the

energy of the atom:

$$E = \int_0^R \left\{ \frac{3}{10}(3\pi^2)^{2/3}\rho^{2/3} - \frac{Z}{r} + \frac{1}{2}\int_0^R \frac{1}{r_>}\, 4\pi r'^2 \rho(r')dr' \right\} 4\pi r^2 \rho(r) dr\,. \quad (2.107)$$

The density is determined from a variational principle; the energy is required to be a minimum with respect to variations of the density, with the constraint that the number of electrons is N. Introducing a Lagrange multiplier λ, the variational principal $\delta(E - \lambda N) = 0$ can be written

$$\int_0^R \left\{ \frac{1}{2}(3\pi^2)^{2/3}\rho^{2/3} - \frac{Z}{r} + \int_0^R \frac{1}{r_>}\, 4\pi r'^2 \rho(r')dr' - \lambda \right\} 4\pi r^2 \delta\rho(r) dr = 0. \quad (2.108)$$

Requiring that this condition be satisfied for arbitrary variations $\delta\rho(r)$ leads to the following integral equation for $\rho(r)$:

$$\frac{1}{2}(3\pi^2)^{2/3}\rho^{2/3} - \frac{Z}{r} + \int_0^R \frac{1}{r_>}\, 4\pi r'^2 \rho(r')dr' = \lambda\,. \quad (2.109)$$

Evaluating this equation at the point $r = R$, where $\rho(R) = 0$, we obtain

$$\lambda = -\frac{Z}{R} + \frac{1}{R}\int_0^R 4\pi r'^2 \rho(r')dr' = -\frac{Z-N}{R} = V(R)\,, \quad (2.110)$$

where $V(r)$ is the sum of the nuclear and atomic potentials at r. Combining (2.110) and (2.109) leads to the relation between the density and potential,

$$\frac{1}{2}(3\pi^2)^{2/3}\rho^{2/3} = V(R) - V(r)\,. \quad (2.111)$$

Since $V(r)$ is a spherically symmetric potential obtained from purely classical arguments, it satisfies the radial Laplace equation,

$$\frac{1}{r}\frac{d^2}{dr^2} rV(r) = -4\pi\rho(r)\,, \quad (2.112)$$

which can be rewritten

$$\frac{1}{r}\frac{d^2}{dr^2} r[V(R) - V(r)] = 4\pi\rho(r)\,. \quad (2.113)$$

Substituting for $\rho(r)$ from (2.111) leads to

$$\frac{d^2}{dr^2} r[V(R) - V(r)] = \frac{8\sqrt{2}}{3\pi}\,\frac{(r[V(R) - V(r)])^{3/2}}{r^{1/2}}\,. \quad (2.114)$$

It is convenient to change variables to ϕ and x, where

$$\phi(r) = \frac{r[V(R) - V(r)]}{Z}\,, \quad (2.115)$$

and

$$x = r/\xi\,, \tag{2.116}$$

with

$$\xi = \left(\frac{9\pi^2}{128Z}\right)^{1/3}. \tag{2.117}$$

With the aid of this transformation, we can rewrite the *Thomas-Fermi equation* (2.114) in dimensionless form:

$$\frac{d^2\phi}{dx^2} = \frac{\phi^{3/2}}{x^{1/2}}\,. \tag{2.118}$$

Since $\lim_{r\to 0} r[V(r) - V(R)] = -Z$, the desired solution to (2.118) satisfies the boundary condition $\phi(0) = 1$. From $\rho(R) = 0$, it follows that $\phi(X) = 0$ at $X = R/\xi$.

By choosing the initial slope appropriately, we can find solutions to the Thomas-Fermi equation that satisfy the two boundary conditions for a wide range of values X. The correct value of X is found by requiring that the normalization condition (2.105) is satisfied. To determine the point X, we write Eq.(2.113) as

$$r\frac{d^2\phi}{dr^2} = \frac{1}{Z}\,4\pi r^2\rho(r)\,. \tag{2.119}$$

From this equation, it follows that $N(r)$, the number of electrons inside a sphere of radius r, is given by

$$\frac{N(r)}{Z} = \int_0^r r\,\frac{d^2\phi(r)}{dr^2}dr \tag{2.120}$$

$$= \left(r\frac{d\phi}{dr} - \phi\right)_0^r \tag{2.121}$$

$$= r\frac{d\phi}{dr} - \phi(r) + 1\,. \tag{2.122}$$

Evaluating this expression at $r = R$, we obtain the normalization condition

$$X\left(\frac{d\phi}{dx}\right)_X = -\frac{Z-N}{Z}. \tag{2.123}$$

An iterative scheme is set up to solve the Thomas-Fermi differential equation. First, two initial values of X are guessed: $X = X_a$ and $X = X_b$. The Thomas-Fermi equation (2.118) is integrated inward to $r = 0$ twice: the first time starting at $x = X_a$, using initial conditions $\phi(X_a) = 0$, $d\phi/dx(X_a) = -(Z-N)/X_aZ$, and the second time starting at $x = X_b$, using initial conditions $\phi(X_b) = 0$, $d\phi/dx(X_b) = -(Z-N)/X_bZ$. We examine the quantities $\phi(0) - 1$ in the two cases. Let us designate this quantity by f; thus, f_a is the value of $\phi(0) - 1$ for the first case, where initial conditions are imposed at $x = X_a$, and f_b is the value of $\phi(0) - 1$ in the second case. If the product $f_af_b > 0$, we choose two new points and repeat the above steps until $f_af_b < 0$.

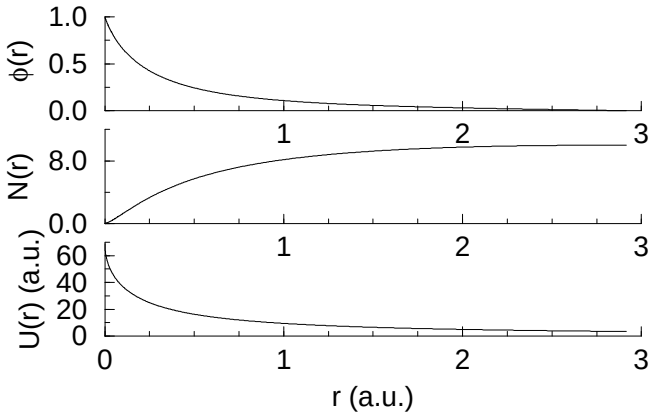

Figure 2.4: Thomas-Fermi functions for the sodium ion, $Z = 11$, $N = 10$. Upper panel: the Thomas-Fermi function $\phi(r)$. Center panel: $N(r)$, the number of electrons inside a sphere of radius r. Lower panel: $U(r)$, the electron contribution to the potential.

If $f_a f_b < 0$, then it follows that the correct value of X is somewhere in the interval between X_a and X_b. Assuming that we have located such an interval, we continue the iteration by interval halving: choose $X = (X_a + X_b)/2$ and integrate inward, test the sign of $f f_a$ and $f f_b$ to determine which subinterval contains X and repeat the above averaging procedure. This interval halving is continued until $|f| < \epsilon$, where ϵ is a tolerance parameter. The value chosen for ϵ determines how well the boundary condition at $x = 0$ is to be satisfied.

In the routine THOMAS, we use the fifth-order Runge-Kutta integration scheme given in Abramowitz and Stegun (1964) to solve the Thomas-Fermi equation. We illustrate the solution obtained for the sodium ion, $Z = 11, N = 10$ in Fig. 2.4. The value of R obtained on convergence was $R = 2.914$ a.u.. In the top panel, we show $\phi(r)$ in the interval 0 - R. In the second panel, we show the corresponding value of $N(r)$, the number of electrons inside a sphere of radius r. In the bottom panel, we give the electron contribution to the potential. Comparing with Fig. 2.3, we see that the electron-electron potential $U(r)$ from the Thomas-Fermi potential has the same general shape as the electron-interaction contribution to the parametric potential $V_b(r)$. This is consistent with the previous observation that $V_b(r)$ led to an accurate inner-shell energy for sodium.

2.6 Separation of Variables for Dirac Equation

To describe the fine structure of atomic states from first principles, it is necessary to treat the bound electrons relativistically. In the independent particle picture, this is done by replacing the one-electron Schrödinger orbital $\psi(\mathbf{r})$ by the corresponding Dirac orbital $\varphi(\mathbf{r})$. The orbital $\varphi(\mathbf{r})$ satisfies the single-particle Dirac equation

$$h_D\varphi = E\varphi, \tag{2.124}$$

where h_D is the Dirac Hamiltonian. In atomic units, h_D is given by

$$h_D = c\boldsymbol{\alpha}\cdot\boldsymbol{p} + \beta c^2 + V(r)\,. \tag{2.125}$$

The constant c is the speed of light; in atomic units, $c = 137.0359895\ldots$. The quantities $\boldsymbol{\alpha}$ and β in Eq.(2.125) are 4×4 Dirac matrices:

$$\boldsymbol{\alpha} = \begin{pmatrix} 0 & \boldsymbol{\sigma} \\ \boldsymbol{\sigma} & 0 \end{pmatrix}, \quad \beta = \begin{pmatrix} 1 & 0 \\ 0 & -1 \end{pmatrix}. \tag{2.126}$$

The 2×2 matrix $\boldsymbol{\sigma}$ is the Pauli spin matrix, discussed in Sec. 1.2.1.

The total angular momentum is given by $\mathbf{J} = \mathbf{L} + \mathbf{S}$, where $\mathbf{L}$ is the orbital angular momentum, and $\mathbf{S}$ is the 4×4 spin angular momentum matrix,

$$\mathbf{S} = \frac{1}{2}\begin{pmatrix} \boldsymbol{\sigma} & 0 \\ 0 & \boldsymbol{\sigma} \end{pmatrix}. \tag{2.127}$$

It is not difficult to show that $\mathbf{J}$ commutes with the Dirac Hamiltonian. We may, therefore, classify the eigenstates of h_D according to the eigenvalues of energy, J^2 and J_z .The eigenstates of J^2 and J_z are easily constructed using the two-component representation of $\boldsymbol{S}$. They are the spherical spinors $\Omega_{\kappa m}(\hat{r})$.

If we seek a solution to the Dirac equation (2.125) having the form

$$\varphi_\kappa(\mathbf{r}) = \frac{1}{r}\begin{pmatrix} iP_\kappa(r) & \Omega_{\kappa m}(\hat{r}) \\ Q_\kappa(r) & \Omega_{-\kappa m}(\hat{r}) \end{pmatrix}, \tag{2.128}$$

then we find, with the help of the identities (1.124,1.126), that the radial functions $P_\kappa(r)$ and $Q_\kappa(r)$ satisfy the coupled first-order differential equations:

$$(V + c^2)\,P_\kappa + c\left(\frac{d}{dr} - \frac{\kappa}{r}\right)Q_\kappa = EP_\kappa \tag{2.129}$$

$$-c\left(\frac{d}{dr} + \frac{\kappa}{r}\right)P_\kappa + (V - c^2)\,Q_\kappa = EQ_\kappa \tag{2.130}$$

where $V(r) = V_{nuc}(r) + U(r)$. The normalization condition for the orbital $\varphi_\kappa(\mathbf{r})$,

$$\int \varphi_\kappa^\dagger(\mathbf{r})\varphi_\kappa(\mathbf{r})d^3r = 1, \tag{2.131}$$

can be written

$$\int_0^\infty [\, P_\kappa^2(r) + Q_\kappa^2(r)\,]dr = 1, \tag{2.132}$$

when expressed in terms of the radial functions $P_\kappa(r)$ and $Q_\kappa(r)$. The radial eigenfunctions and their associated eigenvalues, E, can be determined analytically for a Coulomb potential. In practical cases, however, the eigenvalue problem must be solved numerically.

2.7 Radial Dirac Equation for a Coulomb Field

In this section, we seek analytical solutions to the radial Dirac equations (2.129) and (2.130) for the special case $V(r) = -Z/r$. As a first step in our analysis, we examine these equations at large values of r. Retaining only dominant terms as $r \to \infty$, we find

$$c\frac{dQ_\kappa}{dr} = (E - c^2)P_\kappa\,, \tag{2.133}$$

$$c\frac{dP_\kappa}{dr} = -(E + c^2)Q_\kappa\,. \tag{2.134}$$

This pair of equations can be converted into the second-order equation

$$c^2\frac{d^2P_\kappa}{dr^2} + (E^2 - c^4)P_\kappa = 0, \tag{2.135}$$

which has two linearly independent solutions, $e^{\pm\lambda r}$, with $\lambda = \sqrt{c^2 - E^2/c^2}$. The physically acceptable solution is

$$P_\kappa(r) = e^{-\lambda r}\,. \tag{2.136}$$

The corresponding solution Q_κ is given by

$$Q_\kappa(r) = \sqrt{\frac{c^2 - E}{c^2 + E}}e^{-\lambda r}. \tag{2.137}$$

Factoring the asymptotic behavior, we express the radial functions in the form

$$P_\kappa = \sqrt{1 + E/c^2}e^{-\lambda r}(F_1 + F_2)\,, \tag{2.138}$$

$$Q_\kappa = \sqrt{1 - E/c^2}e^{-\lambda r}(F_1 - F_2)\,. \tag{2.139}$$

Substituting this *ansatz* into (2.129) and (2.130), we find that the functions F_1 and F_2 satisfy the coupled equations

$$\frac{dF_1}{dx} = \frac{EZ}{c^2\lambda x}F_1 + \left(\frac{Z}{\lambda x} - \frac{\kappa}{x}\right)F_2\,, \tag{2.140}$$

$$\frac{dF_2}{dx} = -\left(\frac{Z}{\lambda x} + \frac{\kappa}{x}\right)F_1 + \left(1 - \frac{EZ}{c^2\lambda x}\right)F_2\,, \tag{2.141}$$

where $x = 2\lambda r$.

We seek solutions to Eqs.(2.140,2.141) that have the limiting forms $F_1 = a_1 x^\gamma$ and $F_2 = a_2 x^\gamma$ as $x \to 0$. Substituting these expressions into (2.140) and (2.141) and retaining only the most singular terms, we find:

$$\frac{a_2}{a_1} = \frac{\gamma - EZ/c^2\lambda}{-\kappa + Z/\lambda} = \frac{-\kappa - Z/\lambda}{\gamma + EZ/c^2\lambda}. \tag{2.142}$$

Clearing fractions in the right-hand equality, leads to the result $\gamma^2 = \kappa^2 - Z^2/c^2 = \kappa^2 - \alpha^2 Z^2$. Here, we have used the fact that $c = 1/\alpha$ in atomic units. The physically acceptable value of γ is given by the positive square root, $\gamma = \sqrt{\kappa^2 - \alpha^2 Z^2}$. Next, we use Eq.(2.140) to express F_2 in terms of F_1,

$$F_2 = \frac{1}{-\kappa + Z/\lambda}\left[x\frac{dF_1}{dx} - \frac{EZ}{c^2\lambda}F_1\right]. \tag{2.143}$$

This equation, in turn, can be used to eliminate F_2 from Eq.(2.141), leading to

$$x\frac{d^2F_1}{dx^2} + (1-x)\frac{dF_1}{dx} - \left(\frac{\gamma^2}{x^2} - \frac{EZ}{c^2\lambda}\right)F_1 = 0\,. \tag{2.144}$$

Finally, we write

$$F_1(x) = x^\gamma F(x)\,, \tag{2.145}$$

and find that the function $F(x)$ satisfies the Kummer's equation,

$$x\frac{d^2F}{dx^2} + (b-x)\frac{dF}{dx} - aF = 0\,, \tag{2.146}$$

where $a = \gamma - EZ/c^2\lambda$, and $b = 2\gamma + 1$. This equation is identical to Eq.(2.18) except for the values of the parameters a and b. The solutions to Eq.(2.146) that are regular at the origin are the Confluent Hypergeometric functions written out in Eq.(2.19). Therefore,

$$F_1(x) = x^\gamma\, F(a,b,x)\,. \tag{2.147}$$

The function $F_2(x)$ can also be expressed in terms of Confluent Hypergeometric functions. Using Eq.(2.143), we find

$$F_2(x) = \frac{x^\gamma}{(-\kappa + Z/\lambda)}\left(x\frac{dF}{dx} + aF\right) = \frac{(\gamma - EZ/c^2\lambda)}{(-\kappa + Z/\lambda)}x^\gamma F(a+1,b,x)\,. \tag{2.148}$$

Combining these results, we obtain the following expressions for the radial Dirac functions:

$$\begin{aligned} P_\kappa(r) &= \sqrt{1+E/c^2}\,e^{-x/2}x^\gamma[(-\kappa + Z/\lambda)F(a,b,x) \\ &\quad +(\gamma - EZ/c^2\lambda)F(a+1,b,x)\big], \end{aligned} \tag{2.149}$$

$$\begin{aligned} Q_\kappa(r) &= \sqrt{1-E/c^2}\,e^{-x/2}x^\gamma[(-\kappa + Z/\lambda)F(a,b,x) \\ &\quad -(\gamma - EZ/c^2\lambda)F(a+1,b,x)\big]. \end{aligned} \tag{2.150}$$

These solutions have yet to be normalized.

We now turn to the eigenvalue problem. First, we examine the behavior of the radial functions at large r. We find:

$$F(a,b,x) \;\rightarrow\; \frac{\Gamma(b)}{\Gamma(a)}\, e^x x^{a-b}[1+O(|x|^{-1})]\,, \tag{2.151}$$

$$aF(a+1,b,x) \;\rightarrow\; \frac{\Gamma(b)}{\Gamma(a)}\, e^x x^{a+1-b}[1+O(|x|^{-1})]\,. \tag{2.152}$$

From these equations, it follows that the radial wave functions are normalizable if, and only if, the coefficients of the exponentials in Eqs.(2.151) and (2.152) vanish. As in the nonrelativistic case, this occurs when $a = -n_r$, where $n_r = 0, -1, -2, \cdots$. We define the principal quantum number n through the relation, $n = k + n_r$, where $k = |\kappa| = j + 1/2$. The eigenvalue equation, therefore, can be written

$$EZ/c^2\lambda = \gamma + n - k\,.$$

The case $a = -n_r = 0$ requires special attention. In this case, one can solve the eigenvalue equation to find $k = Z/\lambda$. From this, it follows that the two factors $-\kappa + Z/\lambda$ and $\gamma - EZ/c^2\lambda$ in Eqs.(2.149) and (2.150) vanish for $\kappa = k > 0$. States with $n_r = 0$ occur only for $\kappa < 0$. Therefore, for a given value of $n > 0$ there are $2n-1$ possible eigenfunctions: n eigenfunctions with $\kappa = -1, -2, \cdots -n$, and $n-1$ eigenfunctions with $\kappa = 1, 2, \cdots n-1$.

Solving the eigenvalue equation for E, we obtain

$$E_{n\kappa} = \frac{c^2}{\sqrt{1 + \frac{\alpha^2 Z^2}{(\gamma+n-k)^2}}}\,. \tag{2.153}$$

It is interesting to note that the Dirac energy levels depend only on $k = |\kappa|$. Those levels having the same values of n and j, but different values of ℓ are degenerate. Thus, for example, the $2s_{1/2}$ and $2p_{1/2}$ levels in hydrogenlike ions are degenerate. By contrast, levels with the same value of n and ℓ but different values of j, such as the $2p_{1/2}$ and $2p_{3/2}$ levels, have different energies. The separation between two such levels is called the fine-structure interval.

Expanding (2.153) in powers of αZ, we find

$$E_{n\kappa} = c^2 - \frac{Z^2}{2n^2} - \frac{\alpha^2 Z^4}{2n^3}\left(\frac{1}{k} - \frac{3}{4n}\right) + \cdots\,. \tag{2.154}$$

The first term in this expansion is just the electron's rest energy (mc^2) expressed in atomic units. The second term is precisely the nonrelativistic Coulomb-field binding energy. The third term is the leading fine-structure correction. The fine-structure energy difference between the $2p_{3/2}$ and $2p_{1/2}$ levels in hydrogen is predicted by this formula to be

$$\Delta E_{2p} = \frac{\alpha^2}{32}\,\text{a.u.} = 0.3652\,\text{cm}^{-1}\,,$$

in close agreement with the measured separation. The separation of the $2s_{1/2}$ and $2p_{1/2}$ levels in hydrogen is measured to be $0.0354\,\text{cm}^{-1}$. The degeneracy

between these two levels predicted by the Dirac equation is lifted by the Lamb-shift!

Let us introduce the (noninteger) parameter $N = Z/\lambda = (\gamma + n - k)c^2/E$. From (2.153), we find $N = \sqrt{n^2 - 2(n-k)(k-\gamma)}$. Thus, $N = n$ when $n = k$. With this definition, the coefficients of the hypergeometric functions in Eqs.(2.149) and (2.150) can be written

$$(-\kappa + Z/\lambda) = (N - \kappa)\,, \tag{2.155}$$

$$(\gamma - EZ/c^2\lambda) = -(n-k)\,. \tag{2.156}$$

Introducing the normalization factor

$$N_{n\kappa} = \frac{1}{N\,\Gamma(2\gamma+1)}\sqrt{\frac{Z\,\Gamma(2\gamma+1+n-k)}{2\,(n-k)!\,(N-\kappa)}}\,, \tag{2.157}$$

we can write the radial Dirac Coulomb wave functions as

$$\begin{aligned} P_{n\kappa}(r) &= \sqrt{1+E_{n\kappa}/c^2}\,N_{n\kappa}e^{-x/2}x^{\gamma}\,[(N-\kappa)F(-n+k,2\gamma+1,x) \\ &\quad -(n-k)F(-n+k+1,2\gamma+1,x)]\,, \end{aligned} \tag{2.158}$$

$$\begin{aligned} Q_{n\kappa}(r) &= \sqrt{1-E_{n\kappa}/c^2}\,N_{n\kappa}e^{-x/2}x^{\gamma}\,[(N-\kappa)F(-n+k,2\gamma+1,x) \\ &\quad +(n-k)F(-n+k+1,2\gamma+1,x)]\,. \end{aligned} \tag{2.159}$$

These functions satisfy the normalization condition (2.132). It should be noticed that the ratio of the scale factors in (2.158) and (2.159) is $\sqrt{(1-E_{n\kappa}/c^2)/(1+E_{n\kappa}/c^2)} \approx \alpha Z/2n$. Thus, $Q_{n\kappa}(r)$ is several orders of magnitude smaller than $P_{n\kappa}(r)$ for $Z = 1$. For this reason, $P_{n\kappa}$ and $Q_{n\kappa}$ are referred to as the large and small components of the radial Dirac wave function, respectively.

As a specific example, let us consider the $1s_{1/2}$ ground state of an electron in a hydrogenlike ion with nuclear charge Z. For this state, $n = 1$, $\kappa = -1$, $k = 1$, $\gamma = \sqrt{1-\alpha^2Z^2}$, $E_{n\kappa}/c^2 = \gamma$, $N = 1$, $\lambda = Z$ and $x = 2Zr$. Therefore,

$$P_{1-1}(r) = \sqrt{\frac{1+\gamma}{2}}\sqrt{\frac{2Z}{\Gamma(2\gamma+1)}}\,(2Zr)^{\gamma}e^{-Zr}\,,$$

$$Q_{1-1}(r) = \sqrt{\frac{1-\gamma}{2}}\sqrt{\frac{2Z}{\Gamma(2\gamma+1)}}\,(2Zr)^{\gamma}e^{-Zr}\,.$$

In Fig. 2.5, we plot the $n = 2$ Coulomb wave functions for nuclear charge $Z = 2$. The small components $Q_{2\kappa}(r)$ in the figure are scaled up by a factor of $1/\alpha Z$ to make them comparable in size to the large components $P_{2\kappa}(r)$. The large components are seen to be very similar to the corresponding nonrelativistic Coulomb wave functions $P_{n\ell}(r)$, illustrated in Fig. 2.1. The number of nodes in the $P_{n\kappa}(r)$ is $n - \ell - 1$. The number of nodes in $Q_{n\kappa}(r)$ is also $n - \ell - 1$ for $\kappa < 0$, but is $n - \ell$ for $\kappa > 0$. These rules for the nodes will be useful in designing a numerical eigenvalue routine for the Dirac equation. It should be noticed that, except for sign, the large components of the $2p_{1/2}$ and $2p_{3/2}$ radial wave functions are virtually indistinguishable.

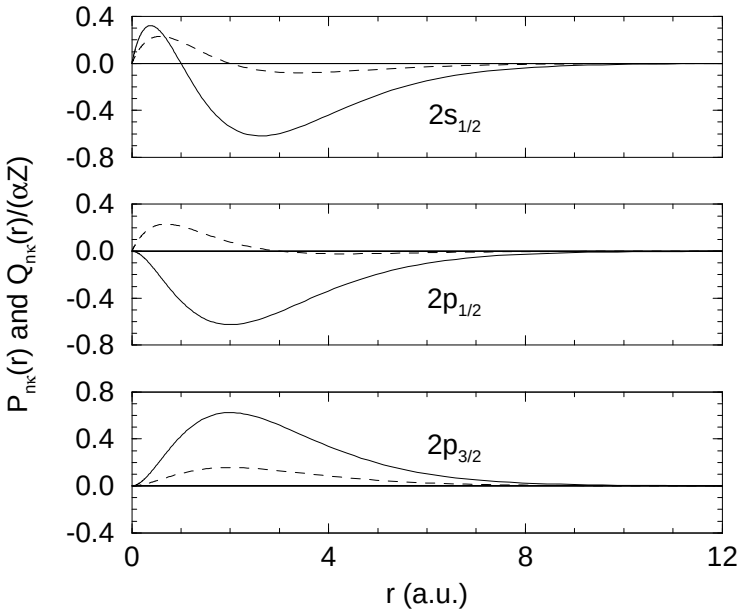

Figure 2.5: Radial Dirac Coulomb wave functions for the $n = 2$ states of hydrogenlike helium, $Z = 2$. The solid lines represent the large components $P_{2\kappa}(r)$ and the dashed lines represent the scaled small components, $Q_{2\kappa}(r)/\alpha Z$.

2.8 Numerical Solution to Dirac Equation

The numerical treatment of the radial Dirac equation closely parallels that used previously to solve the radial Schrödinger equation. The basic point-by-point integration of the radial equations is performed using the Adams-Moulton scheme (ADAMS). We obtain the values of the radial functions near the origin necessary to start the outward integration using an algorithm based on Lagrangian differentiation (OUTDIR). The corresponding values of the radial functions near the practical infinity, needed to start the inward integration, are obtained from an asymptotic expansion of the radial functions (INDIR). A scheme following the pattern of the nonrelativistic routine MASTER is then used to solve the eigenvalue problem. In the paragraphs below we describe the modifications of the nonrelativistic routines that are needed in the Dirac case.

To make comparison with nonrelativistic calculations easier, we subtract the rest energy c^2 a.u. from E_κ in our numerical calculations. In the sequel, we use $W_\kappa = E_\kappa - c^2$ instead of E as the value of the energy in the relativistic case.

The choice of radial grid is identical to that used in the nonrelativistic case; $r(t)$ gives the value of the distance coordinate on the uniformly-spaced t grid. The radial Dirac equations on the t grid take the form

$$\frac{dy}{dt} = f(y,t)\,, \tag{2.160}$$

where $y(t)$ and $f(y,t)$ are the two-component arrays:

$$y = \begin{pmatrix} P_\kappa \\ Q_\kappa \end{pmatrix}\,, \tag{2.161}$$

$$f(y,t) = r' \begin{pmatrix} -(\kappa/r)\,P_\kappa(r) - \alpha[W_\kappa - V(r) + 2\alpha^{-2}]Q_\kappa(r) \\ (\kappa/r)\,Q_\kappa(r) + \alpha[W_\kappa - V(r)]P_\kappa(r) \end{pmatrix}\,, \tag{2.162}$$

where, $r'(t) = \frac{dr}{dt}$.

2.8.1 Outward and Inward Integrations (ADAMS, OUTDIR, INDIR)

ADAMS: We integrate Eqs.(2.161) and(2.162) forward using the Adams-Moulton algorithm given in Eq.(2.58):

$$y[n+1] = y[n] + \frac{h}{D}\sum_{j=1}^{k+1} a[j]\,f[n-k+j]\,. \tag{2.163}$$

The coefficients $a[j]$ and D for this integration formula are given in Table 2.1. Writing $f(y,t) = G(t)\,y$, equation (2.163) can be put in the form (2.59),

$$\left(1 - \frac{ha[k+1]}{D}G[n+1]\right) y[n+1] = y[n] + \frac{h}{D}\sum_{j=1}^{k} a[j]\,f[n-k+j]\,, \tag{2.164}$$

where G is the 2×2 matrix

$$G(t) = \begin{pmatrix} a(t) & b(t) \\ c(t) & d(t) \end{pmatrix} , \tag{2.165}$$

with

$$\begin{aligned} a(t) &= -r'\,(\kappa/r)\,, & b(t) &= -\alpha\, r'\,(W_\kappa - V(r) + 2\alpha^{-2})\,, \\ c(t) &= \alpha\, r'\,(W_\kappa - V(r))\,, & d(t) &= r'\,(\kappa/r)\,. \end{aligned} \tag{2.166}$$

The matrix $M[n+1] = 1 - \frac{ha[k+1]}{D} G[n+1]$ on the left-hand side of Eq.(2.165) can be inverted to give

$$M^{-1}[n+1] = \frac{1}{\Delta[n+1]} \begin{pmatrix} 1 - \lambda d[n+1] & \lambda b[n+1] \\ \lambda c[n+1] & 1 - \lambda a[n+1] \end{pmatrix} , \tag{2.167}$$

where

$$\begin{aligned} \Delta[n+1] &= 1 - \lambda^2 (b[n+1]c[n+1] - a[n+1]d[n+1])\,, \\ \lambda &= \frac{ha[k+1]}{D}\,. \end{aligned}$$

With these definitions, the radial Dirac equation can be written in precisely the same form as the radial Schrödinger equation (2.64)

$$y[n+1] = M^{-1}[n+1] \left(y[n] + \frac{h}{D} \sum_{j=1}^{k} a[j]\, f[n-k+j] \right) . \tag{2.168}$$

This formula is used in the relativistic version of the routine ADAMS to carry out the step-by-step integration of the Dirac equation.

As in the nonrelativistic case, we must supply values of y_n at the first k grid points. This is done by adapting the procedure used to start the outward integration of the Schrödinger equation to the Dirac case.

OUTDIR: The values of y_n at the first k grid points, needed to start the outward integration using (2.168), are obtained using Lagrangian integration formulas. As a preliminary step, we factor r^γ from the radial functions $P_\kappa(r)$ and $Q_\kappa(r)$, where $\gamma = \sqrt{k^2 - (\alpha Z)^2}$. We write:

$$P_\kappa(r) = r^\gamma u(r(t)), \tag{2.169}$$

$$Q_\kappa(r) = r^\gamma v(r(t)), \tag{2.170}$$

and find,

$$du/dt = a(t)u(t) + b(t)v(t), \tag{2.171}$$

$$dv/dt = c(t)u(t) + d(t)v(t), \tag{2.172}$$

where,

$$\begin{aligned} a(t) &= -(\gamma+\kappa)r'/r, && (2.173)\\ b(t) &= -\alpha(W-V(r)+2\alpha^{-2})r', && (2.174)\\ c(t) &= \alpha(W-V(r))r', && (2.175)\\ d(t) &= -(\gamma-\kappa)r'/r. && (2.176) \end{aligned}$$

We normalize our solution so that, at the origin, $u_0 = u(0) = 1$. It follows that $v_0 = v(0)$ takes the value

$$\begin{aligned} v_0 &= -(\kappa+\gamma)/\alpha Z, \quad \text{for } \kappa > 0, && (2.177)\\ &= \alpha Z/(\gamma-\kappa), \qquad \text{for } \kappa < 0, && (2.178) \end{aligned}$$

provided the potential satisfies

$$V(r) \to -\frac{Z}{r},$$

as $r \to 0$. The two equations (2.177) and (2.178) lead to identical results mathematically; however, (2.177) is used for $\kappa > 0$ and (2.178) for $\kappa < 0$ to avoid unnecessary loss of significant figures by cancelation for small values of αZ. One can express du/dt and dv/dt at the points $t[i]$, $i = 0, 1, \cdots, k$ in terms of $u[i] = u(t[i])$ and $v[i] = v(t[i])$ using the Lagrangian differentiation formulas written down in Eq.(2.70). The differential equations thereby become inhomogeneous matrix equations giving the vectors $(u[1], u[2], \cdots, u[k])$ and $(v[1], v[2], \cdots, v[k])$ in terms of initial values $u[0]$ and $v[0]$:

$$\sum_{j=1}^{k} m[ij]\ u[j] - a[i]\ u[i] - b[i]\ v[i] = -m[i0]\ u[0], \tag{2.179}$$

$$\sum_{j=1}^{k} m[ij]\ v[j] - c[i]\ u[i] - d[i]\ v[i] = -m[i0]\ v[0]. \tag{2.180}$$

This system of $2k \times 2k$ inhomogeneous linear equations can be solved by standard routines to give $u[i]$ and $v[i]$ at the points $i = 1, 2, \cdots, k$. The corresponding values of P_κ and Q_κ are given by

$$\begin{aligned} P_\kappa(r[i]) &= r[i]^\gamma\ u[i], && (2.181)\\ Q_\kappa(r[i]) &= r[i]^\gamma\ v[i]. && (2.182) \end{aligned}$$

These equations are used in the routine OUTDIR to give the k values required to start the outward integration using a $k+1$-point Adams-Moulton scheme.

INDIR: The inward integration is started using an asymptotic expansion of the radial Dirac functions. The expansion is carried out for r so large that the potential $V(r)$ takes on its asymptotic form

$$V(r) = -\frac{\zeta}{r},$$

where $\zeta = Z - N + 1$ is the ionic charge of the atom. We assume that the asymptotic expansion of the radial Dirac functions takes the form

$$P_\kappa(r) = r^\sigma e^{-\lambda r} \left\{ \sqrt{\frac{c^2+E}{2c^2}} \left[1 + \frac{a_1}{r} + \frac{a_2}{r} + \cdots\right] + \sqrt{\frac{c^2-E}{2c^2}} \left[\frac{b_1}{r} + \frac{b_2}{r} + \cdots\right] \right\}, \quad (2.183)$$

$$Q_\kappa(r) = r^\sigma e^{-\lambda r} \left\{ \sqrt{\frac{c^2+E}{2c^2}} \left[1 + \frac{a_1}{r} + \frac{a_2}{r} + \cdots\right] - \sqrt{\frac{c^2-E}{2c^2}} \left[\frac{b_1}{r} + \frac{b_2}{r} + \cdots\right] \right\}, \quad (2.184)$$

where $\lambda = \sqrt{c^2 - E^2/c^2}$. The radial Dirac equations admit such a solution only if $\sigma = E\zeta/c^2\lambda$. The expansion coefficients can be shown to satisfy the following recursion relations:

$$b_1 = \frac{1}{2c}\left(\kappa + \frac{\zeta}{\lambda}\right), \quad (2.185)$$

$$b_{n+1} = \frac{1}{2n\lambda}\left(\kappa^2 - (n-\sigma)^2 - \frac{\zeta^2}{c^2}\right) b_n, \quad n = 1, 2, \cdots, \quad (2.186)$$

$$a_n = \frac{c}{n\lambda}\left(\kappa + (n-\sigma)\frac{E}{c^2} - \frac{\zeta\lambda}{c^2}\right) b_n, \quad n = 1, 2, \cdots. \quad (2.187)$$

In the routine INDIR, Eqs.(2.183) and (2.184) are used to generate the k values of $P_\kappa(r)$ and $Q_\kappa(r)$ needed to start the inward integration.

2.8.2 Eigenvalue Problem for Dirac Equation (MASTER)

The method that we use to determine the eigenfunctions and eigenvalues of the radial Dirac equation is a modification of that used in the nonrelativistic routine MASTER to solve the eigenvalue problem for the Schrödinger equation. We guess an energy, integrate the equation outward to the outer classical turning point a_c using OUTDIR, integrate inward from the practical infinity a_∞ to a_c using INDIR and, finally, scale the solution in the region $r > a_c$ so that the large component $P(r)$ is continuous at a_c. A preliminary adjustment of the energy is made to obtain the correct number of nodes ($= n - l - 1$) for $P(r)$ by adjusting the energy upward or downward as necessary. At this point we have a continuous large component function $P(r)$ with the correct number of radial nodes; however, the small component $Q(r)$ is discontinuous at $r = a_c$. A fine adjustment of the energy is made using perturbation theory to remove this discontinuity.

If we let $P_1(r)$ and $Q_1(r)$ be solutions to the radial Dirac equation corresponding to energy W_1 and let $P_2(r)$ and $Q_2(r)$ be solutions corresponding to

energy W_2, then it follows from the radial Dirac equations that

$$\frac{d}{dr}(P_1Q_2 - P_2Q_1) = \frac{1}{c}(W_2 - W_1)(P_1P_2 + Q_1Q_2)\,. \tag{2.188}$$

Integrating both sides of this equation from 0 to a_c and adding the corresponding integral of both sides from a_c to infinity, we obtain the identity

$$P_1(a_c)(Q_2^- - Q_2^+) + P_2(a_c)(Q_1^+ - Q_1^-) = \frac{1}{c}(W_2 - W_1)\int_0^\infty (P_1P_2 + Q_1Q_2)dr\,, \tag{2.189}$$

where Q_1^+ and Q_2^+ are the values of the small components at a_c obtained from inward integration, and Q_1^- and Q_2^- are the values at a_c obtained from outward integration. If we suppose that Q_1 is discontinuous at a_c and if we require that Q_2 be continuous, then we obtain from (2.189) on approximating $P_2(r)$ and $Q_2(r)$ by $P_1(r)$ and $Q_1(r)$,

$$W_2 \approx W_1 + \frac{cP_1(a_c)(Q_1^+ - Q_1^-)}{\int_0^\infty (P_1^2 + Q_1^2)dr}\,. \tag{2.190}$$

The approximation (2.190) is used iteratively to reduce the discontinuity in $Q(r)$ at $r = a_c$ to insignificance. The Dirac eigenvalue routine DMASTER is written following the pattern of the nonrelativistic eigenvalue routine MASTER, incorporating the routines OUTDIR and INDIR to carry out the point-by-point integration of the radial equations and using the approximation (2.190) to refine the solution.

2.8.3 Examples using Parametric Potentials

As in the nonrelativistic case, it is possible to devise parametric potentials to approximate the effects of the electron-electron interaction. Two potentials that have been used with some success to describe properties of large atoms having one valence electron are the Tietz potential, Tietz (1954),

$$V(r) = -\frac{1}{r}\left[1 + \frac{(Z-1)e^{-\gamma r}}{(1+tr)^2}\right]\,, \tag{2.191}$$

and the Green potential, Green et al. (1969),

$$V(r) = -\frac{1}{r}\left[1 + \frac{Z-1}{H(e^{r/d}-1)+1}\right]\,. \tag{2.192}$$

Each of these potentials contain two parameters that can be adjusted to fit experimentally measured energy levels. In Table 2.4, we list values of the parameters for rubidium (Z=37), cesium (Z=55), gold (Z=79) and thallium (Z=81). Energies of low-lying states of these atoms obtained by solving the Dirac equation in the two potentials are listed in Table 2.5. Wave functions obtained by solving the Dirac equation in parametric potentials have been successfully employed to predict properties of heavy atoms (such as hyperfine constants) and

Table 2.4: Parameters for the Tietz and Green potentials.

	Tietz		Green	
Element	t	γ	H	d
Rb	1.9530	0.2700	3.4811	0.7855
Cs	2.0453	0.2445	4.4691	0.8967
Au	2.4310	0.3500	4.4560	0.7160
Tl	2.3537	0.3895	4.4530	0.7234

Table 2.5: Energies obtained using the Tietz and Green potentials.

State	Tietz	Green	Exp.	State	Tietz	Green	Exp.
Rubidium $Z = 37$				Cesium $Z = 55$			
$5s_{1/2}$	-0.15414	-0.15348	-0.15351	$6s_{1/2}$	-0.14343	-0.14312	-0.14310
$5p_{1/2}$	-0.09557	-0.09615	-0.09619	$6p_{1/2}$	-0.09247	-0.09224	-0.09217
$5p_{3/2}$	-0.09398	-0.09480	-0.09511	$6p_{3/2}$	-0.08892	-0.08916	-0.08964
$6s_{1/2}$	-0.06140	-0.06215	-0.06177	$7s_{1/2}$	-0.05827	-0.05902	-0.05865
$6p_{1/2}$	-0.04505	-0.04570	-0.04545	$7p_{1/2}$	-0.04379	-0.04424	-0.04393
$6p_{3/2}$	-0.04456	-0.04526	-0.04510	$7p_{3/2}$	-0.04270	-0.04323	-0.04310
$7s_{1/2}$	-0.03345	-0.03382	-0.03362	$8s_{1/2}$	-0.03213	-0.03251	-0.03230
Gold $Z = 79$				Thallium $Z = 81$			
$6s_{1/2}$	-0.37106	-0.37006	-0.33904	$6p_{1/2}$	-0.22456	-0.22453	-0.22446
$6p_{1/2}$	-0.18709	-0.17134	-0.16882	$6p_{3/2}$	-0.18320	-0.17644	-0.18896
$6p_{3/2}$	-0.15907	-0.14423	-0.15143	$7s_{1/2}$	-0.10195	-0.10183	-0.10382
$7s_{1/2}$	-0.09386	-0.09270	-0.09079	$7p_{1/2}$	-0.06933	-0.06958	-0.06882
$7p_{1/2}$	-0.06441	-0.06313	-0.06551	$7p_{3/2}$	-0.06391	-0.06374	-0.06426
$7p_{3/2}$	-0.05990	-0.05834	-0.06234	$8s_{1/2}$	-0.04756	-0.04771	-0.04792
$8s_{1/2}$	-0.04499	-0.04476	-0.04405	$8p_{1/2}$	-0.03626	-0.03639	-0.03598

to describe the interaction of atoms with electromagnetic fields. The obvious disadvantage of treating atoms using parametric potentials is that there is no *a priori* reason to believe that properties, other than those used as input data in the fitting procedure, will be predicted accurately. In the next chapter, we take up the Hartree-Fock theory, which provides an *ab-initio* method for calculating electronic potentials, atomic energy levels and wave functions.

Chapter 3

Self-Consistent Fields

In this chapter, we consider the problem of determining an approximate wave function for an N-electron atom. We assume that each electron in the atom moves independently in the nuclear Coulomb field and the average field of the remaining electrons. We approximate the electron-electron interaction by a central potential $U(r)$, and we construct an N-electron wave function for the atomic ground state as an antisymmetric product of one-electron orbitals. Next, we evaluate the energy of the atom in its ground state using this wave function. We invoke the variational principle, requiring that the energy be stationary with respect to small changes in the orbitals with the constraint that the wave function remain normalized, to determine the orbitals. This leads to the Hartree-Fock (HF) equations. Solving the HF equations, we determine the one-electron orbitals, the one-electron energies, and the central potential $U(r)$ self-consistently.

3.1 Two-Electron Systems

Let us start our discussion of many-electron atoms by considering a two-electron (heliumlike) ion with nuclear charge Z. The two-electron Hamiltonian may be written

$$H(\mathbf{r_1}, \mathbf{r_2}) = h_0(\mathbf{r_1}) + h_0(\mathbf{r_2}) + \frac{1}{r_{12}}, \tag{3.1}$$

with

$$h_0(\mathbf{r}) = -\frac{1}{2}\nabla^2 - \frac{Z}{r}. \tag{3.2}$$

The term $1/r_{12}$ in Eq.(3.1) is the Coulomb repulsion between the two electrons. The two-electron wave function $\Psi(\mathbf{r}_1, \mathbf{r}_2)$ satisfies the Schrödinger equation

$$H(\mathbf{r_1}, \mathbf{r_2})\Psi(\mathbf{r}_1, \mathbf{r}_2) = E\Psi(\mathbf{r}_1, \mathbf{r}_2). \tag{3.3}$$

We seek bound-state solutions to this equation.

The two-electron Hamiltonian is symmetric with respect to the interchange of the coordinates $\mathbf{r_1}$ and $\mathbf{r_2}$. It follows that $\Psi(\mathbf{r}_2, \mathbf{r}_1)$ is an eigenfunction of H having the same eigenvalue as $\Psi(\mathbf{r}_1, \mathbf{r}_2)$. Moreover, the symmetric and antisymmetric combinations,

$$\Psi(\mathbf{r}_1, \mathbf{r}_2) \pm \Psi(\mathbf{r}_2, \mathbf{r}_1), \tag{3.4}$$

are also eigenfunctions, energy degenerate with $\Psi(\mathbf{r}_1, \mathbf{r}_2)$. The symmetric combination in Eq.(3.4) gives the two-particle wave function appropriate to a system of two interacting bosons; for example, an atom consisting of two π^- mesons in a nuclear Coulomb field repelling one another by the Coulomb force. For electrons and other fermions, the antisymmetric combination in Eq.(3.4) is the appropriate choice.

As an approximation to the two-electron Hamiltonian in Eq.(3.1), let us consider the *Independent-Particle* Hamiltonian

$$H_0(\mathbf{r}_1, \mathbf{r}_2) = h(\mathbf{r}_1) + h(\mathbf{r}_2), \tag{3.5}$$

where

$$h(\mathbf{r}) = h_0(\mathbf{r}) + U(r) = -\frac{1}{2}\nabla^2 + V(r)\,. \tag{3.6}$$

The Hamiltonian H_0 describes the independent motion of two particles in a potential $V(r) = -Z/r + U(r)$. The potential $U(r)$ is chosen to approximate the effect of the Coulomb repulsion $1/r_{12}$. The full Hamiltonian H is then given by $H = H_0 + V(\mathbf{r}_1, \mathbf{r}_2)$, where

$$V(\mathbf{r}_1, \mathbf{r}_2) = \frac{1}{r_{12}} - U(r_1) - U(r_2)\,. \tag{3.7}$$

If we let the orbital $\psi_a(\mathbf{r})$ represent a solution to the one-electron Schrödinger equation,

$$h(\mathbf{r})\,\psi_a(\mathbf{r}) = \epsilon_a \psi_a(\mathbf{r}), \tag{3.8}$$

belonging to eigenvalue ϵ_a, then the product wave function $\Psi_{ab}(\mathbf{r}_1, \mathbf{r}_2) = \psi_a(\mathbf{r_1})\psi_b(\mathbf{r_2})$ is a solution to the two-electron problem,

$$H_0 \Psi_{ab}(\mathbf{r}_1, \mathbf{r}_2) = E_{ab} \Psi_{ab}(\mathbf{r}_1, \mathbf{r}_2), \tag{3.9}$$

belonging to energy $E^{(0)}_{ab} = \epsilon_a + \epsilon_b$.

The lowest energy two-electron eigenstate of H_0 is a product of the two lowest energy one-electron orbitals. For atomic potentials, these are the $1s$ orbitals corresponding to the two possible orientations of spin, $\psi_{1s\mu}(\mathbf{r}) = (P_{1s}(r)/r)Y_{00}(\hat{r})\chi_\mu$, with $\mu = \pm 1/2$. The corresponding antisymmetric product state is

$$\Psi_{1s,1s}(\mathbf{r}_1, \mathbf{r}_2) = \frac{1}{4\pi}\ \frac{1}{r_1}P_{1s}(r_1)\ \frac{1}{r_2}P_{1s}(r_2) \\ \frac{1}{\sqrt{2}}(\chi_{1/2}(1)\chi_{-1/2}(2) - \chi_{-1/2}(1)\chi_{1/2}(2)). \tag{3.10}$$

The factor $1/\sqrt{2}$ is introduced here to insure that $\langle\Psi_{1s1s}|\Psi_{1s1s}\rangle = 1$. The wave function in Eq.(3.10) is an approximation to the ground-state wave function for a two-electron ion.

The orbital angular momentum vector $\mathbf{L} = \mathbf{L}_1 + \mathbf{L}_2$ and the spin angular momentum $\mathbf{S} = \frac{1}{2}\sigma_1 + \frac{1}{2}\sigma_2$ commute with H as well as H_0. It follows that the eigenstates of H and H_0 can also be chosen as eigenstates of L^2, L_z, S^2 and S_z. The combination of spin functions in Eq.(3.10),

$$\frac{1}{\sqrt{2}}(\chi_{1/2}(1)\chi_{-1/2}(2) - \chi_{-1/2}(1)\chi_{1/2}(2)), \tag{3.11}$$

is an eigenstate of S^2 and S_z with eigenvalues 0 and 0, respectively. Similarly, the product of spherical harmonics $Y_{00}(\hat{r}_1)Y_{00}(\hat{r}_2)$ is an eigenstate of L^2 and L_z with eigenvalues 0 and 0, respectively.

Let us approximate the electron interaction by simply replacing the charge Z in the Coulomb potential by an effective charge $\zeta = Z - \sigma$. This corresponds to choosing the electron-electron potential $U(r) = (Z - \zeta)/r$. The potential $V(r)$ in the single-particle Hamiltonian is $V(r) = -\zeta/r$. The one-electron solutions to Eq.(3.8) are then known analytically; they are

$$P_{1s}(r) = 2\zeta^{3/2}\, re^{-\zeta r}. \tag{3.12}$$

The corresponding two-electron energy eigenvalue is $E^{(0)}_{1s1s} = -\zeta^2$ a.u. We can easily obtain the first-order correction to this energy by applying first-order perturbation theory:

$$E^{(1)}_{1s1s} = \langle\Psi_{1s1s}|\frac{1}{r_{12}} - U(r_1) - U(r_2)|\Psi_{1s1s}\rangle\,. \tag{3.13}$$

The first term in (3.13) can be written

$$\langle\Psi_{1s1s}|\frac{1}{r_{12}}|\Psi_{1s1s}\rangle = \frac{1}{(4\pi)^2}\int dr_1 d\Omega_1 \int dr_2 d\Omega_2\, P^2_{1s}(r_1)\, P^2_{1s}(r_2)\,\frac{1}{r_{12}}\,. \tag{3.14}$$

The Coulomb interaction in this equation can be expanded in terms of Legendre polynomials to give

$$\frac{1}{r_{12}} = \frac{1}{|\mathbf{r}_1 - \mathbf{r}_2|} = \sum_{l=0}^{\infty} \frac{r_<^l}{r_>^{l+1}} P_l(\cos\theta), \tag{3.15}$$

where $r_< = \min(r_1, r_2)$ and $r_> = \max(r_1, r_2)$, and where θ is the angle between the vectors $\mathbf{r}_1$ and $\mathbf{r}_2$. With the aid of this expansion, the angular integrals can be carried out to give

$$\langle\Psi_{1s1s}|\frac{1}{r_{12}}|\Psi_{1s1s}\rangle = \int_0^\infty dr_1 P^2_{1s}(r_1) \int_0^\infty dr_2\, P^2_{1s}(r_2)\,\frac{1}{r_>}. \tag{3.16}$$

It should be noted that after the angular integrations, only the monopole contribution from (3.15) survives. The function

$$v_0(1s, r_1) = \int_0^\infty dr_2\, P^2_{1s}(r_2)\,\frac{1}{r_>} \tag{3.17}$$

is just the potential at r_1 of a spherically symmetric charge distribution having radial density $P_{1s}^2(r)$. In terms of this function, we may write

$$\langle \Psi_{1s1s}| \frac{1}{r_{12}} |\Psi_{1s1s}\rangle = \int_0^\infty P_{1s}^2(r)\, v_0(1s,r)\, dr. \tag{3.18}$$

The two remaining integrals in Eq.(3.13) are easily evaluated. We find

$$\langle \Psi_{1s1s}|U(r_1)|\Psi_{1s1s}\rangle = \langle \Psi_{1s1s}|U(r_2)|\Psi_{1s1s}\rangle = \int_0^\infty P_{1s}^2(r) U(r)\, dr\,. \tag{3.19}$$

Combining (3.18) and (3.19), we obtain the following expression for the first-order energy:

$$E_{1s1s}^{(1)} = \int_0^\infty P_{1s}^2(r)\, (v_0(1s,r) - 2U(r))\, dr\,. \tag{3.20}$$

Using the specific form of the $1s$ radial wave function given in Eq.(3.12), we can evaluate $v_0(1s,r)$ analytically using Eq.(3.17) to obtain

$$v_0(1s,r) = (1 - e^{-2\zeta r})/r - \zeta e^{-2\zeta r}\,. \tag{3.21}$$

Using this result, we find

$$\int_0^\infty P_{1s}^2(r)\, v_0(1s,r)\, dr = \frac{5}{8}\zeta\,. \tag{3.22}$$

The integral of $U(r) = (Z-\zeta)/r$ in Eq.(3.20) can be evaluated using the fact that $\langle 1s|1/r|1s\rangle = \zeta$. Altogether, we find

$$E_{1s1s}^{(1)} = \frac{5}{8}\zeta - 2(Z-\zeta)\zeta\,. \tag{3.23}$$

Combining this result with the expression for the lowest-order energy, we obtain

$$E_{1s1s} = E_{1s1s}^{(0)} + E_{1s1s}^{(1)} = -\zeta^2 + \frac{5}{8}\zeta - 2(Z-\zeta)\zeta. \tag{3.24}$$

The specific value of ζ in this equation is determined with the aid of the variational principle, which requires that the parameters in the approximate wave function be chosen to minimize the energy. The value of ζ which minimizes the energy in Eq.(3.24) is found to be $\zeta = Z - 5/16$. The corresponding value of the energy is $E_{1s1s} = -(Z-5/16)^2$. For helium, $Z=2$, this leads to a prediction for the ground-state energy of $E_{1s1s} = -2.848$ a.u., which is within 2% of the experimentally measured energy $E_{1s1s}^{\rm exp} = -2.903$ a.u..

Generally, in the independent-particle approximation, the energy can be expressed in terms of the radial wave function as

$$E_{1s1s} = \langle \Psi_{1s1s}| h_0(\mathbf{r}_1) + h_0(\mathbf{r}_2) + \frac{1}{r_{12}} |\Psi_{1s1s}\rangle\,. \tag{3.25}$$

The expectation values of the single-particle operators $h_0(\mathbf{r}_1)$ and $h_0(\mathbf{r}_2)$ are identical. The first term in (3.25) can be reduced to

$$\langle\Psi_{1s1s}|h_0(\mathbf{r}_1)|\Psi_{1s1s}\rangle = \int_0^\infty dr\left(-\frac{1}{2}P_{1s}(r)\frac{d^2P_{1s}}{dr^2} - \frac{Z}{r}P_{1s}^2(r)\right). \tag{3.26}$$

Integrating by parts, and making use of the previously derived expression for the Coulomb interaction in (3.18), we obtain

$$E_{1s1s} = \int_0^\infty dr\left[\left(\frac{dP_{1s}}{dr}\right)^2 - 2\frac{Z}{r}P_{1s}^2(r) + v_0(1s,r)P_{1s}^2(r)\right]. \tag{3.27}$$

The requirement that the two-particle wave function be normalized, $\langle\Psi_{1s1s}|\Psi_{1s1s}\rangle = 1$, leads to the constraint on the single electron orbital

$$N_{1s} = \int_0^\infty P_{1s}(r)^2 dr = 1. \tag{3.28}$$

We now invoke the variational principle to determine the radial wave functions. We require that the energy be stationary with respect to variations of the radial function subject to the normalization constraint. Introducing the Lagrange multiplier λ, the variational principle may be written

$$\delta(E_{1s1s} - \lambda N_{1s}) = 0\,. \tag{3.29}$$

We designate the variation in the function $P_{1s}(r)$ by $\delta P_{1s}(r)$, and we require $\delta P_{1s}(0) = \delta P_{1s}(\infty) = 0$. Further, we note the identity

$$\delta\frac{dP_{1s}}{dr} = \frac{d}{dr}\delta P_{1s}. \tag{3.30}$$

With the aid of (3.30) we obtain

$$\delta(E_{1s1s} - \lambda N_{1s}) = 2\int_0^\infty\Bigg(-\frac{d^2P_{1s}}{dr^2} - 2\frac{Z}{r}P_{1s}(r) + 2v_0(1s,r)P_{1s}(r) - \lambda P_{1s}(r)\Bigg)\delta P_{1s}(r)\,. \tag{3.31}$$

Requiring that this expression vanish for arbitrary variations $\delta P_{1s}(r)$ satisfying the boundary conditions leads to the Hartree-Fock equation

$$-\frac{1}{2}\frac{d^2P_{1s}}{dr^2} - \frac{Z}{r}P_{1s}(r) + v_0(1s,r)P_{1s}(r) = \epsilon_{1s}P_{1s}(r), \tag{3.32}$$

where we have defined $\epsilon_{1s} = \lambda/2$. The HF equation is just the radial Schrödinger equation for a particle with orbital angular momentum 0 moving in the potential

$$V(r) = -\frac{Z}{r} + v_0(1s,r)\,. \tag{3.33}$$

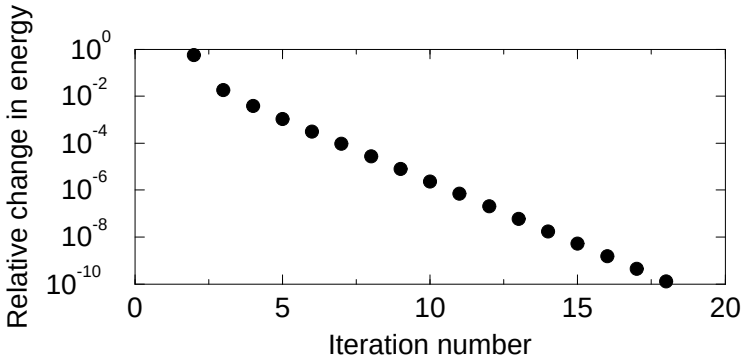

Figure 3.1: Relative change in energy $(E^{(n)} - E^{(n-1)})/E^{(n)}$ as a function of the iteration step number n in the iterative solution of the HF equation for helium, $Z = 2$.

The HF equation is solved iteratively. We start the iterative solution by approximating the radial HF function $P_{1s}(r)$ with a screened $1s$ Coulomb function having effective charge $\zeta = Z - 5/16$. We use this wave function to evaluate $v_0(1s, r)$. We then solve (3.32) using the approximate potential $v_0(1s, r)$. The resulting radial function $P_{1s}(r)$ is used to construct a second approximation to $v_0(1s, r)$, and the iteration is continued until self-consistent values of $P_{1s}(r)$ and $v_0(1s, r)$ are obtained. The pattern of convergence for this iteration procedure is illustrated in Fig. 3.1 where we plot the relative change in the single-particle energy as a function of the iteration step. After 18 steps, the energy has converged to 10 figures.

The resulting value of single-particle energy is found to be $\epsilon_a = -.9179\ldots$ a.u.. The total energy of the two-electron system can be written

$$E_{1s1s} = \langle 1s|2h_0 + v_0(1s, r)|1s\rangle = 2\epsilon_{1s} - \langle 1s|v_0(1s, r)|1s\rangle\,. \tag{3.34}$$

From this, we find $E_{1s,1s} = -2.861\ldots$ a.u., only a slight improvement over the value obtained previously using a screened Coulomb field to approximate the electron-electron interaction. The HF energy is the most accurate that can be obtained within the framework of the independent-particle model. To achieve greater accuracy, we must go beyond the independent-particle model and treat the correlated motion of the two electrons.

In Fig. 3.2, we plot the functions $P_{1s}(r)$ and $v_0(1s, r)$ found by solving the HF equation for neutral helium, $Z = 2$. The potential $v_0(1s, r)$ has the following limiting values:

$$\lim_{r\to 0} v_0(1s, r) = \langle 1s|\frac{1}{r}|1s\rangle, \tag{3.35}$$

$$\lim_{r\to \infty} v_0(1s, r) = \frac{1}{r}. \tag{3.36}$$

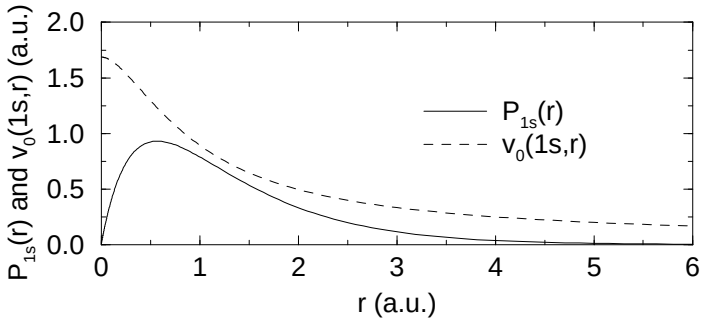

Figure 3.2: Solutions to the HF equation for helium, $Z = 2$. The radial HF wave function $P_{1s}(r)$ is plotted in the solid curve and electron potential $v_0(1s, r)$ is plotted in the dashed curve.

3.2 HF Equations for Closed-Shell Atoms

For a system of N-electrons, the Hamiltonian is

$$H(\mathbf{r_1}, \mathbf{r_2}, \cdots, \mathbf{r}_N) = \sum_{i=1}^{N} h_0(\mathbf{r}_i) + \frac{1}{2} \sum_{i \neq j} \frac{1}{r_{ij}} \,, \tag{3.37}$$

where h_0 is the single-particle operator for the sum of the kinetic energy and the electron-nucleus interaction given in Eq.(3.2), and where $1/r_{ij}$ is the Coulomb interaction energy between the i^{th} and j^{th} electrons. We seek approximate solutions to the N-electron Schrödinger equation

$$H(r_1, \mathbf{r}_2, \cdots, \mathbf{r}_N)\Psi(\mathbf{r}_1, \mathbf{r}_2, \cdots, \mathbf{r}_N) = E\Psi(\mathbf{r}_1, \mathbf{r}_2, \cdots, \mathbf{r}_N). \tag{3.38}$$

The solutions corresponding to electrons (and other fermions) are completely antisymmetric with respect to the interchange of any two coordinates

$$\Psi(\mathbf{r}_1, \cdots, \mathbf{r}_i, \cdots, \mathbf{r}_j, \cdots, \mathbf{r}_N) = -\Psi(\mathbf{r}_1, \cdots, \mathbf{r}_j, \cdots, \mathbf{r}_i, \cdots, \mathbf{r}_N)\,. \tag{3.39}$$

It is perhaps worthwhile repeating here an observation by Hartree (1957, p. 16) concerning "exact" solutions to Eq.(3.38) in the many-electron case. If we consider, for example, the 26 electron iron atom, the function $\Psi(\mathbf{r}_1, \mathbf{r}_2, \cdots, \mathbf{r}_N)$ depends on $3 \times 26 = 78$ variables. Using a course grid of only 10 points for each variable, it would require 10^{78} numbers to tabulate the wave function for iron. Since this number exceeds the estimated number of particles in the solar system, it is difficult to understand how the wave function would be stored even if it could be calculated! Of more practical interest are approximations to "exact" solutions and methods for systematically improving the accuracy of such approximations.

Again, we start with the independent-particle approximation. We write $H = H_0 + V$, with

$$H_0(\mathbf{r_1}, \mathbf{r_2}, \cdots, \mathbf{r}_N) = \sum_{i=1}^{N} h(\mathbf{r}_i)\,, \tag{3.40}$$

$$V(\mathbf{r_1}, \mathbf{r_2}, \cdots, \mathbf{r}_N) = \frac{1}{2}\sum_{i\neq j}\frac{1}{r_{ij}} - \sum_{i=1}^{N} U(r_i)\,, \tag{3.41}$$

where, as in the previous section, $U(r)$ is an appropriately chosen approximation to the electron interaction potential and where $h(r) = h_0 + U(r)$. If we let $\psi_a(\mathbf{r})$ be an eigenfunction of h having eigenvalue ϵ_a, then

$$\psi_a(\mathbf{r}_1)\psi_b(\mathbf{r}_2)\cdots\psi_n(\mathbf{r}_N) \tag{3.42}$$

is an eigenfunction of H_0 with eigenvalue

$$E^{(0)}_{ab\cdots n} = \epsilon_a + \epsilon_b + \cdots + \epsilon_n\,.$$

Moreover, each of the $N!$ product functions obtained by permuting the indices $\mathbf{r}_1, \mathbf{r}_2, \cdots, \mathbf{r}_N$ in the wave function (3.42), is degenerate in energy with that wave function. A completely antisymmetric product wave function is given by the Slater determinant

$$\Psi_{ab\cdots n}(\mathbf{r_1}, \mathbf{r_2}, \cdots, \mathbf{r}_N) = \frac{1}{\sqrt{N!}}\begin{vmatrix} \psi_a(\mathbf{r}_1) & \psi_b(\mathbf{r}_1) & \cdots & \psi_n(\mathbf{r}_1) \\ \psi_a(\mathbf{r}_2) & \psi_b(\mathbf{r}_2) & \cdots & \psi_n(\mathbf{r}_2) \\ \vdots & & & \\ \psi_a(\mathbf{r}_N) & \psi_b(\mathbf{r}_N) & \cdots & \psi_n(\mathbf{r}_N) \end{vmatrix}\,. \tag{3.43}$$

The antisymmetric two-particle wave function $\Psi_{1s1s}(\mathbf{r}_1, \mathbf{r}_2)$ used in the previous section is a special case of a Slater-determinant wave function with $n_a = 1, l_a = 0, m_a = 0, \mu_a = 1/2$ and $n_b = 1, l_b = 0, m_b = 0, \mu_b = -1/2$. Here, we specify the orbitals by their quantum numbers; for example, $a = (n_a, l_a, m_a, \mu_a)$. Since the determinant vanishes if two columns are identical, it follows that the quantum numbers $a, b, \cdots, n$ must be distinct. The fact that the quantum numbers of the orbitals in an antisymmetric product wave function are distinct is called the Pauli exclusion principle.

In the following paragraphs, we will need to evaluate diagonal and off-diagonal matrix elements of many-particle operators between Slater-determinant wave functions. Many-particle operators F of the form

$$F = \sum_{i=1}^{N} f(\mathbf{r}_i)\,, \tag{3.44}$$

such as H_0 itself, are called *one-particle operators*. Operators G of the form

$$G = \frac{1}{2}\sum_{i\neq j} g(r_{ij})\,, \tag{3.45}$$

such as the Coulomb interaction energy, are called *two-particle operators*. The following rules will help us evaluate matrix elements of one- and two-particle operators:

Rule 1

$$\langle \Psi_{a'b'\cdots n'}|F|\Psi_{ab\cdots n}\rangle = 0,$$

if the indices $\{a', b', \cdots, n'\}$ *and* $\{a, b, \cdots, n\}$ *differ in more than one place.*

Rule 2

$$\langle \Psi_{ab\cdots k'\cdots n}|F|\Psi_{ab\cdots k\cdots n}\rangle = f_{k'k}\,,$$

if only the two indices k *and* k' *differ.*

Rule 3

$$\langle \Psi_{ab\cdots n}|F|\Psi_{ab\cdots n}\rangle = \sum_{i=a}^{n} f_{ii}\,,$$

if the indices in the two sets are identical.

Rule 4

$$\langle \Psi_{a'b'\cdots n'}|G|\Psi_{ab\cdots n}\rangle = 0,$$

if the indices $\{a', b', \cdots, n'\}$ *and* $\{a, b, \cdots, n\}$ *differ in more than two places.*

Rule 5

$$\langle \Psi_{ab\cdots k'\cdots l'\cdots n}|G|\Psi_{ab\cdots k\cdots l\cdots n}\rangle = g_{k'l'kl} - g_{k'l'lk}\,,$$

if only the pairs k, l *and* k', l' *in the two sets differ.*

Rule 6

$$\langle \Psi_{ab\cdots k'\cdots n}|G|\Psi_{ab\cdots k\cdots n}\rangle = \sum_{i=a}^{n} \left(g_{k'iki} - g_{k'iik}\right)\,,$$

if only the indices k *and* k' *in the two sets differ.*

Rule 7

$$\langle \Psi_{ab\cdots n}|G|\Psi_{ab\cdots n}\rangle = \frac{1}{2}\sum_{i,j} \left(g_{ijij} - g_{ijji}\right)\,,$$

if the two sets are identical, where both sums extend over all of the indices $\{a, b, \cdots, n\}$

In the above rules, we have introduced the notation:

$$f_{ab} = \langle a|f|b\rangle = \int d^3r \psi_a^\dagger(\mathbf{r}) f(\mathbf{r}) \psi_b(\mathbf{r})\,, \tag{3.46}$$

$$g_{abcd} = \langle ab|g|cd\rangle = \int d^3r_1 \int d^3r_2\, \psi_a^\dagger(\mathbf{r}_1)\psi_b^\dagger(\mathbf{r}_2) g(r_{12}) \psi_c(\mathbf{r}_1)\psi_d(\mathbf{r}_2)\,. \tag{3.47}$$

With the aid of these rules, we easily work out the expectation value of the H_0 and H, using a Slater determinant wave function:

$$E^{(0)}_{ab\cdots n} = \sum_a (h_0)_{aa} + \sum_a U_{aa} \,, \tag{3.48}$$

$$E^{(1)}_{ab\cdots n} = \frac{1}{2}\sum_{ab} (g_{abab} - g_{abba}) - \sum_a U_{aa} \,, \tag{3.49}$$

$$E_{ab\cdots n} = \sum_a (h_0)_{aa} + \frac{1}{2}\sum_{ab} (g_{abab} - g_{abba}) \,, \tag{3.50}$$

where the sums extend over all one-electron orbital quantum numbers in the set $\{a, b, \cdots, n\}$. The terms g_{abab} and g_{abba} are matrix elements of the Coulomb interaction $g(r_{12}) = 1/r_{12}$. The term g_{abab} is called the *direct* matrix element of the operator $g(r_{12})$ and g_{abba} is called the *exchange* matrix element.

The lowest-energy eigenstate of H_0 for an N-electron atom is a product of the N lowest-energy one-electron orbitals. For two-electron atoms, these are the two $1s$ orbitals with different spin projections. In atomic model potentials, such as those discussed in the previous chapter, the lowest few orbital eigenvalues are ordered in the sequence $\epsilon_{1s} < \epsilon_{2s} < \epsilon_{2p} < \epsilon_{3s} < \epsilon_{3p}$. (The ordering beyond this point depends on the potential to some extent and will be considered later.)

For three- or four-electron atoms (lithium and beryllium), the ground state-wave function is taken to be a Slater determinant made up of two $1s$ orbitals, and one or two $2s$ orbitals. The radial probability density functions for these atoms have two distinct maxima, one corresponding to the $1s$ electrons near $1/Z$ a.u., and a second corresponding to the $2s$ electron near 1 a.u.. This variation of the density is referred to as the atomic shell structure. Electronic orbitals having the same principal quantum number n belong to the same shell; their contribution to the radial density is localized. Orbitals having the same principal quantum number, but different angular quantum numbers, belong to different subshells. They contribute fine structure to the radial density function of the atom. The $2s$ subshell is complete after including the two $2s$ orbitals with different spin projections. We continue through the first row of the periodic table, adding successive $2p$ electrons with different values of m and μ until the $n = 2$ shell is complete at neon, $Z = 10$. This building up scheme can be continued throughout the periodic system.

Slater-determinant wave functions for atoms with closed subshells can be shown to be eigenstates of L^2, L_z, S^2 and S_z. The eigenvalues of all four of these operators are 0. Similarly, Slater-determinant wave function for atoms with one electron beyond closed subshells, or for atoms with a single hole in an otherwise filled subshell, are also angular momentum eigenstates. To construct angular momentum eigenstates for other open-shell atoms, linear combinations of Slater determinants, coupled together with Clebsch-Gordan coefficients, are used. We defer further discussion of open-shell atoms until the next chapter and concentrate here on the case of atoms with closed subshells.

We define the configuration of an atomic state to be the number and type of one-electron orbitals present in the Slater-determinant wave function represent-

ing that state. A configuration having k orbitals with principal quantum number n and angular quantum number l is designated by $(nl)^k$. The configurations of the ground states of the closed-shell atoms being considered are: helium $(1s)^2$; beryllium $(1s)^2(2s)^2$; neon $(1s)^2(2s)^2(2p)^6$; magnesium $(1s)^2(2s)^2(2p)^6(3s)^2$; argon $(1s)^2(2s)^2(2p)^6(3s)^2(3p)^6$, calcium $(1s)^2(2s)^2(2p)^6(3s)^2(3p)^6(4s)^2$; and so forth.

The orbitals $\psi_a(\mathbf{r})$ are decomposed into radial, angular, and spin components as $\psi_a(\mathbf{r}_i) = (P_{n_a l_a}(r_i)/r_i)Y_{l_a m_a}(\hat{r}_i)\chi_{\mu_a}(i)$, and the terms in the expression for the energy (3.50) are worked out. First, we evaluate $(h_0)_{aa}$ to obtain:

$$(h_0)_{aa} = \int_0^\infty dr P_{n_a l_a}\left(-\frac{1}{2}\frac{d^2 P_{n_a l_a}}{dr^2} + \frac{l_a(l_a+1)}{2r^2}P_{n_a l_a} - \frac{Z}{r}P_{n_a l_a}\right). \quad (3.51)$$

We note that this term has the same value for each of the $2(2l_a+1)$ orbitals in the $n_a l_a$ subshell. The integral on the right-hand side of this equation is often denoted by $I(n_a l_a)$. On integrating by parts, we can rewrite Eq. (3.51) as

$$I(n_a l_a) = \int_0^\infty dr\left[\frac{1}{2}\left(\frac{dP_{n_a l_a}}{dr}\right)^2 + \frac{l_a(l_a+1)}{2r^2}P^2_{n_a l_a} - \frac{Z}{r}P^2_{n_a l_a}\right]. \quad (3.52)$$

We will need this term later in this section.

Next, we examine the direct Coulomb matrix element g_{abab}. To evaluate this quantity, we make use of the decomposition of $1/r_{12}$ given in Eq.(3.15). Further, we use the well-known identity

$$P_l(\cos\theta) = \sum_{m=-l}^{l}(-1)^m C^l_{-m}(\hat{r}_1)C^l_m(\hat{r}_2)\,, \quad (3.53)$$

to express the Legendre polynomial of $\cos\theta$, where θ is the angle between the two vectors $\mathbf{r}_1$ and $\mathbf{r}_2$, in terms of the angular coordinates of the two vectors in an arbitrary coordinate system. Here, as in Chapter 1, the quantities $C^l_m(\hat{r})$ are tensor operators, defined in terms of spherical harmonics by:

$$C^l_m(\hat{r}) = \sqrt{\frac{4\pi}{2l+1}}Y_{lm}(\hat{r})\,.$$

With the aid of the above decomposition, we find:

$$g_{abab} = \sum_{l=0}^{\infty}\sum_{m=-l}^{l}(-1)^m \int_0^\infty dr_1 P^2_{n_a l_a}(r_1)\int d\Omega_1 Y^*_{l_a m_a}(\hat{r}_1)C^l_{-m}(\hat{r}_1)Y_{l_a m_a}(\hat{r}_1)$$
$$\int_0^\infty dr_2 P^2_{n_b l_b}(r_2)\left(\frac{r^l_<}{r^{l+1}_>}\right)\int d\Omega_2 Y^*_{l_b m_b}(\hat{r}_2)C^l_m(\hat{r}_2)Y_{l_b m_b}(\hat{r}_2). \quad (3.54)$$

The angular integrals can be expressed in terms of reduced matrix elements of

the tensor operator C^l_m using the Wigner-Eckart theorem. We find

$$g_{abab} = \sum_{l=0}^{\infty} - \quad l0 \quad - \quad l0 \quad \langle l_a||C^l||l_a\rangle\langle l_b||C^l||l_b\rangle\, R_l(n_a l_a, n_b l_b, n_a l_a, n_b l_b)\,, \tag{3.55}$$

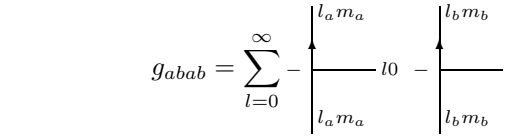

where

$$R_l(a,b,c,d) = \int_0^\infty dr_1 P_a(r_1) P_c(r_1) \int_0^\infty dr_2 P_b(r_2) P_d(r_2) \left(\frac{r_<^l}{r_>^{l+1}}\right). \tag{3.56}$$

These integrals of products of four radial orbitals are called Slater integrals. The Slater integrals can be written in terms of multipole potentials. We define the potentials $v_l(a,b,r)$ by

$$v_l(a,b,r_1) = \int_0^\infty dr_2 P_a(r_2) P_b(r_2) \left(\frac{r_<^l}{r_>^{l+1}}\right). \tag{3.57}$$

We may then write

$$R_l(a,b,c,d) = \int_0^\infty dr P_a(r) P_c(r) v_l(b,d,r) \tag{3.58}$$

$$= \int_0^\infty dr P_b(r) P_d(r) v_l(a,c,r)\,. \tag{3.59}$$

The potentials $v_l(a,b,r)$ are often expressed in the form $v_l(a,b,r) = Y_l(a,b,r)/r$. The functions $Y_l(a,b,r)$ are called Hartree screening functions. Later, we will designate the functions $v_l(a,a,r)$ using the slightly simpler notation $v_l(a,r)$. The function $v_0(a,r)$ is the potential at r due to a spherically symmetric charge distribution with radial density $P_a(r)^2$. The functions $v_l(b,r)$ have the following limiting forms which will be used later:

$$\lim_{r\to 0} v_l(a,r) = r^l \langle a|\frac{1}{r^{l+1}}|a\rangle\,, \tag{3.60}$$

$$\lim_{r\to \infty} v_l(a,r) = \frac{1}{r^{l+1}} \langle a|r^l|a\rangle\,. \tag{3.61}$$

Following the outline of the calculation for the direct integral g_{abab}, we may write the exchange integral g_{abba} as

$$g_{abba} = \sum_{l=0}^{\infty} \sum_{m=-l}^{l} \delta_{\mu_a\mu_b} - \quad lm \quad - \quad lm \quad \langle l_b||C^l||l_a\rangle^2\, R_l(n_a l_a, n_b l_b, n_b l_b, n_a l_a)\,. \tag{3.62}$$

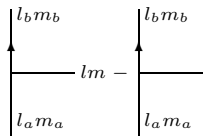

Let us carry out the sum over the magnetic quantum numbers m_b and μ_b in Eq.(3.55). We make use of the identity

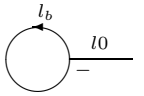

$$= \delta_{l0}\sqrt{2l_b+1} \tag{3.63}$$

to obtain

$$\begin{aligned}\sum_{m_b\mu_b} g_{abab} &= 2\sqrt{\frac{2l_b+1}{2l_a+1}}\langle l_a||C^0||l_a\rangle\langle l_b||C^0||l_b\rangle\, R_0(n_al_a,n_bl_b,n_al_a,n_bl_b)\\ &= 2(2l_b+1)R_0(n_al_a,n_bl_b,n_al_a,n_bl_b)\,. \end{aligned} \tag{3.64}$$

To carry out the sum over the magnetic quantum numbers m_b and μ_b and m in Eq.(3.62), we use the identity

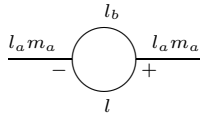

$$= \frac{1}{2l_a+1} \tag{3.65}$$

and find

$$\sum_{m_b\mu_b} g_{abba} = \sum_l \frac{\langle l_b||C^l||l_a\rangle^2}{2l_a+1}\, R_l(n_al_a,n_bl_b,n_bl_b,n_al_a)\,. \tag{3.66}$$

The sum over l extends over all values permitted by the angular momentum and parity selection rules contained in $\langle l_b||C^l||l_a\rangle$, namely, $|l_a-l_b|\le l\le l_a+l_b$, with the constraint that the sum l_a+l_b+l is an even integer.

We are now in a position to evaluate the expression for the energy given in Eq.(3.50). We find

$$\begin{aligned}E_{ab\cdots n} = \sum_{n_al_a} 2(2l_a+1)\Bigg\{ I(n_al_a) + \sum_{n_bl_b}(2l_b+1)\Bigg(R_0(n_al_a,n_bl_b,n_al_a,n_bl_b)\\ - \sum_l \Lambda_{l_all_b} R_l(n_al_a,n_bl_b,n_bl_b,n_al_a)\Bigg)\Bigg\},\end{aligned} \tag{3.67}$$

with

$$\Lambda_{l_all_b} = \frac{\langle l_a||C^l||l_b\rangle^2}{2(2l_a+1)(2l_b+1)} = \frac{1}{2}\begin{pmatrix} l_a & l & l_b\\ 0 & 0 & 0\end{pmatrix}^2. \tag{3.68}$$

The coefficients $\Lambda_{l_all_b}$ are symmetric with respect to an arbitrary interchange of indices. Values of $\Lambda_{l_all_b}$ for $0\le l_a\le l_b\le 4$ are given in Table 3.1.

To maintain normalization of the many-electron wave function, we must require that the radial functions corresponding to a fixed value of l be orthonormal. Therefore,

$$N_{n_al_a,n_bl_a} = \int_0^\infty dr P_{n_al_a}(r)P_{n_bl_a}(r) = \delta_{n_an_b}\,. \tag{3.69}$$

Introducing Lagrange multipliers to accommodate the constraints in Eq.(3.69), we can express the variational principle as:

$$\delta(E_{ab\cdots n} - \sum_{n_an_bl_a} \lambda_{n_al_a,n_bl_a}N_{n_al_a,n_bl_a}) = 0\,, \tag{3.70}$$

and we demand $\lambda_{n_al_a,n_bl_a} = \lambda_{n_bl_a,n_al_a}$.

Table 3.1: Coefficients of the exchange Slater integrals in the nonrelativistic Hartree-Fock equations: $\Lambda_{l_a l l_b}$. These coefficients are symmetric with respect to any permutation of the three indices.

l_a	l	l_b	$\Lambda_{l_a l l_b}$	l_a	l	l_b	$\Lambda_{l_a l l_b}$	l_a	l	l_b	$\Lambda_{l_a l l_b}$
0	0	0	1/2	2	0	2	1/10	3	1	4	2/63
0	1	1	1/6	2	2	2	1/35	3	3	4	1/77
0	2	2	1/10	2	4	2	1/35	3	5	4	10/1001
0	3	3	1/14	2	1	3	3/70	3	7	4	35/2574
0	4	4	1/18	2	3	3	2/105				
				2	5	3	5/231	4	0	4	1/18
1	0	1	1/6	2	2	4	1/35	4	2	4	10/693
1	2	1	1/15	2	4	4	10/693	4	4	4	9/1001
1	1	2	1/15	2	6	4	5/286	4	6	4	10/1287
1	3	2	3/70					4	8	4	245/21879
1	2	3	3/70	3	0	3	1/14				
1	4	3	2/63	3	2	3	2/105				
1	3	4	2/63	3	4	3	1/77				
1	5	4	5/198	3	6	3	50/300				

The equation obtained by requiring that this expression be stationary with respect to variations $\delta P_{n_a l_a}(r)$ is found to be

$$-\frac{1}{2}\frac{d^2 P_{n_a l_a}}{dr^2} + \frac{l_a(l_a+1)}{2r^2} P_{n_a l_a}(r) - \frac{Z}{r} P_{n_a l_a}(r) + \sum_{n_b l_b} (4l_b+2) \left(v_0(n_b l_b, r) P_{n_a l_a}(r) - \sum_l \Lambda_{l_a l l_b} v_l(n_b l_b, n_a l_a, r) P_{n_b l_b}(r) \right) = \epsilon_{n_a l_a} P_{n_a l_a}(r) + \sum_{n_b \neq n_a} \epsilon_{n_a l_a, n_b l_a} P_{n_b l_a}(r), \quad (3.71)$$

where $\epsilon_{n_a l_a, n_b l_a} = \lambda_{n_a l_a, n_b l_a}/(4l_a+2)$ and $\epsilon_{n_a l_a} = \lambda_{n_a l_a, n_a l_a}/(4l_a+2)$.

For orientation, let us examine several special cases. Let us first consider the case of helium for which there is a single $1s$ orbital and a single HF equation. The only nonvanishing angular coefficient in the second line of Eq.(3.71) is $\Lambda_{000} = 1/2$. The entire second row of the equation reduces to

$$2\left(v_0(1s,r) P_{1s}(r) - \frac{1}{2} v_0(1s,r) P_{1s}(r) \right) = v_0(1s,r) P_{1s}(r)\,.$$

The HF equation, Eq.(3.71), reduces to Eq.(3.32) derived in the previous section.

For the case of beryllium, there are two distinct radial orbitals for the $1s$

and $2s$ shells, respectively. The second line of Eq.(3.71) takes the form

$$\Big(v_0(1s,r)+2v_0(2s,r)\Big)P_{1s}-v_0(2s,1s,r)P_{2s}(r), \quad \text{for } n_a l_a = 1s,$$
$$\Big(2v_0(1s,r)+v_0(2s,r)\Big)P_{2s}-v_0(1s,2s,r)P_{1s}(r), \quad \text{for } n_a l_a = 2s.$$

The two HF equations for beryllium become

$$-\frac{1}{2}\frac{d^2P_{1s}}{dr^2}+\left(-\frac{Z}{r}+v_0(1s,r)+2v_0(2s,r)\right)P_{1s}-v_0(2s,1s,r)P_{2s}(r) = \epsilon_{1s}P_{1s}(r)+\epsilon_{1s,2s}P_{2s}(r), \tag{3.72}$$
$$-\frac{1}{2}\frac{d^2P_{2s}}{dr^2}+\left(-\frac{Z}{r}+2v_0(1s,r)+v_0(2s,r)\right)P_{2s}-v_0(1s,2s,r)P_{1s}(r) = \epsilon_{1s,2s}P_{1s}(r)+\epsilon_{2s}P_{2s}(r). \tag{3.73}$$

The off-diagonal Lagrange multiplier $\epsilon_{1s,2s}$ is chosen so as to insure the orthogonality of the $1s$ and $2s$ radial orbitals. Multiplying Eq.(3.72) by $P_{2s}(r)$ and Eq.(3.73) by $P_{1s}(r)$, subtracting the resulting equations, and integrating from 0 to ∞, we obtain the identity

$$(\epsilon_{1s}-\epsilon_{2s})\int_0^\infty dr P_{1s}(r)P_{2s}(r) = -\frac{1}{2}\left(P_{2s}\frac{dP_{1s}}{dr}-P_{1s}\frac{dP_{2s}}{dr}\right)_0^\infty . \tag{3.74}$$

For solutions regular at 0 and ∞, the right-hand side of this equation vanishes. Since $\epsilon_{2s} \neq \epsilon_{1s}$, the solutions to Eqs.(3.72) and (3.73) are orthogonal for arbitrary values of the off-diagonal Lagrange multiplier. We make the simplest choice here, namely, $\epsilon_{1s,2s} = 0$. The HF equations then reduce to a pair of radial Schrödinger equations coupled together by the potential function $v_0(1s,2s,r) = v_0(2s,1s,r)$.

As in the example of beryllium, it is easily shown for a general closed-shell atom that the orbitals associated with a specific value of l and different values of n are orthogonal no matter what value is chosen for the off-diagonal Lagrange multipliers. We take advantage of this fact to simplify the HF equations by choosing $\epsilon_{n_a l_a, n_b l_a} = 0$ for all values of n_a, n_b and l_a.

Generally, we define the Hartree-Fock potential $V_{\rm HF}$ by specifying its action on a arbitrary radial orbital $P_*(r)$. Writing $V_{\rm HF}\,P_*(r) = V_{\rm dir}\,P_*(r) + V_{\rm exc}\,P_*(r)$ we find,

$$V_{\rm dir}\,P_*(r) = \sum_b (4l_b+2)\,v_0(b,r)P_*(r)\,, \tag{3.75}$$
$$V_{\rm exc}\,P_*(r) = \sum_b (4l_b+2)\sum_l \Lambda_{l_b l l_*}\,v_l(b,*,r)P_b(r)\,. \tag{3.76}$$

In the above equations, the sum over b is understood to mean a sum over n_b and l_b. The direct potential $V_{\rm dir}$ is a multiplicative operator. It is just the potential

due to the spherically averaged charge distribution of all atomic electrons. The exchange potential $V_{\rm exc}$ is, by contrast, a nonlocal operator defined by means of an integral. The direct part of the HF potential has the following limits

$$\lim_{r\to 0} V_{\rm dir}(r) = \sum_b (4l_b+2)\langle b|\frac{1}{r}|b\rangle\,, \tag{3.77}$$

$$\lim_{r\to \infty} V_{\rm dir}(r) = \frac{N}{r}\,, \tag{3.78}$$

where $N=\sum_b(4l_b+2)=$ number of electrons in the atom. For neutral atoms, the direct part of the HF potential precisely cancels the nuclear potential at large r. The asymptotic potential for a neutral atom is, therefore, dominated by the monopole parts of the exchange potential at large r. Using the fact that $\Lambda_{l_b 0 l_a}=\delta_{l_b l_a}/(4l_a+2)$, and the fact that the limiting value of $v_0(n_b l_a, n_a l_a, r)$ is

$$\lim_{r\to\infty} v_0(n_b l_a, n_a l_a, r) = \frac{1}{r}\int_0^\infty dr P_{n_b l_a}(r) P_{n_a l_a}(r) = \frac{\delta_{n_b n_a}}{r}\,, \tag{3.79}$$

we find that

$$\lim_{r\to\infty} V_{\rm exc} P_a(r) = -\frac{1}{r}P_a(r)\,. \tag{3.80}$$

The sum of the nuclear potential and the HF potential, therefore, approaches the ionic potential $(N-1)/r$ for large r. With the above definitions, we may write the HF equation for an atom with closed subshells as

$$-\frac{1}{2}\frac{d^2P_a}{dr^2} + \left(V_{\rm HF} - \frac{Z}{r} + \frac{l_a(l_a+1)}{2r^2}\right)P_a(r) = \epsilon_a P_a(r)\,, \tag{3.81}$$

where the index a ranges over the occupied subshells $(n_a l_a)$. The HF equations are a set of radial Schrödinger equations for electrons moving in a common central potential $V(r)=-Z/r+U(r)$. By comparison with Eq.(2.12), the "best" value for the average central potential $U(r)$ is seen to be the nonlocal HF potential $V_{\rm HF}$.

Once the HF equations have been solved, the energy can be determined from Eq.(3.50), which may be written in terms of radial orbitals as

$$E_{ab\cdots n} = \sum_a \epsilon_a - \sum_a (V_{\rm HF})_{aa} + \frac{1}{2}\sum_{ab}(g_{abab}-g_{abba}) \tag{3.82}$$

$$= \sum_a \epsilon_a - \frac{1}{2}\sum_{ab}(g_{abab}-g_{abba})\,. \tag{3.83}$$

Here, we have made use of the fact that $(V_{\rm HF})_{aa}=\sum_b(g_{abab}-g_{abba})$. Expressing the energy in terms of Slater integrals, we find

$$E_{ab\cdots n} = \sum_a 2[l_a]\left[\epsilon_a - \sum_b [l_b]\left(R_0(a,b,a,b) - \sum_l \Lambda_{l_a l l_b} R_l(a,b,b,a)\right)\right], \tag{3.84}$$

with $[l_a]\stackrel{\rm def}{=}2l_a+1$.

The HF energy eigenvalue ϵ_c is related to the energy required to remove an electron from the subshell c. If we calculate the energy of an ion with closed subshells except for a vacancy in subshell c, using a Slater determinant wave function, then we obtain

$$E_{\rm ion} = \sum_a \langle a|h_0|a\rangle - \langle c|h_0|c\rangle + \frac{1}{2}\sum_{ab}(g_{abab} - g_{abba}) - \sum_a (g_{acac} - g_{caac})\,. \quad (3.85)$$

Let us use the orbitals from the closed-shell HF approximation for the atom to evaluate this expression. We then obtain

$$E_{\rm ion} - E_{\rm atom} = -\langle c|h_0|c\rangle - \sum_a (g_{acac} - g_{caac}) = -\langle c|h_0 + V_{\rm HF}|c\rangle = -\epsilon_c\,. \quad (3.86)$$

Thus we find that the removal energy, calculated using HF wave functions for the atom, is the negative of the corresponding HF eigenvalue. This result is called Koopmans' theorem.

In Section 3.1, we have discussed the numerical solution to the HF equation for the $1s$ orbital in helium. In Section 3.3, we discuss the numerical solution to the coupled system of HF equations that arise for other closed-subshell atoms and ions.

3.3 Numerical Solution to the HF Equations

As in the case of helium, the Hartree-Fock equations (3.81) for a general closed-shell atom are solved iteratively. We approximate the HF orbitals by unscreened Coulomb field orbitals initially. This is a fair approximation for the innermost $1s$ orbitals, but a very poor approximation for the outer orbitals. To create a more realistic starting potential, we do a preliminary self-consistent calculation of the direct part of the HF potential scaled to give the correct ionic charge. The Coulomb orbitals are gradually modified until self-consistency at the level is achieved at a level of 1 part in 10^3. The resulting potential is a good local approximation to HF potential and the resulting orbitals are good approximations to the final HF orbitals for outer as well as inner shells. Moreover, orbitals with the same value of l but different values of n are orthogonal. These screened orbitals are used to start the iterative solution of the HF equations. The iteration of the HF equations, including both direct and exchange terms, is then performed until self-consistency is achieved at a level of 1 part in 10^9.

3.3.1 Starting Approximation (HART)

As outlined above, we carry out a self-consistent calculation of single-particle orbitals in a model potential $U(r)$ as a preliminary step in the solution to the HF equations. The model potential is obtained by scaling the direct part of the HF potential to give a potential with the proper asymptotic behavior.

We choose $U(r) = 0$, initially, and use the routine MASTER to solve the radial Schrödinger equation in the unscreened nuclear Coulomb field $V(r) = -Z/r$ for

Table 3.2: Energy eigenvalues for neon. The initial Coulomb energy eigenvalues are reduced to give model potential values shown under $U(r)$. These values are used as initial approximations to the HF eigenvalues shown under $V_{\rm HF}$.

State	Coulomb	$U(r)$	$V_{\rm HF}$
$1s$	-50.00000	-29.27338	-32.77244
$2s$	-12.50000	-1.42929	-1.93039
$2p$	-12.50000	-0.65093	-0.85041

each occupied orbital $P_a(r)$. We accumulate the radial charge density $\rho(r) = \sum_a (4l_a+2)P_a(r)^2$. The direct part of the HF potential is given in terms of $\rho(r)$ by

$$V_{\rm dir}(r) = \int_0^\infty dr' \, \frac{\rho(r')}{r_>} \, . \tag{3.87}$$

Asymptotically, $\lim_{r\to\infty} V_{\rm dir}(r) = N/r$, where N is the number of atomic electrons. To create a model potential with the correct asymptotic behavior, we multiply $V_{\rm dir}$ by the factor $(N-1)/N$. We use the potential $U(r) = (1-1/N)V_{\rm dir}(r)$, calculated self-consistently, as our starting approximation. We add $U(r)$ to the nuclear potential and solve the radial equations once again to obtain a second approximation. This second approximation is used to obtain new values of $\rho(r)$ and $U(r)$. These values are used to obtain a third approximation. This iteration procedure is continued until the potential is stable to some desired level of accuracy.

Since this potential is only used as an initial approximation in solving the HF equations, it is not necessary to carry out the self-consistent iteration accurately. We terminate the iterative solution to the equations when the relative change in the eigenvalue for each orbital, from loop to loop in the iteration, is less than 1 part in 10^3.

The iteration procedure described above does not converge in general, but oscillates from loop to loop with increasing amplitude. To eliminate such oscillations, we change the initial Coulomb interaction gradually. If we designate the value of $U(r)$ from the $n^{\rm th}$ iteration loop as $U^{(n)}(r)$, then at the $(n+1)^{\rm st}$ loop we use the combination

$$U(r) = \eta U^{(n+1)}(r) + (1-\eta)U^{(n)}(r)$$

rather than $U^{(n+1)}(r)$ to continue the iteration. Choosing η in the range $0.375-0.5$ leads to convergence in all cases.

The subroutine HART is designed to carry out the iteration. For the case of neon, it required 13 iterations to obtain the model potential $U(r)$ self-consistent to 1 part in 10^3 using $\eta = 0.5$. The resulting eigenvalues are compared with the initial Coulomb eigenvalues and the final HF eigenvalues in Table 3.2.

A comment should be made in connection with the use of the subroutine MASTER. As discussed previously, the routine MASTER itself uses an iterative procedure to determine the radial wave functions. MASTER requires only a few iterations if an accurate estimate of the eigenvalue is provided initially. To produce such an estimate, we use perturbation theory to determine the change in the eigenvalues induced by changing the potential. A small loop is introduced after $U(r)$ is changed at the end of an iteration step to calculate the first-order change in each of the energy eigenvalues. Perturbation theory gives

$$\delta\epsilon_a = \int_0^\infty dr\,[U^{(n+1)}(r) - U^{(n)}(r)]\,P_a^2(r)\,. \tag{3.88}$$

This correction to the energy at the end of the $n^{\rm th}$ iteration is added to the output energy ϵ_a from MASTER and used as the input energy for the $(n+1)^{\rm st}$ loop.

After the iteration in the routine HART is completed, we have a model potential $U(r)$ and a set of orbitals $P_a(r)$ and energies ϵ_a that provide a suitable starting point for the iterative solution to the HF equations.

3.3.2 Refining the Solution (NRHF)

The HF equation for orbital P_a is written as a pair of inhomogeneous differential equations

$$\frac{dP_a}{dr} - Q_a = 0\,, \tag{3.89}$$

$$\frac{dQ_a}{dr} + f_a P_a = 2(V_{\rm HF} - U)P_a\,, \tag{3.90}$$

where

$$f_a(r) = 2\left(\epsilon_a - \frac{l_a(l_a+1)}{2r^2} + \frac{Z}{r} - U(r)\right)\,. \tag{3.91}$$

These equations are to be solved iteratively. We start with functions $P_a^{(0)}(r)$ and $\epsilon_a^{(0)}$ obtained from the routine HART described in the previous section. To solve the HF equations, we set up an iteration scheme in which $P_a(r)$ is replaced by $P_a^{(n-1)}(r)$ on the right-hand side of Eq.(3.90) in the $n^{\rm th}$ approximation. Thus we write,

$$\frac{dP_a^{(n)}}{dr} - Q_a^{(n)} = 0\,, \tag{3.92}$$

$$\frac{dQ_a^{(n)}}{dr} + f_a^{(n)} P_a^{(n)} = 2(V_{\rm HF}^{(n-1)} - U)P_a^{(n-1)}\,, \tag{3.93}$$

where $f_a^{(n)}$ is given by Eq.(3.91) with ϵ_a replaced by $\epsilon_a^{(n)}$. The functions $P_a^{(0)}(r)$ and $Q_a^{(0)}(r)$ satisfy the homogeneous equations obtained from Eqs.(3.89-3.90)

by dropping the right-hand side and replacing f_a by $f^{(0)}$. From Eqs.(3.92-3.93), we readily obtain the relation

$$\epsilon_a^{(n)} = \epsilon_a^{(0)} + \frac{\int_0^\infty dr P_a^{(0)}(r) \left(V_{\rm HF}^{(n-1)} - U(r) \right) P_a^{(n-1)}(r)}{\int_0^\infty dr P_a^{(0)}(r)\, P_a^{(n)}(r)} \,. \tag{3.94}$$

We use this equation, with $P_a^{(n)}(r)$ replaced by $P_a^{(n-1)}(r)$ in the denominator, to obtain an approximate value of $\epsilon_a^{(n)}$ to use in the function $f_a^{(n)}(r)$. This approximate value of $\epsilon_a^{(n)}$ will be readjusted later in the iteration step to give a properly normalized orbital. The equations (3.92-3.93) are solved by using the method of variation of parameters.

Solving the inhomogeneous equations: Consider the pair of inhomogeneous differential equations

$$\frac{dP(r)}{dr} - Q(r) = 0 \,, \tag{3.95}$$

$$\frac{dQ(r)}{dr} + f(r)P(r) = R(r) \,. \tag{3.96}$$

We can obtain solutions to the homogeneous equations (obtained by setting $R(r) = 0$) that are regular at the origin using the routine OUTSCH described in Chapter 2. We designate these solutions by P_0 and Q_0. Similarly, we can obtain solutions to the homogeneous equations that are regular at infinity by inward integration using the routine INSCH. We designate these solutions by P_∞ and Q_∞. We seek a solution to the inhomogeneous equations (3.95-3.96) in the form

$$P(r) = A(r)P_0(r) + B(r)P_\infty(r) \,, \tag{3.97}$$

$$Q(r) = A(r)Q_0(r) + B(r)Q_\infty(r) \,, \tag{3.98}$$

where $A(r)$ and $B(r)$ are functions that are to be determined. Substituting into Eqs.(3.95-3.96), we find that the functions $A(r)$ and $B(r)$ satisfy the differential equations

$$\frac{dA}{dr} = -\frac{1}{W} P_\infty(r) R(r) \,, \tag{3.99}$$

$$\frac{dB}{dr} = \frac{1}{W} P_0(r) R(r) \,, \tag{3.100}$$

where $W = P_0(r)Q_\infty(r) - Q_0(r)P_\infty(r)$ is a constant (independent of r) known as the Wronskian of the two solutions. Integrating Eqs.(3.99-3.100), we obtain

a solution to Eqs.(3.95-3.96) regular at the origin and infinity:

$$P(r) = \frac{1}{W}\left(P_\infty(r)\int_0^r dr' P_0(r')R(r') + P_0(r)\int_r^\infty dr' P_\infty(r')R(r')\right), \tag{3.101}$$

$$Q(r) = \frac{1}{W}\left(Q_\infty(r)\int_0^r dr' P_0(r')R(r') + Q_0(r)\int_r^\infty dr' P_\infty(r')R(r')\right). \tag{3.102}$$

This method of solving a linear inhomogeneous set of equations is known as the method of variation of parameters. We use the resulting formulas to obtain numerical solutions to Eqs.(3.92-3.93) at each stage of iteration.

Normalizing the orbitals: The orbitals obtained using Eqs.(3.101-3.102) are regular at the origin and infinity, however, they are not properly normalized. To obtain normalized orbitals at the n^{th} step of iteration, it is necessary to adjust the eigenvalue $\epsilon_a^{(n)}$ from the approximate value given in (3.94). Let us suppose that the norm of the solution to the inhomogeneous equations is

$$\int_0^\infty dr P^2(r) = N \neq 1\,. \tag{3.103}$$

We modify the energy eigenvalue by a small amount $\delta\epsilon$. This induces small changes δP and δQ in the radial functions $P(r)$ and $Q(r)$. These small changes in the solution satisfy the pair of inhomogeneous equations

$$\frac{d\delta P}{dr} - \delta Q(r) = 0\,, \tag{3.104}$$

$$\frac{d\delta Q}{dr} + f(r)\,\delta P(r) = -2\delta\epsilon\, P(r)\,. \tag{3.105}$$

The solution to this equation, found by variation of parameters, is

$$\delta P(r) = -2\delta\epsilon\,\hat{P}(r)\,, \tag{3.106}$$

$$\delta Q(r) = -2\delta\epsilon\,\hat{Q}(r)\,, \tag{3.107}$$

with

$$\hat{P}(r) = \frac{1}{W}\left(P_\infty(r)\int_0^r dr' P_0(r')P(r') + P_0(r)\int_r^\infty dr' P_\infty(r')P(r')\right), \tag{3.108}$$

$$\hat{Q}(r) = \frac{1}{W}\left(Q_\infty(r)\int_0^r dr' P_0(r')P(r') + Q_0(r)\int_r^\infty dr' P_\infty(r')P(r')\right). \tag{3.109}$$

We must choose $\delta\epsilon$ to insure that the orbital $P + \delta P$ is properly normalized. Thus, we require (neglecting terms of order δP^2) that

$$\int_0^\infty dr P(r)^2 + 2\int_0^\infty dr P(r)\delta P(r) = 1\,. \tag{3.110}$$

This equation can be rewritten as

$$\delta\epsilon = \frac{N-1}{4\int_0^\infty dr P(r)\hat{P}(r)}\,. \tag{3.111}$$

Equation (3.111) is itself used iteratively to obtain a properly normalized orbital. Usually a single iteration is sufficient to obtain functions normalized to parts in 10^{12}, although occasionally two iterations are required to obtain this accuracy.

Once starting orbitals have been obtained from the routine HART, first-order and second-order corrections are made to each orbital. A selection scheme is then set up in which the orbitals with the largest values of the relative change in energy are treated in order. For example, if we are considering the Be atom which has 2 orbitals, we iterate the $1s$ orbital twice then we iterate the $2s$ orbital twice. At this point, we chose the orbital with the largest value of $|\epsilon_a^{(2)} - \epsilon_a^{(1)}|/|\epsilon_a^{(2)}|$ and iterate this orbital until the relative change in energy is no longer the larger of the two. We then iterate the other orbital until the relative change in energy is no longer the larger. The selection procedure continues until the changes in relative energies of both orbitals are less than one part in 10^9.

Once the iteration has converged to this level of accuracy, we calculate the total energy, check the orthogonality and normalization of the orbitals, and write the radial functions to an output data file for use in other applications.

In Table 3.3, we list the HF eigenvalues and total energies for the noble gases helium, neon, argon, krypton and xenon. In this table, we also give the average values of r and $1/r$ for each individual subshell. It should be noticed that $\langle nl|r|nl\rangle$ and $\langle nl|1/r|nl\rangle$ depend strongly on the principal quantum number n but only weakly on the angular momentum quantum number l within a shell. For comparison, we also give the negative of the removal energy (-B_{nl}) for an electron in the shell nl which, according to Koopmans' theorem, is approximately the HF eigenvalue ϵ_{nl}. The experimental binding energies presented in this table are averages over the fine-structure components.

In Fig. 3.3, we show the radial wave functions for the occupied orbitals in neon and argon. The $1s$ orbitals peak at about $1/Z$ a.u. whereas the outer orbitals peak at about 1 a.u. and become insignificant beyond 4 a.u. for both elements. In Fig. 3.4, we plot the radial densities for the elements beryllium, neon, argon and krypton. The shell structure of these elements is evident in the figure.

3.4 Atoms with One Valence Electron

Let us consider the alkali-metal atoms lithium, sodium, potassium, rubidium and cesium, all of which have one valence electron outside of closed shells. We

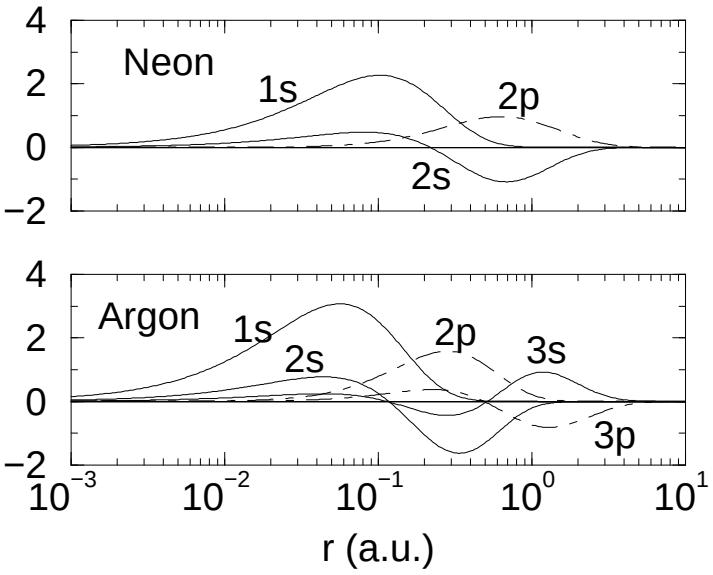

Figure 3.3: Radial HF wave functions for neon and argon.

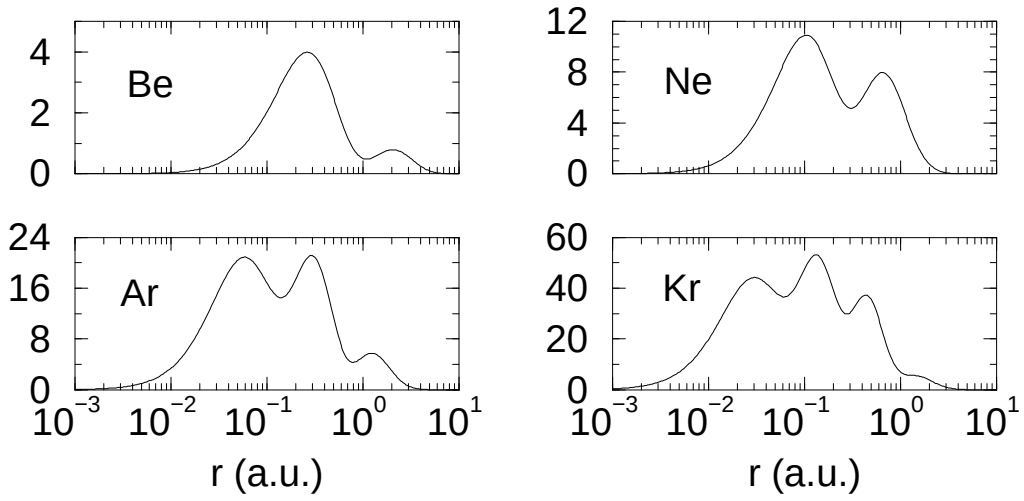

Figure 3.4: Radial HF densities for beryllium, neon, argon and krypton.

Table 3.3: HF eigenvalues ϵ_{nl} , average values of r and $1/r$ for noble gas atoms. The negative of the experimental removal energies -B_{exp} from Bearden and Burr (1967, for inner shells) and Moore (1957, for outer shell) is also listed for comparison.

Atom	nl	ϵ_{nl}	$\langle r \rangle$	$\langle 1/r \rangle$	-B_{exp}
Helium					
	$1s$	-.917956	.92727	1.68728	-0.903
	E_{tot}	-2.861680			
Neon					
	$1s$	-32.772443	.15763	9.61805	-31.86
	$2s$	-1.930391	.89211	1.63255	-1.68
	$2p$	-.850410	.96527	1.43535	-0.792
	E_{tot}	-128.547098			
Argon					
	$1s$	-118.610350	.08610	17.55323	-117.70
	$2s$	-12.322153	.41228	3.55532	-12.00
	$2p$	-9.571466	.37533	3.44999	-9.10
	$3s$	-1.277353	1.42217	.96199	-0.93
	$3p$	-.591017	1.66296	.81407	-0.579
	E_{tot}	-526.817512			
Krypton					
	$1s$	-520.165468	.04244	35.49815	-526.47
	$2s$	-69.903082	.18726	7.91883	-70.60
	$2p$	-63.009785	.16188	7.86843	-62.50
	$3s$	-10.849467	.53780	2.63756	···
	$3p$	-8.331501	.54263	2.52277	-8.00
	$3d$	-3.825234	.55088	2.27694	-3.26
	$4s$	-1.152935	1.62939	.80419	-0.88
	$4p$	-.524187	1.95161	.66922	-0.514
	E_{tot}	-2752.054983			
Xenon					
	$1s$	-1224.397777	.02814	53.46928	-1270.14
	$2s$	-189.340123	.12087	12.30992	-200.39
	$2p$	-177.782449	.10308	12.29169	-181.65
	$3s$	-40.175663	.31870	4.44451	-36.72
	$3p$	-35.221662	.30943	4.52729	-34.44
	$3d$	-26.118869	.28033	4.30438	-24.71
	$4s$	-7.856302	.74527	1.84254	···
	$4p$	-6.008338	.77702	1.74149	···
	$4d$	-2.777881	.87045	1.50874	···
	$5s$	-.944414	1.98096	.64789	···
	$5p$	-.457290	2.33798	.54715	-0.446
	E_{tot}	-7232.138370			

take the wave function of an alkali-metal atom to be a Slater determinant composed of orbitals from the closed shells and a single valence orbital ψ_v. The energy is given by the expression

$$E_{ab\cdots nv} = \sum_a \langle a|h_0|a\rangle + \langle v|h_0|v\rangle + \frac{1}{2}\sum_{ab}(g_{baba} - g_{abba}) + \sum_a (g_{avav} - g_{vaav})\,, \tag{3.112}$$

where the sums over a and b extend over all closed subshells. We can use the results from the previous section to carry out the sums over the magnetic substates of the closed shells to obtain

$$E_{ab\cdots nv} = E_{ab\cdots n} + I(n_v l_v) + \sum_{n_a l_a} 2[l_a]\left(R_0(avav) - \sum_k \Lambda_{l_a k l_v} R_k(vaav)\right), \tag{3.113}$$

where $E_{ab\cdots n}$ is the energy of the closed core given in Eq.(3.67). Let us assume that the orbitals for the closed shells have been determined from a HF calculation for the closed ionic core. The core energy in Eq.(3.113) is then fixed. The valence orbital in Eq.(3.113) is determined variationally. The requirement that the energy be stationary under variations of the valence electron radial function $P_v(r)$, subject to the constraint that the valence orbital remain normalized, leads to the differential equation

$$-\frac{1}{2}\frac{d^2P_v}{dr^2} + \left(V_{\rm HF} - \frac{Z}{r} + \frac{l_v(l_v+1)}{2r^2}\right)P_v = \epsilon_v P_v\,, \tag{3.114}$$

where $V_{\rm HF}$ is the core HF potential written down in Eqs.(3.75-3.76). This homogeneous equation can be solved using the variation of parameters scheme described in the previous section, once the core orbitals are known. Since the equation is homogeneous, the solution can be trivially normalized. The potential in Eq.(3.113) is the HF potential of the $N-1$ electron ion; it is referred to as the $V_{\rm HF}^{N-1}$ potential.

Since the valence electron and those core electrons that have the same orbital angular momentum as the valence electron move in precisely the same potential, it follows that the corresponding radial functions are orthogonal. Thus,

$$\int_0^\infty dr P_v(r)P_a(r) = 0 \;\text{ for } l_a = l_v\,. \tag{3.115}$$

The total energy of the atom can be expressed in terms of the HF eigenvalue ϵ_v as

$$E_{ab\cdots nv} = E_{ab\cdots n} + \epsilon_v, \tag{3.116}$$

where, again, $E_{ab\cdots n}$ is the energy of the ionic core. It follows that the binding energy of the valence electron is just the negative of the corresponding eigenvalue $B_v = E_{\rm ion} - E_{\rm atom} = -\epsilon_v$.

Eigenvalues of the low-lying states of the alkali-metal atoms are presented in Table 3.4. These values agree with measured binding energies at the level of a few percent for lithium. This difference between HF eigenvalues and experiment grows to approximately 10% for cesium.

Table 3.4: Energies of low-lying states of alkali-metal atoms as determined in a $V_{\rm HF}^{N-1}$ Hartree-Fock calculation.

Lithium		Sodium		Potassium		Rubidium		Cesium	
nl	ϵ_{nl}	nl	ϵ_{nl}	nl	ϵ_{nl}	nl	ϵ_{nl}	nl	ϵ_{nl}
$2s$	-.196304	$3s$	-.181801	$4s$	-.146954	$5s$	-.137201	$6s$	-.123013
$3s$	-.073797	$4s$	-.070106	$5s$	-.060945	$6s$	-.058139	$7s$	-.053966
$4s$	-.038474	$5s$	-.037039	$6s$	-.033377	$7s$	-.032208	$8s$	-.030439
$5s$	-.023570	$6s$	-.022871	$7s$	-.021055	$8s$	-.020461	$9s$	-.019551
$2p$	-.128637	$3p$	-.109438	$4p$	-.095553	$5p$	-.090135	$6p$	-.084056
$3p$	-.056771	$4p$	-.050321	$5p$	-.045563	$6p$	-.043652	$7p$	-.041463
$4p$	-.031781	$5p$	-.028932	$6p$	-.026773	$7p$	-.025887	$8p$	-.024858
$5p$	-.020276	$6p$	-.018783	$7p$	-.017628	$8p$	-.017147	$9p$	-.016584
$3d$	-.055562	$3d$	-.055667	$3d$	-.058117	$4d$	-.060066	$5d$	-.066771
$4d$	-.031254	$4d$	-.031315	$4d$	-.032863	$5d$	-.033972	$6d$	-.037148
$5d$	-.020002	$5d$	-.020038	$5d$	-.020960	$6d$	-.021570	$7d$	-.023129

3.5 Dirac-Fock Equations

The Hartree-Fock theory is easily extended to include relativistic effects. We start with a many-body Hamiltonian patterned after its nonrelativistic counterpart:

$$H(\mathbf{r}_1, \mathbf{r}_2, \cdots, \mathbf{r}_N) = \sum_{i=1}^{N} h_0(\mathbf{r}_i) + \frac{1}{2} \sum_{i \neq j} \frac{1}{r_{ij}} \,. \tag{3.117}$$

In the relativistic case, the one-electron Hamiltonian $h_0(\mathbf{r})$ is taken to be the Dirac Hamiltonian

$$h_0(\mathbf{r}) = c\boldsymbol{\alpha} \cdot \boldsymbol{p} + \beta c^2 - Z/r \,. \tag{3.118}$$

The resulting many-body Hamiltonian is called the Dirac-Coulomb Hamiltonian. It provides a useful starting point for discussions of relativistic effects in atoms. The Dirac-Coulomb Hamiltonian must be supplemented by the Breit interaction to understand fine-structure corrections precisely. We will ignore the Breit interaction initially, and return to it after we have derived the Dirac-Fock equations.

The reader must be cautioned that there are difficulties associated with applications of the Dirac-Coulomb Hamiltonian (with or without the Breit Interaction) in higher-order perturbation theory calculations. These difficulties can only be resolved by recourse to Quantum Electrodynamics. We will discuss these difficulties and their solution when we take up relativistic many-body perturbation theory. For doing calculations at the Hartree-Fock level of approximation,

the Dirac-Coulomb Hamiltonian is the appropriate point of departure.

As in the nonrelativistic case, we introduce an average central potential $U(r)$ and the corresponding one-electron Hamiltonian $h(\mathbf{r})$:

$$h(\mathbf{r}) = c\boldsymbol{\alpha}\cdot\boldsymbol{p} + \beta c^2 + V(r)\,, \tag{3.119}$$

with $V(r) = -Z/r + U(r)$. The Dirac-Coulomb Hamiltonian can then be written as $H = H_0 + V$ with

$$H_0 = \sum_i h(\mathbf{r}_i) \tag{3.120}$$

$$V = \frac{1}{2}\sum_{i\neq j}\frac{1}{r_{ij}} - \sum_{i=1}^{N} U(r_i)\,. \tag{3.121}$$

If $\varphi_a(\mathbf{r})$ is an eigenfunction of the one-electron Dirac Hamiltonian $h(\mathbf{r})$ with eigenvalue ϵ_a, then the product wave function

$$\varphi_a(\mathbf{r}_1)\varphi_b(\mathbf{r}_2)\cdots\varphi_n(\mathbf{r}_N) \tag{3.122}$$

is an eigenfunction of H_0 with eigenvalue

$$E^{(0)}_{ab\cdots n} = \epsilon_a + \epsilon_b + \cdots + \epsilon_n\,.$$

A properly antisymmetrized product wave function is given by the Slater determinant:

$$\Psi_{ab\cdots n}(\mathbf{r}_1,\mathbf{r}_2,\cdots,\mathbf{r}_N) = \frac{1}{\sqrt{N!}}\begin{vmatrix} \varphi_a(\mathbf{r}_1) & \varphi_b(\mathbf{r}_1) & \cdots & \varphi_n(\mathbf{r}_1) \\ \varphi_a(\mathbf{r}_2) & \varphi_b(\mathbf{r}_2) & \cdots & \varphi_n(\mathbf{r}_2) \\ \vdots & & & \\ \varphi_a(\mathbf{r}_N) & \varphi_b(\mathbf{r}_N) & \cdots & \varphi_n(\mathbf{r}_N) \end{vmatrix}\,. \tag{3.123}$$

We take the wave function for the ground-state of a closed-shell atom to be a Slater determinant formed from the N lowest-energy single-particle orbitals and evaluate the expectation value of the energy. We find that

$$E_{ab\cdots n} = \sum_a \langle a|h_0|a\rangle + \frac{1}{2}\sum_{ab}(g_{abab} - g_{abba})\,. \tag{3.124}$$

This is just the expression obtained previously in the nonrelativistic case. Here, however, the Coulomb matrix elements g_{abcd} are to be evaluated using Dirac orbitals rather than nonrelativistic orbitals. As in Chapter 2, we write the one-electron Dirac orbital $\varphi_a(\mathbf{r})$ in terms of spherical spinors as

$$\varphi_a(\mathbf{r}) = \frac{1}{r}\begin{pmatrix} iP_a(r)\,\Omega_{\kappa_a m_a}(\hat{r}) \\ Q_a(r)\,\Omega_{-\kappa_a m_a}(\hat{r}) \end{pmatrix}\,. \tag{3.125}$$

Before we can carry out the sums over magnetic quantum numbers, it is necessary to do an angular momentum decomposition of the Coulomb integrals

g_{abcd}. In making this decomposition, we use the fact that

$$\begin{aligned}\varphi_a^\dagger(\mathbf{r})\,\varphi_c(\mathbf{r}) = \\ &\frac{1}{r^2}[P_a(r)P_c(r)\,\Omega^\dagger_{\kappa_a m_a}(\hat{r})\Omega_{\kappa_c m_c}(\hat{r}) + Q_a(r)Q_c(r)\,\Omega^\dagger_{-\kappa_a m_a}(\hat{r})\Omega_{-\kappa_c m_c}(\hat{r})] \\ &= \frac{1}{r^2}[P_a(r)P_c(r) + Q_a(r)Q_c(r)]\,\Omega^\dagger_{\kappa_a m_a}(\hat{r})\Omega_{\kappa_c m_c}(\hat{r})\,. \qquad (3.126)\end{aligned}$$

Introducing the expansion

$$\frac{1}{r_{12}} = \sum_{kq}\frac{r_<^k}{r_>^{k+1}}(-1)^q C^k_{-q}(\hat{r}_1)C^k_q(\hat{r}_2)\,, \qquad (3.127)$$

the Coulomb integral g_{abcd} can be written

$$g_{abcd} = \sum_{kq}(-1)^q\langle\kappa_a m_a|C^k_{-q}|\kappa_c m_c\rangle\langle\kappa_b m_b|C^k_q|\kappa_d m_d\rangle R_k(abcd)\,, \qquad (3.128)$$

where $R_k(abcd)$ is the (relativistic) Slater integral defined by

$$\begin{aligned}R_k(abcd) = \int_0^\infty dr_1[P_a(r_1)P_c(r_1) + Q_a(r_1)Q_c(r_1)]\times \\ \int_0^\infty dr_2\frac{r_<^k}{r_>^{k+1}}[P_b(r_2)P_d(r_2) + Q_b(r_2)Q_d(r_2)]. \qquad (3.129)\end{aligned}$$

The angular matrix elements in Eq.(3.128) are given by

$$\langle\kappa_a m_a|C^k_q|\kappa_b m_b\rangle = \int d\Omega\,\Omega^\dagger_{\kappa_a m_a}(\hat{r})\,C^k_q(\hat{r})\,\Omega_{\kappa_b m_b}(\hat{r})\,. \qquad (3.130)$$

Since the spherical spinors are angular momentum eigenstates and since the functions $C^k_q(\hat{r})$ are spherical tensor operators, the Wigner-Eckart theorem may be used to infer the dependence on the magnetic quantum numbers. We obtain,

$$\langle\kappa_a m_a|C^k_q|\kappa_b m_b\rangle = -$$

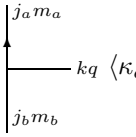

$$\langle\kappa_a||C^k||\kappa_b\rangle\,. \qquad (3.131)$$

The reduced matrix element $\langle\kappa_a||C^k||\kappa_b\rangle$ is found to be

$$\langle\kappa_a||C^k||\kappa_b\rangle = (-1)^{j_a+1/2}\sqrt{[j_a][j_b]}\begin{pmatrix} j_a & j_b & k \\ -1/2 & 1/2 & 0\end{pmatrix}\Pi(l_a+k+l_b)\,, \qquad (3.132)$$

where

$$\Pi(l) = \begin{cases} 1, & \text{if } l \text{ is even} \\ 0, & \text{if } l \text{ is odd}\end{cases}\,. \qquad (3.133)$$

With these definitions, we may write

$$g_{abcd} = \sum_k -$$

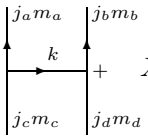

$$X_k(abcd)\,, \qquad (3.134)$$

where

$$X_k(abcd) = (-1)^k \langle \kappa_a || C^k || \kappa_c \rangle \langle \kappa_b || C^k || \kappa_d \rangle R_k(abcd)\,. \tag{3.135}$$

Let us carry out the sum over m_b of the direct and exchange Coulomb matrix elements in Eq.(3.124). To this end, we make use of the easily verified identities

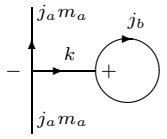

$$= \sqrt{\frac{[j_b]}{[j_a]}}\,\delta_{k0}\,, \tag{3.136}$$

and

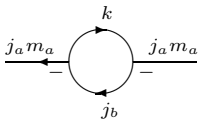

$$= (-1)^{j_a - j_b + k}\,\frac{1}{[j_a]}\,. \tag{3.137}$$

With the aid of the first of these identities, we find

$$\begin{aligned} \sum_{m_b} g_{abab} &= \sqrt{\frac{[j_b]}{[j_a]}}\,X_0(abab) \\ &= [j_b]\,R_0(abab)\,, \end{aligned} \tag{3.138}$$

where we have used the fact that

$$\langle \kappa_a || C^0 || \kappa_a \rangle = \sqrt{[j_a]}\,. \tag{3.139}$$

Using the second graphical identity above, we find that

$$\sum_{m_b} g_{abba} = \sum_k (-1)^{j_a - j_b + k}\,\frac{1}{[j_a]}\,X_k(abba) \tag{3.140}$$

$$= [j_b] \sum_k \Lambda_{\kappa_a k \kappa_b}\,R_k(abba)\,, \tag{3.141}$$

with

$$\Lambda_{\kappa_a k \kappa_b} = \frac{\langle \kappa_a || C^k || \kappa_b \rangle^2}{[j_a][j_b]} = \begin{pmatrix} j_a & j_b & k \\ -1/2 & 1/2 & 0 \end{pmatrix}^2 \Pi(l_a + k + l_b)\,. \tag{3.142}$$

It is now a simple matter to carry out the double sum over magnetic quantum numbers in the expression for the Coulomb energy in Eq.(3.124). We obtain

$$\frac{1}{2} \sum_{m_a m_b} (g_{abab} - g_{abba}) = \frac{1}{2}\,[j_a][j_b] \left(R_0(abab) - \sum_k \Lambda_{\kappa_a k \kappa_b}\,R_k(abba) \right). \tag{3.143}$$

The terms $\langle a|h_0|a\rangle$ in Eq.(3.124) are independent of m_a. They are given by the radial integral

$$\begin{aligned} I_a = \langle a|h_0|a\rangle = \int_0^\infty dr \Big\{ & P_a \left(-\frac{Z}{r} + c^2 \right) P_a + c P_a \left(\frac{d}{dr} - \frac{\kappa}{r} \right) Q_a \\ & - c Q_a \left(\frac{d}{dr} + \frac{\kappa}{r} \right) P_a + Q_a \left(-\frac{Z}{r} - c^2 \right) Q_a \Big\}\,. \end{aligned} \tag{3.144}$$

The energy can therefore be expressed as

$$E_{ab\cdots n} = \sum_a [j_a] \left\{ I_a + \frac{1}{2} \sum_b [j_b] \left[R_0(abab) - \sum_k \Lambda_{\kappa_a k \kappa_b} R_k(abba) \right] \right\} , \quad (3.145)$$

where the indices a and b refer to $(n_a\kappa_a)$ and $(n_b\kappa_b)$, respectively.

Again, as in the nonrelativistic case, we require that $E_{ab\cdots n}$ be stationary with the constraint that the radial functions having the same angular quantum number κ but different principal quantum numbers n be orthogonal. This requirement is combined with the normalization condition in the equation

$$N_{n_a\kappa_a, n_b\kappa_a} = \int_0^\infty dr [P_{n_a\kappa_a}(r) P_{n_b\kappa_a}(r) + Q_{n_a\kappa_a}(r) Q_{n_b\kappa_a}(r)] = \delta_{n_a n_b} . \quad (3.146)$$

Introducing Lagrange multipliers $\lambda_{n_a\kappa_a, n_b\kappa_a}$ (assumed to be symmetric with respect to n_a and n_b), the variational condition is

$$\delta(E_{ab\cdots n} - \sum_{ab} \delta_{\kappa_a\kappa_b} \lambda_{n_a\kappa_a, n_b\kappa_a} N_{n_a\kappa_a, n_b\kappa_b}) = 0 , \quad (3.147)$$

with respect to variations in the radial functions P_a and Q_a. The variations $\delta P_a(r)$ and $\delta Q_a(r)$ are required to vanish at the origin and infinity. After an integration by parts, the variational condition immediately leads to the "Dirac-Fock" differential equations

$$\left(V_{\rm HF} - \frac{Z}{r} + c^2 \right) P_a + c \left(\frac{d}{dr} - \frac{\kappa}{r} \right) Q_a = \epsilon_a P_a + \sum_{n_b \neq n_a} \epsilon_{n_a\kappa_a,\, n_b\kappa_a} P_{n_b\kappa_a} \quad (3.148)$$

$$-c \left(\frac{d}{dr} + \frac{\kappa}{r} \right) P_a + \left(V_{\rm HF} - \frac{Z}{r} - c^2 \right) Q_a = \epsilon_a Q_a + \sum_{n_b \neq n_a} \epsilon_{n_a\kappa_a,\, n_b\kappa_a} Q_{n_b\kappa_a} . \quad (3.149)$$

Here, the HF potential $V_{\rm HF}$ is defined by its action on a radial orbital. Thus, if $R_a(r)$ represents either the large component radial function $P_a(r)$ or the small component function $Q_a(r)$, then

$$V_{\rm HF} R_a(r) = \sum_b [j_b] \left(v_0(b,b,r) R_a(r) - \sum_k \Lambda_{\kappa_a k \kappa_b} v_k(b,a,r) R_b(r) \right) . \quad (3.150)$$

The (relativistic) screening potentials in this equation are given by

$$v_k(a,b,r) = \int_0^\infty dr' \frac{r_<^k}{r_>^{k+1}} [P_a(r') P_b(r') + Q_a(r') Q_b(r')] . \quad (3.151)$$

In Eqs.(3.148, 3.149), we have introduced the notation $\epsilon_a = \lambda_{n_a\kappa_a, n_a\kappa_a}/[j_a]$ and $\epsilon_{n_a\kappa_a,\, n_b\kappa_a} = \lambda_{n_a\kappa_a, n_b\kappa_a}/[j_a]$.

Just as in the nonrelativistic case, the radial orbitals belonging to a particular value of the angular quantum number κ but different values of the principal quantum number n are orthogonal for arbitrary values of the off-diagonal Lagrange multiplier $\epsilon_{n_a\kappa_a,\,n_b\kappa_a}$. We make the simplest choice here, namely, $\epsilon_{n_a\kappa_a,\,n_b\kappa_a} = 0$. With this choice, the Dirac-Fock equations become a set of coupled, non-linear eigenvalue equations. These equations are to be solved self-consistently to obtain the occupied orbitals and the associated energy eigenvalues.

The total energy of the atom may be easily calculated, once the Dirac-Fock equations have been solved using Eq.(3.145). Alternatively, it can be written in terms of the Dirac-Fock eigenvalues as

$$E_{ab\cdots n} = \sum_a [j_a]\epsilon_a - \frac{1}{2}\sum_{ab}[j_a][j_b]\left(R_0(abab) - \sum_k \Lambda_{\kappa_a k\kappa_b} R_k(abba)\right) . \quad (3.152)$$

As in the nonrelativistic case, Koopman's theorem leads to the interpretation of the energy eigenvalue ϵ_a as the negative of the removal energy of an electron from subshell a ($-B_a$).

Numerical Considerations: The numerical techniques used to solve the Dirac-Fock equations are similar to those used in the nonrelativistic case. Starting from Coulomb wave functions, a model potential $U(r)$, taken to be the direct part of the HF potential scaled to give the correct asymptotic behavior, is obtained iteratively using the Dirac routine MASTER. The Dirac-Fock equations are rewritten as inhomogeneous equations, in a form suitable for iteration starting from the model-potential orbitals:

$$\left(U - \frac{Z}{r} + c^2 - \epsilon_a^{(n)}\right) P_a^{(n)} + c\left(\frac{d}{dr} - \frac{\kappa}{r}\right) Q_a^{(n)} = - \left(V_{\rm HF}^{(n-1)} - U\right) P_a^{(n-1)} \quad (3.153)$$

$$-c\left(\frac{d}{dr} + \frac{\kappa}{r}\right) P_a^{(n)} + \left(U - \frac{Z}{r} - c^2 - \epsilon_a^{(n)}\right) Q_a^{(n)} = - \left(V_{\rm HF}^{(n-1)} - U\right) Q_a^{(n-1)}. \quad (3.154)$$

These equations are solved at each stage of iteration and the energy adjusted using a variation of parameters scheme similar to that used in the nonrelativistic case. We leave it to the reader to write out the detailed formulas for solving the inhomogeneous equations. The iteration procedure is continued until the relative change in energy for each orbital is less than one part in 10^9. At this point the total energy is calculated, the orthogonality of the orbitals is checked and the wave functions are written to an external file for use in other applications.

As an example, we present the eigenvalues obtained from a Dirac-Fock calculation of the closed-shell mercury atom (Z=80) in Table 3.5. These eigenvalues

Table 3.5: Dirac-Fock eigenvalues (a.u.) for mercury, $Z = 80$. $E_{\rm tot} = -19648.8585$ a.u.. For the inner shells, we also list the experimental binding energies from Bearden and Burr (1967) for comparison.

nl_j	ϵ_{nl_j}	$-B_{nl_j}$	nl_j	ϵ_{nl_j}	$-B_{nl_j}$
$1s_{1/2}$	-3074.2259	-3054.03			
$2s_{1/2}$	-550.2508	-545.35			
$3s_{1/2}$	-133.1130	-125.86			
$4s_{1/2}$	-30.6482	-27.88			
$5s_{1/2}$	-5.1030	-3.96			
$6s_{1/2}$	-0.3280	-0.384			
$2p_{1/2}$	-526.8546	-522.17	$2p_{3/2}$	-455.1566	-451.44
$3p_{1/2}$	-122.6388	-120.48	$3p_{3/2}$	-106.5451	-104.63
$4p_{1/2}$	-26.1240	-24.88	$4p_{3/2}$	-22.1886	-20.98
$5p_{1/2}$	-3.5379	-2.64	$5p_{3/2}$	-2.8420	-2.12
$3d_{3/2}$	-89.4368		$3d_{5/2}$	-86.0201	
$4d_{3/2}$	-14.7967		$4d_{5/2}$	-14.0526	
$5d_{3/2}$	-0.6501		$5d_{5/2}$	-0.5746	
$4f_{5/2}$	-4.4729		$4f_{7/2}$	-4.3117	

are also compared with experimental removal energies in the table. The ground-state configuration consists of 22 subshells: $(1s_{1/s})^2 \cdots (5d_{3/2})^4 (5d_{5/2})^6 (6s_{1/s})^2$. The fine-structure splitting between levels having the same n and l but different j is evident in both the theoretical and experimental energies. The differences between the experimental and theoretical energies is partly due to the approximation involved in interpreting energy eigenvalues as binding energies (Koopman's theorem) and partly to the neglect of the Breit interaction and QED corrections. When these effects are considered, the agreement between theory and experiment improves to one part in 10^5 the inner electrons.

Nuclear Finite Size: In this example, we have included the effects of nuclear finite size by replacing the nuclear Coulomb potential $-Z/r$ with the potential of a finite charge distribution. We assume that the nucleus is described by a uniform ball of charge of radius R. Under this assumption, the nuclear potential can be written

$$V_{\rm nuc}(r) = \begin{cases} -Z/R\left(3/2 - r^2/2R^2\right) & r < R \\ -Z/r & r \geq R \end{cases} \tag{3.155}$$

The root-mean-square radius of a uniform charge distribution $R_{\rm rms}$ is related to its radius R through

$$R = \sqrt{5/3}\, R_{\rm rms}\,. \tag{3.156}$$

Table 3.6: Dirac-Fock eigenvalues ϵ of valence electrons in Cs ($Z = 55$) and theoretical fine-structure intervals Δ are compared with measured energies (Moore). $\Delta_{nl} = \epsilon_{nlj=l+1/2} - \epsilon_{nlj=l-1/2}$

nl_j	ϵ	Δ_{nl}	$-B_{\rm exp}$	$\Delta_{\rm exp}$
$6s_{1/2}$	-.1273680		-0.143100	
$6p_{1/2}$	-.0856159		-0.092168	
$6p_{3/2}$	-.0837855	0.001830	-0.089643	0.002525
$5d_{3/2}$	-.0644195		-0.077035	
$5d_{5/2}$	-.0645296	-0.000110	-0.076590	0.000445
$7s_{1/2}$	-.0551873		-0.058646	
$7p_{1/2}$	-.0420214		-0.043928	
$7p_{3/2}$	-.0413681	0.000653	-0.043103	0.000825
$6d_{3/2}$	-.0360870		-0.040177	
$6d_{5/2}$	-.0360899	-0.000029	-0.039981	0.000196
$8s_{1/2}$	-.0309524		-0.032302	
$4f_{5/2}$	-.0312727		-0.031596	
$4f_{7/2}$	-.0312737	0.000000	-0.031595	-0.000001

High-energy electron-nucleus scattering experiments and measurements of energies of muonic xrays allow one to determine $R_{\rm rms}$ for many nuclei reliably. A tabulation of R and $R_{\rm rms}$ throughout the periodic table by analysis of such experiments is given by Johnson and Soff (1985). The radii of nucleii for which no direct measurements are available can be estimated using the empirical formula

$$R_{\rm rms} = 0.836A^{1/3} + 0.570 \text{ fm} \quad A > 9, \tag{3.157}$$

which fits the available data to ± 0.05 fm.

Atoms with One-Valence Electron: Again, in parallel with the nonrelativistic theory, we can obtain wave functions for atoms with one-electron beyond closed shells by solving the valence orbital Dirac-Fock equations in the fixed $V_{\rm HF}^{N-1}$ potential of the closed shell ion. As an example, we show the Dirac-Fock eigenvalues for the 13 lowest states in Cs ($Z = 55$) in Table 3.6. For this atom, theoretical eigenvalues and experimental removal energies agree to about 10%. The theoretical fine-structure splitting for np levels ($\Delta_{np} = \epsilon_{np_{3/2}} - \epsilon_{np_{1/2}}$) agrees with experiment only in order of magnitude, whereas, the fine-structure interval for nd levels disagrees with experiment even in sign. To understand these differences, we must consider correlation effects as well as the Breit interaction. In the following chapter, we introduce perturbation theoretic methods for treating correlation corrections.

Chapter 4

Atomic Multiplets

In this chapter, we extend the study of atomic structure from atoms with one valence electron to those with two or more valence electrons. As illustrated in the two previous chapters, excited states of one valence electron atoms having a given angular momentum and parity can be described in the independent-particle model using a single Slater determinant. For atoms with two or more electrons, a linear combination of two or more Slater determinants are typically needed to describe a particular state. In addition to the state of interest, this linear combination describes one or more closely related states; the collection of states given by the linear combination of Slater determinants is referred to as a multiplet. To study multiplets, it is convenient to replace the description of states using Slater determinants by the equivalent second-quantization description of the following section. The rules of second-quantization rules are familiar from studies of the harmonic oscillator in quantum mechanics. A more complete discussion may be found in Lindgren and Morrison (1985).

4.1 Second-Quantization

We start our discussion of second quantization by examining the description of one- and two-electron states. As in the previous chapters, we let a single index k designate the set of one-particle quantum numbers $(n_k l_k m_k \mu_k)$. The one-electron state $|k\rangle$, describe by its wave function $\psi_k(\mathbf{r})$ previously, is represented in second quantization by an operator $a_k^\dagger$ acting on the *vacuum* state $|0\rangle$

$$|k\rangle = a_k^\dagger |0\rangle \,. \tag{4.1}$$

The vacuum state is the state in which there are no electrons; it is assumed to be normalized

$$\langle 0|0\rangle = 1 \,. \tag{4.2}$$

The adjoint to the state $|k\rangle$ is given by

$$\langle k| = \langle 0|a_k \,. \tag{4.3}$$

We assume that a_k operating on the vacuum state vanishes; therefore,

$$a_k|0\rangle = 0 \quad \text{and} \quad \langle 0|a_k^\dagger = 0\,. \tag{4.4}$$

The operators $a_k^\dagger$ and a_k are called *creation* and *annihilation* operators, respectively. The creation and annihilation operators are assumed to satisfy the following anticommutation relations:

$$\{a_j^\dagger, a_k^\dagger\} = a_j^\dagger\, a_k^\dagger + a_k^\dagger\, a_j^\dagger = 0\,, \tag{4.5}$$

$$\{a_j, a_k\} = a_j\, a_k + a_k\, a_j = 0\,, \tag{4.6}$$

$$\{a_j, a_k^\dagger\} = a_j a_k^\dagger + a_k^\dagger a_j = \delta_{jk}\,. \tag{4.7}$$

The third of these relations (4.7) can be used to prove the orthonormality of the one-electron states $|j\rangle$ and $|k\rangle$:

$$\langle j|k\rangle = \langle 0|a_j a_k^\dagger|0\rangle = \langle 0|\delta_{jk} - a_k^\dagger a_j|0\rangle = \delta_{jk}\langle 0|0\rangle = \delta_{jk}\,. \tag{4.8}$$

The antisymmetric two-electron state, represented previously by a Slater determinant $\Psi_{jk}(\mathbf{r}_1, \mathbf{r}_2)$, is represented in second quantization by

$$|jk\rangle = a_j^\dagger a_k^\dagger|0\rangle\,. \tag{4.9}$$

The anticommutation relations (4.5) insure the antisymmetry of the state $|jk\rangle$. Similarly, the antisymmetry of the adjoint state follows from the relation (4.6). The normalization condition for a two-electron state $|jk\rangle$ can be written:

$$\begin{aligned}\langle jk|jk\rangle &= \langle 0|a_k a_j a_j^\dagger a_k^\dagger|0\rangle \\ &= \langle 0|a_k a_k^\dagger - a_k a_j^\dagger a_j a_k^\dagger|0\rangle \\ &= \langle 0|1 - a_k^\dagger a_k - a_j^\dagger a_j + a_j^\dagger a_k^\dagger a_k a_j|0\rangle = 1\,.\end{aligned} \tag{4.10}$$

If we define the number operator for a state $|k\rangle$ by $\mathcal{N}_k = a_k^\dagger a_k$, then, by virtue of the anticommutation relations, we obtain

$$\mathcal{N}_k^2 = a_k^\dagger a_k a_k^\dagger a_k = a_k^\dagger a_k - a_k^\dagger a_k^\dagger a_k a_k = a_k^\dagger a_k = \mathcal{N}_k\,. \tag{4.11}$$

Therefore, the number operator satisfies the identity $\mathcal{N}_k^2 - \mathcal{N}_k = 0$. If n_k is an eigenvalue of $\mathcal{N}_k$, then n_k satisfies the same equation, $n_k^2 - n_k = 0$. From this, it follows that the possible eigenvalues of $\mathcal{N}_k$ are 0 and 1. The one-electron state $|k\rangle$ is an eigenstate of $\mathcal{N}_k$ with eigenvalue 1,

$$\mathcal{N}_k|k\rangle = a_k^\dagger a_k a_k^\dagger|0\rangle = (a_k^\dagger - a_k^\dagger a_k^\dagger a_k)|0\rangle = a_k^\dagger|0\rangle = |k\rangle\,. \tag{4.12}$$

A general N-particle state described by a Slater determinant wave function formed from a product of the orbitals $\psi_a\,\psi_b \cdots \psi_n$ is represented in second quantization as

$$|ab\cdots n\rangle = a_a^\dagger a_b^\dagger \cdots a_n^\dagger|0\rangle\,. \tag{4.13}$$

This state is antisymmetric with respect to the interchange of any two indices; moreover, it is normalized to 1. Defining the number operator $\mathcal{N}$ by

$$\mathcal{N} = \sum_k \mathcal{N}_k = \sum_k a_k^\dagger a_k \,, \tag{4.14}$$

where the sum extends over all single-particle quantum numbers, it can easily be shown that $|ab\cdots n\rangle$ is an eigenstate of $\mathcal{N}$ with eigenvalue N. In a similar way, we see that the state $|ab\cdots n\rangle$ is an eigenstate of the unperturbed Hamiltonian operator H_0 defined by

$$H_0 = \sum_k \epsilon_k a_k^\dagger a_k \,, \tag{4.15}$$

with eigenvalue

$$E^{(0)} = \epsilon_a + \epsilon_b + \cdots + \epsilon_n \,. \tag{4.16}$$

Here ϵ_k is the eigenvalue of the one-electron Hamiltonian $h(\mathbf{r})$ belonging to the eigenfunction $\psi_k(\mathbf{r})$:

$$h\psi_k(\mathbf{r}) = \epsilon_k \psi_k(\mathbf{r}) \,.$$

Equation (4.15) gives the representation of the unperturbed Hamiltonian H_0 in second quantization. This equation can be rewritten

$$H_0 = \sum_k \langle k|h|k\rangle \, a_k^\dagger a_k \,. \tag{4.17}$$

A general single-particle operator $F = \sum_{i=1}^N f(\mathbf{r}_i)$ is represented in second quantization as

$$F = \sum_{kl} \langle k|f|l\rangle \, a_k^\dagger a_l \,. \tag{4.18}$$

This operator acting on the state $|ab\cdots n\rangle$ gives

$$F\,|ab\cdots n\rangle = \sum_{kc} \langle k|f|c\rangle \, |ab\cdots c \to k\cdots n\rangle \,, \tag{4.19}$$

where $|ab\cdots c \to k\cdots n\rangle$ is identical to the state $|ab\cdots n\rangle$ with the operator $a_c^\dagger$ replaced by $a_k^\dagger$. In this expression, c is a state occupied in $|ab\cdots n\rangle$ and the sum extends over all such states. The state k is either identical to c or is a state *not* occupied in $|ab\cdots n\rangle$. The matrix element of F between a state $|a'b'\cdots n'\rangle$ and $|ab\cdots n\rangle$ is nonvanishing only if the sets $\{ab\cdots n\}$ and $\{a'b'\cdots n'\}$ differ in at most one place. Thus

$$\langle ab\cdots c'\cdots n|F|ab\cdots c\cdots n\rangle = \langle c'|f|c\rangle \,. \tag{4.20}$$

Furthermore,

$$\langle ab\cdots n|F|ab\cdots n\rangle = \sum_c \langle c|f|c\rangle \,. \tag{4.21}$$

These rules are precisely the same as those developed in Chapter 2 to calculate matrix-elements of single-particle operators between Slater determinant wave functions.

The two-particle operator,

$$G = \frac{1}{2}\sum_{i\neq j} g(r_{ij})\,,$$

is represented in second quantization by:

$$G = \frac{1}{2}\sum_{ijkl} g_{ijkl}\, a_i^\dagger a_j^\dagger a_l a_k\,, \tag{4.22}$$

where, as before,

$$g_{ijkl} = \int d^3r_1 d^3r_2 \psi_i^\dagger(\mathbf{r}_1)\psi_j^\dagger(\mathbf{r}_2) g(r_{12})\psi_k(\mathbf{r}_1)\psi_l(\mathbf{r}_2)\,.$$

Again, it is simple to verify that matrix elements of G satisfy precisely the rules written down in the previous chapter for calculating matrix elements of two-particle operators between determinant wave functions. As an example, let us consider the expectation value of G in the two-particle state $|ab\rangle$. We have

$$\langle ab|G|ab\rangle = \frac{1}{2}\sum_{ijkl} g_{ijkl}\langle 0|a_b a_a a_i^\dagger a_j^\dagger a_l a_k a_a^\dagger a_b^\dagger|0\rangle\,. \tag{4.23}$$

With the aid of the anticommutation relations, the product $a_b a_a a_i^\dagger a_j^\dagger$ on the left in Eq.(4.23) can be rearranged to give

$$\begin{aligned} a_b a_a a_i^\dagger a_j^\dagger &= \delta_{ia}\delta_{jb} - \delta_{ib}\delta_{ja} \\ &\quad -\delta_{ia}a_j^\dagger a_b + \delta_{ib}a_j^\dagger a_a - \delta_{jb}a_i^\dagger a_a + \delta_{ja}a_i^\dagger a_b + a_i^\dagger a_j^\dagger a_b a_a. \end{aligned} \tag{4.24}$$

Since $\langle 0|a_j^\dagger = 0$, only the first two terms on the right-hand side of this equation contribute in (4.23). Similarly, the product of operators $a_l a_k a_a^\dagger a_b^\dagger$ can be written

$$\begin{aligned} a_l a_k a_a^\dagger a_b^\dagger &= \delta_{ka}\delta_{lb} - \delta_{la}\delta_{kb} \\ &\quad -\delta_{ka}a_b^\dagger a_l + \delta_{kb}a_a^\dagger a_l + \delta_{la}a_b^\dagger a_k - \delta_{lb}a_a^\dagger a_k + a_a^\dagger a_b^\dagger a_l a_k\,. \end{aligned} \tag{4.25}$$

Only the first two terms in this expression contribute to (4.23) since $a_k|0\rangle = 0$. Therefore,

$$\langle ab|G|ab\rangle = \frac{1}{2}\sum_{ijkl} g_{ijkl}\langle 0|(\delta_{ia}\delta_{jb} - \delta_{ib}\delta_{ja})(\delta_{ka}\delta_{lb} - \delta_{la}\delta_{kb})|0\rangle = g_{abab} - g_{abba}\,. \tag{4.26}$$

This is precisely the result that we obtain in configuration space using a Slater determinant wave function.

Schrödinger Hamiltonian: With the aid of the second quantization expressions for one- and two-body operators, we write the expression for the Hamiltonian in second quantization as $H = H_0 + V$, where

$$H_0 = \sum_k \epsilon_k \, a_k^\dagger a_k \,, \tag{4.27}$$

$$V = \frac{1}{2} \sum_{ijkl} g_{ijkl} \, a_i^\dagger a_j^\dagger a_l a_k - \sum_{ik} U_{ik} \, a_i^\dagger a_k \,. \tag{4.28}$$

Here, ϵ_k is the eigenvalue of the one-electron Schrödinger equation in a potential $-Z/r + U(r)$, the quantity g_{ijkl} is a two-electron matrix element of the Coulomb potential $g(r_{12}) = 1/r_{12}$ and U_{ik} is the one-electron matrix element of the background potential $U(r)$:

$$U_{ik} = \int d^3r \, \psi_i^\dagger(\mathbf{r}) U(r) \psi_k(\mathbf{r}) \,. \tag{4.29}$$

No-Pair Hamiltonian: The Dirac-Coulomb Hamiltonian of the previous chapter can also be cast in second-quantized form. Again, $H = H_0 + V$, where H_0 and V are given by the formulas (4.27-4.28). For the Dirac case, ϵ_k in (4.27) is an eigenvalue of the one-electron Dirac Hamiltonian in a potential $-Z/r + U(r)$, and g_{ijkl} is a two-electron Coulomb integral evaluated with Dirac orbitals. In the expression for the Hamiltonian, the operators are restricted to be creation and annihilation operators for *positive-energy* solutions to the Dirac equation. These are the solutions associated with electron states. Contributions from negative-energy (positron) states are omitted from the Hamiltonian entirely. The resulting Hamiltonian is called the *no-pair* Hamiltonian. Since positron states are not present in the no-pair Hamiltonian, effects of virtual electron-positron pairs on atomic structure are omitted. To account for these small effects, we must carry out a separate QED calculation. The no-pair Hamiltonian is free from the problems mentioned in the previous chapter in connection with the Dirac-Coulomb Hamiltonian; it can be used in higher-order perturbation theory calculations. The no-pair Hamiltonian was introduced in a slightly different form by Brown and Ravenhall (1951) and has been discussed in great detail by Mittleman (1971, 1972, 1981) and Sucher (1980).

4.2 6-j Symbols

Before continuing our discussion of many-body techniques, it is necessary to make a short digression into angular momentum theory to describe various ways of combining more than two angular momentum eigenstates to form a product state that is also an angular momentum eigenstate. The Wigner 6-j symbols arise when we consider coupling three states to give a state of definite angular momentum. It is clear that we can couple three states with angular momenta j_1, j_2 and j_3 to a total angular momentum J in various ways. For example, we

can first couple j_1 and j_2 to an intermediate angular momentum J_{12}, and then couple J_{12} and j_3 to J and M, leading to the state

$$|(j_1 j_2) J_{12} j_3\,, JM\rangle = \sum_{\substack{m_1 m_2 m_3 \\ M_{12}}} - \begin{array}{c} j_1 m_1 \\ \vdots \\ J_{12} M_{12} \\ \vdots \\ j_2 m_2 \end{array} - \begin{array}{c} J_{12} M_{12} \\ \vdots \\ JM \\ \vdots \\ j_3 m_3 \end{array} \quad |j_1 m_1\rangle |j_2 m_2\rangle |j_3 m_3\rangle\,. \tag{4.30}$$

Alternatively, we can couple j_2 and j_3 to J_{23}, and then couple j_1 to J_{23} to give the resulting value of J and M. This order of coupling leads to the state

$$|j_1 (j_2 j_3) J_{23}\,, JM\rangle = \sum_{\substack{m_1 m_2 m_3 \\ M_{23}}} - \begin{array}{c} j_2 m_2 \\ \vdots \\ J_{23} M_{23} \\ \vdots \\ j_3 m_3 \end{array} - \begin{array}{c} j_1 m_1 \\ \vdots \\ JM \\ \vdots \\ J_{23} M_{23} \end{array} \quad |j_1 m_1\rangle |j_2 m_2\rangle |j_3 m_3\rangle\,. \tag{4.31}$$

States obtained from either of these two coupling schemes can be expressed as linear combinations of states obtained using the other scheme. Thus, for example, we may write

$$|j_1 (j_2 j_3) J_{23}\,, JM\rangle = \sum_{J_{12}} |(j_1 j_2) J_{12} j_3\,, JM\rangle \, \langle (j_1 j_2) J_{12} j_3\,, JM | j_1 (j_2 j_3) J_{23}\,, JM\rangle\,. \tag{4.32}$$

The resulting recoupling coefficient $\langle (j_1 j_2) J_{12} j_3\,, JM | j_1 (j_2 j_3) J_{23}\,, JM\rangle$ is independent of M. We evaluate this coefficient by connecting the lines corresponding to j_1, j_2 and j_3 in the graphs from (4.30) and (4.31) above. The resulting graph has two free ends, both labeled by JM. Since the recoupling coefficient is independent of M, we may obtain the coefficient by averaging over M. This is done by connecting the free ends and dividing by $[J]$. The resulting coefficient can be expressed as

$$\begin{aligned} &\langle (j_1 j_2) J_{12} j_3\,, JM | j_1 (j_2 j_3) J_{23}\,, JM\rangle = \\ &\qquad (-1)^{j_1 + j_2 + j_3 + J} [J_{12}][J_{23}] \left\{ \begin{array}{ccc} j_1 & j_2 & J_{12} \\ j_3 & J & J_{23} \end{array} \right\}, \end{aligned} \tag{4.33}$$

where the expression in curly brackets can be brought into the graphical form

$$\left\{ \begin{array}{ccc} j_1 & j_2 & J_{12} \\ j_3 & J & J_{23} \end{array} \right\} = \; + \; \begin{array}{c} \\ \\ \\ \\ \\ \\ \\ \end{array} \tag{4.34}$$

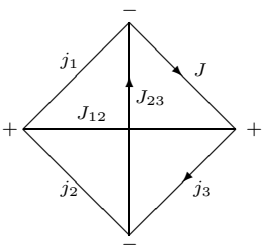

The quantity

$$\left\{ \begin{array}{ccc} j_1 & j_2 & J_{12} \\ j_3 & J & J_{23} \end{array} \right\}$$

is a 6-j symbol. This quantity vanishes unless angular momentum triangle inequalities are satisfied by the triples $j_1 j_2 J_{12}$, $j_3 J J_{12}$, $j_3 j_2 J_{23}$ and $j_1 J J_{23}$. Moreover, the 6-j symbols satisfy the symmetry relations

$$\left\{ \begin{array}{ccc} j_a & j_b & j_c \\ l_a & l_b & l_c \end{array} \right\} = \left\{ \begin{array}{ccc} j_b & j_a & j_c \\ l_b & l_a & l_c \end{array} \right\} = \left\{ \begin{array}{ccc} j_b & j_c & j_a \\ l_b & l_c & l_a \end{array} \right\} . \tag{4.35}$$

In other words, the 6-j symbol is invariant with respect to a permutation (even or odd) of columns. Further, the 6-j symbol satisfies the symmetry relations

$$\left\{ \begin{array}{ccc} j_a & j_b & j_c \\ l_a & l_b & l_c \end{array} \right\} = \left\{ \begin{array}{ccc} j_a & l_b & l_c \\ l_a & j_b & j_c \end{array} \right\} = \left\{ \begin{array}{ccc} l_a & j_b & l_c \\ j_a & l_b & j_c \end{array} \right\} ; \tag{4.36}$$

i.e, the 6-j symbol is invariant under inversion of the arguments in any two columns.

The graphical representation of the 6-j symbol leads to its analytical expression in terms of 3-j symbols

$$\begin{aligned} \left\{ \begin{array}{ccc} j_a & j_b & j_c \\ j_d & j_e & j_f \end{array} \right\} = & \sum_{m's} (-1)^K \times \\ & \left(\begin{array}{ccc} j_a & j_b & j_c \\ -m_a & -m_b & -m_c \end{array} \right) \left(\begin{array}{ccc} j_a & j_e & j_f \\ m_a & -m_e & m_f \end{array} \right) \times \\ & \left(\begin{array}{ccc} j_b & j_f & j_d \\ m_b & -m_f & m_d \end{array} \right) \left(\begin{array}{ccc} j_c & j_d & j_e \\ m_c & -m_d & m_e \end{array} \right) , \end{aligned} \tag{4.37}$$

with

$$K = j_a - m_a + j_b - m_b + j_c - m_c + j_d - m_d + j_e - m_e + j_f - m_f$$

A useful formula (Edmonds, 1974) for calculating 6-j symbols is

$$\begin{aligned} \left\{ \begin{array}{ccc} j_a & j_b & j_c \\ j_d & j_e & j_f \end{array} \right\} = & \Delta(j_a j_b j_c) \Delta(j_a j_e j_f) \Delta(j_d j_b j_f) \Delta(j_d j_e j_c) \times \\ & \sum_k \left[\frac{(-1)^k (k+1)!}{(k - j_a - j_b - j_c)!\,(k - j_a - j_e - j_f)!} \times \right. \\ & \frac{1}{(k - j_d - j_b - j_f)!\,(k - l_d - j_e - j_c)!\,(j_a + j_b + j_d + j_e - k)!} \times \\ & \left. \frac{1}{(j_b + j_c + j_e + j_f - k)!\,(j_c + j_a + j_f + j_d - k)!} \right] , \end{aligned} \tag{4.38}$$

where

$$\Delta(j_a j_b j_c) = \sqrt{\frac{(j_a + j_b - j_c)!\,(j_a - j_b + j_c)!\,(-j_a + j_b + j_c)!}{(j_a + j_b + j_c + 1)!}} . \tag{4.39}$$

The 6-j symbols satisfy the following orthogonality relation

$$\sum_{j_f} [j_c][j_f] \left\{ \begin{array}{ccc} j_a & j_b & j_c \\ j_d & j_e & j_f \end{array} \right\} \left\{ \begin{array}{ccc} j_a & j_b & j'_c \\ j_d & j_e & j_f \end{array} \right\} = \delta_{j_c j'_c} . \tag{4.40}$$

Additionally, they satisfy the following two sum rules: (Racah)

$$\sum_{j_f}(-1)^{j_c+j+j_f}[j_f]\left\{\begin{array}{ccc} j_a & j_b & j_c \\ j_d & j_e & j_f \end{array}\right\}\left\{\begin{array}{ccc} j_a & j_d & j \\ j_b & j_e & j_f \end{array}\right\}=\left\{\begin{array}{ccc} j_a & j_b & j_c \\ j_e & j_d & j \end{array}\right\}, \tag{4.41}$$

and (Biedenharn, 1953; Elliott, 1953)

$$\sum_{k}(-1)^{S+k}[k]\left\{\begin{array}{ccc} l_1 & j_2 & l_3 \\ l_3' & l_2' & k \end{array}\right\}\left\{\begin{array}{ccc} j_2 & j_3 & j_1 \\ l_1' & l_3' & k \end{array}\right\}\left\{\begin{array}{ccc} l_1 & j_3 & l_2 \\ l_1' & l_2' & k \end{array}\right\}$$
$$=\left\{\begin{array}{ccc} j_1 & j_2 & j_3 \\ l_1 & l_2 & l_3 \end{array}\right\}\left\{\begin{array}{ccc} l_3 & j_1 & l_2 \\ l_1' & l_2' & l_3' \end{array}\right\}, \tag{4.42}$$

where $S=j_1+j_2+j_3+l_1+l_2+l_3+l_1'+l_2'+l_3'$. The following special case is often useful

$$\left\{\begin{array}{ccc} j_1 & j_2 & j_3 \\ l_1 & l_2 & 0 \end{array}\right\}=\delta_{j_1 l_2}\delta_{j_2 l_1}\frac{(-1)^{j_1+j_2+j_3}}{\sqrt{[j_1][j_2]}}\,. \tag{4.43}$$

4.3 Two-Electron Atoms

In this Section, we use second quantization to study the excited states of two-electron atoms and ions. We start our discussion by considering a two-electron state $|ab\rangle$. This is an eigenstate of H_0, with eigenvalue $E_{ab}^{(0)}=\epsilon_a+\epsilon_b$:

$$H_0\,|ab\rangle=(\epsilon_a+\epsilon_b)\,|ab\rangle\,. \tag{4.44}$$

The state $|ab\rangle$ is $2[l_a]\times 2[l_b]$-fold degenerate. It is not necessarily an angular momentum eigenstate. We make use of the degeneracy to construct eigenstates of L^2, L_z, S^2 and S_z from $|ab\rangle$. To this end, we first couple l_a and l_b to give an eigenstate of L^2 and L_z, then we couple s_a ($s_a=1/2$) and s_b ($s_b=1/2$) to give an eigenstate of S^2 and S_z. The possible eigenvalues of S^2 are $S(S+1)$, where $S=0$ or 1. States with $S=0$ are referred to as singlet states, since there is only one such state with $M_S=0$. States with $S=1$ are called triplet states. The resulting eigenstates of L^2, L_z, S^2 and S_z are called LS-coupled states. Singlet states are also eigenstates of J ($\mathbf{J}=\mathbf{L}+\mathbf{S}$) with $J=L$. Triplet states can be further combined to give eigenstates of J having eigenvalues $L-1$, L, $L+1$. Nonrelativistically, the triplet states with different values of J are degenerate. This degeneracy is lifted in relativistic calculations. The observed spectrum of helium consists of singlets and triplets of various angular symmetries S, P, ... corresponding to $L=0,1,\ldots$. The triplets are slightly split by relativistic effects. LS-coupled states with orbital angular momentum L, spin angular momentum S, and total angular momentum J are designated by the spectroscopic notation $^{2S+1}L_J$. In Fig. 4.1, we show the approximate ordering of the low-lying singlet and triplet levels of helium in an energy level (or Grotrian) diagram.

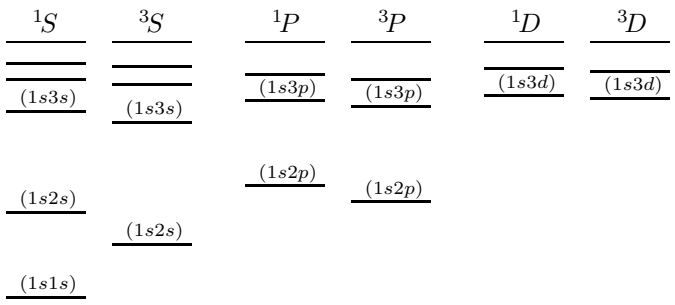

Figure 4.1: Energy level diagram for helium

To form the LS-coupled states, we combine the degenerate states according to

$$|ab, LM_L, SM_S\rangle = \eta \sum_{m_a m_b \mu_a \mu_b} - \begin{array}{|l} l_a m_a \\ \\ l_b m_b \end{array}^{LM_L} - \begin{array}{|l} 1/2\mu_a \\ \\ 1/2\mu_b \end{array}^{SM_S} a_a^\dagger a_b^\dagger |0\rangle \,. \tag{4.45}$$

Here, η is a normalization factor. The norm of this coupled state is easily shown to be

$$\langle ab, LM_L, SM_s | ab, LM_L, SM_s\rangle = \eta^2 (1 + (-1)^{S+L} \delta_{n_b n_a} \delta_{l_a l_b}) \,. \tag{4.46}$$

For states with $n_b \neq n_a$ or $l_b \neq l_a$, we obtain a normalized state by choosing $\eta = 1$. For states formed from identical orbitals ($n_b = n_a$ and $l_b = l_a$), the sum $L + S$ must be even in order to have a normalizable state. To normalize such a state, we choose $\eta = 1/\sqrt{2}$. An example of a state formed from identical orbitals is the $(1s)^2$ ground state. This state has $L = 0$ and $S = 0$; it is a $^1S_0$ state.

The first-order correction to the energy of an LS-coupled state is given by

$$E^{(1)}_{ab,LS} = \langle ab, LM_L, SM_S | V | ab, LM_L, SM_S\rangle \,. \tag{4.47}$$

This result can be written

$$E^{(1)}_{ab,LS} = \eta^2 \sum_{m' s \mu' s} - \begin{array}{|l} l_a m_a \\ \\ l_b m_b \end{array}^{LM_L} - \begin{array}{|l} 1/2\mu_a \\ \\ 1/2\mu_b \end{array}^{SM_S} - \begin{array}{|l} l'_a m'_a \\ \\ l'_b m'_b \end{array}^{LM_L} - \begin{array}{|l} 1/2\mu'_a \\ \\ 1/2\mu'_b \end{array}^{SM_S}$$

$$\Big[g_{a'b'ab} \delta_{\mu'_a \mu_a} \delta_{\mu'_b \mu_b} - g_{a'b'ba} \delta_{\mu'_a \mu_b} \delta_{\mu'_b \mu_a} - (\delta_{a'a} \delta_{b'b} - \delta_{a'b} \delta_{b'a})(U_{aa} + U_{bb}) \Big] \,.$$

We make use of the identity

$$g_{abcd} = \sum_k - \begin{array}{|l} l_a m_a \\ \\ \\ l_c m_c \end{array}^{\quad k \quad} + \begin{array}{|l} l_b m_b \\ \\ \\ l_d m_d \end{array} \quad X_k(abcd) \,, \tag{4.48}$$

where

$$X_k(abcd) = (-1)^k \langle l_a||C^k||l_c\rangle \langle l_b||C^k||l_d\rangle R_k(abcd)\,. \tag{4.49}$$

Substituting this into the expression for the first-order energy, we find

$$E^{(1)}_{ab,LS} = \eta^2 \sum_k \left[(-1)^{L+k+l_a+l_b} \left\{ \begin{array}{ccc} l_a & l_b & L \\ l_b & l_a & k \end{array} \right\} X_k(abab) \right.$$
$$\left. + (-1)^{S+k+l_a+l_b} \left\{ \begin{array}{ccc} l_a & l_b & L \\ l_a & l_b & k \end{array} \right\} X_k(abba) \right] - U_{aa} - U_{bb}\,. \tag{4.50}$$

Let us consider the special case where a is a $1s$ state and b is an nl excited state. Such states are single-particle excitations of the helium ground state. All of the bound levels of helium are of this type; doubly-excited states of helium are not bound! We, therefore, set $l_a = 0$ and $l_b = l$ in Eq.(4.50). In the first term, $k = 0$ so the sum reduces to

$$R_0(1s, nl, 1s, nl)\,.$$

Here, we have made use of Eq.(4.43) and the fact that $\langle s||C^k||s\rangle = \delta_{k0}$ and $\langle l||C^0||l\rangle = \sqrt{[l]}$. In the second term, we find from Eq.(4.43) that $k = L = l$. Furthermore, $\langle l||C^l||s\rangle = 1$, and $\langle s||C^l||l\rangle = (-1)^l$. Therefore, the second term reduces to

$$(-1)^S \frac{1}{[l]} R_l(1s, nl, nl, 1s)\delta_{Ll}\,.$$

Combining these results, we obtain for $(1snl)$ states

$$E^{(1)}_{1snl,LS} = \left[\eta^2 \left(R_0(1s, nl, 1s, nl) + (-1)^S \frac{1}{[l]} R_l(1s, nl, nl, 1s) \right) \right.$$
$$\left. - U_{1s1s} - U_{nlnl} \right] \delta_{Ll}. \tag{4.51}$$

First, let us consider the case $nl = 1s$. In this case, as discussed above, $S = 0$ and $\eta = 1/\sqrt{2}$, leading to the result

$$E^{(1)}_{1s1s,00} = R_0(1s, 1s, 1s, 1s) - 2U_{1s1s}\,. \tag{4.52}$$

This is precisely the expression obtained in the previous section for the first-order correction to the ground-state energy of a heliumlike ion. For states with $nl \neq 1s$, $\eta = 1$ and we find

$$E^{(1)}_{1snl,LS} = \left(R_0(1s, nl, 1s, nl) + (-1)^S \frac{1}{[l]} R_l(1s, nl, nl, 1s) \right.$$
$$\left. - U_{1s1s} - U_{nlnl} \right) \delta_{Ll}. \tag{4.53}$$

The lowest-order energy of these states, $\epsilon_{1s} + \epsilon_{nl}$, is independent of S. The separation between the singlet and triplet states is, therefore, given by

$$\Delta E = E_{1snl,S=0} - E_{1snl,S=1} = \frac{2}{[l]} R_l(1s, nl, nl, 1s)\,.$$

Table 4.1: Energies of $(1snl)$ singlet and triplet states of helium (a.u.). Comparison of a model-potential calculation with experiment (Moore, 1957).

	Singlet		Triplet		ΔE	
nl	Theory	Exp.	Theory	Exp.	Theory	Exp.
$2s$	-.153734	-.145954	-.172019	-.175212	.018285	.029258
$3s$	-.063228	-.061264	-.068014	-.068682	.004785	.007418
$4s$	-.034363	-.033582	-.036265	-.036508	.001902	.002925
$5s$	-.021562	-.021174	-.022502	-.022616	.000940	.001442
$2p$	-.121827	-.123823	-.130465	-.133154	.008638	.009331
$3p$	-.054552	-.055126	-.057337	-.058075	.002785	.002939
$4p$	-.030820	-.031065	-.032022	-.032321	.001202	.001258
$5p$	-.019779	-.019903	-.020400	-.020549	.000621	.000645
$3d$	-.055546	-.055614	-.055572	-.055629	.000026	.000015
$4d$	-.031244	-.031276	-.031260	-.031285	.000015	.000008
$5d$	-.019997	-.020014	-.020006	-.020018	.000009	.000005
$4f$	-.031250	-.031246	-.031250	-.031249	.000000	.000003
$5f$	-.020000	-.020005	-.020000	-.019999	.000000	-.000007

In Table 4.1, we compare a first-order perturbation theory calculation of the energies of the singlet and triplet S, P, D, and F states of helium with experiment. For the purposes of this calculation, we assume that the $1s$ electron moves in the unscreened potential of the nucleus, but that the excited nl electrons move in the field of the nucleus screened by the monopole potential $v_0(1s, r)$ of the $1s$ electron. This somewhat exotic potential can be formally described in terms of projection operators. We let $P = |1s\rangle\langle 1s|$ be the projection operator onto the $1s$ state, and Q be the projection operator onto the complement to the $1s$ state:

$$Q = \sum_{nl \neq 1s} |nl\rangle\langle nl| \,.$$

It follows that $P + Q = 1$. We represent the screening potential by

$$U = Q\, v_0\, Q = v_0 - P\, v_0 - v_0\, P + P\, v_0\, P \,. \tag{4.54}$$

Note that

$$U|1s\rangle = v_0|1s\rangle - |1s\rangle\langle 1s|v_0|1s\rangle - v_0\,|1s\rangle + |1s\rangle\langle 1s|v_0\,|1s\rangle = 0\,, \tag{4.55}$$

while for $nl \neq 1s$ we find,

$$U|nl\rangle = v_0|nl\rangle - |1s\rangle\langle 1s|v_0|nl\rangle \,. \tag{4.56}$$

For states with $l \neq 0$, the second term in the above expression vanishes and $U = v_0(1s, r)$. For states with $l = 0$, the second term insures that the resulting radial wave function is orthogonal to the $1s$ wave function. Notice that $U_{1s1s} = 0$ for this potential, and that $U_{nlnl} = R_0(1s, nl, 1s, nl)$. For comparison with experiment, we evaluate the energy relative to that of the hydrogenlike ion formed when the nl electron is removed. The energy of the hydrogenic ion is precisely ϵ_{1s}. The energy relative to the ion in this model potential is, therefore, given by

$$E_{1snl,LS} - E_{\rm ion} = \epsilon_{nl} + (-1)^S \frac{1}{[l]} R_l(1s, nl, nl, 1s)\,. \tag{4.57}$$

Values obtained from this formula are tabulated in Table 4.1. As seen from this Table, this simple model potential suffices to predict the multiplet structure in helium at the few-percent level of accuracy.

4.4 Atoms with One or Two Valence Electrons

In this section, we study states of atoms that have one or two valence electrons beyond closed shells. For atoms with one valence electron, the present section is an extension of our previous discussion using the $V_{\rm HF}^{N-1}$ potential. For atoms with two valence electrons, the material here is an extension of the discussion of excited states of helium given in the previous section.

We let $|0_c\rangle$ represent the ionic core, which is assumed to consists of filled subshells,

$$|0_c\rangle = a_a^\dagger a_b^\dagger \cdots |0\rangle\,. \tag{4.58}$$

The states of interest can then be described as

$$|v\rangle = a_v^\dagger |0_c\rangle\,, \tag{4.59}$$

$$|vw\rangle = a_v^\dagger a_w^\dagger |0_c\rangle\,, \tag{4.60}$$

where the indices v and w designate orbitals that are different from any of those occupied in the core. Here and later, we adopt the notation that letters at the beginning of the alphabet a, b, $\cdots$, designate core orbitals, letters in the middle of the alphabet i, j, $\cdots$, designate either core or excited (outside of the core) orbitals, letters m, n, $\cdots$, represent excited orbitals, and letters at the end of the alphabet v, w, $\cdots$, represent valence orbitals. Valence orbitals are, of course, special cases of excited orbitals.

It is useful to introduce the normal product of operators here. The normal product of two operators is defined as the product rearranged so that core creation operators are always put to the right of core annihilation operators and excited state annihilation operators are always put to the right of excited state creation operators. In carrying out that rearrangement, a sign change is made for each operator transposition. Normal products are designated by enclosing the operators between pairs of colons; thus $: a_a^\dagger a_n :$ represents the normal product of the operators $a_a^\dagger$ and a_n. Normal products of two creation

operators or two annihilation operators are just the product of the two operators. Moreover,

$$\begin{aligned} :a_m^\dagger a_n: &= a_m^\dagger a_n\,, \\ :a_n a_m^\dagger: &= -a_m^\dagger a_n\,, \\ :a_a^\dagger a_b: &= -a_b a_a^\dagger\,, \\ :a_b a_a^\dagger: &= a_b a_a^\dagger\,. \end{aligned}$$

This definition can be extended to arbitrary products of operators. The normal product of N operators is the product of the N operators rearranged so that core creation operators are to the right of core annihilation operators and excited state annihilation operators are to the right of excited state creation operators with a sign change for each transposition of two operators. With this definition, it follows that the expectation value of the normal product of two operators calculated in the core state vanishes:

$$\langle 0_c| :o_i o_j \cdots o_l: |0_c\rangle = 0\,. \tag{4.61}$$

Here o_i designates either a creation operator $a_i^\dagger$ or an annihilation operator a_i.

The Hamiltonian H can be expressed in terms of normal products by

$$H = H_0 + V\,, \tag{4.62}$$

$$H_0 = E_0 + \sum_k \epsilon_k :a_k^\dagger a_k:\,, \tag{4.63}$$

$$\begin{aligned} V &= \frac{1}{2}\sum_{ijkl} g_{ijkl} :a_i^\dagger a_j^\dagger a_l a_k: + \sum_{ij} (V_{\rm HF} - U)_{ij} :a_i^\dagger a_j: \\ &\quad + V_0\,. \end{aligned} \tag{4.64}$$

Here

$$E_0 = \sum_a \epsilon_a\,,$$

and

$$V_0 = \sum_a \left[\frac{1}{2}(V_{\rm HF})_{aa} - U_{aa}\right]\,.$$

In the above equations we have used the notation

$$(V_{\rm HF})_{ij} = \sum_b \left(g_{ibjb} - g_{ibbj}\right)\,. \tag{4.65}$$

The quantity $V_{\rm HF}$ is just the Hartree-Fock potential of the closed core. We should notice that

$$E_{\rm core} = \langle 0_c|H|0_c\rangle = E_0 + V_0 = \sum_a \epsilon_a + \frac{1}{2}\sum_{ab}\left(g_{abab} - g_{abba}\right) - \sum_a U_{aa}\,. \tag{4.66}$$

This result was derived previously by manipulating Slater determinants.

One valence electron: Let us first consider an atom with one valence electron in a state v. To help evaluate the expectation value of H_0, we make use of the easily established identity

$$\begin{aligned} a_v : a_k^\dagger a_k : a_v^\dagger =: a_v a_k^\dagger a_k a_v^\dagger : \\ +\delta_{kv} : a_k a_v^\dagger : +\delta_{kv} : a_v a_k^\dagger : + : a_k^\dagger a_k : +\delta_{kv}. \end{aligned} \tag{4.67}$$

From this identity, it follows that

$$\langle v| : a_k^\dagger a_k : |v\rangle = \langle 0_c|a_v : a_k^\dagger a_k : a_v^\dagger|0_c\rangle = \delta_{kv}\,. \tag{4.68}$$

Therefore, from Eq.(4.63) it follows that,

$$E_v^{(0)} = \langle v|H_0|v\rangle = E_0 + \epsilon_v\,. \tag{4.69}$$

To evaluate the first-order energy, we make use of the identities

$$\langle 0_c|a_v : a_i^\dagger a_j^\dagger a_l a_k : a_v^\dagger|0_c\rangle = 0\,, \tag{4.70}$$

$$\langle 0_c|a_v : a_i^\dagger a_j : a_v^\dagger|0_c\rangle = \delta_{iv}\delta_{jv}\,. \tag{4.71}$$

Combining these relations with the expression for V given in Eq.(4.64), we find

$$E_v^{(1)} = \langle v|V|v\rangle = V_0 + (V_{\rm HF} - U)_{vv}\ . \tag{4.72}$$

To first order, we therefore have

$$E_v = E_{\rm core} + \epsilon_v + (V_{\rm HF} - U)_{vv}\ . \tag{4.73}$$

If we let U be the Hartree-Fock potential of the core, then the valence orbital is just the $V_{\rm HF}^{N-1}$ orbital discussed in the previous section. As we found previously, ϵ_v is the difference between the energy of the atom and ion. This rule will, of course, be modified when we consider corrections from higher-order perturbation theory. For atoms with one valence electron, the second-quantization approach leads easily to results obtained previously by evaluating matrix elements using Slater determinants.

Two valence electrons: Now, let us turn to atoms having two valence electrons. As an aid to evaluating the energy for such atoms, we make use of the identities

$$\begin{aligned} \langle 0_c|a_w a_v : a_i^\dagger a_j^\dagger a_l a_k : a_v^\dagger a_w^\dagger|0_c\rangle &= (\delta_{iv}\delta_{jw} - \delta_{jv}\delta_{iw}) \times \\ &\quad (\delta_{kv}\delta_{lw} - \delta_{lv}\delta_{kw})\,, \end{aligned} \tag{4.74}$$

$$\langle 0_c|a_w a_v : a_i^\dagger a_j : a_v^\dagger a_w^\dagger|0_c\rangle = \delta_{iv}\delta_{jv} + \delta_{iw}\delta_{jw}\,. \tag{4.75}$$

From these identities, we find for the lowest-order energy,

$$E_{vw}^{(0)} = \langle vw|H_0|vw\rangle = E_0 + \epsilon_v + \epsilon_w\,, \tag{4.76}$$

and for the first-order energy,

$$\begin{aligned} E^{(1)}_{vw} &= \langle vw|V|vw\rangle \\ &= V_0 + (V_{\rm HF}-U)_{vv} + (V_{\rm HF}-U)_{ww} + g_{vwvw} - g_{vwwv}\,. \end{aligned} \tag{4.77}$$

Combining, we find to first order

$$E_{vw} = E_{\rm core} + \epsilon_v + \epsilon_w + (V_{\rm HF}-U)_{vv} + (V_{\rm HF}-U)_{ww} + g_{vwvw} - g_{vwwv}\,. \tag{4.78}$$

For the purpose of illustration, we assume that $U = V_{\rm HF}$ in Eq.(4.78), and we measure energies relative to the closed core. We then have $E^{(0)}_{vw} = \epsilon_v + \epsilon_w$ and $E^{(1)}_{vw} = g_{vwvw} - g_{wvvw}$. As in the case of helium, the degenerate states v and w can be combined to form eigenstates of L^2, L_z, S^2 and S_z. The expression for $E^{(1)}$ in an LS basis is found from (4.50) to be:

$$\begin{aligned} E^{(1)}_{vw,LS} = \eta^2 \sum_k \Bigg[&(-1)^{L+k+l_v+l_w} \begin{Bmatrix} l_v & l_w & L \\ l_w & l_v & k \end{Bmatrix} X_k(vwvw) \\ &+(-1)^{S+k+l_v+l_w} \begin{Bmatrix} l_v & l_w & L \\ l_v & l_w & k \end{Bmatrix} X_k(vwwv) \Bigg]\,. \end{aligned} \tag{4.79}$$

Here $\eta = 1/\sqrt{2}$ for the case of identical particles ($n_v = n_w$ and $l_v = l_w$), and $\eta = 1$ otherwise. For the identical-particle case, the sum $L+S$ must be an even integer.

As specific examples, let us consider the atoms such as beryllium or magnesium which, in the ground state, have two s electrons outside closed shells. In the ground state, beryllium ($Z = 4$) has two $2s$ electrons outside a heliumlike core and magnesium ($Z = 12$) has two $3s$ electrons outside of a neonlike core. Other such atoms are calcium, zinc, mercury and radium. The low-lying excited states of these atoms are ($2snl$) singlet or triplet states for beryllium, ($3snl$) singlet or triplet states for magnesium, etc.. For such states, the expression for the first-order energy simplifies to a form similar to that obtained for helium:

$$E^{(1)}_{ksnl,LS} = \eta^2 \left(R_0(ks,nl,ks,nl) + (-1)^S \frac{1}{[l]} R_l(ks,nl,nl,ks) \right) \delta_{Ll}\,. \tag{4.80}$$

Combining this with the lowest-order energy, we find for the $(ks)^2$ ground-state energy,

$$E_{ksks,00} = 2\epsilon_{ks} + R_0(ks,ks,ks,ks)\,, \tag{4.81}$$

and for ($ksnl$) excited states,

$$E_{ksnl,LS} = \epsilon_{ks} + \epsilon_{nl} + \left(R_0(ks,nl,ks,nl) + (-1)^S \frac{1}{[l]} R_l(ks,nl,nl,ks) \right) \delta_{Ll}\,. \tag{4.82}$$

For beryllium, magnesium and calcium, doubly excited $|(2p)^2, LS\rangle$, $|(3p)^2, LS\rangle$ and $|(4p)^2, LS\rangle$ states, respectively, are also observed in the bound state spectrum. Furthermore, doubly-excited $|3d4p, LS\rangle$ states are observed in the spectrum of calcium.

For $(kp)^2$ configurations, the sum $L+S$ must be even. Therefore, the possible states are ^1S, ^3P and ^1D. The first-order energy for these states is given by

$$E^{(1)}_{kpkp,00} = R_0(kp,kp,kp,kp) + \frac{2}{5}R_2(kp,kp,kp,kp), \quad (4.83)$$

$$E^{(1)}_{kpkp,11} = R_0(kp,kp,kp,kp) - \frac{1}{5}R_2(kp,kp,kp,kp), \quad (4.84)$$

$$E^{(1)}_{kpkp,20} = R_0(kp,kp,kp,kp) + \frac{1}{25}R_2(kp,kp,kp,kp). \quad (4.85)$$

From this, it is predicted in first-order that the ^3P state has the lowest energy and that the ^1S state has the highest energy.

Both carbon ($Z = 6$) and silicon ($Z = 14$) have two kp electrons beyond closed $(ks)^2$ shells in their ground states. We therefore expect the ground states of these atoms to be ^3P state and we expect the next two excited states to be ^1D and ^1S states, respectively. The collection of states from the $(kp)^2$ configuration is called the ground-state multiplet.

The lowest state in the observed spectrum of both carbon and silicon is a ^3P state as predicted, and the next two states are ^1D and ^1S states, as expected. From Eqs.(4.83-4.85), we predict that

$$R = \frac{E(kpkp,00) - E(kpkp,20)}{E(kpkp,00) - E(kpkp,11)} = \frac{3}{5}\,.$$

For carbon the observed ratio is $R = 0.529$, while for silicon $R = 0.591$.

Another interesting example is titanium ($Z = 24$) which has a ground-state configuration $(3d)^2$. For this case, the ground-state multiplet consists of the ^1S, ^3P, ^1D, ^3F and ^1G states. The first-order energy is given by

$$E^{(1)}_{3d3d,00} = R_0 + \frac{2}{7}R_2 + \frac{2}{7}R_4, \quad (4.86)$$

$$E^{(1)}_{3d3d,11} = R_0 + \frac{1}{7}R_2 - \frac{4}{21}R_4, \quad (4.87)$$

$$E^{(1)}_{3d3d,20} = R_0 - \frac{3}{49}R_2 + \frac{4}{49}R_4, \quad (4.88)$$

$$E^{(1)}_{3d3d,31} = R_0 - \frac{8}{49}R_2 - \frac{1}{49}R_4, \quad (4.89)$$

$$E^{(1)}_{3d3d,40} = R_0 + \frac{4}{49}R_2 + \frac{1}{441}R_4, \quad (4.90)$$

where $R_k \equiv R_k(3d,3d,3d,3d)$. From Eqs.(4.86-4.90), we expect the order of the levels in the ground-state multiplet of titanium to be (from lowest to highest): ^3F, ^1D, ^3P, ^1G and ^1S. This ordering of levels is indeed observed in the ground-state multiplet.

4.5 Particle-Hole Excited States

The low-lying excited states of noble gas atoms are those in which an outer-shell electron is promoted to a single-particle state outside of the core, leaving

a vacancy (or hole) in the closed shell. The particle-hole state in which a core electron with quantum numbers a is excited to a state with quantum numbers v is represented by the state vector $|va\rangle$:

$$|va\rangle = a_v^\dagger a_a |0_c\rangle \tag{4.91}$$

This state is an eigenstate of H_0 with eigenvalue

$$E_{va}^{(0)} = E_0 + \epsilon_v - \epsilon_a \, .$$

The state is $2[l_v] \times 2[l_a]$-fold degenerate. Again, we make use of the degeneracy to form LS-coupled angular momentum states. Here, some caution is required. A state with a hole in substate $\cdots m_a, \mu_a$, has angular momentum properties of a particle with angular momemtum components $\cdots - m_a, -\mu_a$. Moreover, if the state $|0_c\rangle$ is formed by applying creation operators to the vacuum in descending order; namely,

$$|0_c\rangle = \cdots a^\dagger_{n_a l_a, l_a, 1/2} a^\dagger_{n_a l_a, l_a, -1/2} a^\dagger_{n_a l_a, l_a-1, 1/2} a^\dagger_{n_a l_a, l_a-1, -1/2} \cdots a^\dagger_{n_a l_a, -l_a, 1/2} a^\dagger_{n_a l_a, -l_a, -1/2} |0\rangle \, ,$$

then an extra factor of

$$(-1)^{l_a - m_a} \times (-1)^{1/2 - \mu_a}$$

is obtained in transposing the operator a_a to the position to the left of $a_a^\dagger$ in the wave function, where we can replace the product $a_a a_a^\dagger$ by 1. Thus, the state vector corresponding to a particle with angular momentum l_v, m_v, μ_v and hole with angular momentum $l_a, -m_a, -\mu_a$ is

$$(-1)^{l_a - m_a} (-1)^{1/2 - \mu_a} a_v^\dagger a_a |0_c\rangle \, .$$

States of this type can be combined to form an LS state. We find,

$$|va, LS\rangle = \sum_{\substack{m_v m_a \\ \mu_v \mu_a}} (-1)^{l_a - m_a} -$$
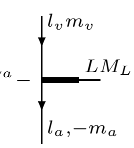

$$(-1)^{1/2 - \mu_a} -$$
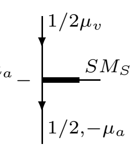

$$a_v^\dagger a_a |0_c\rangle$$

$$= \sum_{\substack{m_v m_a \\ \mu_v \mu_a}} -$$
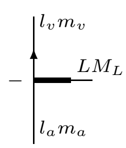

$$-$$
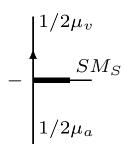

$$a_v^\dagger a_a |0_c\rangle \, . \tag{4.92}$$

These states are properly normalized:

$$\langle va | va \rangle = 1 \, .$$

The first-order energy for the state $|va, LS\rangle$ is evaluated using the relations

$$\langle 0_c | a_c^\dagger a_w : a_i^\dagger a_j : a_v^\dagger a_a | 0_c \rangle = \delta_{jv} \delta_{iw} \delta_{ac} - \delta_{jc} \delta_{ia} \delta_{vw} \, , \tag{4.93}$$

$$\langle 0_c | a_c^\dagger a_w : a_i^\dagger a_j^\dagger a_l a_k : a_v^\dagger a_a | 0_c \rangle = (\delta_{lv} \delta_{kc} - \delta_{kv} \delta_{lc}) \times (\delta_{ja} \delta_{iw} - \delta_{ia} \delta_{jw}). \tag{4.94}$$

Table 4.2: Comparison of $V_{\rm HF}^{N-1}$ energies of $(3s2p)$ and $(3p2p)$ particle-hole excited states of neon and neonlike ions with measurements.

Ion	$V_{\rm HF}^{N-1}$	Exp.	$V_{\rm HF}^{N-1}$	Exp.	$V_{\rm HF}^{N-1}$	Exp.	$V_{\rm HF}^{N-1}$	Exp.
	$(3s2p)\ ^3$P		$(3s2p)\ ^1$P		$(3p2p)\ ^3$S		$(3p2p)\ ^1$S	
Mg^{2+}	1.9942	1.9424	2.0234	1.9662	2.1778	2.1296	2.4162	2.2073
Na^{+}	1.2602	1.2089	1.2814	1.2246	1.3840	1.3360	1.5416	1.4073
Ne	0.6638	0.6118	0.6757	0.6192	0.7263	0.6755	0.7927	0.6970
	$(3p2p)\ ^3$P		$(3p2p)\ ^1$P		$(3p2p)\ ^3$D		$(3p2p)\ ^1$D	
Mg^{2+}	2.2300	2.1830	2.2300	2.1797	2.2091	2.1622	2.2275	2.1754
Na^{+}	1.4178	1.3681	1.4178	1.3664	1.4043	1.3558	1.4160	1.3632
Ne	0.7404	0.6877	0.7404	0.6870	0.7348	0.6826	0.7394	0.6849

From these relations, we conclude that the matrix element of V between uncoupled particle-hole states is

$$\langle wc|V|va\rangle = g_{wacv} - g_{wavc} + (V_{\rm HF}-U)_{wv}\delta_{ac} - (V_{\rm HF}-U)_{ac}\delta_{wv}\,. \tag{4.95}$$

For coupled states, we obtain

$$E^{(1)}_{va,LS} = \sum_{\substack{m_v\mu_v m_w\mu_w\\ m_a\mu_a m_c\mu_c}} - \begin{vmatrix} l_v m_v & & 1/2\mu_v & & l_w m_w & & 1/2\mu_w \\ & LM_L & & SM_S & & LM_L & & SM_S \\ l_a m_a & & 1/2\mu_a & & l_c m_c & & 1/2\mu_c \end{vmatrix}$$

$$[g_{wacv} - g_{wavc} + (V_{\rm HF}-U)_{wv}\delta_{ac} - (V_{\rm HF}-U)_{ac}\delta_{wv}]\,, \tag{4.96}$$

where $(n_w,l_w) = (n_v,l_v)$ and $(n_c,l_c) = (n_a,l_a)$. Carrying out the sums over magnetic substates, we obtain

$$\begin{aligned} E^{(1)}_{va,LS} &= (-1)^{l_v+l_a+l}\left(\frac{2}{[L]}\delta_{S0}X_L(vaav) - \sum_k \begin{Bmatrix} l_v & l_a & L \\ l_a & l_v & k \end{Bmatrix} X_k(vava)\right) \\ &+ (V_{\rm HF}-U)_{vv} - (V_{\rm HF}-U)_{aa}\,. \end{aligned} \tag{4.97}$$

This expression is simplified by choosing the potential U to be the $V_{\rm HF}^{N-1}$ potential, defined for closed shells as

$$V_{\rm HF}^{N-1} \stackrel{\rm def}{=} V_{\rm HF} + Q\Delta V Q\,. \tag{4.98}$$

The term $Q\Delta VQ$ subtracts the contribution of one core electron (assumed to have quantum numbers h) from the HF potential, when it acts on an excited-state orbital:

$$\Delta V P_n = -v_0(h,r)P_n + \sum_k \Lambda_{l_h k l_n} v_k(h,n,r)P_h\,. \tag{4.99}$$

In Eq.(4.98), $Q = 1 - P$ is the projection operator onto excited states:

$$P = \sum_a |a\rangle\langle a| \,, \tag{4.100}$$

$$Q = \sum_n |n\rangle\langle n| \,. \tag{4.101}$$

Setting $U = V_{\rm HF}^{N-1}$, we obtain

$$UP_a = V_{\rm HF} P_a \,, \tag{4.102}$$

$$UP_n = (V_{\rm HF} + \Delta V)\, P_n - \sum_a \langle a|\Delta V|n\rangle P_a \,. \tag{4.103}$$

It follows that $(V_{\rm HF} - U)_{aa} = 0$ and $(V_{\rm HF} - U)_{vv} = -(\Delta V)_{vv}$.

As an example, let us consider the excited states of Ne (Z=10) and the neonlike ions Na^+ (Z=11) and Mg^{2+} (Z=12). The low-lying states of these systems are the odd parity $(va) = (3s2p)$, ^3P and ^1P states. Just above these states are the even parity $(3p2p)$ ^3S, ^3D, ^1D, ^3P, ^1P and ^1S states. In Table 4.2, we show the results of calculations of the energies of these states using Eq.(4.97) with a $V_{\rm HF}^{N-1}$ potential. This model for the excited states of closed-shell systems leads to energies that agree with observation at the 10% level of accuracy. To improve the agreement, it is necessary to consider corrections from higher-order perturbation theory.

4.6 9-j Symbols

Let us consider the problem of coupling spin and orbital angular momenta of two electrons to total angular momentum J. This problem requires us to consider ways of coupling four angular momentum vectors, which can be done in several ways. For example, we may couple the orbital angular momenta l_1 and l_2 of the electrons to L, the spin angular momenta s_1 and s_2 to S, then couple the resulting L and S to a final J. This method of coupling the angular momenta of two electrons is referred to as LS coupling. The angular part of the two-electron wave function for an LS-coupled state is

$$|[(l_1 l_2)L]\,[(s_1 s_2)S]\,JM\rangle =$$

$$\sum_{\substack{m_1 m_2 \mu_1 \mu_2 \\ M_L M_S}} - \begin{array}{|l} l_1 m_1 \\ \\ l_2 m_2 \end{array} \begin{array}{l} \\ LM_L \\ \\ \end{array} - \begin{array}{|l} s_1 \mu_1 \\ \\ s_2 \mu_2 \end{array} \begin{array}{l} \\ SM_S \\ \\ \end{array} - \begin{array}{|l} LM_L \\ \\ SM_S \end{array} \begin{array}{l} \\ JM \\ \\ \end{array} \quad |l_1 m_1\rangle |l_2 m_2\rangle |s_1 \mu_1\rangle |s_2 \mu_2\rangle \tag{4.104}$$

As an alternative to LS coupling, we can first couple l_1 and s_1 to j_1, then couple l_2 and s_2 to j_2, and finally couple the resulting j_1 and j_2 to J. This is referred to as the jj coupling scheme. The angular parts of the one-electron wave function that results from coupling l_i and s_i to j_i are just the spherical spinors $\Omega_{\kappa_i m_i}$.

The angular part of the two-electron wave function in the jj coupling scheme is

$$|[(l_1 s_1)j_1]\,[(l_2 s_2)j_2]\,JM\rangle =$$

$$\sum_{\substack{m_1 m_2 \mu_1 \mu_2 \\ M_1 M_2}} -$$

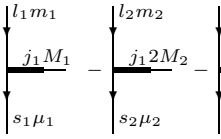

$$|l_1 m_1\rangle|l_2 m_2\rangle|s_1 \mu_1\rangle|s_2 \mu_2\rangle \quad (4.105)$$

Either scheme can be used to describe possible two-electron wave functions; the LS scheme is a more convenient starting point for describing states in atoms with low nuclear charge where relativistic (spin-orbit) effects are negligible, while the jj scheme is more convenient for atoms with high nuclear charge where relativistic effects are important. The natural starting point for relativistic calculations of two electron systems, where single-particle orbitals are taken from the Dirac equation, is the jj-scheme.

We may write each jj coupled wave functions as a linear combinations of LS wave functions:

$$|[(l_1 s_1)j_1]\,[(l_2 s_2)j_2]\,JM\rangle = \sum_{LS} \langle L\,S\,J \mid j_1\,j_2\,J\rangle\; |[(l_1 l_2)L]\,[(s_1 s_2)S]\,JM\rangle, \quad (4.106)$$

where the orthogonal matrix $\langle L\,S\,J \mid j_1\,j_2\,J\rangle$ is given diagrammatically by

$$\langle L\,S\,J \mid j_1\,j_2\,J\rangle = (-1)^R \sqrt{[L][S][j_1][j_2]}$$

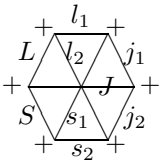

. (4.107)

The phase factor $R = l_1 + l_2 + s_1 + s_2 + j_1 + j_2 + L + S + J$ is the sum of all 9 angular momentum quantum numbers. The hexagonal diagram above serves to define the 9-j symbol:

$$\left\{ \begin{array}{ccc} a & b & c \\ d & e & f \\ g & h & j \end{array} \right\} =$$

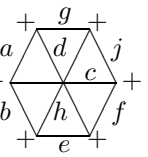

. (4.108)

The 9-j symbol can be expressed conveniently as a product of 3-j symbols:

$$\left\{ \begin{array}{ccc} a & b & c \\ d & e & f \\ g & h & j \end{array} \right\} = \sum_x (-1)^{2x}[x] \left\{ \begin{array}{ccc} a & b & c \\ f & j & x \end{array} \right\} \left\{ \begin{array}{ccc} d & e & f \\ b & x & h \end{array} \right\} \left\{ \begin{array}{ccc} g & h & j \\ x & a & d \end{array} \right\}. \quad (4.109)$$

The 9-j symbol is invariant under an even permutation of rows or columns. An odd permutation of rows or columns gives rise to a phase factor $(-1)^R$, where

R is the previously defined sum of nine angular momenta. The 9-j symbol is also symmetric with respect to a transposition of rows and columns. Thus, for example

$$\left\{ \begin{array}{ccc} a & b & c \\ d & e & f \\ g & h & j \end{array} \right\} = \left\{ \begin{array}{ccc} d & e & f \\ g & h & j \\ a & b & c \end{array} \right\} = (-1)^R \left\{ \begin{array}{ccc} d & e & f \\ a & b & c \\ g & h & j \end{array} \right\} = \left\{ \begin{array}{ccc} a & d & g \\ b & e & h \\ c & f & j \end{array} \right\} \tag{4.110}$$

With the aid of the symmetry relations, we may write the transformation matrix from the LS to jj scheme as

$$\langle L\, S\, J \mid j_1\, j_2\, J\rangle = \sqrt{[L][S][j_1][j_2]} \left\{ \begin{array}{ccc} L & S & J \\ l_1 & s_1 & j_1 \\ l_2 & s_2 & j_2 \end{array} \right\}. \tag{4.111}$$

A useful special case to bear in mind is that in which one angular momentum is zero. In that case, one finds:

$$\left\{ \begin{array}{ccc} a & b & c \\ d & e & f \\ g & h & 0 \end{array} \right\} = \delta_{cf}\delta_{gh} \frac{(-1)^{b+d+c+g}}{\sqrt{[c][g]}} \left\{ \begin{array}{ccc} a & b & c \\ e & d & g \end{array} \right\}. \tag{4.112}$$

The transformation from LS to jj coupling leads us into a discussion of relativistic effects in atoms.

4.7 Relativity and Fine Structure

In the preceding (nonrelativistic) discussion of excited-state energy levels, we found that on transforming to LS-coupled states, the interaction Hamiltonian V became diagonal. Each of the resulting LS states is still $[L]\times[S]$-fold degenerate. We can, of course, combine these degenerate LS states into eigenstates of J^2 and J_z, but the degeneracy of the resulting $|LS, JM_J\rangle$ states (designated by the spectroscopic notation $^{2S+1}L_J$) remains. In the case of one-electron atoms, where the eigenstates of orbital angular momentum split into eigenstates of J^2 with $j = l \pm 1/2$, the $2[l]$ fold degeneracy of the orbital angular momentum eigenstates is removed. The splitting between the states with a given value of l but different values of j is referred to as the "fine-structure" splitting. In a similar way, nonrelativistic many-particle LS states split into fine-structure components having different J values when relativistic effects are introduced.

4.7.1 He-like ions

Let us consider the relativistic two-particle state $|ab\rangle = a_a^\dagger a_b^\dagger |0\rangle$, where the single-particle indices $a = (n_a\kappa_a m_a)$ and $b = (n_b\kappa_b m_b)$ refer to quantum numbers of Dirac orbitals. This state is an eigenstate of the unperturbed part, H_0, of the no-pair Hamiltonian with eigenvalue $E^{(0)} = \epsilon_a + \epsilon_b$:

$$H_0|ab\rangle = (\epsilon_a + \epsilon_b)|ab\rangle\,. \tag{4.113}$$

The states $|ab\rangle$ are $[j_a] \times [j_b]$-fold degenerate. They can be combined to form eigenstates of J^2 and J_z ($|ab, JM_J\rangle$) using Clebsch-Gordan coefficients. The resulting states are referred to as jj-coupled states. We have

$$|ab, JM_J\rangle = \eta \sum_{m_a m_b} - \begin{array}{c} j_a m_a \\ \Big| \\ \hline\hline \\ \Big| \\ j_b m_b \end{array} \begin{array}{l} \\ JM_J \\ \\ \\ \end{array} a_a^\dagger a_b^\dagger |0\rangle \,. \tag{4.114}$$

These states are also eigenstates of parity with eigenvalue $P = (-1)^{l_a + l_b}$. The norm of the jj state in Eq.(4.114) is

$$\langle ab, JM_J | ab, JM_J \rangle = 1 + (-1)^J \delta_{ab} \,. \tag{4.115}$$

Thus, identical-particle states ($n_b = n_a$ and $\kappa_b = \kappa_a$) couple to even values of J only. It follows that we must introduce a normalization factor $\eta = 1/\sqrt{2}$ for identical-particle states, and $\eta = 1$ for other states. With this normalization, we obtain the following expression for the first-order energy:

$$\begin{aligned} E^{(1)}_{ab,J} = \eta^2 \sum_k \Bigg[& (-1)^{J+k+j_a+j_b} \left\{ \begin{array}{ccc} j_a & j_b & J \\ j_b & j_a & k \end{array} \right\} X_k(abab) \\ & + (-1)^{k+j_a+j_b} \left\{ \begin{array}{ccc} j_a & j_b & J \\ j_a & j_b & k \end{array} \right\} X_k(abba) \Bigg] - U_{aa} - U_{bb}, \end{aligned} \tag{4.116}$$

where the quantities $X_k(abcd)$ are given by the Dirac counterpart of Eq.(4.49),

$$X_k(abcd) = (-1)^k \langle \kappa_a || C^k || \kappa_c \rangle \langle \kappa_b || C^k || \kappa_d \rangle R_k(abcd) \,. \tag{4.117}$$

For heliumlike ions, the ground state is a $(1s1s)_{J=0}$. Although it is possible to couple two $j = 1/2$ states to form a $J = 1$ state, the above rule (J is even for identical-particle states) prohibits $J = 1$ in the $(1s)^2$ configuration. The lowest excited state nonrelativistically is the $(1s2s)$ $^3S_1$ state. Relativistically, this is the $(1s2s)_{J=1}$ state. The $(1s2s)$ $^1S_0$ state has the $(1s2s)_{J=0}$ state as its relativistic counterpart. The relativistic $(1s2p_{1/2})_{J=0}$ and $(1s2p_{3/2})_{J=2}$ states correspond to the nonrelativistic $^3P_0$ and $^3P_2$, respectively. The correspondence between nonrelativistic and relativistic $(1s2p)$ states is ambiguous for the case $J = 1$. Relativistically, we have two such states $(1s2p_{1/2})_1$ and $(1s2p_{3/2})_1$, while in the nonrelativistic case, we have the two states $^3P_1$ and $^1P_1$. On general grounds, we expect to be able to express the relativistic states that have $^3P_1$ and $^1P_1$ states as their nonrelativistic limits as linear combinations of the $(1s2p_{1/2})_1$ and $(1s2p_{3/2})_1$ states. Thus, we are led to consider the linear combination of relativistic states

$$|1s2p, 1\rangle = c_1 |1s2p_{1/2}, 1\rangle + c_2 |1s2p_{3/2}, 1\rangle \,, \tag{4.118}$$

with $c_1^2 + c_2^2 = 1$. The lowest-order energy in this state is given by

$$E^{(0)}_{1s2p} = c_1^2 \, \epsilon_{2p_{1/2}} + c_2^2 \, \epsilon_{2p_{3/2}} \,, \tag{4.119}$$

and the corresponding interaction energy is given by

$$\begin{aligned} E^{(1)}_{1s2p,1} &= c_1^2\left(\langle 1s2p_{1/2},1|V|1s2p_{1/2},1\rangle - U_{2p_{1/2},2p_{1/2}}\right) \\ &+ 2c_1c_2\,\langle 1s2p_{3/2},1|V|1s2p_{1/2},1\rangle \\ &+ c_2^2\left(\langle 1s2p_{3/2},1|V|1s2p_{3/2},1\rangle - U_{2p_{3/2},2p_{3/2}}\right). \end{aligned} \tag{4.120}$$

In the first of these two equations we have dropped a term ϵ_{1s} which is independent of the expansion coefficients c_1 and c_2, and, in the second equation, we have dropped a similar c-independent term $-U_{1s,1s}$. Diagonalizing the energy $E^{(0)}_{1s2p,1} + E^{(1)}_{1s2p,1}$ leads to the 2×2 eigenvalue equation:

$$\begin{pmatrix} \epsilon_{2p_{1/2}} + V_{1/2,1/2} - U_{1/2,1/2} & V_{1/2,3/2} \\ V_{3/2,1/2} & \epsilon_{2p_{3/2}} + V_{3/2,3/2} - U_{3/2,3/2} \end{pmatrix} \begin{pmatrix} c_1 \\ c_2 \end{pmatrix} = E \begin{pmatrix} c_1 \\ c_2 \end{pmatrix}, \tag{4.121}$$

where

$$U_{j,j'} = U_{2p_j,2p_{j'}}\delta_{jj'}\,, \tag{4.122}$$

$$\begin{aligned} V_{j,j'} &= \langle 1s2p_j,1|V|1s2p_{j'},1\rangle = R_0(1s,2p_j,1s,2p_{j'})\delta_{jj'} \\ &- 2\begin{Bmatrix} 1/2 & j & 1 \\ 1/2 & j' & 1 \end{Bmatrix} \begin{pmatrix} j & 1/2 & 1 \\ -1/2 & 1/2 & 0 \end{pmatrix} \begin{pmatrix} j' & 1/2 & 1 \\ -1/2 & 1/2 & 0 \end{pmatrix} \\ &\times R_1(1s,2p_j,2p_{j'},1s)\,. \end{aligned} \tag{4.123}$$

We must add $\epsilon_{1s} - U_{1s1s}$ to the eigenvalues of Eq. (4.121) to obtain the energies of the two relativistic $J = 1$ states. This additive term is, of course, just the energy of the one-electron ion formed when the two-electron system is ionized and is omitted when energies are calculated relative to the ionization threshold.

It is instructive to consider the nonrelativistic limit of the energies of the four $|1s2p_j,\,J\rangle$ states. For the $J = 0$ and $J = 2$ states, we find

$$E_{1s2p_{1/2},0} = \epsilon_{2p} + R_0(1s,2p,1s,2p) - \frac{1}{3}R_1(1s,2p,2p,1s) - U_{2p,2p} \tag{4.124}$$

$$E_{1s2p_{3/2},2} = \epsilon_{2p} + R_0(1s,2p,1s,2p) - \frac{1}{3}R_1(1s,2p,2p,1s) - U_{2p,2p}. \tag{4.125}$$

Since we are considering the nonrelativistic limit, we do not distinguish between $2p_{1/2}$ and $2p_{3/2}$. These two levels are degenerate in the nonrelativistic limit and have precisely the energy obtained in Eq. (4.53) for a nonrelativistic ^3P state. The 2×2 eigenvalue problem for the $J = 1$ case simplifies to

$$\begin{aligned} &(E - \epsilon_{2p} - R_0(1s2s1s2p) + U_{2p,2p}) \begin{pmatrix} c_1 \\ c_2 \end{pmatrix} \\ &\qquad = R_1(1s,2p,2p,1s) \begin{pmatrix} -1/9 & \sqrt{8}/9 \\ \sqrt{8}/9 & 1/9 \end{pmatrix} \begin{pmatrix} c_1 \\ c_2 \end{pmatrix}. \end{aligned} \tag{4.126}$$

Table 4.3: First-order relativistic calculations of the $(1s2s)$ and $(1s2p)$ states of heliumlike neon ($Z = 10$), illustrating the fine-structure of the ^3P multiplet.

Term	$^3S_1$	$^1S_0$	$^3P_0$	$^3P_1$	$^3P_2$	$^1P_1$
$E^{(0)}$	-12.5209	-12.5209	-12.5209	-12.5125	-12.5042	-12.5125
$E^{(1)}$	1.8834	2.3247	2.2641	2.2596	2.2592	2.6049
$E_{\rm tot}$	-10.6375	-10.1962	-10.2568	-10.2529	-10.2450	-9.9076

The eigenvalues of the small matrix on the right-hand side of this equation are $\pm 1/3$. From this, it follows that the energies of the $J = 1$ states are

$$E_{1s\,2p_{1/2},\,1} = \epsilon_{2p} + R_0(1s, 2p, 1s, 2p) \mp \frac{1}{3}\, R_1(1s, 2p, 2p, 1s) - U_{2p,2p}. \quad (4.127)$$

The energy associated with the $-$ sign agrees with the energies of the $|s_{1/2}\, p_{1/2},\, 0\rangle$ and $|s_{1/2}\, p_{3/2},\, 2\rangle$ states given in Eq. (4.125) while the energy associated with the $+$ sign agrees with the energy of the nonrelativistic ^1P state given in Eq (4.53). Thus, the energies predicted for the $|1s\, 2p_j,\, 1\rangle$ states reduce to nonrelativistic values obtained previously. Furthermore, the orthogonal matrix that diagonalizes the small matrix in Eq. (4.126) is

$$\begin{pmatrix} \sqrt{1/3} & \sqrt{2/3} \\ \sqrt{2/3} & -\sqrt{1/3} \end{pmatrix}.$$

This is precisely the matrix, obtained in a more direct way in Sec. 4.6, that transforms the jj coupled states

$$\begin{bmatrix} (s_{1/2}\, p_{1/2})_1 \\ (s_{1/2}\, p_{3/2})_1 \end{bmatrix}$$

to the LS coupled states

$$\begin{bmatrix} (sp)\ ^1P_1 \\ (sp)\ ^3P_1 \end{bmatrix}.$$

We leave it as an exercise to verify this assertion.

The degeneracy of LS multiplets is lifted in relativistic calculations, giving to a J-dependent fine-structure of ^{2S+1}L states. As a specific example, let us consider heliumlike neon ($Z = 10$). For simplicity, we choose $U = 0$, and calculate the energies of the two $(1s2s)$ states and the four $(1s2p)$ states. In Table 4.3, we show the lowest-order and first-order energies $E^{(0)}$ and $E^{(1)}$ together with the resulting sum. These energies are all given relative to the one-electron ion. The energies of the $^3P_1$ and $^1P_1$ states were obtained by solving the 2×2 eigenvalue problem in Eq.(4.121). The three ^3P_J states have slightly different energies in this relativistic calculation; the J-dependent fine structure of the ^3P state obvious from the table.

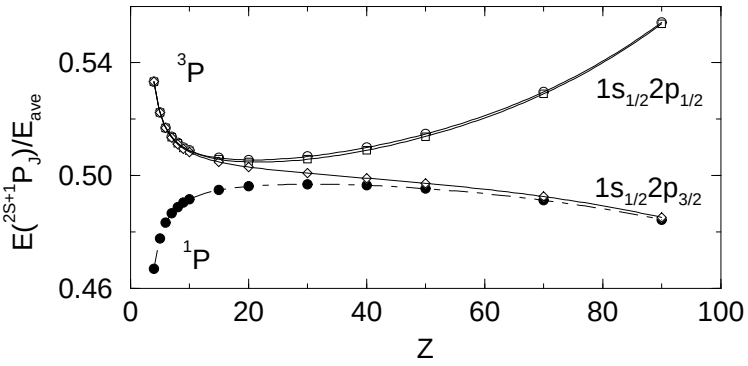

Figure 4.2: Variation with nuclear charge of the energies of $1s2p$ states in heliumlike ions. At low Z the states are LS-coupled states, while at high Z, they become jj-coupled states. Solid circles $^1P_1$; Hollow circles $^3P_0$; Hollow squares $^3P_1$; Hollow diamonds $^3P_2$.

In Fig. 4.2, we illustrate the transition from LS to jj coupling as Z increases along the helium isoelectronic sequence by presenting the results of a series of calculations of the energies of $(1s2p)$ states for two electron ions with nuclear charges ranging from $Z = 4$ to $Z = 90$. We plot the ratio of the energy of each of the four substates to the average energy of the states. For low values of Z, near the nonrelativistic limit, the states divide into a singlet state and a triplet state. As Z increases the triplet state splits apart into J dependent fine-structure components. For large Z, the states come together again to form the two jj states $(1s_{1/2}2p_{1/2})$ and $(1s_{1/2}2p_{3/2})$.

4.7.2 Atoms with Two Valence Electrons

The fine-structure of atoms with two valence electrons beyond closed shells can be treated in much the same way as the fine structure of heliumlike ions. Let us consider the nonrelativistic LS-coupled state ^{2S+1}L (with $S = 0$ or $S = 1$) made up from the configurations $(n_v l_v n_w l_w)$. A single nonrelativistic two-electron configuration $(n_v l_v n_w l_w)$ corresponds to four relativistic configurations $(n_v l_v n_w l_w)$ with $j_v = l_v \pm 1/2$ and $j_w = l_w \pm 1/2$. A jj-coupled state having the state $^{2S+1}L_J$ as its nonrelativistic limit is generally made up as a linear combination

$$|JM\rangle = \sum_{vw} c_{vw} |vw, J\rangle \,. \tag{4.128}$$

Here $|vw, J\rangle$ are normalized jj-coupled and c_{vw} are expansion coefficients satisfying

$$\sum_{vw} c_{vw}^2 = 1 \,. \tag{4.129}$$

As a specific example, let us consider the even-parity $^3D_2$ state obtained nonrelativistically from the configuration $(2p3p)$. There are three relativistic configurations contributing to this state; $(2p_{1/2}3p_{3/2})_{J=2}$, $(2p_{3/2}3p_{1/2})_{J=2}$ and $(2p_{3/2}3p_{3/2})_{J=2}$. The configuration $(2p_{1/2}3p_{1/2})$ can not contribute since two single-particle states with $j = 1/2$ cannot couple to $J = 2$!

The lowest-order energy for the state $|JM\rangle$ in Eq.(4.128) is

$$E_J^{(0)} = \sum_{vw} c_{vw}^2(\epsilon_v + \epsilon_w)\,. \tag{4.130}$$

The first-order energy is given by the quadratic form

$$E_J^{(1)} = \sum_{vw,xy} c_{vw}c_{xy}V_{vw,xy} + \sum_{vw} c_{vw}^2[(V_{\rm HF} - U)_{vv} + (V_{\rm HF} - U)_{ww}]\,. \tag{4.131}$$

The interaction potential $V_{vw,xy}$ in Eq.(4.131) is given by

$$V_{vw,xy} = \eta_{vw}\eta_{xy}\sum_k \left[(-1)^{j_w+j_x+J+k}\left\{\begin{array}{ccc} j_v & j_w & J \\ j_y & j_x & k \end{array}\right\} X_k(vwxy) \right.$$
$$\left. +(-1)^{j_w+j_x+k}\left\{\begin{array}{ccc} j_v & j_w & J \\ j_x & j_y & k \end{array}\right\} X_k(vwyx)\right], \tag{4.132}$$

where, as usual, the normalization factor $\eta_{vw} = 1/\sqrt{2}$ for identical particle configurations ($n_w = n_v$ and $\kappa_w = \kappa_v$) and $\eta_{vw} = 1$ otherwise. It can be easily seen that $V_{vw,xy} = V_{xy,vw}$

As in the mixed-configuration case described previously for heliumlike ions, diagonalizing the quadratic form in Eq.(4.131) leads to the algebraic eigenvalue equation for the energy:

$$\sum_{xy}\Big([\epsilon_x + (V_{\rm HF} - U)_{xx} + \epsilon_y + (V_{\rm HF} - U)_{yy}]\,\delta_{vw,xy} + V_{vw,xy}\Big)c_{xy} = E\,c_{vw}\,. \tag{4.133}$$

4.7.3 Particle-Hole States

Because of the relatively large separation between energies of subshells with a given value of l and different values of j in closed shell atoms (even an atom as light as neon), the fine-structure splitting of particle-hole states is particularly important. The arguments in the preceding paragraphs apply with obvious modifications to the particle-hole states as well.

First, we construct an angular momentum eigenstate as a linear combination of those relativistic particle-hole configurations $(n_v l_v n_a l_a)$ with $j_v = l_v \pm 1/2$ and $j_a = l_a \pm 1/2$ that couple to a given value of J:

$$|JM\rangle = \sum_{va} c_{va}|va, JM\rangle\,, \tag{4.134}$$

where the expansion coefficients satisfy the normalization constraint $\sum_{va} c_{va}^2 = 1$. Again, the first-order energy is a quadratic form in the expansion coefficients. Diagonalizing this quadratic form leads to an algebraic eigenvalue problem for the energy and the expansion coefficients. In the particle-hole case, the eigenvalue problem takes the form

$$\sum_{va}\Big([\epsilon_v + (V_{\rm HF} - U)_{vv} - \epsilon_a - (V_{\rm HF} - U)_{aa}]\,\delta_{vw}\delta_{ab} + V_{wb,va}\Big)c_{va} = E\,c_{wb}\,, \tag{4.135}$$

where the (symmetric) interaction matrix is given by

$$\begin{aligned} V_{wb,va} = (-1)^{J+j_w-j_b}\frac{1}{[J]}X_J(wabv) \\ + \sum_k (-1)^{J+j_w-j_b}\left\{\begin{array}{ccc} j_w & j_b & J \\ j_a & j_v & k \end{array}\right\} X_k(wavb). \end{aligned} \tag{4.136}$$

Chapter 5

Hyperfine Interaction & Isotope Shift

In this Chapter, we apply methods developed earlier in the text to investigate two small corrections to atomic energy levels: the hyperfine interaction, which is caused by interaction of atomic electrons with the electric and magnetic multipole moments of the nucleus, and the isotope shift, which results from the motion of the nucleus relative to the atomic center of mass. The hyperfine interaction leads to further splitting the atomic fine-structure levels, whereas the isotope shift leads to a dependence of energy levels on the nuclear mass.

5.1 Hyperfine Structure

The electric and magnetic multipole moments of a nucleus with angular momentum I, which are proportional to nuclear matrix elements of electric and magnetic multipole fields, are limited by angular momentum and parity selection rules.

Angular momentum selection rules limit the multipolarity k of the moments to $k \leq 2I$. Parity selection rules further limit the moments to even-order electric moments and odd-order magnetic moments. Thus a nucleus with spin $I = 0$ can have only an electric monopole moment; the nuclear charge $|e|Z$. A nucleus with angular momentum $I = 1/2$ can also have a magnetic dipole moment, while a nucleus with $I = 1$ can have a magnetic dipole moment and an electric quadrupole moment in addition to its charge. Low-order nuclear moments give the most significant contributions to the hyperfine interaction. Here, we concentrate on the dominant interactions, those of the magnetic dipole and electric quadrupole moments. The present analysis follows that given by Schwartz (1955).

The hyperfine interaction of a (relativistic) electron with the nucleus is just the electromagnetic interaction with the scalar and vector potentials generated

by the nuclear moments

$$h_{\rm hfs}(\mathbf{r}) = e\phi(\mathbf{r}) - ec\,\boldsymbol{\alpha}\cdot\mathbf{A}(\mathbf{r})\,. \tag{5.1}$$

Nonrelativistic limits can be worked out as needed.

If we let $\boldsymbol{\mu}$ designate the nuclear magnetic moment, then the corresponding magnetic vector potential is given by

$$\mathbf{A}(\mathbf{r}) = \frac{\mu_0}{4\pi}\,\frac{[\boldsymbol{\mu}\times\mathbf{r}]}{r^3}\,.$$

It is convenient to express the interaction $-ec\,\boldsymbol{\alpha}\cdot\mathbf{A}(\mathbf{r})$ in a spherical basis. For this purpose, we rewrite

$$\boldsymbol{\alpha}\cdot[\boldsymbol{\mu}\times\mathbf{r}] = [\mathbf{r}\times\boldsymbol{\alpha}]\cdot\boldsymbol{\mu} = \sum_\lambda (-1)^\lambda [\mathbf{r}\times\boldsymbol{\alpha}]_\lambda\,\mu_{-\lambda}\,.$$

For an arbitrary vector $\mathbf{v}$, one may show,

$$[\mathbf{r}\times\mathbf{v}]_\lambda = -i\sqrt{2}\,r\,\mathbf{C}^{(0)}_{1\lambda}(\hat{r})\cdot\mathbf{v}\,,$$

where $\mathbf{C}^{(0)}_{1\lambda}(\hat{r})$ is a normalized vector spherical harmonic defined by

$$\mathbf{C}^{(0)}_{kq}(\hat{r}) = \sqrt{\frac{4\pi}{2k+1}}\,\mathbf{Y}^{(0)}_{kq}(\hat{r})\,.$$

Using this relation, we can write the magnetic hyperfine interaction as:

$$\frac{e}{4\pi\epsilon_0}\sum_\lambda (-1)^\lambda\,\frac{i\sqrt{2}\,[\boldsymbol{\alpha}\cdot\mathbf{C}^{(0)}_{1\lambda}(\hat{r})]}{cr^2}\,\mu_{-\lambda}\,.$$

The quantity $[\boldsymbol{\alpha}\cdot\mathbf{C}^{(0)}_{1\lambda}(\hat{r})]$ is an irreducible tensor operator of rank 1 acting in the space of electron coordinates and spin. Quantum mechanically, μ_λ is an irreducible tensor operator of rank 1 acting in the space of nuclear coordinates and spin. The c-number magnetic moment μ is the expectation value of the operator μ_0 in the "extended" state of the nucleus, $M_I = I$:

$$\mu \stackrel{\rm def}{=} \langle II|\mu_0|II\rangle\,. \tag{5.2}$$

The nuclear magnetic moment μ is measured in units of the nuclear magneton μ_N:

$$\mu_N = \frac{|e|\hbar}{2M_p}\,,$$

where M_p is the mass of the proton. We write μ in terms of the angular momentum quantum number I as:

$$\mu = g_I\,I\,\mu_N\,. \tag{5.3}$$

The dimensionless factor g_I is called the gyromagnetic ratio. For the proton, the gyromagnetic ratio has the numerical value $g_I = 5.5856948(1)$.

If we let Q_{ij} represent the nuclear quadrupole moment tensor, then the scalar potential is given by

$$\phi(\mathbf{r}) = \frac{1}{4\pi\epsilon_0} \sum_{ij} \frac{x_i x_j}{2r^5} Q_{ij} \,.$$

The quadrupole tensor Q_{ij} is a traceless symmetric tensor of rank 2; it therefore has 5 independent components. For a classical charge distribution $\rho(\mathbf{r})$ the Cartesian components of the quadrupole tensor are given by

$$Q_{ij} = \int d^3r \, (3x_i x_j - r^2 \delta_{ij}) \rho(\mathbf{r}) \,.$$

The components of this tensor can be transformed to a spherical basis and expressed in terms of the five components of the second-rank spherical tensor Q_λ defined by,

$$Q_\lambda = \int d^3r \, r^2 C^2_\lambda(\hat{r}) \rho(\mathbf{r}) \,,$$

where $C^2_\lambda(\hat{r})$ is a normalized spherical tensor of rank 2. In particular, $Q_{33} = 2Q_0$. The potential due to the quadrupole, expressed in a spherical basis, is

$$\phi(\mathbf{r}) = \frac{1}{4\pi\epsilon_0} \sum_\lambda (-1)^\lambda \frac{C^2_\lambda(\hat{r})}{r^3} Q_{-\lambda} \,.$$

Here, Q_λ is an irreducible tensor operator of rank 2 acting in the space of nucleon coordinates and spins. The c-number quadrupole moment of the nucleus Q is given in terms of the expectation value of the operator Q_0 in the extended state:

$$Q \stackrel{\text{def}}{=} 2\langle II|Q_0|II\rangle \,. \tag{5.4}$$

The nuclear quadrupole moment Q is dimensionally a charge times a length squared. It is commonly written in units of $|e| \times$ barn.

The hyperfine interaction Hamiltonian for a relativistic electron with the nuclear magnetic dipole and electric quadrupole moments becomes

$$h_{\rm hfs}(\mathbf{r}) = \frac{e}{4\pi\epsilon_0} \left\{ \sum_\lambda (-1)^\lambda \frac{i\sqrt{2}\,[\boldsymbol{\alpha} \cdot \mathbf{C}^{(0)}_{1\lambda}(\hat{r})]}{cr^2} \mu_{-\lambda} + \sum_\lambda (-1)^\lambda \frac{C^2_\lambda(\hat{r})}{r^3} Q_{-\lambda} \right\} . \tag{5.5}$$

Both the electric and magnetic interactions are thereby expressed in terms of tensor operators and the hyperfine interaction Hamiltonian takes the form

$$h_{\rm hfs}(\mathbf{r}) = \sum_{k\lambda} (-1)^\lambda \, t^k_\lambda(\hat{r}) \, T^k_{-\lambda} \,,$$

where $t^k_q(\mathbf{r})$ is an irreducible tensor operator of rank k that acts on electron coordinates and spin, and T^k_q is a rank k irreducible tensor operator that acts

on nuclear coordinates and spin. Here, $k = 1$ for the magnetic dipole interaction and $k = 2$ for the electric quadrupole interaction. Specifically,

$$t^1_\lambda(\mathbf{r}) = -\frac{|e|}{4\pi\epsilon_0}\,\frac{i\sqrt{2}\,[\boldsymbol{\alpha}\cdot\mathbf{C}^{(0)}_{1\lambda}(\hat{r})]}{cr^2}\,, \tag{5.6}$$

$$t^2_\lambda(\mathbf{r}) = -\frac{|e|}{4\pi\epsilon_0}\,\frac{C^2_\lambda(\hat{r})}{r^3}\,, \tag{5.7}$$

and

$$T^1_\lambda = \mu_\lambda\,, \tag{5.8}$$

$$T^2_\lambda = Q_\lambda\,. \tag{5.9}$$

For a collection of N electrons $h_{\rm hfs}(\mathbf{r})$ is replaced by the single-particle operator

$$H_{\rm hfs} = \sum_{i=1}^{N} h_{\rm hfs}(\mathbf{r}_i) = \sum_\lambda (-1)^\lambda \mathcal{T}^k_\lambda\, T^k_{-\lambda}\,, \tag{5.10}$$

with

$$\mathcal{T}^k_\lambda = \begin{cases} \sum_{i=1}^N t^k_\lambda(\mathbf{r}_i) & \text{in first quantization}\,, \\ \sum_{ij}\langle i|t^k_\lambda|j\rangle a^\dagger_i a_j & \text{in second quantization}\,. \end{cases} \tag{5.11}$$

Let us consider an atomic angular momentum eigenstate $|J, M_J\rangle$ and a nuclear angular momentum eigenstate $|I, M_I\rangle$. These states are coupled to give a eigenstate of total angular momentum $\mathbf{F} = \mathbf{I} + \mathbf{J}$,

$$|(IJ), FM_F\rangle = \sum_{M_I M_J} - \begin{array}{l} IM_I \\ \hline\hline FM_F \\ \hline JM_J \end{array} |I, M_I\rangle\,|J, M_J\rangle.$$

The first-order correction to the energy in this state is just the expectation value of $H_{\rm hfs}$, which is easily shown to be

$$\begin{aligned} W_F &= \langle (IJ), FM_F|H_{\rm hfs}|(IJ), FM_F\rangle \\ &= \sum_k (-1)^{I+J+F} \left\{ \begin{array}{ccc} I & J & F \\ J & I & k \end{array} \right\} \langle J||\mathcal{T}^k||J\rangle\langle I||T^k||I\rangle. \end{aligned} \tag{5.12}$$

We can write this equation in a somewhat more convenient way by introducing

$$(-1)^{I+J+F} \left\{ \begin{array}{ccc} I & J & F \\ J & I & k \end{array} \right\} = \frac{(2I)!\,(2J)!}{\sqrt{(2I-k)!(2I+k+1)!(2J-k)!(2J+k+1)!}} M(IJ, Fk),$$

where

$$M(IJ,Fk) = \begin{cases} \frac{K}{2IJ}\,, & \text{for } k=1\,, \\ \frac{6K(K+1)-8J(J+1)I(I+1)}{2I(2I-1)2J(2J-1)}\,, & \text{for } k=2\,, \end{cases}$$

with $K = F(F+1) - I(I+1) - J(J+1)$. With the aid of the identity

$$\begin{pmatrix} J & k & J \\ -J & 0 & J \end{pmatrix} = \frac{(2J)!}{\sqrt{(2J-k)!\,(2J+k+1)!}}\,, \tag{5.13}$$

it follows that

$$\langle JJ|\mathcal{T}_0^k|JJ\rangle = \frac{(2J)!}{\sqrt{(2J-k)!\,(2J+k+1)!}}\langle J||\mathcal{T}^k||J\rangle\,. \tag{5.14}$$

Combining Eqs.(5.12) and (5.14), we obtain for the energy the expression

$$W_F = \sum_k M(IJ,Fk)\langle JJ|\mathcal{T}_0^k|JJ\rangle\langle II|T_0^k|II\rangle\,. \tag{5.15}$$

The two terms in this sum can be written out explicitly as

$$W_F = \frac{1}{2}\,Ka + \frac{1}{2}\,\frac{3K(K+1) - 4J(J+1)I(I+1)}{2I(2I-1)2J(2J-1)}\,b\,, \tag{5.16}$$

where

$$a = \frac{1}{IJ}\langle JJ|\mathcal{T}_0^1|JJ\rangle\langle II|T_0^1|II\rangle = \frac{\mu}{IJ}\,\langle JJ|\mathcal{T}_0^1|JJ\rangle\,, \tag{5.17}$$

$$b = 4\langle JJ|\mathcal{T}_0^2|JJ\rangle\langle II|T_0^2|II\rangle = 2Q\,\langle JJ|\mathcal{T}_0^2|JJ\rangle\,. \tag{5.18}$$

The problem of evaluating the energy shift due to the atomic hyperfine interaction is now reduced to that of determining the expectation values of the tensor operators $\mathcal{T}_0^k$ in atomic states.

Let us suppose that $b = 0$. The interaction energy then reduces to $W_F = Ka/2$, with $K = F(F+1) - I(I+1) - J(J+1)$. This is precisely the energy that would have been obtained from an effective Hamiltonian of the form

$$H_{\text{eff}} = a\,\mathbf{I}\cdot\mathbf{J}\,.$$

We find that an eigenstate of J breaks up into $2J+1$ sublevels for the case $I \geq J$ or $2I+1$ sublevels for $J < I$. Let us consider the case $I \geq J = 1/2$. In this case, an eigenstate of J breaks up into 2 sublevels,

$$W_F = \begin{cases} Ia/2 & \text{for } F = I + 1/2\,, \\ -(I+1)a/2 & \text{for } F = I - 1/2\,. \end{cases}$$

The splitting between the two sublevels is $\Delta W = (I+1/2)a$. For $I \geq J = 1$, an eigenstate of J splits into three components separated by $(I+1)a$ and Ia, respectively. Generally, for the case $I \geq J$, the hyperfine pattern has $2J+1$ components; the splitting between two adjacent sublevels being $W_{F+1} - W_F = Fa$. By counting the hyperfine components in the case $J > I$ we can determine the nuclear angular momentum I, while measurements of the separation between sublevels permits us to evaluate the nuclear gyromagnetic ratio g_I.

Units: Dimensionally, the magnetic hyperfine interaction energy is given by

$$\begin{aligned}
[W^{\mathrm{m.d.}}] &= \frac{|e|}{4\pi\epsilon_0}\frac{|e|\hbar}{2M_p}\frac{1}{ca_0^2} \\
&= \frac{1}{2M_p c} = 1.987131\times 10^{-6}\,\text{a.u.} \\
&= 0.4361249\,\text{cm}^{-1} \\
&= 13074.69\,\text{MHz}\,.
\end{aligned}$$

Similarly, the electric quadrupole hyperfine interaction energy is, dimensionally,

$$\begin{aligned}
[W^{\mathrm{e.q.}}] &= \frac{|e|}{4\pi\epsilon_0}\,|e|\times\text{barn}\,\frac{1}{a_0^3} \\
&= 3.571064\times 10^{-8}\,\text{a.u.} \\
&= 7.837580\times 10^{-3}\,\text{cm}^{-1} \\
&= 234.965\,\text{MHz}\,.
\end{aligned}$$

In the following, we express the nuclear magnetic moment in units of μ_N, the quadrupole moment in terms of $|e|\times$ barn, and omit the constants $e/4\pi\epsilon_0$ and c in expressions given previously for the interaction. The results will then be in terms of the units given in this paragraph.

5.2 Atoms with One Valence Electron

We now turn to the problem of determining W_F for an atom having a single valence electron in the state $v = (n_v\kappa_v m_v)$,

$$|v\rangle = a_v^\dagger|O_c\rangle\,.$$

The atomic angular momentum components J and M_J are given by $J = j_v$ and $M_J = m_v$ for this state, and the many-body expectation value of the tensor operator $\mathcal{T}^k_\lambda$ is given by

$$\langle v|\mathcal{T}^k_\lambda|v\rangle = \langle v|t^k_\lambda(\mathbf{r})|v\rangle + \sum_a \langle a|t^k_\lambda(\mathbf{r})|a\rangle\,,$$

where the sum over a extends over all core states. The core sum is easily shown to vanish:

$$\sum_a \langle a|t^k_\lambda(\mathbf{r})|a\rangle = \sum_a -$$

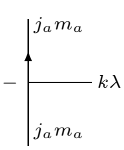

$$\langle a||t^k||a\rangle = \sum_{n_a\kappa_a}$$

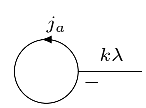

$$\langle a||t^k||a\rangle$$

$$= \sum_{n_a\kappa_a} \delta_{k0}\delta_{\lambda 0}\sqrt{[j_a]}\,\langle a||t^k||a\rangle = 0\,.$$

The expectation value of $\mathcal{T}^k_\lambda$, therefore reduces to the valence electron expectation value of $t^k_\lambda(\mathbf{r})$. For a one valence electron atom, we therefore have,

$$a = \frac{g_I}{j_v}\langle n_v\kappa_v m_v = j_v|t^1_0|n_v\kappa_v m_v = j_v\rangle \times 13074.7\,\mathrm{MHz}\,, \tag{5.19}$$

$$b = 2Q\langle n_v\kappa_v m_v = j_v|t^2_0|n_v\kappa_v m_v = j_v\rangle \times 234.965\,\mathrm{MHz}\,. \tag{5.20}$$

In the magnetic case, $k = 1$, we obtain from Eq.(5.6)

$$\langle w|t^1_\lambda(\mathbf{r})|v\rangle = -i\sqrt{2}\int\frac{dr}{r^2}\Big(-iP_{n_w\kappa_w}(r)Q_{n_v\kappa_v}(r)\,\langle\kappa_w m_w|\boldsymbol{\sigma}\cdot\mathbf{C}^{(0)}_{10}(\hat{r})|-\kappa_v m_v\rangle$$
$$+iQ_{n_w\kappa_w}(r)P_{n_v\kappa_v}(r)\,\langle-\kappa_w m_w|\boldsymbol{\sigma}\cdot\mathbf{C}^{(0)}_{10}(\hat{r})|\kappa_v m_v\rangle\Big)\,, \tag{5.21}$$

where, for example,

$$\langle\kappa_w m_w|\boldsymbol{\sigma}\cdot\mathbf{C}^{(0)}_{kq}|-\kappa_v m_v\rangle = \int d\Omega\,\Omega^\dagger_{\kappa_w m_w}(\hat{r})\,\boldsymbol{\sigma}\cdot\mathbf{C}^{(0)}_{kq}(\hat{r})\,\Omega_{-\kappa_v m_v}(\hat{r})\,.$$

Often in relativistic calculations, one encounters angular matrix elements, such as those in the above equation, of $\boldsymbol{\sigma}$ times a normalized vector spherical harmonic $\mathbf{C}^{(\nu)}_{kq}$. Such matrix elements are easily reduced to matrix elements of normalized spherical harmonics. We find:

$$\langle\kappa_b m_b|\boldsymbol{\sigma}\cdot\mathbf{C}^{(-1)}_{kq}|\kappa_a m_a\rangle = -\langle-\kappa_b m_b|C^k_q|\kappa_a m_a\rangle\,, \tag{5.22}$$

$$\langle\kappa_b m_b|\boldsymbol{\sigma}\cdot\mathbf{C}^{(0)}_{kq}|\kappa_a m_a\rangle = \frac{\kappa_a-\kappa_b}{\sqrt{k(k+1)}}\langle\kappa_b m_b|C^k_q|\kappa_a m_a\rangle\,, \tag{5.23}$$

$$\langle\kappa_b m_b|\boldsymbol{\sigma}\cdot\mathbf{C}^{(1)}_{kq}|\kappa_a m_a\rangle = \frac{\kappa_a+\kappa_b}{\sqrt{k(k+1)}}\langle-\kappa_b m_b|C^k_q|\kappa_a m_a\rangle\,. \tag{5.24}$$

With the aid of Eq.(5.23), we obtain

$$\langle w|t^1_\lambda(\mathbf{r})|v\rangle = (\kappa_v+\kappa_w)\,\langle-\kappa_w m_w|C^1_\lambda|\kappa_v m_v\rangle\left(\frac{1}{r^2}\right)_{wv}\,, \tag{5.25}$$

where

$$\left(\frac{1}{r^2}\right)_{wv} = \int_0^\infty\frac{dr}{r^2}(P_{n_w\kappa_w}(r)Q_{n_v\kappa_v}(r)+Q_{n_w\kappa_w}(r)P_{n_v\kappa_v}(r))\,. \tag{5.26}$$

Here we have used the symmetry relation

$$\langle-\kappa_w m_w|C^1_\lambda|\kappa_v m_v\rangle = \langle\kappa_w m_w|C^1_\lambda|-\kappa_v m_v\rangle\,. \tag{5.27}$$

Therefore, we have in the case $k = 1$,

$$\langle n_v\kappa_v j_v|t^1_0|n_v\kappa_v j_v\rangle = 2\kappa_v\langle-\kappa_v j_v|C^1_0|\kappa_v j_v\rangle\left(\frac{1}{r^2}\right)_{vv}\,. \tag{5.28}$$

A similar, but simpler calculation for $k = 2$ gives

$$\langle n_v \kappa_v j_v | t_0^2 | n_v \kappa_v j_v \rangle = -\langle \kappa_v j_v | C_0^2 | \kappa_v j_v \rangle \left\langle \frac{1}{r^3} \right\rangle_{vv} , \tag{5.29}$$

where

$$\left\langle \frac{1}{r^3} \right\rangle_{wv} = \int_0^\infty \frac{dr}{r^3} (P_{n_w \kappa_w}(r) P_{n_v \kappa_v}(r) + Q_{n_w \kappa_w}(r) Q_{n_v \kappa_v}(r)) . \tag{5.30}$$

The angular matrix elements in Eqs.(5.28) and (5.29) are evaluated to give

$$\langle -\kappa_v j_v | C_0^1 | \kappa_v j_v \rangle = -\frac{1}{2j_v + 2} ,$$
$$\langle \kappa_v j_v | C_0^2 | \kappa_v j_v \rangle = -\frac{2j_v - 1}{4j_v + 4} ,$$

from which it follows that

$$a = -\frac{g_I \, \kappa_v}{j_v(j_v + 1)} \left\langle \frac{1}{r^2} \right\rangle_{vv} \times 13074.7 \, \text{MHz} , \tag{5.31}$$

$$b = Q \frac{2j_v - 1}{2j_v + 2} \left\langle \frac{1}{r^3} \right\rangle_{vv} \times 234.965 \, \text{MHz} . \tag{5.32}$$

5.2.1 Pauli Approximation

To obtain the nonrelativistic limit of the expression for the dipole hyperfine constant a in Eq.(5.31), we consider an approximation to the radial Dirac equation referred to as the Pauli approximation. We set $W_{n\kappa} = E_{n\kappa} - c^2$ and write the radial Dirac equations as

$$c \left(\frac{d}{dr} - \frac{\kappa}{r} \right) Q_{n\kappa} = (W_{n\kappa} - V) P_{n\kappa} , \tag{5.33}$$

$$(2c^2 + W_{n\kappa} - V) Q_{n\kappa} = -c \left(\frac{d}{dr} + \frac{\kappa}{r} \right) P_{n\kappa} . \tag{5.34}$$

The Pauli approximation consists of neglecting $W_{n\kappa} - V$ compared to $2c^2$ in Eq.(5.34), leading to the relation

$$Q_{n\kappa} \approx -\frac{1}{2c} \left(\frac{d}{dr} + \frac{\kappa}{r} \right) P_{n\kappa} . \tag{5.35}$$

Substituting this approximation into Eq.(5.34), gives the differential equation

$$\frac{1}{2} \frac{d^2 P_{n\kappa}}{dr^2} + \left(W_{n\kappa} - V - \frac{\kappa(\kappa + 1)}{2r^2} \right) P_{n\kappa} = 0 , \tag{5.36}$$

for the large component radial function $P_{n\kappa}$. This is just the radial Schrödinger equation for orbital angular momentum l, since $\kappa(\kappa + 1) = l(l + 1)$ for the two

possible κ values associated with a given value of l ($\kappa = l$ and $\kappa = -l-1$). Therefore, in the Pauli approximation, the large component radial function $P_{n\kappa}$ goes over to the corresponding nonrelativistic radial function P_{nl}. The small component radial function in the Pauli approximation is found from Eq.(5.35) with $P_{n\kappa}$ replaced by P_{nl}. With the aid of the Pauli approximation, we therefore obtain

$$\begin{aligned}\left(\frac{1}{r^2}\right)_{vw} &= -\frac{1}{2c}\int_0^\infty \frac{dr}{r^2}\left[P_{n_v l_v}\left(\frac{d}{dr}+\frac{\kappa_w}{r}\right)P_{n_w l_w} + P_{n_w l_w}\left(\frac{d}{dr}+\frac{\kappa_v}{r}\right)P_{n_v l_v}\right] \\ &= -\frac{1}{2c}\int_0^\infty dr\left[\frac{d}{dr}\left(\frac{P_{n_v l_v}P_{n_w l_w}}{r^2}\right) + \frac{\kappa_v+\kappa_w+2}{r^3}P_{n_v l_v}P_{n_w l_w}\right] \\ &= \frac{1}{2c}\left(\frac{P_{n_v l_v}P_{n_w l_w}}{r^2}\right)_{r=0} - \frac{\kappa_v+\kappa_w+2}{2c}\left\langle\frac{1}{r^3}\right\rangle_{vw}, \end{aligned} \tag{5.37}$$

where the radial matrix element of $1/r^3$ on the last line is to be evaluated using nonrelativistic wave functions. The first term on the last line of Eq.(5.37) contributes if, and only if, both states v and w are s states, since the nonrelativistic radial wave functions $P_{nl}(r)$ are proportional to r^{l+1}. Indeed, if we let

$$\lim_{r\to 0}\left(\frac{P_{n_v l_v}(r)}{r}\right) = N_v \delta_{l_v 0}\,,$$

then we obtain the following nonrelativistic limiting values for the dipole hyperfine constant:

$$a_{\rm NR} = \frac{2}{3}\,g_I N_v^2 \times 95.4016\,{\rm MHz}, \quad \text{for } l_v = 0, \tag{5.38}$$

$$a_{\rm NR} = \frac{l_v(l_v+1)}{j_v(j_v+1)}\,g_I\left\langle\frac{1}{r^3}\right\rangle_{vv} \times 95.4016\,{\rm MHz}, \quad \text{for } l_v \neq 0. \tag{5.39}$$

The overall scale here is set by the constant $13074.69 \times \alpha = 95.4106\,{\rm MHz}$. For the ground state of hydrogen, $N_{1s} = 2$, and Eq.(5.38) leads to the result

$$a_{\rm NR} = \frac{2}{3} \times 5.5856948 \times 2^2 \times 95.4016\,{\rm MHz} = 1421.16\,{\rm MHz}. \tag{5.40}$$

This number is to be compared with the experimental value $a_{\rm Exp.} = 1420.406\,{\rm MHz}$. The difference between these values arises from radiative, reduced-mass and relativistic corrections. These corrections are discussed, for example, in Bethe and Salpeter (1957).

In Table 5.1, we compare results of HF calculations of the hyperfine constants for the ground states of alkali-metal atoms with measurements. These values are seen to be in only qualitative agreement with experiment. The agreement between theory and experiment can be improved to the level of 5% or better by including corrections from first-order and second-order perturbation theory. For the heavier alkali atoms, a significant part of the difference between calculation and measurement is due to the use of the nonrelativistic approximation. For example, if we use the relativistic expression Eq.(5.31) rather than Eq.(5.38) to evaluate a for rubidium, we obtain $a = 643.9\,{\rm MHz}$ instead of the value $a = 542.0\,{\rm MHz}$ given in the table.

Table 5.1: Nonrelativistic HF calculations of the magnetic dipole hyperfine constants a (MHz) for ground states of alkali-metal atoms compared with measurements.

Atom	Z	A	I	State	g_I	$a_{\rm NR}$	$a_{\rm Exp.}$
Li	3	7	3/2	$2s_{1/2}$	2.17065	284.2	401.752
Na	11	23	3/2	$3s_{1/2}$	1.47749	615.9	885.813
K	19	39	3/2	$4s_{1/2}$	0.26064	140.8	230.860
Rb	37	85	5/2	$5s_{1/2}$	0.54121	542.0	1011.911

5.3 Isotope Shift

All of the previous calculations were carried out assuming that the nuclear mass is infinite. In this section, we consider corrections associated with finite nuclear mass. These corrections lead to *isotope shifts* of atomic energy levels. We evaluate isotope shifts using many-body methods, following earlier pioneering work by Mårtensson and Salomonson (1982). We first discuss the various contributions to the isotope shift, then go on to several specific examples.

Consider a nonrelativistic atom with N electrons of mass m at $(\boldsymbol{r}_1, \boldsymbol{r}_2, \cdots)$ and a nucleus of mass M_A at $\boldsymbol{r}_0$. The Hamiltonian for the $N+1$ particle atom may be written

$$H(\boldsymbol{r}_0, \boldsymbol{r}_1, \boldsymbol{r}_2, \cdots, \boldsymbol{p}_0, \boldsymbol{p}_1, \boldsymbol{p}_2, \cdots) = \frac{p_0^2}{2M_A} + \sum_i \frac{p_i^2}{2m} + \sum_i V_{e-N}(\boldsymbol{r}_i - \boldsymbol{r}_0) + \frac{1}{2}\sum_{i\neq j} V_{e-e}(\boldsymbol{r}_i - \boldsymbol{r}_j)\,. \tag{5.41}$$

Let us transform to relative coordinates:

$$\boldsymbol{\rho}_i = \boldsymbol{r}_i - \boldsymbol{r}_0 \tag{5.42}$$

$$\boldsymbol{R} = \frac{M_A\ \boldsymbol{r_0} + m\sum_i \boldsymbol{r}_i}{M_T}\,, \tag{5.43}$$

where $M_T = M_A + N\,m$. The generalized momenta conjugate to $\boldsymbol{\rho}_i$ and $\boldsymbol{R}$ are:

$$\boldsymbol{\pi}_i = \frac{1}{i}\boldsymbol{\nabla}_{\rho_i} \tag{5.44}$$

$$\boldsymbol{P} = \frac{1}{i}\boldsymbol{\nabla}_R \tag{5.45}$$

We find using the four previous equations:

$$\boldsymbol{p}_i = \boldsymbol{\pi}_i + \frac{m}{M_T}\boldsymbol{P} \tag{5.46}$$

$$\boldsymbol{p}_0 = -\sum_i \boldsymbol{\pi}_i + \frac{M_A}{M_T}\boldsymbol{P} \tag{5.47}$$

The kinetic energy term in the original Hamiltonian can be rewritten

$$\begin{aligned}
\text{K. E.} &= \frac{1}{2m}\left[\sum_i \pi_i^2 + 2\frac{m}{M_T}\sum_i \boldsymbol{\pi}_i\cdot\boldsymbol{P} + \frac{Nm^2}{M_T^2}P^2\right] \\
&+ \frac{1}{2M_A}\left[\left(\sum_i \boldsymbol{\pi}_i\right)^2 - 2\frac{M_A}{M_T}\sum_i \boldsymbol{\pi}_i\cdot\boldsymbol{P} + \frac{M_A^2}{M_T^2}P^2\right] \\
&= \frac{m+M_A}{2\,m\,M_A}\sum_i \pi_i^2 + \frac{1}{2M_A}\sum_{i\neq j}\boldsymbol{\pi}_i\cdot\boldsymbol{\pi}_j + \frac{1}{2M_T}P^2 \qquad (5.48)
\end{aligned}$$

The wave function for the atom is therefore factorizable into a product of plane wave describing the center of mass motion and an N-electron wave function describing the motion relative to the nucleus. The Hamiltonian for the relative motion is

$$\begin{aligned}
H(\boldsymbol{\rho}_1,\boldsymbol{\rho}_2,\cdots,\boldsymbol{\pi}_1,\boldsymbol{\pi}_2,\cdots) &= \sum_i \frac{\pi_i^2}{2\,\mu} + \sum_i V_{e-N}(\boldsymbol{\rho}_i) + \frac{1}{2}\sum_{i\neq j} V_{e-e}(\boldsymbol{\rho}_i-\boldsymbol{\rho}_j) \\
&+ \frac{1}{2M_A}\sum_{i\neq j}\boldsymbol{\pi}_i\cdot\boldsymbol{\pi}_j\,. \qquad (5.49)
\end{aligned}$$

where the reduced mass μ is given by

$$\mu = \frac{M_A\,m}{M_A+m}\,. \qquad (5.50)$$

5.3.1 Normal and Specific Mass Shifts

We write the Hamiltonian as a sum

$$\begin{aligned}
H(\boldsymbol{\rho}_1,\boldsymbol{\rho}_2,\cdots,\boldsymbol{\pi}_1,\boldsymbol{\pi}_2,\cdots) &= H_\mu + \Delta H \qquad (5.51)\\
H_\mu(\boldsymbol{\rho}_1,\boldsymbol{\rho}_2,\cdots,\boldsymbol{\pi}_1,\boldsymbol{\pi}_2,\cdots) &= \sum_i \frac{\pi_i^2}{2\,\mu} + \sum_i V_{e-N}(\boldsymbol{\rho}_i) \\
&+ \frac{1}{2}\sum_{i\neq j} V_{e-e}(\boldsymbol{\rho}_i-\boldsymbol{\rho}_j) \qquad (5.52)\\
\Delta H(\boldsymbol{\pi}_1,\boldsymbol{\pi}_2,\cdots) &= \frac{1}{2M_A}\sum_{i\neq j}\boldsymbol{\pi}_i\cdot\boldsymbol{\pi}_j\,. \qquad (5.53)
\end{aligned}$$

Normal Mass Shift The effect of the finite nuclear mass on the first term in ΔH is to scale the infinite mass energies by the ratio $\mu/m = M_A/(M_A+m)$. (The infinite mass energy levels are commonly measured in units of the Rydberg constant R_∞ which has the value 1/2 (a.u.) = 109737.31 cm^{-1}.) The shift of the energy from the infinite-mass value is is referred to as the *normal mass shift*.

The value of the normal mass shift is

$$\delta E_{\rm NMS} = E_\mu - E_m = \left(\frac{M_A}{M_A+m} - 1\right) E_m = -\frac{m}{M_A+m}\, E_m \equiv -\frac{m}{M_A}\, E_\mu \,. \tag{5.54}$$

Here E_m is the value of the energy in atomic units calculated with the infinite-mass Rydberg constant. We may use the above expression with E_μ replaced by the experimental energy to evaluate the normal mass shift to obtain an accurate approximation to the normal mass shift.

Specific Mass Shift The correction to the energy from ΔH is referred to as the *specific mass shift*. The value of the specific mass shift is

$$\delta E_{\rm SMS} = \frac{1}{2M_A} \left\langle \sum_{i\neq j} \boldsymbol{\pi}_i \cdot \boldsymbol{\pi}_j \right\rangle . \tag{5.55}$$

The energy is proportional to the mass (μ for H_μ) or (m for H_m) in the denominator of the kinetic energy. It follows that lengths vary inversely with mass and that kinetic energy varies directly as mass. The scaling of kinetic energy implies that momentum is proportional to mass. With the aid of these scaling relations, one may rewrite

$$\delta E_{\rm SMS} = \frac{M_A}{2(M_A+m)^2} \left\langle \sum_{i\neq j} \boldsymbol{p}_i \cdot \boldsymbol{p}_j \right\rangle , \tag{5.56}$$

in the center of mass system. This scaling is required since we evaluate the SMS matrix element using infinite nuclear mass wave functions. The prescription is as follows:

(a) Express all answers in terms of the R_∞, the infinite mass Rydberg constant.

(b) Multiply the total energy by $-m/(M_A+m)$ to obtain the the normal mass shift.

(c) Multiply the matrix element of $\sum \boldsymbol{p}_i \cdot \boldsymbol{p}_j$ by $M_A/2(M_A+m)^2$ to find the specific mass shift.

Alternatively, we may use experimental energies for E_μ and evaluate the normal mass shift as

$$\delta E_{\rm NMS} = -\frac{m}{M_A}\, E_{\rm expt} \,. \tag{5.57}$$

5.4 Calculations of the SMS

Whereas values the NMS can be obtained directly from the energy, determining the SMS represents a non-trivial many-body problem. Ignoring the coefficient

$M_A/(M_a+m)^2$ for the moment, the specific mass shift operator

$$T = \frac{1}{2}\sum_{i\neq j} \boldsymbol{p}_i \cdot \boldsymbol{p}_j$$

can be expressed in second quantization as

$$\frac{1}{2}\sum_{ijkl} t_{ijkl} a_i^\dagger a_j^\dagger a_l a_k \ ,$$

where

$$t_{ijkl} = \langle ij|\, \boldsymbol{p}_1 \cdot \boldsymbol{p}_2 \,|kl\rangle \ . \tag{5.58}$$

5.4.1 Angular Decomposition

The two-particle operator t_{ijkl} may be decomposed in an angular-momentum basis as

$$t_{ijkl} = \sum_\lambda (-1)^\lambda \langle i|\, p_\lambda \,|k\rangle \langle j|\, p_{-\lambda} \,|l\rangle \,, \tag{5.59}$$

which, in turn, can be expressed diagrammatically as

$t_{ijkl} = -$ 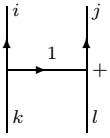 $+ \quad T_1(ijkl)\,,$ (5.60)

where

$$T_1(ijkl) = -\langle i||C^1||k\rangle \, \langle j||C^1||l\rangle \, P(ac)\, P(bd)\,. \tag{5.61}$$

In Eq. (5.61), the quantities $P(ik)$ are radial matrix elements of the momentum operator. We give explicit forms for these reduced matrix elements in the following subsection.

Nonrelativistic case

We write $\boldsymbol{p} = \frac{1}{i}\boldsymbol{\nabla}$ and note that in the nonrelativistic case

$$\begin{aligned}
\langle b|\boldsymbol{\nabla}|a\rangle &= \int d^3r \, \frac{1}{r} P_b(r)\, Y^\star_{l_b m_b} \boldsymbol{\nabla} \left(\frac{1}{r} P_a(r)\, Y_{l_a m_a} \right) \\
&= \int_0^\infty dr\, P_b(r) \left(\frac{dP_a}{dr} - \frac{1}{r} P_a(r) \right) \int d\Omega \ Y^\star_{l_b m_b} \hat{r}\, Y_{l_a m_a} \\
&+ \int_0^\infty dr\, P_b(r) P_a(r) \int d\Omega \ Y^\star_{l_b m_b} \boldsymbol{\nabla}\, Y_{l_a m_a}
\end{aligned} \tag{5.62}$$

We can rewrite the operators on spherical harmonics in terms of vector spherical harmonics as

$$\hat{r} Y_{lm}(\hat{r}) = \boldsymbol{Y}^{(-1)}_{lm}(\hat{r}) \tag{5.63}$$

$$\boldsymbol{\nabla} Y_{lm}(\hat{r}) = \frac{\sqrt{l(l+1)}}{r}\, \boldsymbol{Y}^{(1)}_{lm}(\hat{r}) \tag{5.64}$$

Using the expansion of vector spherical harmonics in terms of $\boldsymbol{Y}_{JLM}(\hat{r})$, we easily establish that

$$\langle l_b m_b|\boldsymbol{\nabla}|l_a m_a\rangle = \begin{cases} (l_a+1)\langle l_b m_b|\hat{r}|l_a m_a\rangle & \text{for } l_b = l_a - 1, \\ -l_a\langle l_b m_b|\hat{r}|l_a m_a\rangle & \text{for } l_b = l_a + 1\ . \end{cases} \tag{5.65}$$

With the aid of this expression, We find

$$\langle b|\boldsymbol{\nabla}|a\rangle = \langle l_b m_b|\hat{r}|l_a m_a\rangle \int_0^\infty dr P_b(r)\left(\frac{dP_a}{dr} + \frac{l_a}{r}P_a\right), \quad l_b = l_a - 1, \tag{5.66}$$

and

$$\langle b|\boldsymbol{\nabla}|a\rangle = \langle l_b m_b|\hat{r}|l_a m_a\rangle \int_0^\infty dr P_b(r)\left(\frac{dP_a}{dr} - \frac{l_a+1}{r}P_a\right), \quad l_b = l_a + 1. \tag{5.67}$$

We may therefore write, as in Eq. (5.61),

$$\langle b|p_\lambda|a\rangle = \langle l_b m_b|\, C^1_\lambda\, |l_a m_a\rangle\ P(ba),$$

where the radial matrix element $P(ab)$ is

$$\begin{aligned} P(ba) &= \frac{1}{i}\int_0^\infty dr P_b(r)\left(\frac{dP_a}{dr} + \frac{l_a}{r}P_a\right), \quad l_b = l_a - 1, \\ &= \frac{1}{i}\int_0^\infty dr P_b(r)\left(\frac{dP_a}{dr} - \frac{l_a+1}{r}P_a\right), \quad l_b = l_a + 1. \end{aligned} \tag{5.68}$$

Relativistic case:

It is simple to generalize the previous nonrelativistic matrix element to the relativistic case. We may write

$$\langle b|p_\lambda|a\rangle = \langle \kappa_b m_b|\, C^1_\lambda\, |\kappa_a m_a\rangle\ P(ba),$$

where the relativistic radial matrix elements $P(ab)$ is

$$P(ba) = \frac{1}{i}\int_0^\infty dr\left[P_b(r)\left(\frac{dP_a}{dr} + \frac{\eta_a}{r}P_a\right) + Q_b(r)\left(\frac{dQ_a}{dr} + \frac{\zeta_a}{r}Q_a\right)\right], \tag{5.69}$$

with $\eta_a = l_a$ or $-l_a - 1$, for $l_b = l_a - 1$ or $l_b = l_a + 1$, respectively; and $\zeta_a = l'_a$ or $-l'_a - 1$ for $l'_b = l'_a - 1$ or $l'_b = l'_a + 1$, respectively. Here $l' = l(-\kappa)$. This is the proper form for the matrix element of the momentum operator. Actually, this can be written in a somewhat more convenient form by noting that only the values $\kappa_b = -\kappa_a$ or $\kappa_b = \kappa_a \pm 1$ are permitted by angular momentum selection rules. We find:

κ_b	η_a	ζ_a
$\kappa_a - 1$	$-\kappa_a$	$-\kappa_b$
$-\kappa_a$	κ_b	κ_a
$\kappa_a + 1$	κ_b	κ_a

One should note that $P(ab) = P(ba)^*$.

Table 5.2: Lowest-order matrix elements of the specific-mass-shift operator T for valence states of Li and Na.

Lithium $Z=3$			Sodium $Z=3$		
State	$E_{\rm HF}$	$\langle v\|T\|v\rangle$	State	$E_{\rm HF}$	$\langle v\|T\|v\rangle$
$2s$	-0.19632	0.00000	$3s$	-0.18203	-0.06150
$2p_{1/2}$	-0.12864	-0.04162	$3p_{1/2}$	-0.10949	-0.03201
$2p_{3/2}$	-0.12864	-0.04162	$3p_{3/2}$	-0.10942	-0.03199

5.4.2 Application to One-Electron Atom

Consider an atom with a single valence electron and assume that the many-electron wave function is given in the frozen-core HF approximation. The lowest-order matrix element of T in a state v is then given by

$$\langle v|T|v\rangle = \sum_a [t_{vava} - t_{vaav}]$$

Since only angular momentum $l = 1$ contributes to matrix elements P_{ab}, one easily establishes that the "direct" term $\sum_a t_{vava}$ vanishes. The exchange term is given by

$$-\sum_a t_{vaav} = -\sum_a -$$

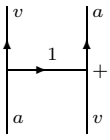

$$+ \quad T_1(vaav)\,.$$

We can carry out the sum over magnetic substates using standard graphical rules to find:

$$\langle v|T|v\rangle = -\sum_a \frac{1}{[v]}\,|\langle v||C^1||a\rangle|^2\,|P(va)|^2\,. \tag{5.70}$$

where we have used the fact that

$$P(ba) = P(ab)^\star\,.$$

Results of HF calculations of $\langle v|T|v\rangle$ using Eq.(5.70) for low-lying states in Li and Na are given in Table 5.2. For Li, the $2s$ contribution vanishes because of parity selection rules. Only the $2p$ level contributes to the SMS of the $2p-2s$ spectral line in the HF approximation. The frequency difference of the $2p-2s$ line between isotopes ^{7}Li and ^{6}Li predicted in the HF approximation is 3563 MHz. [Note that the conversion factor from atomic units (a.u.) to GHz is 3609.49 with M_A expressed in atomic mass units (u).] The corresponding NMS is 5813 MHz, and the resulting sum is 9376 MHz. This theoretical value is within about 10% of the measured isotope shift 10533 MHz. The difference is accounted for primarily by correlation corrections to the $2s$ SMS, which increases the $2p-2s$

value by 1100 MHz and leads to a theoretical value 10487 MHz for the isotope shift, in excellent agreement with measurement.

HF calculations of the SMS for Na and heavier elements are unreliable. For example, correlation corrections change the sign of the $3s$ matrix element given in Table 5.2 and reduce the $3p$ value by a factor of 3. We return to the analysis of the IS in Na in Chap. 8.

5.5 Field Shift

In addition to the normal and specific mass shifts, we also have a shift arising from the change in nuclear *radius* from one isotope to the next. This shift is referred to as the field shift and is parameterized as

$$\delta E = -F\delta\left\langle r^2\right\rangle\,, \tag{5.71}$$

where $\delta\left\langle r^2\right\rangle$ is the change in the root-mean-square radius of the nucleus. An empirical formula for the r.m.s. radius is given in Eq. (3.157).

Assuming that the nucleus can be described as a uniformly charged ball of radius R, the nuclear potential is

$$V(r,R) = \begin{cases} -(Z/2R)\,\left[3 - r^2/R^2\right]\,, & r < R \\ -Z/r\,, & r \geq R \end{cases} \tag{5.72}$$

For a uniform charge distribution, the mean square radius $\left\langle r^2\right\rangle$ is related to R^2 by

$$\left\langle r^2\right\rangle = \frac{3}{5}R^2.$$

The change in $V(r,R)$ induced by a change δR in the radius is

$$\delta V = \frac{3Z}{2R^2}\left[1 - \frac{r^2}{R^2}\right]\,\delta R, \quad r \leq R\,.$$

Expressing this result in terms of $\delta\left\langle r^2\right\rangle$, we find

$$\delta V = \frac{5Z}{4R^3}\left[1 - \frac{r^2}{R^2}\right]\,\delta\left\langle r^2\right\rangle, \quad r \leq R\,. \tag{5.73}$$

With this result in mind, we can introduce the single-particle operator $F(r)$

$$\begin{aligned} F(r) &= -\frac{5Z}{4R^3}\left[1 - \frac{r^2}{R^2}\right], \quad r \leq R \\ &= 0, \quad r > R \end{aligned}$$

and determine the field-shift parameter F from the equation

$$F = \langle F(r)\rangle\,. \tag{5.74}$$

In atomic structure calculations, the above assumption of a uniform nuclear charge density is often replaced by the more realistic assumption of a nuclear charge density given by a Fermi distribution function:

$$\rho_{\rm nuc}(r) = \frac{\rho_0}{1+\exp[(r-c)/a]}.$$

In this formula, c is the 50% fall-off radius of the density, and a is related to the 90%–10% fall-off distance t by $t = 4\ln(3)\,a$. (Nuclear models predict that $a \approx 0.5$ fm.) The corresponding nuclear potential is

$$V_{\rm nuc}(r) = \begin{cases} -\dfrac{Z}{\mathcal{N}\,c}\left[\left(\dfrac{3}{2} - \dfrac{r^2}{2\,c^2} + \dfrac{\pi^2\,a^2}{2\,c^2} + \dfrac{3\,a^2}{c^2}\,P_2\right) + \dfrac{6\,a^3}{c^2 r}\,(S_3 - P_3)\right], & \text{for } r \le c, \\ -\dfrac{Z}{\mathcal{N}\,r}\left[1 + \dfrac{\pi^2\,a^2}{c^2} + \dfrac{6\,a^3}{c^3}\,(S_3 - P_3) - \dfrac{3\,r a^2}{c^3} P_2\right], & \text{for } r > c, \end{cases} \tag{5.75}$$

where

$$S_k = \sum_{n=1}^{\infty} \frac{(-1)^{n-1}}{k^n}\ \exp\left[-n\,c/a\right],$$
$$P_k = \sum_{n=1}^{\infty} \frac{(-1)^{n-1}}{k^n}\ \exp\left[-n\,(r-c)/a\right].$$

Here,

$$\mathcal{N} = 1 + \frac{\pi^2\,a^2}{c^2} + \frac{6\,a^3}{c^3}\,S_3.$$

The root-mean-square radius of the nuclear charge distribution is related to the 50% fall off radius C by

$$R_{\rm rms} = c\sqrt{\frac{3}{5}\left(\frac{\mathcal{M}}{\mathcal{N}}\right)},$$

with

$$\mathcal{M} = 1 + \frac{10\,\pi^2\,a^2}{3\,c^2} + \frac{7\pi^4 a^4}{3\,c^4} + \frac{120\,a^5}{c^5}\,S_5.$$

In Fig. 5.1, we compare the potential $V(r)$ and the field-shift distribution function $F(r)$ for a uniform distribution with corresponding values for a Fermi distribution. It can be seen that the field-shift parameter is insensitive to details of the nuclear charge distribution.

Owing to the fact that $F(r)$ is independent of angle, calculations of atomic matrix elements in the HF approximation are very simple. Thus, for an atom with a single valence electron,

$$\langle v|F|v\rangle = f_{vv} + \sum_a [j_a] f_{aa} \tag{5.76}$$

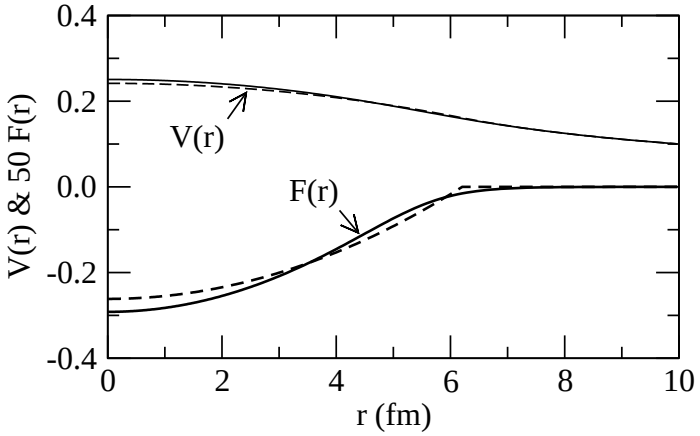

Figure 5.1: Comparison of the nuclear potential $|V(r)|$ and field-shift factor $F(r)$ calculated assuming a uniform distribution (given by solid lines) with values calculated assuming a Fermi distribution (dashed lines).

Where

$$f_{bb} = \int_0^\infty dr P_b(r)^2 F(r) \qquad \text{nonrelativistic}$$
$$= \int_0^\infty dr \left(P_b(r)^2 + Q_b(r)^2\right) F(r) \qquad \text{relativistic}$$

It should be noted that core orbitals give non-vanishing contributions to matrix elements of F in contrast to the hyperfine case studies earlier, where only the valence electron contributed.

As was found earlier for the SMS, HF calculations of the FS for heavier atoms are substantially modified by correlation corrections. Thus, for example, the HF value of F for the $6s$ state of cesium $F = -1270$ MHz/fm^2 becomes -1894 MHz/fm^2, after correlation corrections are included in the calculation.

Chapter 6

Radiative Transitions

In this chapter, we study the absorption and emission of radiation by atoms. We start with a brief review of Maxwell's equations for the radiation field and plane-wave solutions to these equations. We introduce the quantized electromagnetic field, and expand the atom-field interaction Hamiltonian in terms of photon creation and annihilation operators. The interaction between the atom and field is described using the perturbation expansion of the S-matrix. Spontaneous and induced emission are explained, and expressions for the Einstein A and B coefficients are derived. We give the multipole decomposition of the fields and discuss selection rules and intensity ratios. Detailed studies are made of transitions in one- and two-electron atoms.

6.1 Review of Classical Electromagnetism

The electric field $\mathbf{E}(\mathbf{r},t)$ and magnetic field $\mathbf{B}(\mathbf{r},t)$ (magnetic flux density vector) generated by a charge density $\rho(\mathbf{r},t)$ and a current density $\mathbf{J}(\mathbf{r},t)$ are governed by Maxwell's equations, which (in S.I. units) are

$$\begin{aligned} \boldsymbol{\nabla}\cdot\mathbf{E} &= \tfrac{1}{\epsilon_0}\,\rho, & \boldsymbol{\nabla}\cdot\mathbf{B} &= 0, \\ \boldsymbol{\nabla}\times\mathbf{B} &= \mu_0\,\mathbf{J} + \tfrac{1}{c^2}\,\frac{\partial\mathbf{E}}{\partial t}, & \boldsymbol{\nabla}\times\mathbf{E} &= -\frac{\partial\mathbf{B}}{\partial t}. \end{aligned} \tag{6.1}$$

These fields couple to the atomic electrons through the scalar and vector potentials, so let us start with a review of these potentials.

6.1.1 Electromagnetic Potentials

The fields $\mathbf{E}(\mathbf{r},t)$ and $\mathbf{B}(\mathbf{r},t)$ are represented in terms of a scalar potential $\phi(\mathbf{r},t)$ and a vector potential $\mathbf{A}(\mathbf{r},t)$ through the differential relations

$$\begin{aligned} \mathbf{E}(\mathbf{r},t) &= -\boldsymbol{\nabla}\phi(\mathbf{r},t) - \frac{\partial \mathbf{A}(\mathbf{r},t)}{\partial t}, & (6.2)\\ \mathbf{B}(\mathbf{r},t) &= \boldsymbol{\nabla}\times\mathbf{A}(\mathbf{r},t). & (6.3) \end{aligned}$$

The homogeneous Maxwell equations are satisfied identically by these relations and the inhomogeneous Maxwell equations can be written

$$\begin{aligned} \nabla^2\phi - \frac{1}{c^2}\frac{\partial^2\phi}{\partial t^2} &= -\frac{1}{\epsilon_0}\,\rho(\mathbf{r},t), & (6.4)\\ \nabla^2\mathbf{A} - \frac{1}{c^2}\frac{\partial^2\mathbf{A}}{\partial t^2} &= -\mu_0\,\mathbf{J}(\mathbf{r},t), & (6.5) \end{aligned}$$

provided the potentials satisfy the Lorentz condition,

$$\boldsymbol{\nabla}\cdot\mathbf{A} + \frac{1}{c^2}\frac{\partial\phi}{\partial t} = 0. \tag{6.6}$$

The electric and magnetic fields remain unchanged when the potentials are subjected to a *gauge transformation*,

$$\begin{aligned} \mathbf{A}(\mathbf{r},t) &\rightarrow \mathbf{A}'(\mathbf{r},t) = \mathbf{A}(\mathbf{r},t) + \boldsymbol{\nabla}\chi(\mathbf{r},t), & (6.7)\\ \phi(\mathbf{r},t) &\rightarrow \phi'(\mathbf{r},t) = \phi(\mathbf{r},t) - \frac{\partial\chi(\mathbf{r},t)}{\partial t}. & (6.8) \end{aligned}$$

From the Lorentz condition, it follows that the gauge function $\chi(\mathbf{r},t)$ satisfies the wave equation,

$$\nabla^2\chi(\mathbf{r},t) - \frac{1}{c^2}\frac{\partial^2\chi(\mathbf{r},t)}{\partial t^2} = 0. \tag{6.9}$$

Let us consider harmonic electromagnetic fields with time dependence $\exp(\mp i\omega t)$. The corresponding potentials are written

$$\begin{aligned} \mathbf{A}(\mathbf{r},t) &= \mathbf{A}_\pm(\mathbf{r},\omega)\,e^{\mp i\omega t},\\ \phi(\mathbf{r},t) &= \phi_\pm(\mathbf{r},\omega)\,e^{\mp i\omega t}. \end{aligned}$$

For such waves, the Lorentz condition becomes

$$c\,\boldsymbol{\nabla}\cdot\mathbf{A}_\pm(\mathbf{r},\omega) \mp ik\,\phi_\pm(\mathbf{r},\omega) = 0, \tag{6.10}$$

where $k = \omega/c$. Equations (6.7) and (6.8) describing a gauge transformation become

$$\begin{aligned} \mathbf{A}_\pm(\mathbf{r},\omega) &\rightarrow \mathbf{A}'_\pm(\mathbf{r},\omega) = \mathbf{A}_\pm(\mathbf{r},\omega) + \boldsymbol{\nabla}\chi_\pm(\mathbf{r},\omega), & (6.11)\\ \phi_\pm(\mathbf{r},\omega) &\rightarrow \phi'_\pm(\mathbf{r},\omega) = \phi_\pm(\mathbf{r},\omega) \pm i\omega\,\chi_\pm(\mathbf{r},\omega), & (6.12) \end{aligned}$$

and the wave equation (6.9) reduces to the Helmholtz equation

$$\nabla^2\chi_\pm(\mathbf{r},\omega) + k^2\chi_\pm(\mathbf{r},\omega) = 0. \tag{6.13}$$

Gauge transformations can be used to bring potentials into various convenient forms. One particularly important form, referred to as the *transverse gauge*, is defined by the condition

$$\boldsymbol{\nabla}\cdot\mathbf{A}_\pm(\mathbf{r},\omega) = 0. \tag{6.14}$$

It follows from the Lorentz condition that, in the transverse gauge, the scalar potential vanishes:

$$\phi_\pm(\mathbf{r},\omega) = 0. \tag{6.15}$$

Any given set of potentials ($\mathbf{A}_\pm(\mathbf{r},\omega)$, $\phi_\pm(\mathbf{r},\omega)$) satisfying the Lorentz condition can, of course, be transformed into the transverse gauge by a suitably chosen gauge transformation. In the transverse gauge, the electric and magnetic fields are given by

$$\mathbf{E}_\pm(\mathbf{r},\omega) = \pm i\omega\mathbf{A}_\pm(\mathbf{r},\omega), \tag{6.16}$$

$$\mathbf{B}_\pm(\mathbf{r},\omega) = \boldsymbol{\nabla}\times\mathbf{A}_\pm(\mathbf{r},\omega). \tag{6.17}$$

6.1.2 Electromagnetic Plane Waves

Let us consider plane-wave solutions to the source-free Maxwell equations. If we suppose that these plane waves are propagating in the direction $\hat{k}$, then the transverse-gauge vector potential is

$$\mathbf{A}_\pm(\mathbf{r},\omega) = \hat{\epsilon}\, e^{\pm i\mathbf{k}\cdot\mathbf{r}}. \tag{6.18}$$

The vector $\mathbf{k} = k\hat{k}$ is called the propagation vector, and the unit vector $\hat{\epsilon}$ is called the polarization vector. From the relation (6.14) it follows that the polarization vector is orthogonal to the propagation vector. The two-dimensional space perpendicular to $\hat{k}$ is spanned by two orthogonal polarization vectors. If, for example, we suppose $\hat{k}$ is along the z axis, then the unit vector along the x axis, $\hat{\imath}$, and the unit vector along the y axis, $\hat{\jmath}$, span the two-dimensional space of polarization vectors. Fields described by these unit vectors are *linearly polarized* along the x axis and y axis, respectively. From Eqs.(6.16,6.17), it follows that for plane waves linearly polarized along direction $\hat{\imath}$, the electric field $\mathbf{E}$ is along $\hat{\imath}$ and the magnetic field $\mathbf{B}$ is along $\hat{\jmath} = [\hat{k}\times\hat{\imath}]$.

A *real* linear combination, $\hat{\epsilon} = \cos\varphi\,\hat{\imath} + \sin\varphi\,\hat{\jmath}$ describes a wave that is linearly polarized at angle φ to the x axis. Moreover, the combinations

$$\hat{\epsilon}_\pm = \frac{1}{\sqrt{2}}\,(\hat{\imath} \pm i\hat{\jmath})$$

describe *left- and right-circularly polarized* waves, respectively. For circularly-polarized waves, the electric field vector at a fixed point in space rotates in a

circle in the plane perpendicular to $\hat{k}$, the sense of rotation being positive or negative for left- or right-circularly polarized waves, respectively. Generally, we let $\hat{\epsilon}_\lambda$ (with $\lambda = \pm 1$) represent two orthogonal unit vectors, spanning the space of polarization vectors. We take these vectors to be either two real vectors describing linear polarization or the two complex vectors describing circular polarization. In either case we have

$$\begin{array}{lll} \hat{\epsilon}_1^* \cdot \hat{\epsilon}_1 = 1, & \hat{\epsilon}_{-1}^* \cdot \hat{\epsilon}_{-1} = 1, & \hat{\epsilon}_1^* \cdot \hat{\epsilon}_{-1} = 0, \\ \hat{k} \cdot \hat{\epsilon}_1 = 0, & \hat{k} \cdot \hat{\epsilon}_{-1} = 0, & \hat{k} \cdot \hat{k} = 1. \end{array}$$

A plane-wave solution is, therefore, characterized by frequency ω, propagation direction $\hat{k}$, and polarization vector $\hat{\epsilon}_\lambda$. To simplify our notation somewhat, we use a single index i to refer to the entire set of parameters $i = (\omega, \hat{k}, \hat{\epsilon}_\lambda)$ describing the wave.

The general solution to the time-dependent wave equation in the transverse gauge can be written as a superposition of plane wave solutions

$$\mathbf{A}(\mathbf{r}, t) = \sum_i \mathbf{A}_i(\mathbf{r}, t), \tag{6.19}$$

where

$$\mathbf{A}_i(\mathbf{r}, t) = c_i \, \hat{\epsilon}_\lambda \, e^{i\mathbf{k}\cdot\mathbf{r} - i\omega t} + c_i^* \, \hat{\epsilon}_\lambda^* \, e^{-i\mathbf{k}\cdot\mathbf{r} + i\omega t}. \tag{6.20}$$

The constants c_i and c_i^* are Fourier expansion coefficients. From Eq.(6.20), it follows that the vector potential is real.

6.2 Quantized Electromagnetic Field

We carry out the quantization of the electromagnetic field in a box of volume V. The vector $\mathbf{k}$ in Eq.(6.20) then takes on discrete values depending on boundary conditions at the surface of the box, with the number of distinct vectors in the interval d^3k given by $d^3n = V d^3k/(2\pi)^3$. To quantize the field, we interpret the expansion coefficients c_i and c_i^* in Eq.(6.20) as quantum mechanical operators. In this way we obtain the operator $\mathbf{A}_i(\mathbf{r}, t)$ representing a photon with frequency ω, propagation direction $\hat{k}$, and polarization vector $\hat{\epsilon}_\lambda$:

$$\mathbf{A}_i(\mathbf{r}, t) = \sqrt{\frac{\hbar}{2\epsilon_0 \omega V}} \left[c_i \, \hat{\epsilon}_\lambda \, e^{i\mathbf{k}\cdot\mathbf{r} - i\omega t} + c_i^\dagger \, \hat{\epsilon}_\lambda^* \, e^{-i\mathbf{k}\cdot\mathbf{r} + i\omega t} \right]. \tag{6.21}$$

In this equation, c_i and $c_i^\dagger$ are photon annihilation and creation operators, respectively. These operators satisfy the commutation relations

$$[c_i, c_j] = 0, \quad [c_i^\dagger, c_j^\dagger] = 0, \quad [c_i, c_j^\dagger] = \delta_{ij}. \tag{6.22}$$

The coefficient $\sqrt{\hbar/2\epsilon_0\omega V}$ is chosen in such a way that the expression for the energy has an obvious interpretation in terms of photons.

The general expression for the quantized vector potential is a superposition of the photon potentials, as in Eq.(6.19),

$$\mathbf{A}(\mathbf{r},t) = \sum_i \mathbf{A}_i(\mathbf{r},t).$$

The corresponding electric and magnetic fields are given by

$$\mathbf{E}(\mathbf{r},t) = i\sum_i \sqrt{\frac{\hbar\omega}{2\epsilon_0 V}}\,\left[c_i\,\hat{\epsilon}_\lambda\,e^{i\mathbf{k}\cdot\mathbf{r}-i\omega t} - c_i^\dagger\,\hat{\epsilon}_\lambda^*\,e^{-i\mathbf{k}\cdot\mathbf{r}+i\omega t}\right],$$

$$\mathbf{B}(\mathbf{r},t) = \frac{i}{c}\sum_i \sqrt{\frac{\hbar\omega}{2\epsilon_0 V}}\,\left[c_i\,[\hat{k}\times\hat{\epsilon}_\lambda]\,e^{i\mathbf{k}\cdot\mathbf{r}-i\omega t} - c_i^\dagger\,[\hat{k}\times\hat{\epsilon}_\lambda^*]\,e^{-i\mathbf{k}\cdot\mathbf{r}+i\omega t}\right].$$

The Hamiltonian governing the electromagnetic field is

$$\begin{aligned} H_{EM} &= \frac{\epsilon_0}{2}\int d^3r\,\mathbf{E}(\mathbf{r},t)\cdot\mathbf{E}(\mathbf{r},t) + \frac{1}{2\mu_0}\int d^3r\,\mathbf{B}(\mathbf{r},t)\cdot\mathbf{B}(\mathbf{r},t) \\ &= \frac{1}{4}\sum_i \hbar\omega\,\left(\hat{\epsilon}_\lambda^*\cdot\hat{\epsilon}_\lambda + [\hat{k}\times\hat{\epsilon}_\lambda]\cdot[\hat{k}\times\hat{\epsilon}_\lambda^*]\right)\,\left(c_i c_i^\dagger + c_i^\dagger c_i\right) \qquad (6.23) \\ &= \sum_i \hbar\omega\,\left(\mathcal{N}_i + \frac{1}{2}\right), \end{aligned}$$

where $\mathcal{N}_i = c_i^\dagger c_i$ is the photon number operator.

6.2.1 Eigenstates of $\mathcal{N}_i$

Let us say a few words about eigenstates of the number operator $\mathcal{N}_i$, which are also eigenstates of the electromagnetic Hamiltonian. For simplicity, we drop the subscript i and consider an eigenstate of the generic operator $\mathcal{N} = c^\dagger c$. If we let $|\nu\rangle$ be an eigenstate of $\mathcal{N}$

$$\mathcal{N}|\nu\rangle = \nu|\nu\rangle, \qquad (6.24)$$

then it follows from the commutation relation $[c, c^\dagger] = 1$ that $c\,|n\rangle$ is an eigenstate with eigenvalue $\nu - 1$ and $c^\dagger|\nu\rangle$ is an eigenstate with eigenvalue $\nu + 1$. By applying c repeatedly to the state $|\nu\rangle$, we generate a sequence of states with eigenvalues $\nu - 1$, $\nu - 2$, $\cdots$. If we require that the eigenvalues of $\mathcal{N}$ (and therefore the energy) be nonnegative, then it follows that this sequence must terminate after a finite number of steps n. This will happen only if $\nu = n$. Thus, the eigenvalues of the number operator are integers.

We write

$$\begin{aligned} c\,|n\rangle &= \alpha\,|n-1\rangle, \\ c^\dagger|n\rangle &= \beta\,|n+1\rangle. \end{aligned}$$

It is simple to evaluate the constants α and β. For this purpose, we consider

$$\begin{aligned} n &= \langle n|c^\dagger c|n\rangle = \alpha^2\langle n-1|n-1\rangle = \alpha^2, \qquad (6.25) \\ &= \langle n|(-1+cc^\dagger)|n\rangle = -\langle n|n\rangle + \beta^2\langle n+1|n+1\rangle = -1+\beta^2, \qquad (6.26) \end{aligned}$$

From Eq.(6.25), it follows that $\alpha = \sqrt{n}$ and from Eq.(6.26) $\beta = \sqrt{n+1}$. We therefore have

$$c|n\rangle = \sqrt{n}\,|n-1\rangle, \tag{6.27}$$
$$c^\dagger|n\rangle = \sqrt{n+1}\,|n+1\rangle. \tag{6.28}$$

The electromagnetic vacuum state $|0\rangle$ is the state for which $\mathcal{N}_i|0\rangle = 0$ for all i. The vacuum state is an eigenstate of $H_{\rm EM}$ having energy

$$E_0 = \frac{1}{2}\sum_i \hbar\omega_i.$$

This is the (infinite) zero-point energy of the electromagnetic field. Since the zero-point energy is not measurable, it is convenient to subtract it from the electromagnetic Hamiltonian. This is accomplished by replacing the operator products in Eq.(6.23) by normal products. The modified electromagnetic Hamiltonian is

$$H_{\rm EM} = \sum_i \hbar\omega\mathcal{N}_i$$

An eigenstate of the $H_{\rm EM}$ corresponding to a photon in state i with frequency ω, propagation direction $\hat{k}$ and polarization vector $\hat{\epsilon}_\lambda$ is $|1_i\rangle = c_i^\dagger|0\rangle$. The corresponding eigenvalue is $\hbar\omega$. Generally, the state $|n_i\rangle$ is an eigenstate of $H_{\rm EM}$ with eigenvalue $n_i\hbar\omega$.

6.2.2 Interaction Hamiltonian

The interaction of an electron with this external field is described by the Hamiltonian

$$\begin{aligned} h_I(\mathbf{r},t) &= -ec\,\boldsymbol{\alpha}\cdot\boldsymbol{A}(\mathbf{r},t) \\ &= \sum_i \left[h_I(\mathbf{r},\omega)\,c_i\,e^{-i\omega t} + h_I^\dagger(\mathbf{r},\omega)\,c_i^\dagger e^{i\omega t}\right], \end{aligned} \tag{6.29}$$

where

$$h_I(\mathbf{r},\omega) = -ec\sqrt{\frac{\hbar}{2\epsilon_0\omega V}}\,\boldsymbol{\alpha}\cdot\hat{\epsilon}_\lambda\,e^{i\mathbf{k}\cdot\mathbf{r}}. \tag{6.30}$$

The corresponding many-electron interaction Hamiltonian in the Heisenberg representation is given by

$$H_I(t) = \sum_k \left[H_I(\omega)\,c_k\,e^{-i\omega t} + H_I^\dagger(\omega)\,c_k^\dagger\,e^{i\omega t}\right], \tag{6.31}$$

where $H_I(\omega)$ is a sum of one-electron terms,

$$H_I(\omega) = \sum_{i=1}^{N} h_I(\mathbf{r}_i,\omega). \tag{6.32}$$

The interaction Hamiltonian in the Schrödinger representation is just the interaction Hamiltonian in the Heisenberg representation evaluated at $t = 0$.

6.2.3 Time-Dependent Perturbation Theory

Let us now consider the effect of adding the interaction Hamiltonian H_I to the sum of the many-electron Hamiltonian $H_0 + V_I$ and the electromagnetic Hamiltonian $H_{\rm EM}$,

$$H = H_0 + V_I + H_{\rm EM}. \tag{6.33}$$

We let Ψ_k represent an eigenfunction of $H_0 + V_I$ belonging to eigenvalue E_k,

$$(H_0 + V_I)\Psi_k = E_k \Psi_k, \tag{6.34}$$

and we let $|n_k\rangle$ be an n_k photon eigenstate of $H_{\rm EM}$ with eigenvalue $n_k\hbar\omega$,

$$H_{\rm EM}|n_k\rangle = n_k\hbar\omega\,|n_k\rangle.$$

An eigenstate of H corresponding to a many-electron atom in the state Ψ_k and n_k photons is the product state

$$\Phi_k \stackrel{\rm def}{=} \Psi_k\,|n_k\rangle.$$

This is an eigenstate of H with eigenvalue $E_k + n_k\hbar\omega$. We are interested in transitions between such stationary states induced by the interaction H_I.

In the *interaction representation*, the Schrödinger equation for a state $\Phi(t)$ is written

$$i\hbar\frac{\partial\Phi(t)}{\partial t} = \hat{H}_I(t)\,\Phi(t)\,, \tag{6.35}$$

where $\hat{H}_I(t)$ is the time-dependent interaction Hamiltonian

$$\hat{H}_I(t) = e^{iHt/\hbar}H_I e^{-iHt/\hbar}. \tag{6.36}$$

Let us introduce the unitary operator $U(t,t_0)$ describing the evolution of stationary states Φ_k prepared at $t = t_0$,

$$\Phi_k(t) = U(t,t_0)\,\Phi_k.$$

It follows from Eq.(6.35) that $U(t,t_0)$ satisfies

$$\begin{aligned} i\hbar\frac{\partial U(t,t_0)}{\partial t} &= \hat{H}_I U(t,t_0) \\ U(t_0,t_0) &= I\,, \end{aligned} \tag{6.37}$$

where I is the identity operator. These equations can be rewritten as an equivalent integral equation

$$U(t,t_0) = I - \frac{i}{\hbar}\int_{t_0}^{t} dt_1 \hat{H}_I(t_1)\,U(t_1,t_0)\,. \tag{6.38}$$

The iteration solution to Eq.(6.38) is

$$\begin{aligned} U(t,t_0) &= I - \frac{i}{\hbar}\int_{t_0}^{t} dt_1\,\hat{H}_I(t_1) + \frac{(-i)^2}{\hbar^2}\int_{t_0}^{t} dt_1\,\hat{H}_I(t_1)\int_{t_0}^{t_1} dt_2\,\hat{H}_I(t_2)U(t_2,t_0) \\ &= \sum_{n=0}^{\infty}\frac{(-i)^n}{\hbar^n}\int_{t_0}^{t} dt_1\,\hat{H}_I(t_1)\int_{t_0}^{t_1} dt_2\,\hat{H}_I(t_2)\cdots\int_{t_0}^{t_{n-1}} dt_n\,\hat{H}_I(t_n)\,. \end{aligned} \tag{6.39}$$

The S operator is the unitary operator that transforms states prepared at times in the remote past ($t = -\infty$), when the interaction $H_I(t)$ is assumed to vanish, into states in the remote future ($t = \infty$), when $H_I(t)$ is also assumed to vanish. Thus

$$S = U(\infty, -\infty).$$

Expanding S in powers of H_I, we have

$$S = I + \sum_{n=1}^{\infty} S^{(n)},$$

where

$$S^{(n)} = \frac{(-i)^n}{\hbar^n} \int_{-\infty}^{\infty} dt_1 \, \hat{H}_I(t_1) \int_{-\infty}^{t_1} dt_2 \, \hat{H}_I(t_2) \cdots \int_{-\infty}^{t_{n-1}} dt_n \, \hat{H}_I(t_n) \, .$$

To first order in H_I we have

$$S \approx I - \frac{i}{\hbar} \int_{-\infty}^{\infty} dt \, \hat{H}_I(t). \tag{6.40}$$

The first-order transition amplitude for a state Φ_i prepared in the remote past to evolve into a state Φ_f in the remote future is

$$S_{fi}^{(1)} = \langle \Phi_f | S^{(1)} | \Phi_i \rangle = -\frac{i}{\hbar} \int_{-\infty}^{\infty} dt \, \langle \Phi_f^\dagger | e^{iHt/\hbar} H_I e^{-iHt/\hbar} | \Phi_i \rangle \, . \tag{6.41}$$

6.2.4 Transition Matrix Elements

Let us consider an atom in an initial state Ψ_i interacting with n_i photons. The initial state is

$$\Phi_i = \Psi_i \, |n_i\rangle.$$

The operator c_i in $H_I(t)$ will cause transitions to states with $n_i - 1$ photons, while the operator $c_i^\dagger$ will lead to states with $n_i + 1$ photons. Thus, we must consider two possibilities:

1. photon absorption, leading to a final state

$$\Phi_f = \Psi_f | n_i - 1 \rangle, \text{ and}$$

2. photon emission, leading to a final state

$$\Phi_f = \Psi_f | n_i + 1 \rangle.$$

For the case of photon absorption, using the fact that

$$\langle n_i - 1 | c_i | n_i \rangle = \sqrt{n_i},$$

we may write

$$\begin{aligned} S_{fi}^{(1)} &= -\frac{i}{\hbar}\sqrt{n_i}\int_{-\infty}^{\infty} dt\, e^{i(E_f-E_i-\hbar\omega)t/\hbar}\langle\Psi_f|H_I|\Psi_i\rangle \\ &= -2\pi i\delta(E_f-E_i-\hbar\omega)\,\sqrt{n_i}\,\langle\Psi_f|H_I|\Psi_i\rangle. \end{aligned} \tag{6.42}$$

Similarly, for the case of photon emission, we find

$$\begin{aligned} S_{fi}^{(1)} &= -\frac{i}{\hbar}\sqrt{n_i+1}\int_{-\infty}^{\infty} dt\, e^{i(E_f-E_i+\hbar\omega)t/\hbar}\langle\Psi_f|H_I^\dagger|\Psi_i\rangle \\ &= -2\pi i\delta(E_f-E_i+\hbar\omega)\,\sqrt{n_i+1}\,\langle\Psi_f|H_I^\dagger|\Psi_i\rangle. \end{aligned} \tag{6.43}$$

We introduce the *transition amplitude*

$$T_{fi} = \begin{cases} \langle\Psi_f|H_I|\Psi_i\rangle, & \text{for absorption of radiation,} \\ \langle\Psi_f|H_I^\dagger|\Psi_i\rangle, & \text{for emission of radiation.} \end{cases}$$

We treat the two cases simultaneously using

$$S_{fi} = -2\pi\delta(E_f-E_i\mp\hbar\omega)\,T_{fi}\begin{pmatrix}\sqrt{n_i}\\ \sqrt{n_i+1}\end{pmatrix}, \tag{6.45}$$

where the upper contribution refers to absorption and the lower refers to emission. The probability of a transition from state Ψ_i to state Ψ_f is just the square of $S_{fi}^{(1)}$. In evaluating the square, we replace one factor of $2\pi\delta(E_f-E_i\mp\hbar\omega)$ by $T/\hbar$, where T is the total interaction time. Thus, we find that the transition probability per unit time W_{fi} is given by

$$W_{fi} = \frac{2\pi}{\hbar}\delta(E_f-E_i\mp\hbar\omega)\,|T_{fi}|^2\begin{pmatrix}n_i\\ n_i+1\end{pmatrix}. \tag{6.46}$$

In an interval of wave numbers d^3k, there are

$$d^3n_i = \frac{V}{(2\pi)^3}d^3k = \frac{V}{(2\pi c)^3}\omega^2 d\omega d\Omega_k \tag{6.47}$$

photon states of a given polarization. The corresponding number of transitions per second d^3w_{fi} is thus given by

$$d^3w_{fi} = W_{fi}\,d^3n_i = \frac{V}{(2\pi)^2c^3\hbar}\,\delta(E_f-E_i\mp\hbar\omega)\,\omega^2 d\omega d\Omega_k|T_{fi}|^2\begin{pmatrix}n_i\\ n_i+1\end{pmatrix}.$$

Integrating over ω, we obtain

$$d^2w_{fi} = \frac{V}{(2\pi\hbar)^2c^3}\,\omega^2 d\Omega_k|T_{fi}|^2\begin{pmatrix}n_i\\ n_i+1\end{pmatrix},$$

where n_i is now the number of photons with energy $\hbar\omega = E_f - E_i$ for absorption and $\hbar\omega = E_i - E_f$ for emission. Factoring $-ec\sqrt{\hbar/2\epsilon_0\omega V}$ from the interaction Hamiltonian, we obtain

$$d^2w_{fi} = \frac{\alpha}{2\pi}\,\omega\,d\Omega_k|T_{fi}|^2\begin{pmatrix}n_i\\ n_i+1\end{pmatrix}, \tag{6.48}$$

where the single-particle interaction Hamiltonian is now replaced by

$$h_I(\mathbf{r},\omega) \to \boldsymbol{\alpha}\cdot\hat{\epsilon}_\lambda\, e^{i\mathbf{k}\cdot\mathbf{r}}. \tag{6.49}$$

Let us assume that we have a collection of atoms in equilibrium with a radiation field. Further, let us assume that the photons of frequency ω in the radiation field are distributed isotropically and that the number of photons in each of the two polarization states is equal. In this case, the photon number n can be related to the *spectral density function* $\rho(\omega)$ which is defined as the photon energy per unit volume in the frequency interval $d\omega$. One finds from (6.47) that

$$\rho(\omega) = 2\times n\hbar\omega\times\frac{4\pi\omega^2}{(2\pi c)^3} = \frac{\hbar\omega^3}{\pi^2c^3}\,n\,. \tag{6.50}$$

For isotropic, unpolarized radiation, we can integrate Eq.(6.23) over angles Ω_k and sum over polarization states $\hat{\epsilon}_\lambda$, treating n as a multiplicative factor. The resulting absorption probability per second, $w_{b\to a}$, leading from an initial (lower energy) state a to final (higher energy) state b in presence of n photons of energy $\hbar\omega$ is given in terms of the spectral density function $\rho(\omega)$ as

$$w^{\rm ab}_{a\to b} = \frac{\pi^2c^3}{\hbar\omega^3}\rho(\omega)\,\frac{\alpha}{2\pi}\omega\sum_\lambda\int d\Omega_k|T_{ba}|^2. \tag{6.51}$$

Similarly, the emission probability per second leading from state b to state a in the presence of n photons of energy $\hbar\omega$ is given in terms of $\rho(\omega)$ by

$$w^{\rm em}_{b\to a} = \left(1+\frac{\pi^2c^3}{\hbar\omega^3}\rho(\omega)\right)\frac{\alpha}{2\pi}\omega\sum_\lambda\int d\Omega_k|T_{ab}|^2. \tag{6.52}$$

The emission probability consists of two parts, a *spontaneous emission* contribution, $w^{\rm sp}_{b\to a}$, that is independent of $\rho(\omega)$, and an *induced* or *stimulated* emission contribution, $w^{\rm ie}_{b\to a}$ that is proportional to $\rho(\omega)$.

Let the state a be a member of a g-fold degenerate group of levels γ, and b be a member of a g'-fold degenerate group of levels γ'. If we assume that the atom can be in any of the degenerate initial levels with equal probability, then the average transition probability from $\gamma\to\gamma'$ is found by summing over sublevels a and b and dividing by g, whereas the average transition probability from $\gamma'\to\gamma$ is given by the sum over a and b divided by γ'. The Einstein A- and B-coefficients are defined in terms of average transition probabilities per second between degenerate levels through the relations

$$B_{\gamma\gamma'}\rho(\omega) = w^{\rm ab}_{\gamma\gamma'} = \frac{1}{g}\sum_{ab} w^{\rm ab}_{a\to b}, \tag{6.53}$$

$$A_{\gamma'\gamma} = w^{\rm sp}_{\gamma'\gamma} = \frac{1}{g'}\sum_{ab} w^{\rm sp}_{b\to a}, \tag{6.54}$$

$$B_{\gamma'\gamma}\rho(\omega) = w^{\rm ie}_{\gamma'\gamma} = \frac{1}{g'}\sum_{ab} w^{\rm ie}_{b\to a}. \tag{6.55}$$

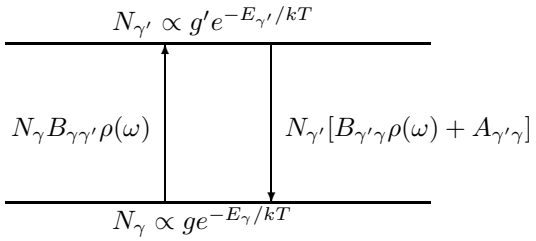

Figure 6.1: Detailed balance for radiative transitions between two levels.

It follows from Eqs.(6.51-6.52), that the three Einstein coefficients are related by equations

$$g' B_{\gamma'\gamma} = g B_{\gamma\gamma'}, \tag{6.56}$$

$$A_{\gamma'\gamma'} = \frac{\hbar\omega^3}{\pi^2 c^3} B_{\gamma'\gamma}. \tag{6.57}$$

If we suppose that there are N_γ atoms in the lower level γ, and $N_{\gamma'}$ atoms in the upper level γ', then, on average, there will be $N_\gamma B_{\gamma\gamma'}\rho(\omega)$ upward transitions to level γ' per second, and $N_{\gamma'}[B_{\gamma'\gamma}\rho(\omega) + A_{\gamma'\gamma}]$ downward transitions from γ' to γ per second. The principle of detailed balance requires that, in equilibrium, the number of upward transitions per second between the two levels equals the number of downward transitions per second. This, in turn, leads to the relation

$$\frac{N_{\gamma'}}{N_\gamma} = \frac{B_{\gamma\gamma'}\rho(\omega)}{A_{\gamma'\gamma} + B_{\gamma'\gamma}\rho(\omega)}. \tag{6.58}$$

Assuming that the number of atomic states of energy E_γ in the equilibrium distribution at temperature T is proportional to $exp(-E_\gamma/kT)$, where k is Boltzmann's constant, we have

$$\frac{N_{\gamma'}}{N_\gamma} = \frac{g' e^{-E_{\gamma'}/kT}}{g e^{-E_\gamma/kT}} = \frac{g'}{g} e^{-\hbar\omega/kT}.$$

Substituting this relation into (6.58), and making use of the symmetry relations between the Einstein coefficients, (6.56-6.57), leads to Planck's formula for the spectral energy density,

$$\rho(\omega) = \frac{1}{\pi^2 c^3} \frac{\hbar\omega^3}{e^{\hbar\omega/kT} - 1}. \tag{6.59}$$

In the low-energy limit, this reduces to the classical Rayleigh-Jeans formula

$$\lim_{\omega\to 0} \rho(\omega) = \frac{\omega^2}{\pi^2 c^3}\, kT.$$

The Planck formula is a direct consequence of the fact that the photon creation and annihilation operators satisfy the commutation relations (6.22). Conversely,

the fact that radiation in equilibrium with matter is found to satisfy the Planck formula experimentally is strong evidence for the quantum mechanical nature of the electromagnetic field.

6.2.5 Gauge Invariance

Let us consider the interaction of an electron with a field described by potentials

$$\mathbf{A}(\mathbf{r},\omega)e^{-i\omega t} \quad \text{and} \quad \phi(\mathbf{r},\omega)e^{-i\omega t},$$

such as those associated with absorption of a photon with frequency ω. The corresponding interaction Hamiltonian can be written

$$h(\mathbf{r},t) = h(\mathbf{r},\omega)e^{-i\omega t},$$

with

$$h_I(\mathbf{r},\omega) = e\left\{-c\boldsymbol{\alpha}\cdot A(\mathbf{r},\omega) + \phi(\mathbf{r},\omega)\right\}. \tag{6.60}$$

A gauge transformation induces the following change in $h_I(\mathbf{r},\omega)$:

$$\Delta h_I(\mathbf{r},\omega) = e\left\{-c\boldsymbol{\alpha}\cdot\boldsymbol{\nabla}\chi(\mathbf{r},\omega) + i\omega\chi(\mathbf{r},\omega)\right\}. \tag{6.61}$$

This equation can be rewritten in terms of the momentum operator $\boldsymbol{p}$ in the form

$$\Delta h_I = e\left\{-i\frac{c}{\hbar}\boldsymbol{\alpha}\cdot\boldsymbol{p}\chi + i\omega\chi\right\}. \tag{6.62}$$

The first term in braces can be reexpressed in terms of the commutator of the single-particle Dirac Hamiltonian,

$$h_0 = c\boldsymbol{\alpha}\cdot\boldsymbol{p} + \beta mc^2 + V_{\rm nuc}(r) + U(r), \tag{6.63}$$

with the gauge function $\chi(\mathbf{r},\omega)$, leading to

$$\Delta h_I = -i\frac{e}{\hbar}\left\{[h_0,\chi] - \hbar\omega\chi\right\}. \tag{6.64}$$

It is important to note that the expressions(6.62) and (6.64) for Δh_I are equivalent for local potentials but *not* for the non-local Hartree-Fock potential.

The transition amplitude from an initial state $|a\rangle$ to a final state $|b\rangle$, both assumed to be eigenstates of h_0, is proportional to the matrix element $\langle b|h_I|a\rangle$. The change in this matrix element induced by a gauge transformation is given by

$$\langle b|\Delta h_I|a\rangle = -i\frac{e}{\hbar}\langle b|[h_0,\chi] - \hbar\omega\chi|a\rangle = -i\frac{e}{\hbar}\left(\epsilon_b - \epsilon_a - \hbar\omega\right)\langle b|\chi|a\rangle. \tag{6.65}$$

It follows that, for states $|a\rangle$ and $|b\rangle$ that satisfy $\hbar\omega = \epsilon_b - \epsilon_a$, transition amplitudes calculated using single-particle orbitals in a local potential are gauge invariant.

Later, we will encounter the expression

$$\left\langle b \left| \frac{d\Delta h_I}{d\omega} \right| a \right\rangle .$$

This can be rewritten with the aid of the above identities as

$$\left\langle b \left| \frac{d\Delta h_I}{d\omega} \right| a \right\rangle = -i\frac{e}{\hbar} \left\langle b \left| [h_0, \frac{d\chi}{d\omega}] - \hbar\omega \frac{d\chi}{d\omega} - \hbar\chi \right| a \right\rangle = ie \left\langle b|\chi|a \right\rangle , \qquad (6.66)$$

where the identity on the right-hand side is valid only for states satisfying $\hbar\omega = \epsilon_b - \epsilon_a$.

6.2.6 Electric Dipole Transitions

Let us consider a one-electron atom and examine the transition amplitude

$$T_{ba} = \int d^3r \, \psi_b^\dagger(\mathbf{r}) \, \boldsymbol{\alpha}\cdot \hat{\epsilon} \, e^{i\mathbf{k}\cdot\mathbf{r}} \, \psi_a(\mathbf{r}). \qquad (6.67)$$

The values of r for which there are significant contributions to this integral are those less than a few atomic radii, which, for an ion with charge Z, is of order $1/Z$ a.u.. The photon energy for transitions between states having different principal quantum numbers in such an ion is of order Z^2 a.u.. For transitions between states with the same principal quantum number, the photon energy is of order Z a.u.. Using the fact that $k = \omega/c$, the factor kr in the exponent is, therefore, of order αZ for transitions between states with different principal quantum numbers and of order α for transitions between states having the same principal quantum number. In either case, for neutral atoms or ions with small ionic charge Z, the quantity $|\mathbf{k}\cdot\mathbf{r}| \leq kr \ll 1$, so one can accurately approximate the exponential factor in Eq.(6.67) by 1. In this approximation, the transition amplitude T_{ba} is just the matrix element of $\boldsymbol{\alpha}\cdot\hat{\epsilon}$.

We will first examine the transition amplitude in the nonrelativistic limit. To obtain a nonrelativistic expression for the transition amplitude, we turn to the Pauli approximation. We write the Dirac wave function $\psi_a(\mathbf{r})$ in terms of two-component functions $\phi_a(\mathbf{r})$ and $\chi_a(\mathbf{r})$,

$$\psi_a(\mathbf{r}) \approx \begin{pmatrix} \phi_a(\mathbf{r}) \\ \chi_a(\mathbf{r}) \end{pmatrix}. \qquad (6.68)$$

In the Pauli approximation, the large-component ϕ_a is the nonrelativistic wave function,

$$\left(\frac{p^2}{2m} + V(r) \right) \phi_a(\mathbf{r}) = W_a \phi_a(\mathbf{r}), \qquad (6.69)$$

and the small component $\chi_a(\mathbf{r})$ is given in terms of $\phi_a(\mathbf{r})$ by

$$\chi_a(\mathbf{r}) = \frac{\boldsymbol{\sigma}\cdot\boldsymbol{p}}{2mc} \phi_a(\mathbf{r}). \qquad (6.70)$$

The transition amplitude reduces to

$$T_{ba} = \frac{1}{2mc}\int d^3r\,\phi_b^\dagger(\mathbf{r})\,[\boldsymbol{\sigma}\cdot\boldsymbol{p}\;\boldsymbol{\sigma}\cdot\hat{\epsilon}+\boldsymbol{\sigma}\cdot\hat{\epsilon}\;\boldsymbol{\sigma}\cdot\boldsymbol{p}]\;\phi_a(\mathbf{r}) \tag{6.71}$$

$$= \frac{1}{mc}\int d^3r\,\phi_b^\dagger(\mathbf{r})\,\boldsymbol{p}\cdot\hat{\epsilon}\,\phi_a(\mathbf{r}) = \frac{1}{c}\langle b|\boldsymbol{v}|a\rangle\;\cdot\hat{\epsilon}. \tag{6.72}$$

This is known as the *velocity-form* of the transition matrix element. Now, the commutator of the single-particle Schrödinger Hamiltonian $h_{\rm nr} = p^2/2m + V(r)$ with the vector $\boldsymbol{r}$ can be written

$$[h_{\rm nr}, \boldsymbol{r}] = -i\frac{\hbar}{m}\,\boldsymbol{p} = -i\hbar\,\boldsymbol{v}, \tag{6.73}$$

so one can rewrite matrix elements of $\boldsymbol{v}$ in terms of matrix elements of the vector $\boldsymbol{r}$. Using the commutator relation, we find

$$\langle b|\boldsymbol{v}|a\rangle = i\omega_{ba}\langle b|\boldsymbol{r}|a\rangle, \tag{6.74}$$

where $\omega_{ba} = (W_b - W_a)/\hbar$. This allows us to express the transition amplitude in *length-form* as

$$T_{ba} = ik_{ba}\langle b|\boldsymbol{r}|a\rangle\cdot\hat{\epsilon}. \tag{6.75}$$

where $k_{ba} = \omega_{ab}/c$.

The electric dipole operator is $\boldsymbol{d} = e\boldsymbol{r}$ so the transition amplitude in length form is proportional to the matrix element of the electric dipole operator. The amplitudes are therefore referred to as *electric dipole* transition amplitudes. In a spherical basis, the electric dipole operator is an odd-parity irreducible tensor operator of rank one. It follows that T_{ba} is nonvanishing only between states a and b that have different parity and that satisfy the angular momentum triangle relations $|l_a - 1| \le l_b \le l_a + 1$. From parity considerations, it follows that only states satisfying $l_b = l_a \pm 1$ contribute nonvanishing matrix elements. Transitions forbidden by the dipole selection rules can give finite but small contributions to T_{ba} when higher-order terms are included in the expansion of the exponential in Eq.(6.67). These higher-order multipole contributions will be discussed further in the following section.

Let us now consider a transition from a particular atomic substate a to a substate b by spontaneous emission. The spontaneous emission probability is

$$w_{ba}^{\rm sp} = \frac{\alpha}{2\pi}\omega\sum_\lambda\int d\Omega_k|\langle a|\boldsymbol{v}|b\rangle\cdot\hat{\epsilon}_\lambda^*|^2. \tag{6.76}$$

We first examine the dependence of this expression on the photon polarization vector ϵ_λ. For this purpose, consider the quantity $I_\lambda = (\hat{\epsilon}_\lambda^*\cdot\mathbf{A})\,(\hat{\epsilon}_\lambda\cdot\mathbf{A}^*)$, where $\mathbf{A} = \langle a|\boldsymbol{v}|b\rangle$. To carry out the sum over polarization states, we must sum I_λ over both states of polarization. Taking $\hat{k}$ to be along the z axis, this leads to

$$I_1 + I_{-1} = A_xA_x^* + A_yA_y^* = \mathbf{A}\cdot\mathbf{A}^* - \mathbf{A}\cdot\hat{k}\,\mathbf{A}^*\cdot\hat{k} = |\mathbf{A}|^2\sin^2\theta. \tag{6.77}$$

Here, θ is the angle between the emitted photon and the vector $\mathbf{A}$.

The integration over photon angles is carried out next. Choosing $\mathbf{A}$ as an axis, we have

$$\int d\Omega_k \sin^2\theta = 2\pi \int_{-1}^{1} d\mu (1-\mu^2) = \frac{8\pi}{3}.$$

Thus, after summing over photon polarization states and integrating over photon emission angles, we obtain the spontaneous emission probability per second,

$$w_{ba}^{\rm sp} = \frac{4\alpha}{3}\frac{\omega}{c^2}\,|\langle a|\boldsymbol{v}|b\rangle|^2 = \frac{4\alpha}{3}\frac{\omega^3}{c^2}\,|\langle a|\boldsymbol{r}|b\rangle|^2. \tag{6.78}$$

We write the components of $\boldsymbol{r}$ in a spherical basis as r_ν and find

$$\langle a|r_\nu|b\rangle = -$$

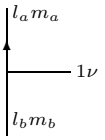

$$\langle a||r||b\rangle \delta_{\sigma_b\sigma_a}, \tag{6.79}$$

where σ_a and σ_b are spin projections, and where the reduced matrix element of $\boldsymbol{r}$ is given by

$$\langle a||r||b\rangle = \langle l_a||C_1||l_b\rangle \int_0^\infty r\,P_a(r)P_b(r)\,dr.$$

The velocity-form of this reduced matrix element is obtained with the aid of Eq.(6.74),

$$\langle b|\boldsymbol{r}|a\rangle = -\frac{i}{m\omega_{ba}}\langle b|\boldsymbol{p}|a\rangle = -\frac{\hbar}{m\omega_{ba}}\langle b|\boldsymbol{\nabla}|a\rangle,$$

together with the expression for the reduced matrix element of $\boldsymbol{\nabla}$,

$$\langle a||\nabla||b\rangle = \langle l_a||C_1||l_b\rangle \begin{cases} \int_0^\infty dr P_b\left(\frac{d}{dr} + \frac{l_a}{r}\right) P_a, & \text{for } l_b = l_a - 1, \\ \int_0^\infty dr P_b\left(\frac{d}{dr} - \frac{l_a+1}{r}\right) P_a, & \text{for } l_b = l_a + 1. \end{cases} \tag{6.80}$$

In evaluating the reduced matrix elements, the formula

$$\langle l_a||C_1||l_b\rangle = \begin{cases} -\sqrt{l_a} & \text{for } l_b = l_a - 1, \\ \sqrt{l_a+1} & \text{for } l_b = l_a + 1, \end{cases} \tag{6.81}$$

is useful.

Summing $w_{ba}^{\rm sp}$ over the magnetic substates m_b and σ_b of the final state, and m_a and σ_a of the initial state, we obtain the Einstein A-coefficient for spontaneous emission:

$$\begin{aligned} A_{ab} &= \frac{1}{2[l_a]} \sum_{\substack{m_a\sigma_a \\ m_b\sigma_b}} w_{ba}^{\rm sp} \\ &= \frac{4\alpha}{3}\frac{\omega^3}{c^2}\frac{1}{[l_a]} \sum_{m_a m_b \nu} (-1)^\nu - \end{aligned}$$

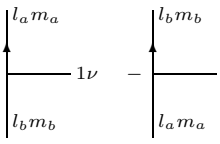

$$\begin{aligned} &\langle a||r||b\rangle\,\langle b||r||a\rangle \\ &= \frac{4\alpha}{3}\frac{\omega^3}{c^2}\frac{1}{[l_a]}\,|\langle a||r||b\rangle|^2. \end{aligned} \tag{6.82}$$

The Einstein A-coefficient is often expressed in terms of the *line strength* $S_{\rm E1}$ which is defined as

$$S_{\rm E1} = |\langle a||r||b\rangle|^2.$$

We can write

$$A_{ab} = \frac{4\alpha}{3}\,\frac{\omega^3}{c^2}\,\frac{S_{\rm E1}}{[l_a]} = \frac{16\pi}{3}k^3\frac{S_{\rm E1}}{[l_a]}R_\infty c = \frac{2.02613\times 10^{18}}{\lambda^3}\,\frac{S_{\rm E1}}{[l_a]}\,s^{-1}. \tag{6.83}$$

In the third term, R_∞ is the Rydberg constant, and in the last term, the wavelength λ is expressed in Å. The line strength in the above equation is in atomic units. In these equations, we have used the fact that the atomic unit of frequency is $4\pi R_\infty c$, where $R_\infty c = 3.28984\times 10^{15}\,{\rm s}^{-1}$.

The *oscillator strength* f_{kn} for a transition $k\to n$ is defined by

$$f_{kn} = \frac{2m\omega_{nk}}{3\hbar}|\langle k|\boldsymbol{r}|n\rangle|^2, \tag{6.84}$$

where $\omega_{nk} = (W_n - W_k)/\hbar$. If the transition is from a lower state to an upper state (absorption), then the oscillator strength is positive. The oscillator strength is a dimensionless quantity. Oscillator strengths satisfies the following important identity, known as the Thomas-Reiche-Kuhn (TRK) sum rule

$$\sum_n f_{kn} = N, \tag{6.85}$$

where N is the total number of atomic electrons. In this equation, n ranges over all states permitted by the dipole selection rules. To prove the TRK sum rule for a one electron atom, we recall that

$$\omega_{kn}\langle k|\boldsymbol{r}|n\rangle = \frac{1}{im}\langle k|\boldsymbol{p}|n\rangle,$$

and write

$$f_{kn} = \frac{m}{3\hbar}\left\{\frac{i}{m}\langle k|\boldsymbol{p}|n\rangle\cdot\langle n|\boldsymbol{r}|k\rangle - \frac{i}{m}\langle k|\boldsymbol{r}|n\rangle\cdot\langle n|\boldsymbol{p}|k\rangle\right\}.$$

Summing over n, we obtain

$$\sum_n f_{kn} = \frac{i}{3\hbar}\langle k|\,[p_x,x]+[p_y,y]+[p_z,z]\,|k\rangle = 1. \tag{6.86}$$

The *reduced oscillator strength* for a transition between degenerate levels is defined as the average over initial substates and the sum over final substates of the oscillator strength. For spontaneous emission in a one-electron atom, this gives

$$\begin{aligned}\bar{f}_{ab} &= -\frac{2m}{3\hbar}\,\frac{\omega}{2[l_a]}\sum_{\substack{m_a\sigma_a\\ m_b\sigma_b}}|\langle a|{\rm r}|b\rangle|^2\\ &= -\frac{2m}{3\hbar}\,\frac{\omega}{[l_a]}S_{\rm E1}\\ &= -\frac{303.756}{[l_a]\lambda}S_{\rm E1}.\end{aligned} \tag{6.87}$$

Table 6.1: Reduced oscillator strengths for transitions in hydrogen

n	$1s \to np$	$2s \to np$	$2p \to ns$	$2p \to nd$	$3s \to np$	$3p \to ns$	$3p \to nd$
1	$\cdots$	$\cdots$	-0.1387	$\cdots$	$\cdots$	-0.0264	$\cdots$
2	0.4162	$\cdots$	$\cdots$	$\cdots$	-0.0408	-0.1450	$\cdots$
3	0.0791	0.4349	0.0136	0.6958	$\cdots$	$\cdots$	$\cdots$
4	0.0290	0.1028	0.0030	0.1218	0.4847	0.0322	0.6183
5	0.0139	0.0419	0.0012	0.0444	0.1210	0.0074	0.1392
6	0.0078	0.0216	0.0006	0.0216	0.0514	0.0030	0.0561
7	0.0048	0.0127	0.0004	0.0123	0.0274	0.0016	0.0290
8	0.0032	0.0082	0.0002	0.0078	0.0165	0.0009	0.0172
9	0.0022	0.0056	0.0002	0.0052	0.0109	0.0006	0.0112
10	0.0016	0.0040	0.0001	0.0037	0.0076	0.0004	0.0077
11	0.0012	0.0030	0.0001	0.0027	0.0055	0.0003	0.0055
12	0.0009	0.0022	0.0001	0.0021	0.0041	0.0002	0.0041
13-∞	0.0050	0.0120	0.0003	0.0108	0.0212	0.0012	0.0210
Discrete	0.5650	0.6489	-0.1189	0.9282	0.7095	-0.1233	0.9094
Cont.	0.4350	0.3511	0.0078	0.1829	0.2905	0.0122	0.2017
Total	1.0000	1.0000	-0.1111	1.1111	1.0000	-0.1111	1.1111

The wavelength λ on the last line is expressed in Å.

Reduced oscillator strengths for transitions between levels in helium are given in Table 6.1. For transitions from s states, the only possible final states are np states. The sum of reduced oscillator strengths over all p states saturates the TRK sum rule

$$\sum_n \bar{f}_{ks\to np} = 1.$$

This sum includes an infinite sum over discrete states and an integral over the p-wave continuum. For the $s \to p$ transitions shown in the table, 30-40% of the oscillator strength is in the continuum. For states of angular momentum $l \neq 0$, the selection rules permit transitions to either $n\,l-1$ or $n\,l+1$ final states. The reduced oscillator strengths for such transitions satisfy the following partial sum rules

$$\begin{aligned}\sum_n \bar{f}_{kl\to nl-1} &= -\frac{l(2l-1)}{3(2l+1)},\\ \sum_n \bar{f}_{kl\to nl+1} &= \frac{(l+1)(2l+3)}{3(2l+1)}.\end{aligned}$$

The sum of the two partial contributions is 1, as expected from the TRK sum rule. These $l \neq 0$ transitions are tabulated for $2p \to ns$, nd and $3p \to ns$, nd transitions in Table 6.1. Again, these oscillator strengths are seen to have substantial contributions from the continuum.

Table 6.2: Hartree-Fock calculations of transition rates A_{if} [s^{-1}] and lifetimes τ [s] for levels in lithium. Numbers in parentheses represent powers of ten.

Transition	A_{if} [s^{-1}]	Transition	A_{if} [s^{-1}]	Transition	A_{if} [s^{-1}]
$5s \to 4p$	2.22(6)	$5p \to 5s$	2.41(5)	$5d \to 5p$	2.08(2)
$5s \to 3p$	2.76(6)	$5p \to 4s$	6.10(3)	$5d \to 4p$	1.39(6)
$5s \to 2p$	4.59(6)	$5p \to 3s$	2.82(4)	$5d \to 3p$	3.45(6)
$5s \to$ all	9.58(6)	$5p \to 2s$	7.15(5)	$5d \to 2p$	1.04(7)
		$5p \to 4d$	2.57(5)	$5d \to 4f$	5.07(4)
		$5p \to 3d$	2.10(5)	$5d \to$ all	1.53(7)
		$5p \to$ all	1.46(6)		
τ_{5s} [s]	1.04(-7)	τ_{5p} [s]	6.86(-7)	τ_{5d} [s]	6.52(-8)
$4s \to 3p$	7.34(6)	$4p \to 4s$	7.96(5)	$4d \to 4p$	5.46(2)
$4s \to 2p$	1.01(7)	$4p \to 3s$	1.73(2)	$4d \to 3p$	6.85(6)
$4s \to$ all	1.74(7)	$4p \to 2s$	1.02(6)	$4d \to 2p$	2.25(7)
		$4p \to 3d$	4.91(5)	$4d \to$ all	2.93(7)
		$4p \to$ all	2.30(6)		
τ_{4s} [s]	5.73(-8)	τ_{4p} [s]	4.34(-7)	τ_{4d} [s]	3.41(-8)
$3s \to 2p$	3.28(7)	$3p \to 3s$	3.82(6)	$3d \to 3p$	1.56(3)
		$3p \to 2s$	7.02(5)	$3d \to 2p$	6.73(7)
		$3p \to$ all	4.52(6)	$3d \to$ all	6.73(7)
τ_{3s} [s]	3.05(-8)	τ_{3p} [s]	2.21(-7)	τ_{3d} [s]	1.48(-8)
		$2p \to 2s$	3.76(7)		
		τ_{2p} [s]	2.66(-8)		

In Table 6.2, we present the results of Hartree-Fock calculations for transitions in lithium. We consider spontaneous transitions from all s, p, and d levels with $n \leq 5$. Both branches $l \to l \pm 1$ are considered, and the A coefficients for all allowed lower states are evaluated. The reciprocal of the resulting sum is the mean lifetime of the state,

$$\tau_a = \frac{1}{\sum_{b \leq a} A_{ab}}. \tag{6.88}$$

The $2p$ lifetime in lithium, for example, is calculated to be $\tau_{2p}^{\text{theory}} = 26.6\,\text{ns}$ compared to the measured lifetime $\tau_{2p}^{\text{exp}} = 27.2\,\text{ns}$. Similarly, a Hartree-Fock calculation for sodium gives a value $\tau_{3p}^{\text{theory}} = 18.0\,\text{ns}$ compared with the experimental value $\tau_{3p}^{\text{exp}} = 16.9\,\text{ns}$.

6.2.7 Magnetic Dipole and Electric Quadrupole Transitions

Including higher-order terms in the expansion of the exponential factor $\exp(i\mathbf{k}\cdot\mathbf{r})$ in the theory presented above leads to higher-order multipole contributions to the transition amplitude. In this section, we consider the contributions obtained by retaining only the first-order terms in the expansion of the exponential $\exp(i\mathbf{k}\cdot\mathbf{r}) \approx 1 + i\mathbf{k}\cdot\mathbf{r}$. Using the Pauli approximation, the transition amplitude becomes

$$T_{ba} = \frac{1}{2mc}\int d^3r \phi_b^\dagger(\mathbf{r})\left[2\mathbf{p}\cdot\hat{\epsilon}\,(1 + i\mathbf{k}\cdot\mathbf{r}) + \hbar\boldsymbol{\sigma}\cdot\mathbf{k}\,\boldsymbol{\sigma}\cdot\hat{\epsilon}\,\right]\phi_a(\mathbf{r}). \tag{6.89}$$

We write $T_{ba} = T_{ba}^{(0)} + T_{ba}^{(1)}$, where $T_{ba}^{(0)}$ is the electric dipole amplitude discussed previously, and where the contributions of interest here are given by

$$T_{ba}^{(1)} = \frac{ik}{2mc}\int d^3r \phi_b^\dagger(\mathbf{r})\left(2\hat{k}\cdot\mathbf{r}\,\mathbf{p}\cdot\hat{\epsilon} + \hbar\boldsymbol{\sigma}\cdot[\hat{k}\times\hat{\epsilon}]\right)\phi_a(\mathbf{r}). \tag{6.90}$$

Let us assume that $\hat{k}$ is directed along z and that $\hat{\epsilon}$ is in the xy plane. It follows that

$$2\hat{k}\cdot\mathbf{r}\,\mathbf{p}\cdot\hat{\epsilon} = 2zp_x\epsilon_x + 2zp_y\epsilon_y.$$

We write

$$2zp_x = (zp_x - xp_z) + (zp_x + xp_z),$$

and use the fact that

$$(zp_x + xp_z) = \frac{im}{\hbar}[h, zx],$$

to obtain

$$2zp_x\epsilon_x = \left(L_y + \frac{im}{\hbar}[h, zx]\right)\epsilon_x.$$

Similarly, we find

$$2zp_y\epsilon_y = \left(-L_x + \frac{im}{\hbar}[h, zy]\right)\epsilon_y.$$

These terms can be recombined in vector form to give

$$2\hat{k}\cdot\mathbf{r}\,\mathbf{p}\cdot\hat{\epsilon} = \boldsymbol{L}\cdot[\hat{k}\times\hat{\epsilon}] + \frac{im}{3\hbar}\sum_{ij}\hat{k}_i\hat{\epsilon}_j[h, Q_{ij}], \tag{6.91}$$

where $Q_{ij} = 3x_ix_j - r^2\delta_{ij}$ is the quadrupole-moment operator. Using the identity (6.91), we find

$$T^{(1)}_{ba} = ik\,\langle b|\boldsymbol{M}|a\rangle\cdot[\hat{k}\times\hat{\epsilon}] - \frac{k\omega_{ba}}{6c}\sum_{ij}\langle b|Q_{ij}|a\rangle\,\hat{k}_i\hat{\epsilon}_j, \tag{6.92}$$

where $\boldsymbol{M}$ is (up to a factor e) the magnetic moment operator

$$\boldsymbol{M} = \frac{1}{2m}\left[\boldsymbol{L} + 2\boldsymbol{S}\right], \tag{6.93}$$

with $\boldsymbol{S} = \frac{1}{2}\boldsymbol{\sigma}$. As in the definition of the electric dipole moment, we have factored the electric charge e in our definition of the magnetic dipole moment. It follows that our magnetic moment has the dimension of a length. Indeed, the coefficient $\hbar/mc = \alpha a_0$ in (6.93) is the electron Compton wavelength.

The first of the contributions in (6.92) is referred to as the magnetic dipole amplitude and the second as the electric quadrupole amplitude. As we will prove later, in the general discussion of multipole radiation, these two amplitudes contribute to the decay rate incoherently. That is to say, we may square each amplitude independently, sum over the photon polarization and integrate over photon angles to determine the corresponding contribution to the transition rate, without concern for possible interference terms.

Magnetic Dipole

Let us consider first the spontaneous magnetic-dipole decay

$$w^{\rm sp}_{a\to b} = \frac{\alpha}{2\pi}\omega\,\frac{k^2}{c^2}\sum_{\lambda}\int d\Omega_k\,|\langle b|\boldsymbol{M}|a\rangle\cdot[\hat{k}\times\hat{\epsilon}_\lambda]|^2.$$

The sum over photon polarization states can easily be carried out to give

$$\sum_{\lambda}|\langle b|\boldsymbol{M}|a\rangle\cdot[\hat{k}\times\hat{\epsilon}_\lambda]|^2 = |\langle b|\boldsymbol{M}|a\rangle|^2\sin^2\theta,$$

where θ is the angle between $\hat{k}$ and the vector matrix element. Integrating $\sin^2\theta$ over angles gives a factor of $8\pi/3$. We therefore obtain for the Einstein A-coefficient

$$A_{ab} = \frac{4}{3}\frac{\omega^3}{c^5}\frac{1}{g_a}\sum_{m}|\langle b|\boldsymbol{M}|a\rangle|^2, \tag{6.94}$$

where g_a is the degeneracy of the initial state and where the sum is over all magnetic substates of a and b. The sums can be carried out just as in the electric dipole case. Defining a magnetic dipole line strength as

$$S_{\rm M1} = |\langle b||L + 2S||a\rangle|^2,$$

we obtain

$$A_{ab} = \frac{1}{3}\frac{\omega^3}{c^5}\frac{S_{\rm M1}}{g_a} = \frac{2.69735\times 10^{13}}{\lambda^3}\frac{S_{\rm M1}}{g_a}{\rm s}^{-1}, \tag{6.95}$$

where the wavelength λ is expressed in Å units and $S_{\rm M1}$ is dimensionless.

The magnetic-dipole selection rules require that $j_b = j_a$ or $j_b = j_a \pm 1$ and that the parity of the initial and final states be the same. For nonrelativistic single-electron states, this implies that $l_b = l_a$. Magnetic dipole transitions of the type $n_a l_a \to n_b l_b$, with $l_b = l_a$ between states with $n_b \neq n_a$, however, vanish because radial wave functions with the same value of l but different principal quantum numbers are orthogonal. It should be mentioned that the amplitudes for such transitions is nonvanishing (but small) in a relativistic calculation.

Fine-structure transitions: As a first example, let us consider transitions between fine-structure components of an nl state The reduced matrix element of $L+2S$ between *coupled* single electron states ($\kappa_a = \mp(j_a+1/2)$ for $j_a = l_a \pm 1/2$, and $\kappa_b = \mp(j_b+1/2)$ for $j_b = l_b \pm 1/2$, with $l_a = l_b = l$) is given by

$$\langle\kappa_b||L+2S||\kappa_a\rangle = (-1)^{j_a+l-1/2}\left\{\begin{array}{ccc} j_a & j_b & 1 \\ l & l & 1/2\end{array}\right\}\sqrt{l(l+1)(2l+1)}$$
$$+(-1)^{j_b+l-1/2}\left\{\begin{array}{ccc} j_a & j_b & 1 \\ 1/2 & 1/2 & l\end{array}\right\}\sqrt{6}$$

For the M1 transition $np_{3/2} \to np_{1/2}$ between the fine-structure components of an np-state, the reduced matrix element becomes

$$\langle j_b = 1/2, \kappa_b = 1||L+2S||j_a = 3/2, \kappa_a = -2\rangle = \frac{2}{\sqrt{3}}$$

The degeneracy of the initial $np_{3/2}$ state is $g_a = 4$, so the ratio $S_{\rm M1}/g_a = 1/3$, leading to

$$A^{\rm M1}_{np_{3/s}\to np_{1/2}} = \frac{1}{3}\,\frac{2.69735\times 10^{13}}{\lambda^3}\,{\rm s}^{-1} \tag{6.96}$$

As a specific example, the wavelength of the $2p_{3/2}-2p_{1/2}$ transition in boronlike argon (13-fold ionized argon) is 4412.56 Å. The lifetime predicted by Eq. (6.96) is 9.56 ms, compared to the measured lifetime 9.573 ms. The excellent agreement found here is a consequence of the fact that the line strength $S_{\rm M1}$ is independent of the radial wave function.

Lifetime of the metastable $F = 1$ hyperfine component of the hydrogen $1s$ state: Let us consider next the magnetic dipole transition between the two ground-state hyperfine levels in hydrogen. The initial and final states are obtained by coupling the $s = 1/2$ electron to the $s = 1/2$ proton to form states with, $F_a = 1$ and $F_b = 0$, respectively. Since both initial and final states have $l = 0$, the magnetic-dipole matrix element becomes

$$\langle a|L_\nu + 2S_\nu|b\rangle = \langle 1/2,\, 1/2,\, F_a|2S_\nu|1/2,\, 1/2,\, F_b\rangle.$$

The corresponding reduced matrix element is easily found to be

$$\langle a||2S||b\rangle = (-1)^{F_b}\sqrt{[F_a][F_b]}\left\{\begin{array}{ccc} F_a & F_b & 1 \\ 1/2 & 1/2 & 1/2 \end{array}\right\}\langle 1/2||\sigma||1/2\rangle.$$

The one-electron reduced matrix element of σ is $\langle 1/2||\sigma||1/2\rangle = \sqrt{6}$, and the six-j symbol above has the value $1/\sqrt{6}$, from which it follows

$$\langle a||2S_\nu||b\rangle = \sqrt{[F_a]} = \sqrt{3}.$$

Since the initial state degeneracy is $g_a = 3$, it follows that

$$A_{ab} = \frac{2.69735\times 10^{13}}{(2.1106)^3\times 10^{27}} = 2.87\times 10^{-15}\,\mathrm{s}^{-1}.$$

Here, we have used the fact that the wavelength of the hyperfine transition is 21.106 cm. The mean lifetime of the $F = 1$ state is $\tau = 11\times 10^6$ years!

Electric Quadrupole

From Eq.(6.92), the electric quadrupole transition amplitude is

$$T^{(1)}_{ba} = -\frac{k^2}{6}\sum_{ij}\langle b|Q_{ij}|a\rangle\,\hat{k}_i\hat{\epsilon}_j, \tag{6.97}$$

where we assume $\omega_{ba} = \omega > 0$ and set $k = \omega/c$. This amplitude must be squared, summed over photon polarization states, and integrated over photon angles. The sum over polarization states of the squared amplitude is easy to evaluate in a coordinate system with k along the z' axis and ϵ_λ in the $x'y'$ plane. In this coordinate system, one obtains

$$\sum_\lambda|\sum_{ij}\langle b|Q_{ij}|a\rangle\,\hat{k}_i\hat{\epsilon}_j|^2 = |\langle b|Q_{z'x'}|a\rangle|^2 + |\langle b|Q_{z'y'}|a\rangle|^2,$$

where $\hat{\epsilon}_j$ is the jth component of $\hat{\epsilon}_\lambda$. To carry out the integral over photon angles, we transform this expression to a fixed coordinate system. This is done with the aid of Euler angles. We suppose that the z' axis is at an angle θ with the fixed z axis and that the x' axis is along the intersection of the plane perpendicular to z' and the xy plane. The variable x' axis, makes an angle ϕ with the fixed x axis. The two coordinate systems are shown in Fig. 6.2. The transformation equations from (x, y, z) to (x', y', z') are

$$\left[\begin{array}{c} x' \\ y' \\ z' \end{array}\right] = \left[\begin{array}{ccc} \cos\phi & \sin\phi & 0 \\ -\cos\theta\sin\phi & \cos\theta\cos\phi & \sin\theta \\ \sin\theta\sin\phi & -\sin\theta\cos\phi & \cos\theta \end{array}\right]\left[\begin{array}{c} x \\ y \\ z \end{array}\right]. \tag{6.98}$$

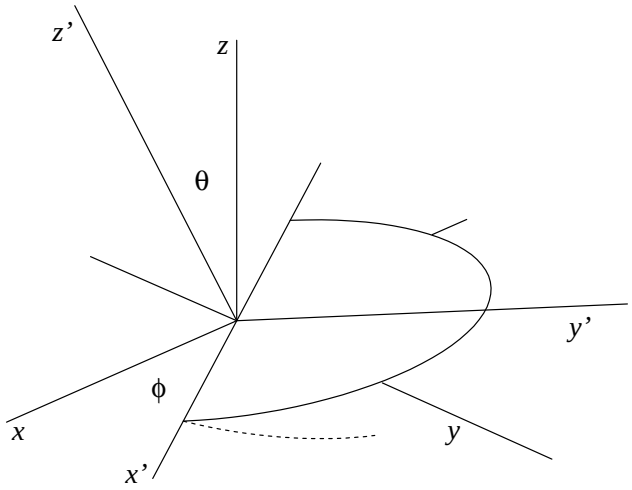

Figure 6.2: The propagation vector $\hat{k}$ is along the z' axis, $\hat{\epsilon}_1$ is along the x' axis and $\hat{\epsilon}_2$ is along the y' axis. The photon angular integration variables are ϕ and θ.

It follows that

$$\begin{aligned} Q_{z'x'} &= \sin\theta \sin 2\phi\,(Q_{xx} - Q_{yy})/2 - \sin\theta\cos 2\phi\, Q_{xy} \\ &\quad + \cos\theta\cos\phi\, Q_{zx} + \cos\theta\sin\phi\, Q_{zy}, \\ Q_{z'y'} &= -\sin\theta\cos\theta(1-\cos 2\phi)\, Q_{xx}/2 - \sin\theta\cos\theta(1+\cos 2\phi)\, Q_{yy}/2 \\ &\quad + \sin\theta\cos\theta\sin 2\phi\, Q_{xy} + (1-2\cos^2\theta)\sin\phi\, Q_{xz} \\ &\quad -(1-2\cos^2\theta)\cos\phi\, Q_{yz} + \cos\theta\sin\theta\, Q_{zz}. \end{aligned}$$

Here, we use Q_{xy} as shorthand for $\langle b|Q_{xy}|a\rangle$. Squaring and integrating over ϕ, we obtain

$$\begin{aligned} \int_0^{2\pi} d\phi |Q_{z'x'}|^2 &= \pi\left[\sin^2\theta\,|Q_{xx}-Q_{yy}|^2/4 + \sin^2\theta\,|Q_{xy}|^2 + \cos^2\theta\,|Q_{zx}|^2 + \cos^2\theta\,|Q_{zy}|^2\right], \\ \int_0^{2\pi} d\phi |Q_{z'y'}|^2 &= \pi\left[\sin^2\theta\cos^2\theta\,|Q_{xx}+Q_{yy}-2Q_{zz}|^2/2 + \sin^2\theta\cos^2\theta\,|Q_{xx}-Q_{yy}|^2/4\right. \\ &\quad \left. + \sin^2\theta\cos^2\theta\,|Q_{xy}|^2 + (1-2\cos^2\theta)^2\,|Q_{xz}|^2 + (1-2\cos^2\theta)^2\,|Q_{yz}|^2\right]. \end{aligned}$$

Integrating the sum of the two terms above over θ gives

$$\int\left[|Q_{z'x'}|^2 + |Q_{z'y'}|^2\right]\, d\Omega = \frac{8\pi}{5}\left[|Q_{xx}|^2 + |Q_{yy}|^2 + |Q_{xy}|^2 + |Q_{xz}|^2 + |Q_{yz}|^2 + \Re(Q_{xx}Q_{yy}^*)\right].$$

The terms in square brackets on the right hand side of this expression can be rewritten in terms of the spherical components of the quadrupole tensor $Q_\nu^{(2)}$ as

$$[\cdots] = 3\sum_\nu |Q_\nu^{(2)}|^2.$$

To prove this relation, we use the fact that the components of the quadrupole moment tensor in a spherical basis are

$$Q_\nu^{(2)} = r^2\, C_\nu^{(2)}(\hat{r}). \tag{6.99}$$

From the definition, we infer the following relations between rectangular and spherical components:

$$\begin{aligned} Q_0^{(2)} &= \frac{1}{2}\, Q_{zz} \\ Q_{\pm 1}^{(2)} &= \mp\frac{1}{\sqrt{6}}\, (Q_{xz} \pm i Q_{yz}) \\ Q_{\pm 2}^{(2)} &= \frac{1}{\sqrt{24}}\, (Q_{xx} - Q_{yy} \pm 2i Q_{xy})\,, \end{aligned}$$

and conversely

$$\begin{aligned} Q_{xx} &= \sqrt{\tfrac{3}{2}}\left(Q_2^{(2)} + Q_{-2}^{(2)}\right) - Q_0^{(2)} & Q_{xy} &= -i\sqrt{\tfrac{3}{2}}\left(Q_2^{(2)} - Q_{-2}^{(2)}\right) \\ Q_{yy} &= -\sqrt{\tfrac{3}{2}}\left(Q_2^{(2)} + Q_{-2}^{(2)}\right) - Q_0^{(2)} & Q_{yz} &= i\sqrt{\tfrac{3}{2}}\left(Q_1^{(2)} + Q_{-1}^{(2)}\right) \\ Q_{zz} &= 2Q_0^{(2)} & Q_{zx} &= -\sqrt{\tfrac{3}{2}}\left(Q_1^{(2)} - Q_{-1}^{(2)}\right). \end{aligned}$$

Summing $|\langle a|Q_\nu^{(2)}|b\rangle|^2$ over ν and magnetic substates of a and b leads to the expression for the Einstein A-coefficient for quadrupole radiation,

$$A_{ab} = \frac{24\pi}{5}\frac{\alpha}{2\pi}\omega\frac{k^4}{36}\frac{1}{g_a}|\langle a||Q^{(2)}||b\rangle|^2 = \frac{1}{15}k^5\,\frac{S_{\rm E2}}{g_a} = \frac{1.1198\times 10^{18}}{\lambda^5}\,\frac{S_{\rm E2}}{g_a}\,{\rm s}^{-1}, \tag{6.100}$$

where the quadrupole line strength, which is is given by

$$S_{E2} = |\langle a||Q^{(2)}||b\rangle|^2,$$

is expressed in atomic units and λ is in Å.

For a one-electron atom, the quadrupole reduced matrix element can be written

$$\langle a||Q^{(2)}||b\rangle = \sqrt{2}\,\langle l_a||C^{(2)}||l_b\rangle \int_0^\infty P_a(r)\, r^2\, P_b(r)\, dr. \tag{6.101}$$

The factor of $\sqrt{2}$ here arises from consideration of the electron spin. It can be omitted from the reduced matrix element, in which case the initial state degeneracy g_a must be replaced by $g_a \to [l_a]$. The quadrupole selection rules require that $|j_a - 2| \le j_b \le j_a + 2$ and that the parity of initial and final states be the same. For the nonrelativistic single-electron case, the selection rules imply that $l_b = l_a \pm 2,\, l_a$.

Electric quadrupole transitions are important in ions such as Ca^+, which has a $4s$ ground state and a $3d$ first excited state. Since the angular momentum of the excited state differs from that of the ground state by 2, the excited state

cannot decay to the ground state by electric or magnetic dipole radiation. The decay is permitted, however, by the electric quadrupole selection rules. The angular reduced matrix element in (6.101) with $l_a = 2$ and $l_b = 0$ has the value

$$\langle 2||C^{(2)}||0\rangle = 1.$$

The radial integral in Eq.(6.101) can be evaluated numerically. We obtain for Ca^+ (and the analogous case Sr^+) from Hartree-Fock calculations the values

$$\begin{array}{ll} \int_0^\infty dr\, P_{4s}(r)\, r^2\, P_{3d}(r) = -10.8304, & \text{for } Ca^+, \\ \int_0^\infty dr\, P_{5s}(r)\, r^2\, P_{4d}(r) = -14.2773, & \text{for } Sr^+. \end{array}$$

The decay rate for the $3d$ state of Ca^+ is

$$A(3d) = \frac{1.1198 \times 10^{18} \times (10.8304)^2}{(7310)^5 \times 5} = 1.259\,\mathrm{s}^{-1},$$

and the corresponding decay rate for the $4d$ state of Sr^+ is

$$A(4d) = \frac{1.1198 \times 10^{18} \times (14.2773)^2}{(6805)^5 \times 5} = 3.128\,\mathrm{s}^{-1},$$

The lifetime of the $4d$ state in Sr^+ has been measured experimentally and found to be 0.40 ± 0.04 sec for the $4d_{3/2}$ state and 0.34 ± 0.03 sec for the $4d_{5/2}$ state, in fair agreement with the value $\tau = 0.320$ sec predicted by the HF calculation.

6.2.8 Nonrelativistic Many-Body Amplitudes

The nonrelativistic theory of electric-dipole transitions can be generalized to many-electron atoms by simply replacing the single-particle transition operator $t = \frac{1}{c}\boldsymbol{v}\cdot\hat{\epsilon}$ by its many-electron counterpart, $T = \sum_i t_i$. In velocity form, we write

$$T = \frac{1}{c}\,\boldsymbol{V}\cdot\hat{\epsilon},$$

where,

$$\begin{array}{lll} \boldsymbol{V} & = \sum_{i=1}^N \boldsymbol{v}_i, & \text{first quantization,} \\ & = \sum_{ij}\langle i|\boldsymbol{v}|j\rangle a_i^\dagger a_j, & \text{second quantization.} \end{array}$$

It is elementary to prove that

$$\boldsymbol{V} = \frac{i}{\hbar}[H, \boldsymbol{R}],$$

where $\boldsymbol{R} = \sum_i \boldsymbol{r}_i$ and where $H = H_0 + V_I$ is the nonrelativistic many-body Hamiltonian. This relation is used to show that the equivalent length-form of the transition operator is obtained through the substitution

$$\langle F|\boldsymbol{V}|I\rangle \to i\omega_{FI}\langle F|\boldsymbol{R}|I\rangle,$$

with $\omega_{FI} = (E_F - E_I)/\hbar$. It should be carefully noted that the length - velocity equivalence in the many-body case is true for *exact* many-body wave functions, but is not, in general, valid for approximate wave functions. Indeed, one can use the difference in length-form and velocity-form amplitudes, in certain cases, as a measure of the quality of the many-body wave functions Ψ_I and Ψ_F.

It follows from the analysis given earlier in this section that the Einstein A-coefficient is

$$A_{IF} = \frac{4}{3}\alpha\frac{\omega^3}{c^2}\frac{S_{\rm E1}}{g_I}, \tag{6.102}$$

where g_I is the initial state degeneracy and where $S_{\rm E1} = |\langle F||R||I\rangle|^2$ is the line strength. The line strength can be evaluated in velocity-form by making the replacement

$$\langle F||R||I\rangle \rightarrow -\frac{\hbar}{m\omega_{FI}}\langle F||\nabla||I\rangle.$$

Let us apply this formalism to study transitions in two-electron atoms. We proceed in two steps. First, we evaluate the matrix element of the dipole operator between two uncoupled states,

$$|I\rangle = a_a^\dagger a_b^\dagger|0\rangle, \tag{6.103}$$

$$|F\rangle = a_c^\dagger a_d^\dagger|0\rangle. \tag{6.104}$$

We easily find

$$\langle F|R_\nu|I\rangle = (r_\nu)_{ca}\delta_{db} - (r_\nu)_{da}\delta_{cb} - (r_\nu)_{cb}\delta_{da} + (r_\nu)_{db}\delta_{ca}.$$

Next, we couple the atomic states in the LS scheme and find

$$\langle L'M'_L S'M'_S|R_\nu|LM_L SM_S\rangle =$$

$$\eta\eta' \sum_{m's\,\mu's} -\begin{array}{c}l_cm_c\\|\\L'M'_L\\|\\l_dm_d\end{array} -\begin{array}{c}1/2\mu_c\\|\\S'M'_S\\|\\1/2\mu_d\end{array} -\begin{array}{c}l_am_a\\|\\LM_L\\|\\l_bm_b\end{array} -\begin{array}{c}1/2\mu_a\\|\\SM_S\\|\\1/2\mu_b\end{array} \times$$

$$\left\{ -\begin{array}{c}l_cm_c\\|\\1\nu\\|\\l_am_a\end{array}\langle c||r||a\rangle\delta_{db} - -\begin{array}{c}l_dm_d\\|\\1\nu\\|\\l_am_a\end{array}\langle d||r||a\rangle\delta_{cb} \right.$$

$$\left. - -\begin{array}{c}l_cm_c\\|\\1\nu\\|\\l_bm_b\end{array}\langle c||r||b\rangle\delta_{da} + -\begin{array}{c}l_dm_d\\|\\1\nu\\|\\l_bm_b\end{array}\langle d||r||b\rangle\delta_{ca} \right\}. \tag{6.105}$$

The spin sums in this equation can be easily carried out leading to a factor of $\delta_{S'S}\delta_{M'_S M_S}$ in the two direct terms and a factor of $(-1)^{S+1}\delta_{S'S}\delta_{M'_S M_S}$ in the two exchange terms. The orbital angular momentum sums are a bit more difficult.

From the Wigner-Eckart theorem, it follows that each of the four terms in the sum must be proportional to

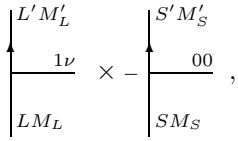

where the proportionality constant is the corresponding contribution to the reduced matrix element. Carrying out the sums over magnetic substates, we obtain

$$\begin{aligned}\langle L'S'||R||LS\rangle = \eta'\eta\sqrt{[S][L'][L]}\,\Bigg[&(-1)^{L+l_c+l_d+1}\left\{\begin{array}{ccc} L' & L & 1 \\ l_a & l_c & l_b \end{array}\right\}\langle c||r||a\rangle\delta_{db} \\ &+(-1)^{L'+L+S+1}\left\{\begin{array}{ccc} L' & L & 1 \\ l_a & l_d & l_b \end{array}\right\}\langle d||r||a\rangle\delta_{cb} \\ &+(-1)^{S+l_b+l_c+1}\left\{\begin{array}{ccc} L' & L & 1 \\ l_b & l_c & l_a \end{array}\right\}\langle c||r||b\rangle\delta_{da} \\ &+(-1)^{L'+l_a+l_b+1}\left\{\begin{array}{ccc} L' & L & 1 \\ l_b & l_d & l_a \end{array}\right\}\langle d||r||b\rangle\delta_{ca}\Bigg]\,, \end{aligned} \tag{6.106}$$

where we have used the fact that

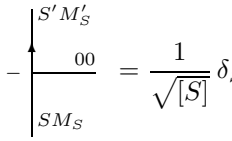

$$= \frac{1}{\sqrt{[S]}}\,\delta_{S'S}\delta_{M'_S M_S}.$$

Let us consider, as specific examples, transitions from excited $(nl1s)$ states to either the $(1s)^2\,{}^1S$ ground state or to a $(2s1s)\,{}^{1,3}S$ excited state. Since $L'=0$ for the final states, the dipole selection rules lead to $L=1$ for the initial states. There are the three possible cases:

1. $(np1s)\,{}^1P \to (1s)^2\,{}^1S$. In this case $S=0$, $\eta=1$, $\eta'=1/\sqrt{2}$, $a=np$ and $b=c=d=1s$. The reduced matrix element in Eq.(6.106) becomes

$$\langle 2\,{}^1S||R||n\,{}^1P\rangle = \sqrt{2}\,\langle 1s||r||np\rangle.$$

2. $(np1s)\,{}^1P \to (2s1s)\,{}^1S$. Here, $S=0$, $\eta=\eta'=1$, $a=np$, $c=2s$ and $b=d=1s$. The reduced matrix element is

$$\langle 2\,{}^1S||R||n\,{}^1P\rangle = \langle 2s||r||np\rangle.$$

3. $(np1s)\,{}^3P \to (2s1s)\,{}^3S$. This case is the same as the previous except $S=1$. The reduced matrix element is

$$\langle 2\,{}^3S||R||n\,{}^3P\rangle = \sqrt{3}\,\langle 2s||r||np\rangle.$$

Table 6.3: Wavelengths and oscillator strengths for transitions in heliumlike ions calculated in a central potential $v_0(1s, r)$. Wavelengths are determined using first-order energies.

Z	λ(Å)	f	λ(Å)	f	λ(Å)	f
	$2\,^1P - 1\,^1S$		$3\,^1P - 1\,^1S$		$4\,^1P - 1\,^1S$	
2	570.5	0.335	527.3	0.086	513.5	0.035
3	197.4	0.528	177.0	0.121	170.7	0.047
4	99.8	0.615	88.1	0.134	84.6	0.051
5	60.1	0.664	52.6	0.140	50.4	0.053
6	40.2	0.695	34.9	0.144	33.4	0.054
7	28.8	0.717	24.9	0.147	23.8	0.055
8	21.6	0.732	18.6	0.148	17.8	0.055
9	16.8	0.744	14.5	0.150	13.8	0.056
10	13.4	0.754	11.6	0.151	11.0	0.056
	$2\,^1P - 2\,^1S$		$3\,^1P - 2\,^1S$		$4\,^1P - 2\,^1S$	
2	27744.0	0.248	3731.2	0.121	3072.5	0.042
3	10651.8	0.176	1473.7	0.194	1128.0	0.058
4	6483.9	0.133	673.7	0.255	511.3	0.071
5	4646.6	0.106	385.3	0.292	291.0	0.078
6	3617.4	0.088	249.3	0.316	187.6	0.083
7	2960.5	0.075	174.4	0.334	131.0	0.086
8	2505.1	0.065	128.9	0.347	96.6	0.088
9	2170.9	0.058	99.1	0.357	74.2	0.090
10	1915.3	0.052	78.6	0.365	58.8	0.092
	$2\,^3P - 2\,^3S$		$3\,^3P - 2\,^3S$		$4\,^3P - 2\,^3S$	
2	10039.4	0.685	5568.2	0.081	4332.4	0.030
3	5292.1	0.355	1179.9	0.242	932.1	0.070
4	3642.8	0.236	577.6	0.297	448.1	0.081
5	2786.5	0.176	342.5	0.328	263.1	0.087
6	2258.9	0.140	226.6	0.348	172.9	0.090
7	1900.2	0.116	161.0	0.362	122.3	0.092
8	1640.3	0.100	120.3	0.372	91.1	0.094
9	1443.2	0.087	93.3	0.379	70.4	0.095
10	1288.4	0.077	74.4	0.385	56.1	0.096

The evaluation of the two-particle reduced matrix element thus reduces to the evaluation of a single-particle matrix element between "active" electrons. We describe the helium ground-state in the Hartree-Fock approximation. The ground-state HF potential $v_0(1s,r)$ is then used as a screening potential $[U(r) = v_0(1s,r)]$ in calculating excited-state orbitals. We find that the lowest-order $2\,^1P - 1\,^1S$ energy difference is $\hbar\omega_0 = 0.7905$, and the first-order energy difference is $\hbar\omega_1 = 0.0081$, leading to a predicted wavelength $\lambda = 570.51$ Å for the transition, in reasonably good agreement with the measured wavelength $\lambda^{\rm exp} = 584.33$ Å. The calculated matrix elements in length- and velocity-form are identical if the lowest-order energy is used in the calculation, but differ if the more accurate energy $\hbar(\omega_0 + \omega_1) = 0.7986$ is used. We find that $\langle 1s||r||2p\rangle_l = 0.561$ compared with $\langle 1s||r||2p\rangle_v = 0.555$. The calculated line strength is $S_{\rm E1} = 0.629$ compared to the exact value $S_{\rm E1}^{\rm exact} = 0.5313$, while the oscillator strength is $f = .335$ compared to the exact result $f^{\rm exact} = 0.2762$. Finally, the value of the Einstein A-coefficient from the approximate calculation is $A = 22.9 \times 10^8\,{\rm s}^{-1}$ compared to the exact value $A^{\rm exact} = 17.99 \times 10^8\,{\rm s}^{-1}$. The exact values given here are from a recent relativistic all-order calculation by Plante. Generally, a simpler nonrelativistic calculation suffices to give an understanding of the transition probabilities in two-electron systems at the level of 10-20%. In Table 6.3, we give results of calculations of wavelengths and oscillator strengths for transitions from $n\,^{1,3}P$ states to the $1\,^1S$ ground state and the $2\,^{1,3}S$ excited states in two-electron ions with Z ranging from 2 to 10. The calculations are of the type described above. The accuracy of the approximate calculations gradually improves along the isoelectronic sequence. At $Z = 10$ the tabulated values are accurate at the 1-2% level. The oscillator strengths are plotted against Z in Fig 6.3.

6.3 Theory of Multipole Transitions

In the following paragraphs, we extend and systematize the decomposition of the transition amplitude into electric dipole, magnetic dipole and electric quadrupole components started the previous sections. The transition amplitude for a one-electron atom is

$$T_{ba} = \int d^3r \psi_b^\dagger \boldsymbol{\alpha}\cdot\mathbf{A}(\mathbf{r},\omega)\,\psi_a, \tag{6.107}$$

where $\mathbf{A}(\mathbf{r},\omega)$ is the transverse-gauge vector potential

$$\mathbf{A}(\mathbf{r},\omega) = \hat{\epsilon}\, e^{i\mathbf{k}\cdot\mathbf{r}}\,.$$

As a first step in the multipole decomposition, we expand the vector potential $\mathbf{A}(\mathbf{r},\omega)$ in a series of vector spherical harmonics

$$\mathbf{A}(\mathbf{r},\omega) = \sum_{JLM} A_{JLM}\mathbf{Y}_{JLM}(\hat{r}). \tag{6.108}$$

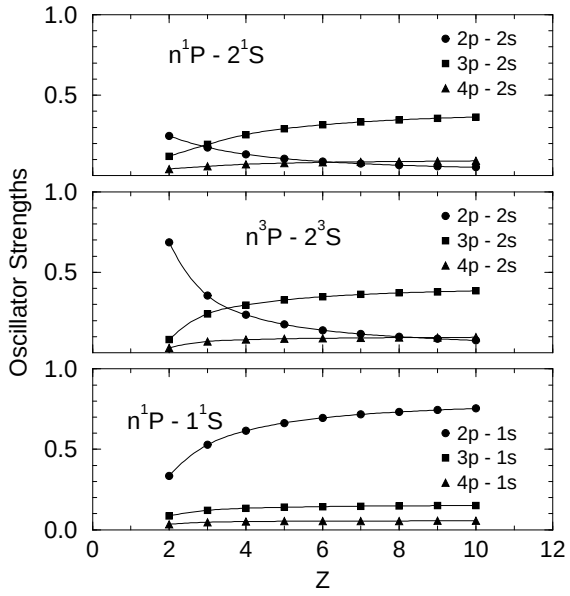

Figure 6.3: Oscillator strengths for transitions in heliumlike ions.

The expansion coefficients are, of course, given by

$$A_{JLM} = \int d\Omega \, (\mathbf{Y}_{JLM}(\hat{r}) \cdot \hat{\epsilon}) \, e^{i\mathbf{k}\cdot\mathbf{r}}. \tag{6.109}$$

In this equation and below, vector operators on the left-hand side are understood to be adjoint operators. Using the well-known expansion of a plane-wave in terms of spherical Bessel functions $j_l(kr)$,

$$e^{i\mathbf{k}\cdot\mathbf{r}} = 4\pi \sum_{lm} i^l j_l(kr) \, Y^*_{lm}(\hat{k}) Y_{lm}(\hat{r}),$$

and carrying out the angular integration in Eq.(6.109), we can rewrite the expansion of the vector potential (6.108) in the form

$$\mathbf{A}(\mathbf{r}, \omega) = 4\pi \sum_{JLM} i^L (\mathbf{Y}_{JLM}(\hat{k}) \cdot \hat{\epsilon}) \, \mathbf{a}_{JLM}(\mathbf{r}), \tag{6.110}$$

where

$$\mathbf{a}_{JLM}(\mathbf{r}) = j_L(kr) \mathbf{Y}_{JLM}(\hat{r}). \tag{6.111}$$

It is more convenient to express this expansion in terms of the vector spherical harmonics $\mathbf{Y}^{(\lambda)}_{JM}(\hat{r})$ rather than $\mathbf{Y}_{JLM}(\hat{r})$. This can be accomplished with the

aid of the relations

$$\mathbf{Y}_{JJ-1M}(\hat{r}) = \sqrt{\frac{J}{2J+1}}\mathbf{Y}^{(-1)}_{JM}(\hat{r}) + \sqrt{\frac{J+1}{2J+1}}\mathbf{Y}^{(1)}_{JM}(\hat{r}), \quad (6.112)$$

$$\mathbf{Y}_{JJM}(\hat{r}) = \mathbf{Y}^{(0)}_{JM}(\hat{r}), \quad (6.113)$$

$$\mathbf{Y}_{JJ+1M}(\hat{r}) = -\sqrt{\frac{J+1}{2J+1}}\mathbf{Y}^{(-1)}_{JM}(\hat{r}) + \sqrt{\frac{J}{2J+1}}\mathbf{Y}^{(1)}_{JM}(\hat{r}). \quad (6.114)$$

This transformation leads immediately to the *multipole expansion* of the vector potential,

$$\mathbf{A}(\mathbf{r},\omega) = 4\pi \sum_{JM\lambda} i^{J-\lambda}(\mathbf{Y}^{(\lambda)}_{JM}(\hat{k})\cdot\hat{\epsilon})\,\mathbf{a}^{(\lambda)}_{JM}(\mathbf{r}). \quad (6.115)$$

The vector functions $\mathbf{a}^{(\lambda)}_{JM}(\mathbf{r})$ are referred to as *multipole potentials*. They are given by

$$\mathbf{a}^{(0)}_{JM}(\mathbf{r}) = \mathbf{a}_{JJM}(\mathbf{r}), \quad (6.116)$$

$$\mathbf{a}^{(1)}_{JM}(\mathbf{r}) = \sqrt{\frac{J+1}{2J+1}}\mathbf{a}_{JJ-1M}(\mathbf{r}) - \sqrt{\frac{J}{2J+1}}\mathbf{a}_{JJ+1M}(\mathbf{r}). \quad (6.117)$$

Only terms with $\lambda = 0$ and $\lambda = 1$ contribute to the multipole expansion (6.115), since $\mathbf{Y}^{(-1)}_{JM}(\hat{k}) = \hat{k}Y_{JM}(\hat{k})$ is orthogonal to $\hat{\epsilon}$. The multipole potentials satisfy the Helmholtz equation

$$\nabla^2\mathbf{a}^{(\lambda)}_{JM} + k^2\mathbf{a}^{(\lambda)}_{JM} = 0, \quad (6.118)$$

and the transversality condition

$$\boldsymbol{\nabla}\cdot\mathbf{a}^{(\lambda)}_{JM} = 0. \quad (6.119)$$

The multipole potentials with $\lambda = 0$ are the *magnetic* multipole potentials and those with $\lambda = 1$ are the *electric* multipole potentials. The interaction $\boldsymbol{\alpha}\cdot\mathbf{a}^{(\lambda)}_{JM}$ is an irreducible tensor operator of rank J. The parity of the multipole potential $\mathbf{a}^{(\lambda)}_{JM}(\mathbf{r})$ is $(-1)^{J+1-\lambda}$. It should be noted that in the multipole expansion, all information concerning the photon's polarization and its propagation direction is contained in the expansion coefficient.

With the aid of Eqs.(6.112-6.114), and the following well-known identities among spherical Bessel functions,

$$j_{n-1}(z) = \frac{n+1}{z}j_n(z) + j'_n(z), \quad (6.120)$$

$$j_{n+1}(z) = \frac{n}{z}j_n(z) - j'_n(z), \quad (6.121)$$

where

$$j'_n(z) = \frac{d}{dz}\,j_n(z),$$

the multipole potentials $\mathbf{a}^{(\lambda)}_{JM}(\mathbf{r})$ can be put in the form

$$\begin{aligned}\mathbf{a}^{(0)}_{JM}(\mathbf{r}) &= j_J(kr)\mathbf{Y}^{(0)}_{JM}(\hat{r}), &(6.122)\\ \mathbf{a}^{(1)}_{JM}(\mathbf{r}) &= \left[j'_J(kr)+\frac{j_J(kr)}{kr}\right]\mathbf{Y}^{(1)}_{JM}(\hat{r}) \\ &\quad +\sqrt{J(J+1)}\,\frac{j_J(kr)}{kr}\,\mathbf{Y}^{(-1)}_{JM}(\hat{r})\,. &(6.123)\end{aligned}$$

Let us examine the small k limit in Eqs.(6.122,6.123) for the special case $J=1$. We find on expanding $j_1(kr)\approx kr/3$,

$$\begin{aligned}\lim_{k\to 0}\mathbf{a}^{(0)}_{1m}(\mathbf{r}) &= \frac{kr}{3}\mathbf{Y}^{(0)}_{1m}(\hat{r}) = -i\sqrt{\frac{3}{8\pi}}\,\frac{k}{3}\,[\mathbf{r}\times\boldsymbol{\xi}_m]\\ \lim_{k\to 0}\mathbf{a}^{(1)}_{1m}(\mathbf{r}) &= \frac{2}{3}\mathbf{Y}^{(1)}_{1m}(\hat{r})+\frac{\sqrt{2}}{3}\mathbf{Y}^{(-1)}_{1m}(\hat{r}) = \sqrt{\frac{3}{8\pi}}\,\frac{2}{3}\,\boldsymbol{\xi}_m\,,\end{aligned}$$

where $\boldsymbol{\xi}_m$ are the three unit spherical basis vectors. With the aid of the Pauli approximation, we can easily show that nonrelativistically the $J=1$ transition operators take the limiting forms

$$\begin{aligned}\boldsymbol{\alpha}\cdot\mathbf{a}^{(0)}_{1m}(\mathbf{r}) &\to \frac{2}{3}\sqrt{\frac{3}{8\pi}}\,\frac{ik}{2mc}\,([\boldsymbol{L}+2\boldsymbol{S}]\cdot\boldsymbol{\xi}_m)\\ \boldsymbol{\alpha}\cdot\mathbf{a}^{(1)}_{1m}(\mathbf{r}) &\to \frac{2}{3}\sqrt{\frac{3}{8\pi}}\,\frac{1}{c}\,(\boldsymbol{v}\cdot\boldsymbol{\xi}_m)\,.\end{aligned}$$

Thus, the $J=1$ components of relativistic multipole operators introduced here are, up to a factor, the *velocity form* of the magnetic and electric dipole operators. We therefore refer to the transverse-gauge operators as velocity-form operators. Later, we will show how to recover the corresponding length-form operators.

The multipole expansion of the vector potential (6.115) leads to a corresponding multipole expansion of the transition operator

$$T_{ba}=4\pi\sum_{JM\lambda}i^{J-\lambda}[\mathbf{Y}^{(\lambda)}_{JM}(\hat{k})\cdot\hat{\epsilon}]\,[T^{(\lambda)}_{JM}]_{ba}, \tag{6.124}$$

where

$$[T^{(\lambda)}_{JM}]_{ba}=\int d^3r\psi^\dagger_b\,\boldsymbol{\alpha}\cdot\mathbf{a}^{(\lambda)}_{JM}(\mathbf{r})\,\psi_a. \tag{6.125}$$

To obtain the transition probability, we must square the amplitude, sum over polarization states, and integrate over photon directions. On squaring the amplitude, we encounter terms of the form

$$[\mathbf{Y}^{(\lambda)}_{JM}(\hat{k})\cdot\hat{\epsilon}_\nu]\,[\hat{\epsilon}_\nu\cdot\mathbf{Y}^{(\lambda')}_{J'M'}(\hat{k})]\,, \tag{6.126}$$

to be summed over polarization directions $\hat{\epsilon}_\nu$. Using the fact that the vector spherical harmonics with $\lambda=0,1$ are orthogonal to $\hat{k}$, the polarization sum

becomes

$$\sum_{\nu}[\mathbf{Y}^{(\lambda)}_{JM}(\hat{k})\cdot\hat{\epsilon}_{\nu}]\,[\hat{\epsilon}_{\nu}\cdot\mathbf{Y}^{(\lambda')}_{J'M'}(\hat{k})] = [\mathbf{Y}^{(\lambda)}_{JM}(\hat{k})\cdot\mathbf{Y}^{(\lambda')}_{J'M'}(\hat{k})]\,. \tag{6.127}$$

This expression is easily integrated over photon directions leading to

$$\int d\Omega_k\,[\mathbf{Y}^{(\lambda)}_{JM}(\hat{k})\cdot\mathbf{Y}^{(\lambda')}_{J'M'}(\hat{k})] = \delta_{JJ'}\delta_{MM'}\delta_{\lambda\lambda'}. \tag{6.128}$$

We therefore obtain for the transition rate

$$w_{ba} = \frac{\alpha}{2\pi}\omega\sum_{\nu}\int d\Omega_k|T_{ba}|^2 = 8\pi\alpha\omega\sum_{JM\lambda}\left|[T^{(\lambda)}_{JM}]_{ba}\right|^2. \tag{6.129}$$

We see that the rate is an incoherent sum of all possible multipoles. Angular momentum selection rules, of course, limit the type and number of multipoles that contribute to the sum.

As shown previously in Sec. 6.2.5, a gauge transformation leaves single-particle amplitudes invariant, provided the energy difference between the initial and final states equals the energy carried off by the photon. The transformed multipole potential can be written

$$\begin{aligned}\mathbf{a}^{(\lambda)}_{JM}(\mathbf{r}) &\rightarrow \mathbf{a}^{(\lambda)}_{JM}(\mathbf{r}) + \boldsymbol{\nabla}\chi_{JM}(\mathbf{r}),\\ \phi_{JM}(\mathbf{r}) &\rightarrow i\omega\,\chi_{JM}(\mathbf{r}),\end{aligned}$$

where the gauge function $\chi_{JM}(\mathbf{r})$ is a solution to the Helmholtz equation. We choose the gauge function to be

$$\chi_{JM}(\mathbf{r}) = -\frac{1}{k}\sqrt{\frac{J+1}{J}}\,j_J(kr)\,Y_{JM}(\hat{r})\,,$$

to cancel the lowest-order (in powers of kr) contribution to the interaction. The resulting transformation has no effect on the magnetic multipoles, but transforms electric multipole potentials to the form

$$\begin{aligned}\mathbf{a}^{(1)}_{JM}(\mathbf{r}) &= -j_{J+1}(kr)\left[\mathbf{Y}^{(1)}_{JM}(\hat{r}) - \sqrt{\frac{J+1}{J}}\mathbf{Y}^{(-1)}_{JM}(\hat{r})\right],\\ \phi^{(1)}_{JM}(kr) &= -ic\sqrt{\frac{J+1}{J}}\,j_J(kr)Y_{JM}(\hat{r})\,.\end{aligned} \tag{6.130}$$

The resulting potentials reduce to the *length-form* multipole potentials in the nonrelativistic limit. We refer to this choice of gauge as the length-gauge in the sequel. Let us examine the nonrelativistic limit of the length-gauge transition operator

$$\boldsymbol{\alpha}\cdot\mathbf{a}^{(1)}_{JM}(\mathbf{r}) - \frac{1}{c}\,\phi_{JM}(\mathbf{r}).$$

Since the vector potential contribution is smaller than the scalar potential by terms of order kr, the interaction can be approximated for small values of kr by

$$\lim_{k\to 0}\left[\boldsymbol{\alpha}\cdot\mathbf{a}^{(1)}_{JM}(\mathbf{r})-\frac{1}{c}\,\phi_{JM}(\mathbf{r})\right]=i\sqrt{\frac{(2J+1)(J+1)}{4\pi J}}\,\frac{k^J}{(2J+1)!!}\,Q_{JM}(\mathbf{r}),$$

where

$$Q_{JM}(\mathbf{r})=r^J\,C_{JM}(\hat{r})$$

is the electric J-pole moment operator in a spherical basis.

In either gauge, the multipole-interaction can be written in terms of a dimensionless multipole-transition operator $t^{(\lambda)}_{JM}(\mathbf{r})$ defined by

$$\left[\boldsymbol{\alpha}\cdot\mathbf{a}^{(\lambda)}_{JM}(\mathbf{r})-\frac{1}{c}\,\phi_{JM}(\mathbf{r})\right]=i\sqrt{\frac{(2J+1)(J+1)}{4\pi J}}\,t^{(\lambda)}_{JM}(\mathbf{r})\,. \tag{6.131}$$

The one-electron reduced matrix elements $\langle i||t^{(\lambda)}_J||j\rangle$ are given by
Transverse Gauge:

$$\begin{aligned}
\langle\kappa_i||t^{(0)}_J||\kappa_j\rangle &= \langle -\kappa_i||C_J||\kappa_j\rangle\int_0^\infty dr\,\frac{\kappa_i+\kappa_j}{J+1}\,j_J(kr)[P_i(r)Q_j(r)+Q_i(r)P_j(r)]\,,\\
\langle\kappa_i||t^{(1)}_J||\kappa_j\rangle &= \langle\kappa_i||C_J||\kappa_j\rangle\int_0^\infty dr\left\{-\frac{\kappa_i-\kappa_j}{J+1}\left[j'_J(kr)+\frac{j_J(kr)}{kr}\right]\times\right.\\
&\qquad\left.[P_i(r)Q_j(r)+Q_i(r)P_j(r)]+J\frac{j_J(kr)}{kr}\,[P_i(r)Q_j(r)-Q_i(r)P_j(r)]\right\},
\end{aligned}$$

and
Length Gauge:

$$\begin{aligned}
\langle\kappa_i||t^{(1)}_J||\kappa_j\rangle = \langle\kappa_i||C_J||\kappa_j\rangle\int_0^\infty dr\left\{j_J(kr)[P_i(r)P_j(r)+Q_i(r)Q_j(r)]+\right.\\
\left.j_{J+1}(kr)\left[\frac{\kappa_i-\kappa_j}{J+1}[P_i(r)Q_j(r)+Q_i(r)P_j(r)]+[P_i(r)Q_j(r)-Q_i(r)P_j(r)]\right]\right\}.
\end{aligned}$$

The functions $P_i(r)$ and $Q_i(r)$ in the above equations are the large and small components, respectively, of the radial Dirac wave functions for the orbital with quantum numbers (n_i,κ_i).

The multipole-transition operators $t^{(\lambda)}_J(\mathbf{r})$ are related to the frequency-dependent multipole-moment operators $q^{(\lambda)}_J(\mathbf{r},\omega)$ by

$$q^{(\lambda)}_J(\mathbf{r},\omega)=\frac{(2J+1)!!}{k^J}\,t^{(\lambda)}_J(\mathbf{r}). \tag{6.132}$$

Both the transition operators and the multipole-moment operators are irreducible tensor operators. For a many-body system, the multipole-transition

operators are given by

$$T^{(\lambda)}_{JM} = \sum_{ij}(t^{(\lambda)}_{JM})_{ij}\, a^\dagger_i a_j, \tag{6.133}$$

$$Q^{(\lambda)}_{JM} = \sum_{ij}(q^{(\lambda)}_{JM})_{ij}\, a^\dagger_i a_j, \tag{6.134}$$

where $(t^{(\lambda)}_{JM})_{ij} = \langle i|t^{(\lambda)}_{JM}(\mathbf{r})|j\rangle$ and $(q^{(\lambda)}_{JM})_{ij} = \langle i|q^{(\lambda)}_{JM}(\mathbf{r},\omega)|j\rangle$.

The Einstein A-coefficient, giving the probability per unit time for emission of a photon with multipolarity $(J\lambda)$ from a state I with angular momentum J_I, to a state F with angular momentum J_F, is

$$A^{(\lambda)}_J = 2\alpha\omega\,\frac{[J]}{[J_I]}\frac{J+1}{J}\,|\langle F||T^{(\lambda)}_J||I\rangle|^2 = \frac{(2J+2)(2J+1)\,k^{2J+1}}{J[(2J+1)!!]^2}\,\frac{|\langle F||Q^{(\lambda)}_J||I\rangle|^2}{[J_I]}, \tag{6.135}$$

where $[J_I] = 2J_I + 1$. This equation leads to the familiar expressions

$$A^{(1)}_1 = \frac{4k^3}{3}\frac{|\langle F||Q_1||I\rangle|^2}{[J_I]}\,,$$

$$A^{(2)}_2 = \frac{k^5}{15}\frac{|\langle F||Q_2||I\rangle|^2}{[J_I]}\,,$$

for electric dipole and quadrupole transitions, where

$$Q_{JM} = Q^{(1)}_{JM}.$$

For magnetic multipole transitions, we factor an additional $\alpha/2$ from the frequency-dependent multipole moment operator $Q^{(0)}_J$ and define

$$M_{JM} = 2cQ^{(0)}_{JM}\,,$$

to facilitate comparison with the previous nonrelativistic theory. The Einstein A-coefficient for magnetic-dipole radiation may thus be written

$$A^{(0)}_1 = \frac{k^3}{3c^2}\frac{|\langle F||M_1||I\rangle|^2}{[J_I]}\,. \tag{6.136}$$

Chapter 7

Introduction to MBPT

In this chapter, we take a step beyond the independent-particle approximation and study the effects of electron correlation in atoms. One of the simplest and most direct methods for treating correlation is many-body perturbation theory (MBPT). In this chapter, we consider first-order MBPT corrections to many-body wave functions and second-order corrections to the energies, where the terms first-order and second-order refer to powers of the interaction potential. Additionally, we give some results from third-order MBPT.

We retain the notation of Chap. 4 and write the many-electron Hamiltonian $H = H_0 + V_I$ in normally-ordered form,

$$H_0 = \sum_i \epsilon_i \, a_i^\dagger a_i \,, \tag{7.1}$$

$$V_I = V_0 + V_1 + V_2 \,, \tag{7.2}$$

$$V_0 = \sum_a \left(\frac{1}{2} V_{\rm HF} - U \right)_{aa} \,, \tag{7.3}$$

$$V_1 = \sum_{ij} (\Delta V)_{ij} \; :a_i^\dagger a_j: \,, \tag{7.4}$$

$$V_2 = \frac{1}{2} \sum_{ijkl} g_{ijkl} \; :a_i^\dagger a_j^\dagger a_l a_k: \,, \tag{7.5}$$

where $(\Delta V)_{ij} = (V_{\rm HF} - U)_{ij}$ with $(V_{\rm HF})_{ij} = \sum_b \left(g_{ibjb} - g_{ibbj} \right)$. The normal ordering here is with respect to a suitably chosen closed-shell reference state $|O_c\rangle = a_a^\dagger a_b^\dagger \cdots a_n^\dagger |0\rangle$. If we are considering correlation corrections to a closed-shell atom, then the reference state is chosen to be the ground-state of the atom. Similarly, if we are treating correlation corrections to states in atoms with one- or two-electrons beyond a closed-shell ion, the reference state is chosen to be the ionic ground-state.

We let Ψ be an exact eigenstate of the many-body Hamiltonian H and let E be the corresponding eigenvalue. We decompose Ψ into an unperturbed wave

function Ψ_0 satisfying

$$H_0\Psi_0 = E_0\Psi_0\,, \tag{7.6}$$

and a perturbation $\Delta\Psi$. For the examples considered in this chapter, the state Ψ_0 is nondegenerate. The wave function Ψ is normalized using the *intermediate normalization* condition $\langle\Psi_0|\Psi\rangle = 1$. Setting $\Psi = \Psi_0 + \Delta\Psi$ and $E = E_0 + \Delta E$, we may rewrite the Schrödinger equation in the form

$$(H_0 - E_0)\Delta\Psi = (\Delta E - V_I)\Psi. \tag{7.7}$$

From this equation, it follows (with the aid of the intermediate normalization condition) that

$$\Delta E = \langle\Psi_0|V_I|\Psi\rangle. \tag{7.8}$$

It is often convenient to work with operators that map the unperturbed wave function Ψ_0 onto Ψ or $\Delta\Psi$ rather than the wave functions Ψ or $\Delta\Psi$ themselves. The *wave operator* Ω is the operator that maps the unperturbed wave function onto the exact wave function

$$\Psi = \Omega\Psi_0\,, \tag{7.9}$$

and the *correlation operator* $\chi = \Omega - 1$ is the operator that maps Ψ_0 onto $\Delta\Psi$,

$$\Delta\Psi = \chi\Psi_0. \tag{7.10}$$

It follows from (7.8) that

$$\Delta E = \langle\Psi_0|V_I\Omega|\Psi_0\rangle = \langle\Psi_0|V_I|\Psi_0\rangle + \langle\Psi_0|V_I\chi|\Psi_0\rangle\,. \tag{7.11}$$

The operator $V_{\rm eff} = V_I\Omega$ is an *effective potential*, in the sense that

$$\Delta E = \langle\Psi_0|V_{\rm eff}|\Psi_0\rangle. \tag{7.12}$$

We expand both $\Delta\Psi$ and ΔE in powers of V_I,

$$\Delta\Psi = \Psi^{(1)} + \Psi^{(2)} + \cdots\,, \tag{7.13}$$

$$\Delta E = E^{(1)} + E^{(2)} + \cdots\,. \tag{7.14}$$

The Schrödinger equation (7.7) then leads to an hierarchy of inhomogeneous equations

$$(H_0 - E_0)\Psi^{(1)} = (E^{(1)} - V_I)\Psi_0, \tag{7.15}$$

$$(H_0 - E_0)\Psi^{(2)} = (E^{(1)} - V_I)\Psi^{(1)} + E^{(1)}\Psi_0, \tag{7.16}$$

$$(H_0 - E_0)\Psi^{(3)} = (E^{(1)} - V_I)\Psi^{(2)} + E^{(2)}\Psi^{(1)} + E^{(3)}\Psi_0, \quad \cdots \tag{7.17}$$

We consider the solution to these equations for several simple cases in the following sections.

7.1 Closed-Shell Atoms

In this section, we work out the lowest-order correlation corrections to the wave function and energy for a closed-shell atom. We take the lowest-order wave function Ψ_0 to be the reference wave function $|O_c\rangle$. The lowest-order energy is then $E_0 = \sum_a \epsilon_a$, where the sum extends over all occupied core states. For a closed-shell atom, the reference state is the unique solution to Eq.(7.6).

Equation (7.15) has a non-trivial solution only if the right-hand side is orthogonal to the solution to the homogeneous equation. This implies that

$$E^{(1)} = \langle \Psi_0 | V_I | \Psi_0 \rangle = \langle O_c | V_I | O_c \rangle = V_0 \,. \tag{7.18}$$

Thus, the solvability condition leads to the previously derived expression for the sum of the lowest- and first-order energy,

$$E_0 + E^{(1)} = \sum_a \left(\epsilon_a + \frac{1}{2} (V_{\rm HF})_{aa} - U_{aa} \right) = \sum_a I_a + \frac{1}{2} \sum_{ab} \left(g_{abab} - g_{abba} \right) \,, \tag{7.19}$$

where $I_a = \langle a | h_0 | a \rangle$ is the one-particle matrix element of the sum of single-particle kinetic energy and the electron-nucleus potential energy. We see that the sum of the lowest- and first-order energies is just the expectation value of the many-body Hamiltonian evaluated using the independent-particle many-body wave function. Indeed, to obtain Hartree-Fock wave functions in Chapter 3, we minimized this sum treated as a functional of single-particle orbitals $\phi_a(r)$.

Since $E^{(1)} = V_0$, the right-hand side of Eq.(7.15) can be simplified, leading to

$$\begin{aligned} (H_0 - E_0)\Psi^{(1)} &= -V_1 \Psi_0 - V_2 \Psi_0 \\ &= \left[- \sum_{na} (\Delta V)_{na} \, a_n^\dagger a_a - \frac{1}{2} \sum_{mnab} g_{mnab} \, a_m^\dagger a_n^\dagger a_b a_a \right] |O_c\rangle \,. \end{aligned} \tag{7.20}$$

Here we have taken advantage of the normal ordering in V_1 and V_2 and retained only the nonvanishing core (a_a or a_b) annihilation operators and excited state ($a_n^\dagger$ or $a_m^\dagger$) creation operators in the sums. (As in previous chapters, we denote core orbitals by subscripts a, b, ... at the beginning of the alphabet and designate excited orbitals by letters m, n, ... in the middle of the alphabet.) The general solution to Eq.(7.15) is the sum of a particular solution to the inhomogeneous equation and the general solution to the homogeneous equation. The intermediate normalization condition implies that the perturbed wave function $\Psi^{(1)}$ is orthogonal to Ψ_0. We therefore seek a solution to (7.15) that is orthogonal to Ψ_0. From an examination of the right-hand side of the inhomogeneous equation, we are led to write $\Psi^{(1)} = \chi^{(1)} \Psi_0$, where the first-order correlation operator $\chi^{(1)}$ is a linear combination of one-particle–one-hole operators $a_n^\dagger a_a$ and two-particle–two-hole operators $a_m^\dagger a_n^\dagger a_b a_a$,

$$\chi^{(1)} = \sum_{an} \chi^{(1)}_{na} a_n^\dagger a_a + \frac{1}{2} \sum_{mnab} \chi^{(1)}_{mnab} a_m^\dagger a_n^\dagger a_b a_a \,. \tag{7.21}$$

The first-order wave function is, in other words, constructed as a linear combination of particle-hole excited states and two-particle–two-hole excited states. Substituting this *ansatz* into Eq.(7.20), we obtain

$$\left[\sum_{an}(\epsilon_n-\epsilon_a)\chi^{(1)}_{na}\,a^\dagger_n a_a+\frac{1}{2}\sum_{mnab}(\epsilon_m+\epsilon_n-\epsilon_a-\epsilon_b)\chi^{(1)}_{mnab}\,a^\dagger_m a^\dagger_n a_b a_a\right]|O_c\rangle$$
$$=\left[-\sum_{na}(\Delta V)_{na}\,a^\dagger_n a_a-\frac{1}{2}\sum_{mnab}g_{mnab}\,a^\dagger_m a^\dagger_n a_b a_a\right]|O_c\rangle\,. \quad (7.22)$$

Identifying coefficients of the particle-hole and two-particle–two-hole operators on the left and right of this equation, we find

$$\chi^{(1)}_{na} = -\frac{(\Delta V)_{na}}{\epsilon_n-\epsilon_a}\,, \quad (7.23)$$
$$\chi^{(1)}_{mnab} = -\frac{g_{mnab}}{\epsilon_m+\epsilon_n-\epsilon_a-\epsilon_b}\,. \quad (7.24)$$

Using these expansion coefficients, we can reconstruct the first-order correlation operator $\chi^{(1)}$ from Eq.(7.21). Then, using $\Psi^{(1)}=\chi^{(1)}\Psi_0$, we have the first-order wave function.

According to Eq.(7.8), the second-order energy is

$$E^{(2)}=\langle\Psi_0|V_I|\Psi^{(1)}\rangle=\langle\Psi_0|V_I\chi^{(1)}|\Psi_0\rangle. \quad (7.25)$$

Substituting the expansion for $\chi^{(1)}$, we find

$$E^{(2)}=\langle O_c|\left[V_0+\sum_{ij}(\Delta V)_{ij}\;:a^\dagger_i a_j:+\frac{1}{2}\sum_{ijkl}g_{ijkl}\;:a^\dagger_i a^\dagger_j a_l a_k:\right]\times$$
$$\left[\sum_{na}\chi^{(1)}_{na}a^\dagger_n a_a+\frac{1}{2}\sum_{nmab}\chi^{(1)}_{nmab}a^\dagger_n a^\dagger_m a_b a_a\right]|O_c\rangle. \quad (7.26)$$

Using Wick's theorem to evaluate the matrix elements of products of creation and annihilation operators, we obtain

$$E^{(2)}=\sum_{na}(\Delta V)_{an}\chi^{(1)}_{na}+\frac{1}{2}\sum_{mnab}\tilde{g}_{abmn}\chi^{(1)}_{mnab}$$
$$=-\sum_{na}\frac{(\Delta V)_{an}(\Delta V)_{na}}{\epsilon_n-\epsilon_a}-\frac{1}{2}\sum_{mnab}\frac{\tilde{g}_{abmn}g_{mnab}}{\epsilon_m+\epsilon_n-\epsilon_a-\epsilon_b}\,. \quad (7.27)$$

To evaluate the second-order correction to the energy, it is first necessary to carry out the sum over magnetic substates and then to evaluate the remaining multiple sums over the remaining quantum numbers numerically.

Closed-Shell: Third-Order Energy

Derivation of the expression for the third-order energy follows the pattern outlined above but is considerably more involved. For a closed-shell atom, the result is (Blundell et al., 1987)

$$\begin{aligned} E^{(3)} &= \sum_{abcmnr} \frac{\tilde{g}_{acnr}\tilde{g}_{nmba}\tilde{g}_{rbmc}}{(\epsilon_n+\epsilon_m-\epsilon_a-\epsilon_b)(\epsilon_r+\epsilon_n-\epsilon_a-\epsilon_c)} \\ &+\frac{1}{2}\sum_{abcdmn} \frac{\tilde{g}_{cdmn}g_{nmba}g_{badc}}{(\epsilon_n+\epsilon_m-\epsilon_a-\epsilon_b)(\epsilon_n+\epsilon_m-\epsilon_c-\epsilon_d)} \\ &+\frac{1}{2}\sum_{abmnrs} \frac{\tilde{g}_{absr}g_{nmba}g_{rsnm}}{(\epsilon_n+\epsilon_m-\epsilon_a-\epsilon_b)(\epsilon_r+\epsilon_s-\epsilon_a-\epsilon_b)}, \end{aligned} \tag{7.28}$$

where we have assumed, for simplicity, that $U = V_{\rm HF}$.

7.1.1 Angular Momentum Reduction

The sum over magnetic quantum numbers for the one-particle–one-hole contribution to the second-order correlation energy is elementary. Since ΔV in Eq. (7.27) is a scalar, it follows that $l_n = l_a$, $m_n = m_a$, and $\sigma_n = \sigma_a$. The sum over magnetic substates can be carried out leaving a sum over all occupied subshells $a = (n_a, l_a)$ and those excited orbitals $n = (n_n, l_n)$ having $l_n = l_a$,

$$E_a^{(2)} = -\sum_{\substack{na \\ l_n=l_a}} 2[l_a]\,\frac{(\Delta V)_{an}(\Delta V)_{na}}{\epsilon_n-\epsilon_a}, \tag{7.29}$$

with

$$(\Delta V)_{an} = \sum_b 2[l_b]\left[R_0(a,b,n,b) - \sum_k \Lambda_{l_a k l_b} R_k(a,b,b,n)\right] - U_{an}.$$

The corresponding formulas in the relativistic case are the same with $2[l_a]$ replaced by $[j_a]$ and $\Lambda_{l_a k l_b}$ replaced by $\Lambda_{\kappa_a k \kappa_b}$.

The sum over magnetic substates is more difficult for the $g_{abmn}\tilde{g}_{mnab}$ term. As a first step, we separate out the dependence on magnetic quantum numbers of the Coulomb matrix element using

$$g_{mnab} = \sum_k - \;\; + \;\; \delta_{\sigma_a\sigma_m}\delta_{\sigma_b\sigma_n}\, X_k(mnab)\,, \tag{7.30}$$

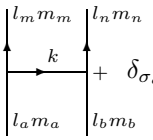

where

$$X_k(mnab) = (-1)^k \langle l_m||C_k||l_a\rangle\langle l_n||C_k||l_b\rangle R_k(mnab)\,. \tag{7.31}$$

The indices σ_i in Eq.(7.30) designate spin quantum numbers. Next, we consider the sum over magnetic quantum numbers of the product,

$$\sum_{m's} - \left| \begin{array}{c} l_a m_a \quad l_b m_b \\ \longrightarrow k \\ l_m m_m \quad l_n m_n \end{array} \right| + \quad \times - \left| \begin{array}{c} l_m m_m \quad l_n m_n \\ \longrightarrow k' \\ l_a m_a \quad l_b m_b \end{array} \right| + \quad = (-1)^{l_m - l_a + l_n - l_b} \frac{1}{[k]} \delta_{k'k} \,, \tag{7.32}$$

and the sum of the exchange product,

$$\sum_{m's} - \left| \begin{array}{c} l_a m_a \quad l_b m_b \\ \longrightarrow k \\ l_n m_n \quad l_m m_m \end{array} \right| + \quad \times - \left| \begin{array}{c} l_m m_m \quad l_n m_n \\ \longrightarrow k' \\ l_a m_a \quad l_b m_b \end{array} \right| + \quad = (-1)^{l_m - l_a + l_n - l_b} \left\{ \begin{array}{ccc} l_a & l_m & k \\ l_b & l_n & k' \end{array} \right\} . \tag{7.33}$$

These two terms are combined to give an expression for the two-particle–two-hole contribution to the correlation energy,

$$E_b^{(2)} = -\sum_k \frac{2}{[k]} \sum_{abmn} \frac{Z_k(mnab) X_k(mnab)}{\epsilon_m + \epsilon_n - \epsilon_b - \epsilon_a}, \tag{7.34}$$

where

$$Z_k(mnab) = X_k(mnab) - \frac{1}{2} \sum_{k'} [k] \left\{ \begin{array}{ccc} l_a & l_m & k \\ l_b & l_n & k' \end{array} \right\} X_{k'}(mnba) \,. \tag{7.35}$$

In summary, the nonrelativistic second-order correlation energy for a closed-shell atom or ion is

$$\begin{aligned} E^{(2)} &= E_a^{(2)} + E_b^{(2)} \\ &= -\sum_{\substack{na \\ l_n = l_a}} 2[l_a] \frac{(\Delta V)_{an} (\Delta V)_{na}}{\epsilon_n - \epsilon_a} \\ &\quad - \sum_k \frac{2}{[k]} \sum_{abmn} \frac{Z_k(mnab) X_k(mnab)}{\epsilon_m + \epsilon_n - \epsilon_b - \epsilon_a} \,. \end{aligned} \tag{7.36}$$

If we assume that our basic orbitals ϕ_m are obtained in the HF potential of the core, then $(\Delta V)_{aa} = (V_{\rm HF} - U)_{aa} = 0$, and the first term in Eq. (7.36) vanishes. This is an example of a general rule: *formulas of MBPT take their simplest form starting from a HF potential.*

Closed Shell Atoms: Relativistic Case

Formula (7.27) gives the second-order Coulomb contribution to the correlation energy in the the relativistic case as well. In the relativistic case, the sums over m and n run over positive energies only as discussed earlier. The angular reduction in the relativistic case is somewhat simpler than in the nonrelativistic case since the magnetic sums are over a single magnetic quantum number m_j rather than two m_l and σ.

Again, we write

$$g_{mnab} = \sum_k - \left| \begin{array}{c} j_m m_m \\ \uparrow \\ \xrightarrow{k} \\ \downarrow \\ j_a m_a \end{array} \right| \left| \begin{array}{c} j_n m_n \\ \uparrow \\ \\ \downarrow \\ j_b m_b \end{array} \right| + \quad X_k(mnab)\,, \tag{7.37}$$

where in the relativistic case

$$X_k(mnab) = (-1)^k \langle \kappa_m || C_k || \kappa_a \rangle \langle \kappa_n || C_k || \kappa_b \rangle R_k(mnab)\,. \tag{7.38}$$

Here, one is reminded, $\kappa_i = \mp(j_i + 1)$ for $j_i = l_i \pm 1$. The relativistic reduced matrix elements $\langle \kappa_m || C_k || \kappa_a \rangle$ contain both angular momentum and parity selection rules. The Slater integrals $R_k(mnab)$ are of course evaluated using radial Dirac wave functions. We must now carry out the sum over magnetic quantum numbers in Eq.(7.27):

$$\sum_{m's} - \left| \begin{array}{c} j_a m_a \\ \uparrow \\ \xrightarrow{k} \\ \downarrow \\ j_m m_m \end{array} \right| \left| \begin{array}{c} j_b m_b \\ \uparrow \\ \\ \downarrow \\ j_n m_n \end{array} \right| + \quad \times - \left| \begin{array}{c} j_m m_m \\ \uparrow \\ \xrightarrow{k'} \\ \downarrow \\ j_a m_a \end{array} \right| \left| \begin{array}{c} j_n m_n \\ \uparrow \\ \\ \downarrow \\ j_b m_b \end{array} \right| + \quad = (-1)^{j_m + j_a + j_n + j_b} \frac{1}{[k]} \delta_{k'k}\,, \tag{7.39}$$

and in the exchange term

$$\sum_{m's} - \left| \begin{array}{c} j_a m_a \\ \uparrow \\ \xrightarrow{k} \\ \downarrow \\ j_n m_n \end{array} \right| \left| \begin{array}{c} j_b m_b \\ \uparrow \\ \\ \downarrow \\ j_m m_m \end{array} \right| + \quad \times - \left| \begin{array}{c} j_m m_m \\ \uparrow \\ \xrightarrow{k'} \\ \downarrow \\ j_a m_a \end{array} \right| \left| \begin{array}{c} j_n m_n \\ \uparrow \\ \\ \downarrow \\ j_b m_b \end{array} \right| + \quad = -(-1)^{j_m + j_a + j_n + j_b} \left\{ \begin{array}{ccc} j_a & j_m & k \\ j_b & j_n & k' \end{array} \right\}\,. \tag{7.40}$$

These two terms are combined in the relativistic case (with the additional assumption $U = V_{\rm HF}$) to give

$$E^{(2)} = -\frac{1}{2} \sum_k \frac{1}{[k]} \sum_{abmn} \frac{Z_k(mnab) X_k(mnab)}{\epsilon_m + \epsilon_n - \epsilon_b - \epsilon_a}, \tag{7.41}$$

where

$$Z_k(mnab) = X_k(mnab) + \sum_{k'} [k] \left\{ \begin{array}{ccc} j_a & j_m & k \\ j_b & j_n & k' \end{array} \right\} X_{k'}(mnba)\,. \tag{7.42}$$

A similar analysis can be applied to the relativistic third-order energy. After

angular reduction, one obtains

$$\begin{aligned}
E^{(3)} &= \sum_L \frac{1}{[L]^2} \sum_{abcmnr} (-1)^{j_a+j_b+j_c+j_m+j_n+j_r+L+1} \\
&\qquad \times \frac{Z_L(acnr)Z_L(mnba)Z_L(rbcm)}{(\epsilon_m+\epsilon_n-\epsilon_a-\epsilon_b)(\epsilon_r+\epsilon_n-\epsilon_a-\epsilon_c)} \\
&+ \frac{1}{2} \sum_{\substack{abcdmn \\ L_1L_2L_3}} (-1)^{j_a+j_b+j_c+j_d} \left\{ \begin{array}{ccc} L_1 & L_2 & L_3 \\ j_b & j_d & j_n \end{array} \right\} \left\{ \begin{array}{ccc} L_1 & L_2 & L_3 \\ j_a & j_c & j_m \end{array} \right\} \\
&\qquad \times \frac{Z_{L_1}(dcnm)X_{L_2}(nmba)X_{L_3}(badc)}{(\epsilon_n+\epsilon_m-\epsilon_a-\epsilon_b)(\epsilon_n+\epsilon_m-\epsilon_c-\epsilon_d)} \\
&+ \frac{1}{2} \sum_{\substack{abmnrs \\ L_1L_2L_3}} (-1)^{j_a+j_b+j_m+j_n} \left\{ \begin{array}{ccc} L_1 & L_2 & L_3 \\ j_n & j_r & j_b \end{array} \right\} \left\{ \begin{array}{ccc} L_1 & L_2 & L_3 \\ j_m & j_s & j_a \end{array} \right\} \\
&\qquad \times \frac{Z_{L_1}(basr)X_{L_2}(nmba)X_{L_3}(rsnm)}{(\epsilon_n+\epsilon_m-\epsilon_a-\epsilon_b)(\epsilon_r+\epsilon_s-\epsilon_a-\epsilon_b)}. \qquad (7.43)
\end{aligned}$$

7.1.2 Example: 2nd-order Energy in Helium

As a simple example, let us evaluate the ground-state correlation energy for helium, starting from the Hartree-Fock approximation. Since the core orbitals a and b are both $1s$ orbitals, one easily shows that the quantities $X_k(abmn)$ vanish unless $l_m = l_n = k$. Furthermore, using the fact that $\langle l||C_l||0\rangle = 1$, we find,

$$X_l(1s,1s,nl,ml) = (-1)^l R_l(1s,1s,nl,nl).$$

Moreover,

$$\left\{ \begin{array}{ccc} 0 & l & k \\ 0 & l & k' \end{array} \right\} = \frac{1}{[l]}\delta_{kl}\delta_{k'l}\,.$$

With the aid of these relations, we rewrite the nonrelativistic equation for the second-order correlation energy (7.36) as

$$E^{(2)} = -\sum_{l=0}^{\infty} \frac{1}{[l]} \sum_{mn} \frac{[R_l(1s,1s,nl,ml)]^2}{\epsilon_{nl}+\epsilon_{ml}-2\epsilon_{1s}}. \qquad (7.44)$$

We are, therefore, faced with the problem of evaluating an infinite sum over angular momentum states l of terms that are represented here as double sums over principal quantum numbers m and n of squares of Slater integrals divided by energy differences. The formalism is a bit misleading in the sense that, except for the $1s$ state, there are no bound states in the HF potential for helium. The double sums in this case represent double integrals over the continuum. In the following two subsection, we describe a method for evaluating expressions such as this numerically. We will return to this example later in the chapter.

7.2 B-Spline Basis Sets

As an aid to evaluating MBPT expressions for the correlation energy, we introduce discrete basis sets and, thereby, reduce the infinite sums and integrals over the real spectrum to finite sums over a pseudospectrum.

Since correlation corrections in atoms have finite range, we restrict our attention to a finite (but large) cavity of radius R. To study the ground-state or low-lying excited states of ions, the radius of this cavity is chosen to be $R \approx 40/Z_{\rm ion}$ a.u., where $Z_{\rm ion}$ is the ionic charge. For large cavities, the results of correlation calculations are independent of the cavity radius. We require that the radial wave functions vanish at the origin and at the cavity boundary. The spectrum in the cavity is discrete but infinite.

Next, we expand the solutions to the radial Schrödinger equation in a finite basis. This basis is chosen to be a set of n B-splines of order k. Following deBoor (1978), we divide the interval $[0, R]$ into segments. The endpoints of these segments are given by the knot sequence $\{t_i\}$, $i = 1, 2, \cdots, n + k$. The B-splines of order k, $B_{i,k}(r)$, on this knot sequence are defined recursively by the relations,

$$B_{i,1}(r) = \begin{cases} 1, & t_i \le r < t_{i+1}, \\ 0, & \text{otherwise}, \end{cases} \tag{7.45}$$

and

$$B_{i,k}(r) = \frac{r - t_i}{t_{i+k-1} - t_i} B_{i,k-1}(r) + \frac{t_{i+k} - r}{t_{i+k} - t_{i+1}} B_{i+1,k-1}(r) \, . \tag{7.46}$$

The function $B_{i,k}(r)$ is a piecewise polynomial of degree $k-1$ inside the interval $t_i \le r < t_{i+k}$ and $B_{i,k}(r)$ vanishes outside this interval. The knots defining our grid have k-fold multiplicity at the endpoints 0 and R; *i.e.* $t_1 = t_2 = \cdots = t_k = 0$ and $t_{n+1} = t_{n+2} = \cdots = t_{n+k} = R$. In applications to atomic physics calculations, the knots $t_{k+1}, t_{k+2}, \cdots, t_n$ are distributed on an exponential scale between 0 and R. In Fig. 7.1, we show 30 B-splines of order k covering the interval $r = 0 - 40$ a.u. This set of B-splines could be used as a basis set for expanding radial wave functions.

The set of B-splines of order k on the knot sequence $\{t_i\}$ forms a complete basis for piecewise polynomials of degree $k - 1$ on the interval spanned by the knot sequence. We represent the solution to the radial Schrödinger equation as a linear combination of these B-splines and we work with the B-spline representation of the wave functions rather than the wave functions themselves.

The radial Schrödinger wave function $P_l(r)$ satisfies the variational equation $\delta S = 0$, where

$$S = \int_0^R \left\{ \frac{1}{2} \left(\frac{dP_l}{dr} \right)^2 + \left(V(r) + \frac{l(l+1)}{2r^2} \right) P_l(r)^2 \right\} - \epsilon \int_0^R P_l(r)^2 dr \, . \tag{7.47}$$

The parameter ϵ is a Lagrange multiplier introduced to insure that the normalization constraint

$$\int_0^R P_l(r)^2 dr = 1 \, , \tag{7.48}$$

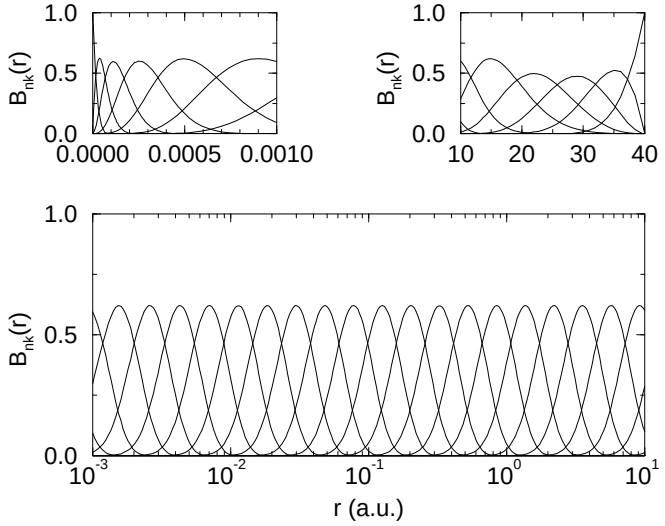

Figure 7.1: We show the $n = 30$ B-splines of order $k = 6$ used to cover the interval 0 to 40 on an "atomic" grid. Note that the splines sum to 1 at each point.

is satisfied. The variational principle $\delta S = 0$, together with the constraints $\delta P_\kappa(0) = 0$ and $\delta P_\kappa(R) = 0$, leads to the radial Schrödinger equation for $P_l(r)$.

We expand $P_l(r)$ in terms of B-splines of order k as

$$P_l(r) = \sum_{i=1}^{n} p_i \, B_i(r) \,, \tag{7.49}$$

where the subscript k has been omitted from $B_{i,k}(r)$ for notational simplicity. The action S becomes a quadratic function of the expansion coefficients p_i when the expansions are substituted into the action integral. The variational principle then leads to a system of linear equations for the expansion coefficients,

$$\frac{\partial S}{\partial p_i} = 0, \quad i = 1, \cdots, n \,. \tag{7.50}$$

The resulting equations can be written in the form of an $n \times n$ symmetric generalized eigenvalue equation,

$$Av = \epsilon B v \,, \tag{7.51}$$

where v is the vector of expansion coefficients,

$$v = (p_1, p_2, \cdots, p_n) \,. \tag{7.52}$$

Table 7.1: Eigenvalues of the generalized eigenvalue problem for the B-spline approximation of the radial Schrödinger equation with $l = 0$ in a Coulomb potential with $Z = 2$. Cavity radius is $R = 30$ a.u. We use 40 splines with $k = 7$.

n	ϵ_n	n	ϵ_n	n	ϵ_n
1	-2.0000000	11	0.5470886		$\cdots$
2	-0.5000000	12	0.7951813		$\cdots$
3	-0.2222222	13	1.2210506		$\cdots$
4	-0.1249925	14	2.5121874	34	300779.9846480
5	-0.0783858	15	4.9347168	35	616576.9524036
6	-0.0379157	16	9.3411933	36	1414036.2030934
7	0.0161116	17	17.2134844	37	4074016.5630432
8	0.0843807	18	31.1163253	38	20369175.6484520
9	0.1754002	19	55.4833327		
10	0.2673078	20	97.9745446		

The matrices A and B are given by

$$A_{ij} = \int_0^R \left\{ \frac{dB_i}{dr}\frac{dB_j}{dr} + 2B_i(r)\left(V(r) + \frac{l(l+1)}{2r^2}\right)B_j(r)\right\}dr, \quad (7.53)$$

$$B_{ij} = \int_0^R B_i(r)B_j(r)dr. \quad (7.54)$$

It should be mentioned that the matrices A and B are diagonally dominant banded matrices. The solution to the eigenvalue problem for such matrices is numerically stable. Routines from the LAPACK library (Anderson et al., 1999) can be used to obtain the eigenvalues and eigenvectors numerically.

Solving the generalized eigenvalue equation, one obtains n real eigenvalues ϵ^λ and n eigenvectors v^λ. The eigenvectors satisfy the orthogonality relations,

$$\sum_{i,j} v_i^\lambda B_{ij} v_j^\mu = \delta_{\lambda\mu} \ , \quad (7.55)$$

which leads to the orthogonality relations

$$\int_0^R P_l^\lambda(r) P_l^\mu(r) dr = \delta_{\lambda\mu}, \quad (7.56)$$

for the corresponding radial wave functions.

The first few eigenvalues and eigenvectors in the cavity agree precisely with the first few bound-state eigenvalues and eigenvectors obtained by numerically integrating the radial Schrödinger equations; but, as the principal quantum number increases, the cavity spectrum departs more and more from the real spectrum. This is illustrated in Table 7.1, where we list the eigenvalues obtained

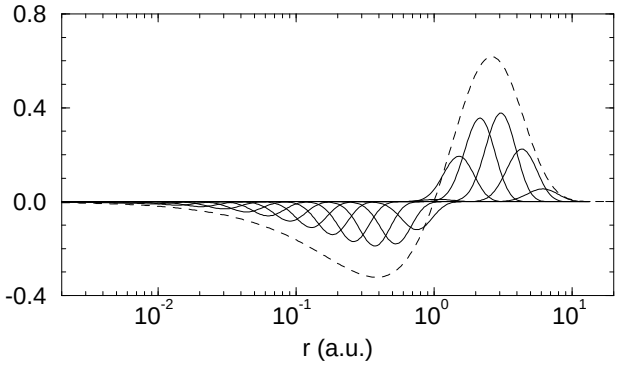

Figure 7.2: B-spline components of the $2s$ state in a Coulomb field with $Z = 2$ obtained using $n = 30$ B-splines of order $k = 6$. The dashed curve is the resulting $2s$ wave function.

for $l = 0$ states in a Coulomb potential with $Z = 2$. In this example we use $n = 40$ splines with $k = 7$. In Fig. 7.2, we show the B-spline components of the $2s$ state in a Coulomb potential with $Z = 2$ obtained using $n = 30$ splines of order $k = 6$.

The cavity spectrum is complete in the space of piecewise polynomials of degree $k - 1$ and, therefore, can be used instead of the real spectrum to evaluate correlation corrections to states confined to the cavity. The quality of the numerically generated B-spline spectrum can be tested by using it to evaluate various energy-weighted sum rules, such as the Thomas-Reiche-Kuhn sum rule. It is found (Johnson et al., 1988a) that the generalized TRK sum rule is satisfied to parts in 10^7 using 40 splines of order 7 for a given l and to parts in 10^9 using 50 splines of order 9.

7.2.1 Hartree-Fock Equation and B-splines

While it is useful to have a finite basis set for the Schrödinger equation in a local potential, it is even more useful to have a basis set for the Hartree-Fock(HF) potential, since in MBPT takes its simplest form when expressed in terms of HF orbitals. One supposes that the HF equations for the occupied orbitals of a closed-shell system have been solved and uses the resulting orbitals to construct the HF potential. Once this potential has been determined, a complete set of single particle orbitals can be constructed. To determine these orbitals using B-splines, it is necessary to modify the potential term in the action integral S and the matrix A in the generalized eigenvalue problem. If we let $V_{\rm HF}$ represent the HF potential, then its contribution to the action integral S for an orbital a

will be

$$\int_0^R P_a(r)V_{\rm HF}P_a(r)dr = \sum_b 2[l_b]\left(R_0(abab) - \sum_k \Lambda_{l_a k l_b} R_k(abba)\right), \quad (7.57)$$

where the sum is over all occupied shells. This contribution to S leads to the following modification of the potential contribution in the matrix element A_{ij},

$$\begin{aligned}\int_0^R & drB_i(r)V_{\rm HF}B_j(r) \\ &= \int_0^R drB_i(r)\sum_b 2[l_b]\Big\{v_0(b,b,r)B_j(r)dr \\ &\qquad - \sum_k \Lambda_{l_a k l_b} v_k(b,B_j,r)P_b(r)\Big\}, \end{aligned} \quad (7.58)$$

where $v_l(a,b,r)$ is the usual Hartree screening potential.

To solve the generalized eigenvalue problem in the HF case, we do a preliminary numerical solution of the nonlinear HF equations to determine the occupied orbitals $P_b(r)$. With the aid of these orbitals, we construct the matrix A using the above formula. The linear eigenvalue problem can then be solved to give the complete spectrum (occupied and unoccupied) of HF states. With this procedure, the states $P_b(r)$ are both input to and output from the routine to solve the eigenvalue equation. By comparing the the eigenfunctions of occupied levels obtained as output with the corresponding input levels, one can monitor the accuracy of the solutions to the eigenvalue problem. It should be noted that this consistency check will work only if the cavity radius is large enough so that boundary effects do not influence the occupied levels in the spline spectrum at the desired level of accuracy.

In Table 7.2, we compare low-lying levels for the sodium atom ($Z = 11$) obtained by solving the generalized eigenvalue problem with values obtained by solving the HF equations numerically. The potential used in this calculation is the HF potential of the closed Na^+ core. It is seen that the B-spline eigenvalues of the occupied $1s$, $2s$ and $2p$ levels agree precisely with the corresponding numerical eigenvalues. The B-spline eigenvalues of higher levels depart from the numerical eigenvalues because of cavity boundary effects.

7.2.2 B-spline Basis for the Dirac Equation

Application of B-splines to obtain a finite basis set for the radial Dirac Equation is described by Johnson et al. (1988a) and follows very closely the pattern described above for the radial Schrödinger equation. Several difference between the relativistic and nonrelativistic expansions should be noted. Firstly, in the

Table 7.2: Comparison of the HF eigenvalues from numerical integration of the HF equations (HF) with those found by solving the HF eigenvalue equation in a cavity using B-splines (spline). Sodium, $Z = 11$, in a cavity of radius $R = 40$ a.u..

nl	HF	spline	nl	HF	spline	nl	HF	spline
$1s$	-40.759750	-40.759750						
$2s$	-3.073688	-3.073688	$2p$	-1.797192	-1.797192			
$3s$	-0.181801	-0.181801	$3p$	-0.109438	-0.109438	$3d$	-0.055667	-0.055667
$4s$	-0.070106	-0.070106	$4p$	-0.050321	-0.050318	$4d$	-0.031315	-0.031021
$5s$	-0.037039	-0.036876	$5p$	-0.028932	-0.027955	$5d$	-0.020038	-0.014308
$6s$	-0.022871	-0.017983	$6p$	-0.018783	-0.008656	$6d$	-0.013912	0.008226
$4f$	-0.031250	-0.031157						
$5f$	-0.020000	-0.016573	$5g$	-0.020000	-0.018710			
$6f$	-0.013889	0.002628	$6g$	-0.013889	-0.003477	$6h$	-0.013889	-0.009268

relativistic case we expand both $P(r)$ and $Q(r)$ in terms of B-splines

$$P(r) = \sum_{i=1}^{n} p_i B_i(r)$$
$$Q(r) = \sum_{i=1}^{n} q_i B_i(r)$$

leading to a $2n \times 2n$ generalized eigenvalue problem for the vector $v = (p_1, p_2, \cdots p_n, q_1, q_2, \cdots q_n)$. The Dirac energy spectrum obtained by solving the eigenvalue problem breaks up into n electron bound and continuum states and n negative-energy states representing positrons. As noted previously, these negative-energy states are omitted in the sums over virtual states in expressions for the correlation energy. Secondly, in the relativistic case, we replace the boundary condition $P(R) = 0$ by the MIT bag-model boundary conditions $P(R) = Q(R)$ (Chodos et al., 1974). This is done to avoid problems associated with the "Klein paradox" (Sakuri, 1967) that arise when one attempts to confine a particle to a cavity using an infinite potential barrier.

7.2.3 Application: Helium Correlation Energy

Let us now return to our discussion of the correlation energy of helium. We introduce a cavity of radius $R = 40$ a.u. and evaluate the B-spline basis functions for $l = 1, 10$. For each value of l, we use $n = 40$ splines of order $k = 6$ and obtain 38 basis functions. These basis functions can be used to replace the exact spectrum to a high degree of accuracy. We evaluate the partial-wave

Table 7.3: Contributions to the second-order correlation energy for helium.

l	E_l	l	E_l
0	-0.013498	5	-0.000168
1	-0.018980	6	-0.000088
2	-0.003194	7	-0.000050
3	-0.000933	8	-0.000031
4	-0.000362	9	-0.000020
		10-∞	-0.000053
	Total		-0.037376

contributions to the correlation energy,

$$E_l^{(2)} = -\frac{1}{[l]} \sum_{mn} \frac{[R_l(1s, 1s, nl, ml)]^2}{\epsilon_{nl} + \epsilon_{ml} - 2\epsilon_{1s}}, \tag{7.59}$$

in Eq.(7.44) by summing over the 38×38 possible basis functions. The resulting contributions to the correlation energy are tabulated for $l = 0$ to 9 in Table 7.3. As $l \to \infty$, the partial-wave contributions are known to fall off as

$$E_l^{(2)} \to -\frac{a}{(l + 1/2)^4}.$$

We use this known asymptotic behavior to estimate the remainder from $l =$ 10 to ∞. The resulting second-order correlation energy for helium is $E^{(2)} = -0.03738$ a.u.. Adding this value to the HF energy $E_{\rm HF} = -2.86168$ a.u., we obtain $E_0 + E^{(1)} + E^{(2)} = -2.89906$ a.u.. The theoretical ionization energy, which is obtained by subtracting the energy of the one-electron helium-like ion, is 0.89906 a.u. compared with the experimental value $E_{\rm exp} = 0.90357$ a.u., the difference being less than 0.5%. Including the third-order energy -0.00368 a.u. leads to a theoretical value of 0.90275 a.u., within 0.08% of the measured value.

7.3 Atoms with One Valence Electron

Let us now turn to the problem of determining the second-order correlation energy for an atom with one valence electron. For simplicity, we start with a "frozen-core" Hartree-Fock formulation. The unperturbed state of the atom is $\Psi_0 = a_v^\dagger |0_c\rangle$, where $|0_c\rangle$ is the HF core state and the corresponding unperturbed energy is $E_0 = \sum_a \epsilon_a + \epsilon_v$.

Since $V_1 = \sum_{ij} (\Delta V)_{ij} : a_i^\dagger a_j := 0$ for a HF potential, it follows that the first-order correction to the energy is $E^{(1)} = V_0$. Thus, $E_0 + E^{(1)} = (E_0 + V_0)_{\rm core} + \epsilon_v$. In other words, there is no first-order correction to the valence removal energy. This result, of course, depends on the fact that the calculation starts from a frozen-core HF potential. In any other potential, there will be a first-order correction to the energy.

7.3.1 Second-Order Energy

Again, since $V_1 = 0$, the first-order wave function will contain only double excitations! There are two possibilities, either two core electrons are excited or one core electron and the valence electron are excited. We correspondingly decompose the first-order correlation operator as

$$\chi^{(1)} = \frac{1}{2}\sum_{abmn} \chi^{(1)}_{mnab} a_m^\dagger a_n^\dagger a_b\, a_a + \sum_{bmn} \chi^{(1)}_{mnvb} a_m^\dagger a_n^\dagger a_b\, a_v. \tag{7.60}$$

Substituting into Eq. (7.15) and matching terms, we find

$$\chi^{(1)}_{mnab} = -\frac{g_{mnab}}{\epsilon_m + \epsilon_n - \epsilon_a - \epsilon_b} \tag{7.61}$$

$$\chi^{(1)}_{mnvb} = -\frac{g_{mnvb}}{\epsilon_m + \epsilon_n - \epsilon_v - \epsilon_b}. \tag{7.62}$$

The second-order energy is obtained from

$$\begin{aligned} E^{(2)} &= \langle\Psi_0|V_2\chi^{(1)}|\Psi_0\rangle = \langle 0_c|a_v\, V_2\chi^{(1)}\, a_v^\dagger|0_c\rangle \\ &= \frac{1}{4}\sum_{ijkl} g_{ijkl}\, \chi^{(1)}_{mnab}\, \langle 0_c|a_v\ :a_i^\dagger a_j^\dagger a_l\, a_k: :a_m^\dagger a_n^\dagger a_b\, a_a: a_v^\dagger|0_c\rangle \\ &+ \frac{1}{2}\sum_{ijkl} g_{ijkl}\, \chi^{(1)}_{mnvb}\, \langle 0_c|a_v\ :a_i^\dagger a_j^\dagger a_l\, a_k: :a_m^\dagger a_n^\dagger a_b: |0_c\rangle. \end{aligned} \tag{7.63}$$

With the aid of Wick's theorem, this reduces to

$$E^{(2)} = \frac{1}{2}\sum_{mnab} \tilde{g}_{abmn}\, \chi^{(1)}_{mnab} - \sum_{nab} \tilde{g}_{abvn}\, \chi^{(1)}_{vnab} + \sum_{mnb} \tilde{g}_{vbmn}\, \chi^{(1)}_{mnvb}.$$

The first term in this equation is just the second-order correction to the core energy $E^{(2)}_{\rm core}$, which is the same for all valence states, and which reduces to

$$E^{(2)}_{\rm core} = -\frac{1}{2}\sum_{mnab} \frac{\tilde{g}_{abmn}\, g_{mnab}}{\epsilon_m + \epsilon_n - \epsilon_a - \epsilon_b}. \tag{7.64}$$

This term can be evaluated using the methods given the previous section. The remaining two terms in second-order correlation energy $E^{(2)}_v$ vary from state to state and represent the correlation correction to the energy relative to the core (the negative of the valence-electron removal energy). The valence correlation energy reduces to

$$E^{(2)}_v = \sum_{nab} \frac{\tilde{g}_{abvn}\, g_{vnab}}{\epsilon_v + \epsilon_n - \epsilon_a - \epsilon_b} - \sum_{mnb} \frac{\tilde{g}_{vbmn}\, g_{mnvb}}{\epsilon_m + \epsilon_n - \epsilon_v - \epsilon_b}. \tag{7.65}$$

This equation is also valid relativistically, with the proviso that negative-energy states be omitted from the sum over excited states.

7.3.2 Angular Momentum Decomposition

To aid in the angular momentum decomposition, we start with an easily proved graphical identity:

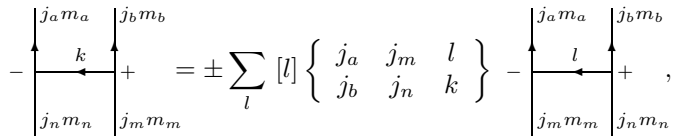

where the + sign pertains to the nonrelativistic case where j_i takes on integer values, and the − sign pertains to the relativistic case where j_i takes on half-integer values. From this identity, it follows that the anti-symmetrized Coulomb matrix element can be written in the nonrelativistic case as:

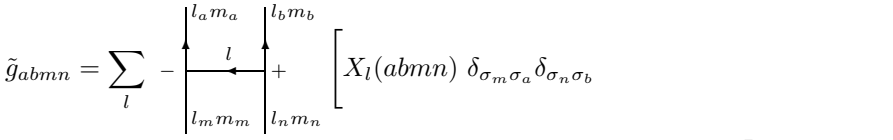

(7.66)

With the aid of this identity, the sum over magnetic quantum numbers in the first term of Eq. (7.65) can be easily carried out giving:

$$\sum_{\substack{m_a m_b m_n \\ \sigma_a \sigma_b \sigma_n}} \tilde{g}_{abvn} g_{vnab} = \sum_k \frac{2}{[k][v]} Z_k(abvn)\, X_k(abvn), \tag{7.67}$$

where $Z_k(abcd)$ is given by Eq.(7.35).

The second term in Eq. (7.65) can be treated similarly leading to the following expression for the nonrelativistic second-order energy:

$$\begin{aligned} E_v^{(2)} = & \sum_k \frac{2}{[k][v]} \sum_{abn} \frac{Z_k(vnab) X_k(vnab)}{\epsilon_v + \epsilon_n - \epsilon_a - \epsilon_b} \\ & - \sum_k \frac{2}{[k][v]} \sum_{bmn} \frac{Z_k(mnvb) X_k(mnvb)}{\epsilon_m + \epsilon_n - \epsilon_v - \epsilon_b}. \end{aligned} \tag{7.68}$$

In Table 7.4, we list the nonrelativistic Hartree-Fock eigenvalues and the corresponding second-order corrections obtained from Eq. (7.68) for a few low lying states in light mono-valent atoms. It is seen in every case that the second-order correlation corrections substantially improve the agreement with experiment. For light atoms, second-order MBPT under estimates the correlation corrections. This trend is reversed for heavy alkali-metal atoms such as cesium, where second-order MBPT substantially overestimates the correlation energy.

Table 7.4: Hartree-Fock eigenvalues ϵ_v with second-order energy corrections $E_v^{(2)}$ are compared with experimental binding energies for a few low-lying states in atoms with one valence electron.

Atom	State	ϵ_v	$E_v^{(2)}$	Sum	Expt.
Li	$2s$	-0.19630	-0.00165	-0.19795	-0.19814
	$2p$	-0.12864	-0.00138	-0.13001	-0.13024
Na	$3s$	-0.18180	-0.00586	-0.18766	-0.18886
	$3p$	-0.10944	-0.00178	-0.11122	-0.11155
	$3d$	-0.05567	-0.00023	-0.05589	-0.05594
K	$4s$	-0.14695	-0.01233	-0.15928	-0.15952
	$4p$	-0.09555	-0.00459	-0.10014	-0.10018
	$3d$	-0.05812	-0.00282	-0.06093	-0.06139
Cu	$4s$	-0.23285	-0.03310	-0.26595	-0.28394
	$4p$	-0.12286	-0.01154	-0.13441	-0.14406
	$4d$	-0.05508	-0.00070	-0.05578	-0.05640
Rb	$5s$	-0.13720	-0.01454	-0.15174	-0.15351
	$5p$	-0.09013	-0.00533	-0.09546	-0.09547
	$4d$	-0.06007	-0.00515	-0.06522	-0.06532

One Valence Electron: Relativistic Case

The relativistic expression for the second-order valence energy in a one-electron atom in state v is

$$\begin{aligned} E_v^{(2)} = & \sum_k \frac{1}{[k][v]} \sum_{abn} \frac{Z_k(vnab) X_k(vnab)}{\epsilon_v + \epsilon_n - \epsilon_a - \epsilon_b} \\ & - \sum_k \frac{1}{[k][v]} \sum_{bmn} \frac{Z_k(mnvb) X_k(mnvb)}{\epsilon_m + \epsilon_n - \epsilon_v - \epsilon_b} \,, \end{aligned} \tag{7.69}$$

Where the functions $X_k(mnvb)$ and $Z_k(mnvb)$ are defined in Eqs.(7.38) and (7.42), respectively. Examples of second-order calculations are given later following our discussion of the Breit Interaction.

7.3.3 Quasi-Particle Equation and Brueckner-Orbitals

As mentioned earlier, there is no first-order correction to the valence-electron energy ϵ_v. There are, however, second- and higher-order corrections. The second-order correction $E_v^{(2)}$ can be written, according to Eq. (7.65), as the diagonal matrix element of a non-local operator $\Sigma^{(2)}(\epsilon_v)$, whose matrix elements are given by

$$\Big[\Sigma^{(2)}(\epsilon_v)\Big]_{ij} = \sum_{nab} \frac{\tilde{g}_{abjn}\, g_{inab}}{\epsilon + \epsilon_n - \epsilon_a - \epsilon_b} - \sum_{mnb} \frac{\tilde{g}_{jbmn}\, g_{mnib}}{\epsilon_m + \epsilon_n - \epsilon - \epsilon_b}. \tag{7.70}$$

The operator $\Sigma(\epsilon)$ is referred to as the self-energy operator; the operator $\Sigma^{(2)}(\epsilon)$ is its second-order approximation. The sum of the zeroth- and second-order energy is the diagonal matrix element of $h_0 + V_{\rm HF} + \Sigma^{(2)}(\epsilon_v)$. We are, therefore, led to consider the generalization of the valence-electron Hartree-Fock equation

$$\Big[h_0 + V_{\rm HF} + \Sigma^{(2)}(\epsilon)\Big]\,\psi = \epsilon\psi. \tag{7.71}$$

This equation is referred to as the quasi-particle equation and its solutions are referred to as (second-order) Brueckner orbitals. The quasi-particle equation describes how the valence orbital is modified by correlation corrections.

One can develop an approximation for $\Sigma^{(2)}(\epsilon)$ in the coordinate representation valid for states that have small overlap with the core. The dominant contribution to the operator for such states arises from the "direct" integral in the second term of Eq. (7.70). The largest contributions are from states m with energies near ϵ_v. Thus,

$$\begin{aligned}\Sigma^{(2)}(\epsilon,\boldsymbol{r},\boldsymbol{r}') \approx -\sum_{mnb}\frac{1}{\epsilon_n-\epsilon_b}\int d^3r_1\frac{\phi^\dagger_m(\boldsymbol{r})\;(\phi^\dagger_n(\boldsymbol{r}_1)\phi_b(\boldsymbol{r}_1))}{|\boldsymbol{r}-\boldsymbol{r}_1|}\;\times \\ \int d^3r_2\frac{(\phi^\dagger_b(\boldsymbol{r}_2)\phi_n(\boldsymbol{r}_2))\;\phi_m(\boldsymbol{r}')}{|\boldsymbol{r}'-\boldsymbol{r}_2|} \\ = -\sum_{nb}\frac{1}{\epsilon_n-\epsilon_b}\int d^3r_1d^3r_2\frac{(\phi^\dagger_n(\boldsymbol{r}_1)\phi_b(\boldsymbol{r}_1))\;(\phi^\dagger_b(\boldsymbol{r}_2)\phi_n(\boldsymbol{r}_2))}{|\boldsymbol{r}-\boldsymbol{r}_1||\boldsymbol{r}-\boldsymbol{r}_2|}\;\delta(\boldsymbol{r}-\boldsymbol{r}'),\end{aligned}$$

where we have made use of the completeness of orbitals ϕ_m. This expression can be expanded for large r to give

$$\Sigma^{(2)}(\epsilon,r,r') \to -\frac{1}{2}\;\frac{\alpha_c}{r^4}\;\delta(\boldsymbol{r}-\boldsymbol{r}'), \tag{7.72}$$

where

$$\alpha_c = \frac{2}{3}\sum_{bn}\frac{\langle b|\,\boldsymbol{r}\,|n\rangle\cdot\langle n|\,\boldsymbol{r}\,|b\rangle}{\epsilon_n-\epsilon_b} \tag{7.73}$$

is the core polarizability. The interpretation of this equation is simple: the valence electron induces a dipole moment in the core and interacts with this induced moment; thus the name self-energy. As an alternative to MBPT, it is possible to describe the effects of the self-energy approximately by adding a phenomenological potential $-\alpha_c/2r^4$ to the HF potential and solving the modified Schrödinger equation. It is worth mentioning that the approximate interaction given in Eq. (7.73) is singular for ns states, so it is necessary to return to the more exact formulation for such states.

Let us now solve Eq. (7.71) perturbatively; neglecting Σ in lowest order. We write $\psi = \phi_v + \delta\phi_v$ and $\epsilon = \epsilon_v + \delta\epsilon_v$, where ϕ_v and ϵ_v are the HF orbital and eigenvalue for state v. We find that the perturbation $\delta\phi_v$ satisfies the inhomogeneous equation

$$(h_0 + V_{\rm HF} - \epsilon_v)\,\delta\phi_v = \Big(\delta\epsilon_v - \Sigma^{(2)}(\epsilon_v)\Big)\,\phi_v. \tag{7.74}$$

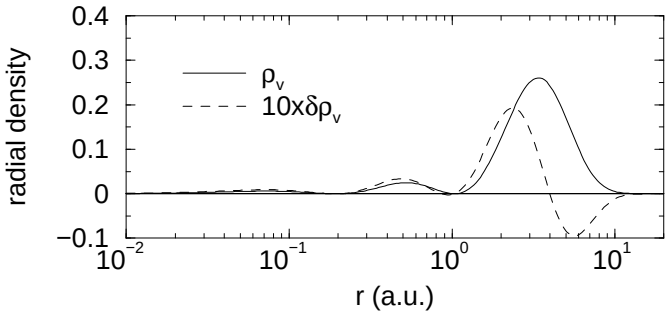

Figure 7.3: The radial charge density ρ_v for the $3s$ state in sodium is shown together with $10\times\delta\rho_v$, where $\delta\rho_v$ is the second-order Brueckner correction to ρ_v.

Since ϵ_v is an eigenvalue of the homogeneous equation, the inhomogeneous equation has a solution if, and only if, the right-hand side is orthogonal ϕ_v. The solvability condition can be written

$$\delta\epsilon_v = \left\langle \phi_v \left| \Sigma^{(2)}(\epsilon_v) \right| \phi_v \right\rangle = \left[\Sigma^{(2)}(\epsilon_v)\right]_{vv},$$

which is just the condition that $\delta\epsilon_v$ be the second-order correlation energy. The solution to (7.74) is then given by

$$\delta\phi_v(\boldsymbol{r}) = -\sum_{i\neq v} \delta_{l_i l_v} \frac{\left[\Sigma^{(2)}(\epsilon_v)\right]_{iv}}{\epsilon_i - \epsilon_v}\ \phi_i(\boldsymbol{r}).$$

If we let $P_v(r)$ and $\delta P_v(r)$ be radial functions associated with ϕ_v and $\delta\phi_v$, respectively, then the radial probability density is $\rho_v(r) = P_v^2(r)$ and the perturbed radial probability density is $\delta\rho_v(r) = 2P_v(r)\ \delta P_v(r)$. We illustrate these radial densities for the $3s$ state of sodium in Fig. 7.3. One sees from this figure that the Brueckner correction draws the valence wave function in toward the atomic core, in harmony with the attractive nature of $\Sigma^{(2)}$.

7.3.4 Monovalent Negative Ions

One interesting application of the quasi-particle equation is the study of negative ions. Consider, for example, a neutral closed-shell atom. The HF potential for such an atom has no bound states other than the occupied core states. Excited states see the neutral potential of the completely shielded nucleus. It is known experimentally, however, that various neutral closed-shell atoms support bound states; the electron binds to the closed core to form a one-electron negative ion. The binding force is provided by the polarization potential of the core $-\alpha_c/2r^4$.

There is an obvious difficulty in describing such an atom within the framework of MBPT; the bound state does not exist in the HF approximation. Indeed, the force responsible for binding shows up first in second-order MBPT.

Table 7.5: Expansion coefficients c_n, $n = 1 \cdot\cdot 20$ of the $5s$ state of Pd^- in a basis of HF orbitals for neutral Pd confined to a cavity of radius $R = 50$ a.u..

n	c_n	n	c_n	n	c_n	n	c_n
1	0.000001	6	0.556972	11	-0.163415	16	-0.009651
2	0.000028	7	0.461970	12	-0.132544	17	-0.002016
3	-0.000294	8	0.344215	13	-0.031214	18	0.000242
4	-0.003225	9	-0.254265	14	-0.074083	19	-0.000009
5	0.458841	10	-0.175688	15	-0.031380	20	-0.000000

One approach that can be used in this case is to solve the quasi-particle equation exactly, without recourse to perturbation theory. To this end, we expand the Brueckner orbital ψ as a linear combination of HF basis orbitals ϕ_k,

$$\psi(\boldsymbol{r}) = \sum_k c_k \phi_k(\boldsymbol{r}).$$

Substituting into Eq. (7.71), we find that the expansion coefficients satisfy the eigenvalue equation

$$\epsilon\ c_i = \sum_j \left[\epsilon_i \delta_{ij} + \left[\Sigma^{(2)}(\epsilon) \right]_{ij} \right]\ c_j. \tag{7.75}$$

For neutral atoms, this equation has solutions that corresponds HF core orbitals modified by the self-energy operator. Other solutions with $\epsilon < 0$ also exist in some cases; the new bound-state solutions being associated with the negative ion. To obtain the solution corresponding to a loosely-bound electron, it is usually sufficient to set $\epsilon = 0$ in the expression for $\Sigma^{(2)}(\epsilon)$.

As a specific example, we consider the case of palladium (Pd), Z=46. This atom has closed $n = 1$, 2, and 3 shells and closed $4s$, $4p$, and $4d$ subshells. The Pd negative ion is found experimentally (Scheer et al., 1998) to have a $5s$ bound state with binding energy, (or affinity) 562.13 meV. The expansion coefficients c_i in Eq. (7.75) for the $5s$ eigenstate are given in Table 7.5. The $5s$ eigen energy is found to be $\epsilon_{5s} = -0.01957$ a.u., corresponding to an electron affinity of 532.5 meV. The radial density of neutral Pd is shown in the lower panel of Fig. 7.4 and the $5s$ Brueckner orbital of Pd^- is shown in the upper panel.

7.4 Relativistic Calculations

Relativistic MBPT calculations closely follow the nonrelativistic pattern described in the paragraphs above with several modifications and caveats. Among the modifications is the replacement of two-component nonrelativistic orbitals $\phi_n(\boldsymbol{r})$ that are products of radial functions $P_{nl}(r)$, spherical harmonics $Y_{lm}(\theta,\, \phi)$

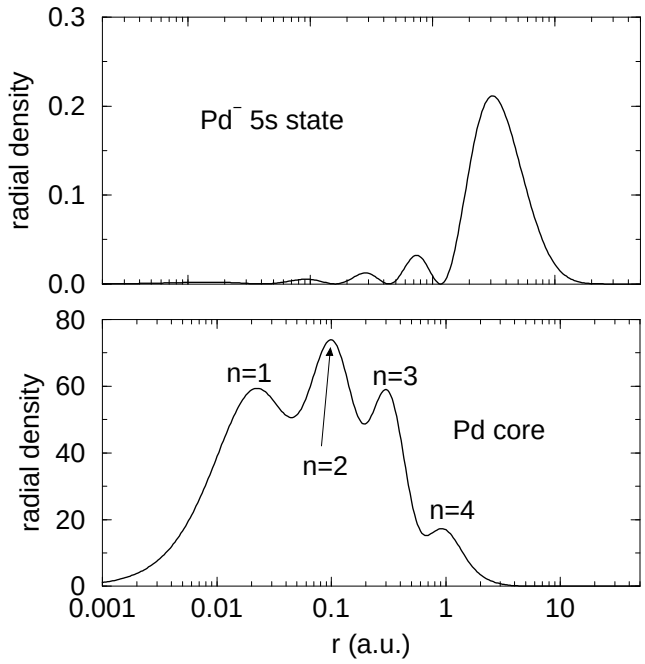

Figure 7.4: Lower panel: radial density of neutral Pd (Z=46). The peaks corresponding to closed $n = 1, 2, \cdots$ shells are labeled. Upper panel: radial density of the $5s$ ground-state orbital of Pd^-. The $5s$ orbital is obtained by solving the quasi-particle equation.

and two-component spinors χ_σ by four-component relativistic orbitals that are products of radial functions ($P_{nl}(r)$, $Q_{nl}(r)$) and spherical spinors $\Omega_{\kappa m}(\theta, \phi)$. In both nonrelativistic and relativistic cases, the many-body theory takes a particularly simple form when the starting potential $U(r)$ is the frozen-core HF potential $V_{\rm HF}$.

In the relativistic case, the Coulomb interaction between electrons is replaced by the sum of the Coulomb and Breit interactions. This later results from transverse photon exchange between electrons. The Breit interaction is relatively smaller (by order $\alpha^2 Z^2$) than the Coulomb interaction, so it follows that higher-order MBPT expressions can, to good accuracy, be linearized in the Breit interaction. Thus, for example, the Breit correction to the expressions for the third-order energy consist of products of two Coulomb matrix elements and one Breit matrix element.

An important caveat in relativistic calculations of energy levels is that contributions from negative-energy states in the spectrum of the Dirac equation ($\epsilon_i \leq -mc^2$) must be omitted from MBPT sums (Brown and Ravenhall, 1951).

Relativistic theory has the distinct advantage that it automatically accounts for the energy separation of nl levels into fine-structure sublevels nlj with $j = l \pm 1/2$. For light atoms this separation is often unimportant and nonrelativistic theory suffices. However, for heavy atoms or highly-charged few-electron ions, where the fine-structure separation is large, a relativistic treatment is essential.

7.4.1 Breit Interaction

The Breit interaction is the contribution to the electron-electron interaction mediated by exchange of transverse photons. The lowest-order energy shift associated with the exchange of a transverse photon between two electrons in states a and b is (Bethe and Salpeter, 1957, p. 170)

$$\begin{aligned} B^{(1)} &= -\frac{1}{2\pi^2}\int d^3r_1 \int d^3r_2 \sum_{ij} \int d^3k\, e^{i\boldsymbol{k}\cdot(\boldsymbol{r}_1-\boldsymbol{r}_2)}\Big(\delta_{ij} - k_i k_j/|\boldsymbol{k}|^2\Big) \\ &\quad \times \left[\frac{1}{\boldsymbol{k}^2}\phi_a^\dagger(\boldsymbol{r}_1)\alpha_i\phi_a(\boldsymbol{r}_1)\phi_b^\dagger(\boldsymbol{r}_2)\alpha_j\phi_b(\boldsymbol{r}_2)\right. \\ &\quad \left. - \frac{1}{\boldsymbol{k}^2 - k_0^2}\phi_a^\dagger(\boldsymbol{r}_1)\alpha_i\phi_b(\boldsymbol{r}_1)\phi_b^\dagger(\boldsymbol{r}_2)\alpha_j\phi_a(\boldsymbol{r}_2)\right], \end{aligned} \tag{7.76}$$

where $k_0 = |\epsilon_a - \epsilon_b|/c$. The integral over d^3k above can be carried out leading to $B^{(1)} = b_{abab} - b_{abba}$, the difference between direct b_{abab} and exchange b_{abba} two-particle matrix elements of the "frequency-dependent" Breit operator

$$b_{12}(k_0) = -\frac{\boldsymbol{\alpha}_1\cdot\boldsymbol{\alpha}_2}{r_{12}}\cos(k_0\, r_{12}) + \boldsymbol{\alpha}_1\cdot\boldsymbol{\nabla}_1\ \boldsymbol{\alpha}_2\cdot\boldsymbol{\nabla}_2\left[\frac{\cos(k_0\, r_{12})-1}{k_0^2\, r_{12}}\right]. \tag{7.77}$$

In the direct matrix element b_{abab}, where $k_0 = 0$, the frequency-dependent Breit interaction reduces to its limiting static form:

$$\begin{aligned} b_{12} &= -\frac{\boldsymbol{\alpha}_1 \cdot \boldsymbol{\alpha}_2}{r_{12}} + \frac{\boldsymbol{\alpha}_1 \cdot \boldsymbol{\alpha}_2 - (\boldsymbol{\alpha}_1 \cdot \hat{r}_{12})\,(\boldsymbol{\alpha}_2 \cdot \hat{r}_{12})}{2r_{12}} \\ &= -\frac{\boldsymbol{\alpha}_1 \cdot \boldsymbol{\alpha}_2 + (\boldsymbol{\alpha}_1 \cdot \hat{r}_{12})\,(\boldsymbol{\alpha}_2 \cdot \hat{r}_{12})}{2r_{12}} \end{aligned} \tag{7.78}$$

The first term on the right-hand side on the first line of Eq. (7.78) is referred to as the Gaunt interaction after Gaunt (1929) who introduced this term to account for the fine-structure in He. The second term on the right-hand side on the first line of Eq. (7.78) (which can be derived, alternatively, in a QED Feynman gauge calculation as the retardation correction to the charge-charge interaction) is referred to as the "retardation" correction. The retardation correction was introduced by Breit (1929, 1930, 1932) who used the entire expression in Eq.(7.78) to study helium fine structure. Below, we separate the two-particle Breit matrix elements b_{ijkl} into a part m_{ijkl} from the Gaunt interaction and a part r_{ijkl} from retardation. Such a separation is particularly convenient when we consider the angular momentum decomposition of the two-particle Breit matrix element.

To summarize, direct matrix elements of the frequency-dependent Breit interaction b_{abab} are evaluated using the static limit, whereas exchange matrix elements b_{abba} are evaluated using Eq. (7.77) with $k_0 = |\epsilon_a - \epsilon_b|/c$. It was shown by Mittleman (1981) that the form of the "frequency-dependent" Breit operator appropriate for evaluating off-diagonal matrix elements b_{abcd} is

$$b_{12}(k_0) \to \frac{1}{2}\, b_{12}(|\epsilon_a - \epsilon_c|/c) + \frac{1}{2}\, b_{12}(|\epsilon_b - \epsilon_d|/c)\ . \tag{7.79}$$

Differences between the frequency-dependent Breit interaction and its static limit given in Eq. (7.78) are of relative order $\alpha^2 Z^2$ and therefore important primarily for highly-charged ions. In the following sections, we use the static version unless otherwise noted.

7.4.2 Angular Reduction of the Breit Interaction

As an aid to the angular decomposition of the two-particle matrix element b_{ijkl} we separate it into two parts $b_{ijkl} = m_{ijkl} + r_{ijkl}$, where m_{ijkl} is the part associated with the Gaunt interaction in Eq.(7.78)

$$m_{ijkl} = -\int\int \frac{d^3r_1 d^3r_2}{|\boldsymbol{r}_1 - \boldsymbol{r}_2|} \phi_i^\dagger(\boldsymbol{r}_1)\boldsymbol{\alpha}\phi_k(\boldsymbol{r}_1) \cdot \phi_j^\dagger(\boldsymbol{r}_2)\boldsymbol{\alpha}\phi_l(\boldsymbol{r}_2), \tag{7.80}$$

and r_{ijkl} is the associated with the retardation correction.

$$r_{ijkl} = \frac{1}{2}\int\int \frac{d^3r_1 d^3r_2}{|\boldsymbol{r}_1 - \boldsymbol{r}_2|} \phi_i^\dagger(\boldsymbol{r}_1)\boldsymbol{\alpha} \cdot \hat{r}_{12}\phi_k(\boldsymbol{r}_1)\ \phi_j^\dagger(\boldsymbol{r}_2)\boldsymbol{\alpha} \cdot \hat{r}_{12}\phi_l(\boldsymbol{r}_2), \tag{7.81}$$

The method used in the decomposition of m_{ijkl} is to expand $\phi_i^\dagger(\boldsymbol{r})\boldsymbol{\alpha}\phi_k(\boldsymbol{r})$ and $\phi_j^\dagger(\boldsymbol{r})\boldsymbol{\alpha}\phi_l(\boldsymbol{r})$ into vector spherical harmonics and then make use of the

orthonormality properties of the vector spherical harmonics to carry out the angular integrations. Details of the reduction can be found in Johnson et al. (1988b) and Mann and Johnson (1971). One obtains

$$m_{ijkl} = \sum_L J(ijkl)\left[M_L(ijkl) + N_L(ijkl)\right], \tag{7.82}$$

where

$J_L(ijkl) = -$ 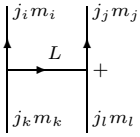 $+$

The radial matrix elements $M_L(ijkl)$ and $N_L(ijkl)$ are

$$\begin{aligned} M_L(ijkl) = (-1)^L &\langle \kappa_i \| C_L \| \kappa_k \rangle \langle \kappa_j \| C_L \| \kappa_l \rangle \\ &\left[\frac{L+1}{2L+3} \int_0^\infty dr_1 \int_0^\infty dr_2 \, \frac{r_<^{L+1}}{r_>^{L+2}} \, Q_{ik}(r_1) Q_{jl}(r_2) \right. \\ &\left. + \frac{L}{2L-1} \int_0^\infty dr_1 \int_0^\infty dr_2 \, \frac{r_<^{L-1}}{r_>^{L}} \, P_{ik}(r_1) P_{jl}(r_2) \right] \end{aligned} \tag{7.83}$$

and

$$\begin{aligned} N_L(ijkl) = (-1)^{L+1} &\langle -\kappa_i \| C_L \| \kappa_k \rangle \langle -\kappa_j \| C_L \| \kappa_l \rangle \\ &\frac{(\kappa_i + \kappa_k)(\kappa_j + \kappa_l)}{L(L+1)} \int_0^\infty dr_1 \int_0^\infty dr_2 \, \frac{r_<^{L}}{r_>^{L+1}} \, V_{ik}(r_1) V_{jl}(r_2), \end{aligned} \tag{7.84}$$

where

$$P_{ik}(r) = U_{ik}(r) + \frac{\kappa_k - \kappa_i}{L} \, V_{ik}(r), \tag{7.85}$$

$$Q_{ik}(r) = -U_{ik}(r) + \frac{\kappa_k - \kappa_i}{L+1} \, V_{ik}(r), \tag{7.86}$$

$$U_{ik}(r) = P_i(r) Q_k(r) - Q_i(r) P_k(r), \tag{7.87}$$

$$V_{ik}(r) = P_i(r) Q_k(r) + Q_i(r) P_k(r). \tag{7.88}$$

The values of the reduced matrix elements $\langle \kappa_i \| C_L \| \kappa_j \rangle$ and $\langle -\kappa_i \| C_L \| \kappa_j \rangle$ in Eqs. (7.83-7.84) depend only on the $|\kappa_i|$, not on the sign. However, the selection rules do depend on the sign. Thus, for example, if $\kappa_i = \kappa_j = -1$, (both $s_{1/2}$ states) then $\langle \kappa_i \| C_L \| \kappa_j \rangle$ is nonzero only for $L = 0$ whereas $\langle -\kappa_i \| C_L \| \kappa_j \rangle$ is nonzero only for $L = 1$.

The matrix element of the retardation part of the Breit interaction takes a similar form, the details being given in Mann and Johnson (1971). One obtains

$$r_{ijkl} = \sum_L J_L(ijkl) O_L(ijkl), \tag{7.89}$$

with

$$
\begin{aligned}
O_L(ijkl) = (-1)^{L+1}&\langle\kappa_i\|C_L\|\kappa_k\rangle\langle\kappa_j\|C_L\|\kappa_l\rangle \\
&\left[\frac{(L+1)^2}{(2L+1)(2L+3)}\int_0^\infty dr_1\int_0^\infty dr_2\ \frac{r_<^{L+1}}{r_>^{L+2}}\ Q_{ik}(r_1)Q_{jl}(r_2)\right. \\
&+\frac{L^2}{(2L+1)(2L-1)}\int_0^\infty dr_1\int_0^\infty dr_2\ \frac{r_<^{L-1}}{r_>^{L}}\ P_{ik}(r_1)P_{jl}(r_2) \\
&+\frac{L(L+1)}{2(2L+1)}\int_0^\infty dr_1\int_0^{r_1} dr_2\ \left(\frac{r_<^{L-1}}{r_>^{L}}-\frac{r_<^{L+1}}{r_>^{L+2}}\right)Q_{ik}(r_1)P_{jl}(r_2) \\
&\left.+\frac{L(L+1)}{2(2L+1)}\int_0^\infty dr_1\int_{r_1}^\infty dr_2\ \left(\frac{r_<^{L-1}}{r_>^{L}}-\frac{r_<^{L+1}}{r_>^{L+2}}\right)P_{ik}(r_1)Q_{jl}(r_2)\right]. \qquad (7.90)
\end{aligned}
$$

Putting this all together, we may write

$$b_{ijkl} = \sum_L - \quad + \ B_L(ijkl), \qquad (7.91)$$

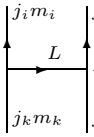

with

$$B_L(ijkl) = M_L(ijkl) + N_L(ijkl) + O_L(ijkl). \qquad (7.92)$$

Matrix elements of the frequency-dependent Breit interaction $b_{12}(k_0)$ are somewhat more complicated; they can be evaluated using the formulas given above with the following substitutions:

(a) In Eqs. (7.83), (7.84) and in the first two lines of Eq. (7.90) replace expressions of the form

$$\frac{r_<^K}{r_>^{K+1}} \to -k_0\,(2K+1)\,j_K(k_0 r_<)\,y_K(k_0 r_>),$$

where $j_K(x)$ and $y_K(x)$ are spherical Bessel and Hankel functions, respectively, and

(b) replace the last two lines of Eq. (7.90) by

$$
\begin{aligned}
\frac{L(L+1)}{(2L+1)}\int_0^\infty dr_1\int_0^{r_1} dr_2\Bigg\{ &-2\left[k_0 j_{L-1}(k_0\,r_2)\,y_{L+1}(k_0\,r_1)+\ \frac{2L+1}{k_0^2}\,\frac{r_2^{L-1}}{r_1^{L+2}}\right] \\
&\times Q_{ik}(r_1)P_{jl}(r_2) - 2\,k_0 j_{L+1}(k_0\,r_2)\,y_{L-1}(k_0\,r_1)P_{ik}(r_1)Q_{jl}(r_2)\Bigg\}.
\end{aligned}
$$

In the following sections, we need sums of the form

$$\sum_{m_a} b_{iaja} = \sqrt{\frac{[j_a]}{[j_i]}}\delta_{j_i j_j}\delta_{m_i m_j}B_0(iaja)$$

over magnetic substates m_a of the state a. Since $P_{aa} = Q_{aa} = 0$, it follows from Eqs.(7.83) and (7.90) that $M_0(iaja) = 0$ and $O_0(iaja) = 0$. Moreover, since $\langle -\kappa_a \| C_0 \| \kappa_a \rangle = 0$, it follows that $N_0(iaja) = 0$ also. Therefore, $\sum_{m_a} b_{iaja} = 0$.

7.4.3 Coulomb-Breit Many-Electron Hamiltonian

Replacing the electron-electron Coulomb interaction by the sum of the Coulomb and Breit interaction,

$$\frac{1}{r_{12}} \to \frac{1}{r_{12}} + b_{12}$$

leads to a modified many-electron interaction potential

$$V_I = \sum_{ijkl} \left[g_{ijkl} + b_{ijkl} \right] a_i^\dagger a_j^\dagger a_l a_k. \tag{7.93}$$

Arranging V_I in normal order with respect to the closed core leads to

$$\begin{aligned} V_I &= V_2 + V_1 + V_0 \\ V_2 &= \frac{1}{2} \sum_{ijkl} \left[g_{ijkl} + b_{ijkl} \right] :a_i^\dagger a_j^\dagger a_l a_k: \qquad (7.94) \\ V_1 &= \sum_{ij} \left(V_{\rm HF} + B_{\rm HF} - U \right)_{ij} :a_i^\dagger a_b: \qquad (7.95) \\ V_0 &= \frac{1}{2} \sum_a (V_{\rm HF} + B_{\rm HF})_{aa}, \qquad (7.96) \end{aligned}$$

where

$$(B_{\rm HF})_{ij} = \sum_b \left[b_{ibjb} - b_{ibbj} \right].$$

The first term on the right hand side of the above equation vanishes, as shown in the previous section.

7.4.4 Closed-Shell Energies

If we choose $U = V_{\rm HF}$ then we find for a closed-shell atom,

$$E = E_0 + E^{(1)} + B^{(1)} + E^{(2)} + B^{(2)} + E^{(3)} + \cdots$$

with $E_0 = \sum_a \epsilon_a$ and $\langle 0_c | V_I | 0_c \rangle = V_0 = E^{(1)} + B^{(1)} = \frac{1}{2} \sum_a (V_{\rm HF} + B_{\rm HF})_{aa}$. Therefore, $E_0 + V_0 = E_{\rm HF} + B^{(1)}$ with

$$B^{(1)} = \frac{1}{2} \sum_a (B_{\rm HF})_{aa}. \tag{7.97}$$

The expression for the second-order energy can be inferred from Eq.(7.27):

$$E^{(2)} + B^{(2)} = -\sum_{na} \frac{(B_{\rm HF})_{an}(B_{\rm HF})_{na}}{\epsilon_n - \epsilon_a} - \frac{1}{2}\sum_{mnab} \frac{(\tilde{g}_{abmn} + \tilde{b}_{abmn})(g_{mnab} + b_{mnab})}{\epsilon_m + \epsilon_n - \epsilon_a - \epsilon_b}\,.$$

Linearizing this expression in powers of b_{ijkl}, we may write this in the form

$$E^{(2)} = -\frac{1}{2}\sum_{mnab} \frac{\tilde{g}_{abmn} g_{mnab}}{\epsilon_m + \epsilon_n - \epsilon_a - \epsilon_b} \tag{7.98}$$

$$B^{(2)} = -\sum_{mnab} \frac{\tilde{g}_{abmn} b_{mnab}}{\epsilon_m + \epsilon_n - \epsilon_a - \epsilon_b}\,. \tag{7.99}$$

Continuing in this way, we can write the perturbation expansion for the energy as a sum of Coulomb energies $E^{(n)}$ and linearized Breit energies $B^{(n)}$.

The relativistic expression for $E^{(2)}$ after angular reduction is given in Eq.(7.41); the corresponding expression for $B^{(2)}$ is

$$B_2^{(2)} = -\sum_k \frac{1}{[k]} \sum_{abmn} \frac{Z_k(mnab) B_k(mnab)}{\epsilon_m + \epsilon_n - \epsilon_b - \epsilon_a}, \tag{7.100}$$

where $Z_k(mnab)$ and $B_k(mnab)$ are defined in Eqs.(7.42) and Eq.(7.91), respectively.

In Table 7.6 and Fig. 7.5, we list values of the above contributions to the ground-state energies of heliumlike ions with nuclear charges Z ranging from 2 to 90. Notice that $E^{(2)}$ is roughly constant and that $E^{(3)}$ falls off approximately as $1/Z$. By contrast, $B^{(1)}$ and $B^{(2)}$ grow as Z^3 and Z^2, respectively. From the table, it is obvious that contributions from $B^{(1)}$ and $B^{(2)}$ are almost negligible for neutral He. However, for $Z > 5$, $B^{(1)}$ is larger than $|E^{(3)}|$ and for $Z > 17$, $B^{(1)}$ is larger than $|E^{(2)}|$. Indeed, beyond $Z = 70$, we even find $|B^{(2)}| > |E^{(2)}|$. Thus, while the Breit interaction is a relatively small perturbation for low Z atoms and ions, it is the dominant correction to the HF energy at high Z.

7.4.5 One Valence Electron

As in the nonrelativistic case the energy of an atom with one valence electron separates into a core contribution that is independent of the valence state and a valence contribution E_v, The valence energy may be written,

$$E_v = \epsilon_v + E_v^{(1)} + B_v^{(1)} + E_v^{(2)} + B_v^{(2)} + E_v^{(3)} + \cdots$$

Expressions for the Coulomb contributions $E_v^{(n)}$, before angular momentum reduction are formally identical to the nonrelativistic expression given earlier.

Table 7.6: Contributions to the ground-state energy for He-like ions.

Z
2
3
4
5
6
7
8
9
10
20
30
40
50
60
70
80
90

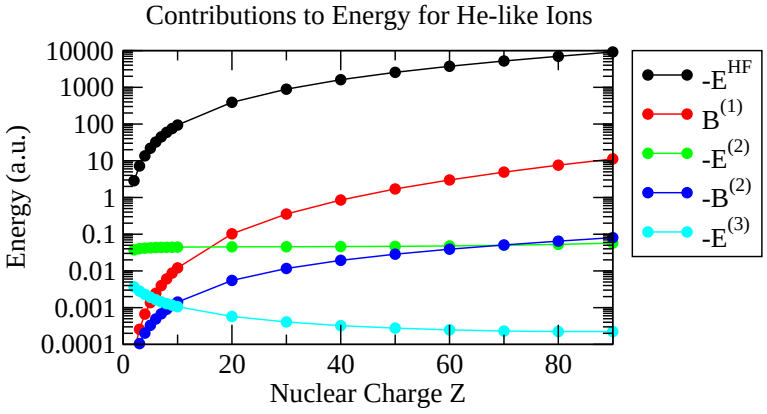

Figure 7.5: MBPT contributions for He-lile ions.

Table 7.7: MBPT Coulomb ($E^{(n)}$), Breit ($B^{(n)}$) and reduced mass – mass polarization (RM/MP) contributions to the energies of $2s$ and $2p$ states of lithiumlike Ne (Johnson et al., 1988b).

Term	$2s_{1/2}$	$2p_{1/2}$	$2p_{3/2}$
$E_{\rm HF}$	-8.78258	-8.19384	-8.18557
$B^{(1)}$	0.00090	0.00160	0.00074
$E^{(2)}$	-0.00542	-0.01012	-0.01003
$B^{(2)}$	-0.00011	-0.00014	-0.00012
$E^{(3)}$	-0.00013	-0.00028	-0.00028
RM/MP	0.00024	0.00010	0.00010
Total	-8.78709	-8.20267	-8.19516
NIST	-8.78672	-8.20282	-8.19530
Δ	0.00037	-0.00015	-0.00014

One easily establishes the following formulas for the low order linearized Breit corrections:

$$B^{(1)} = (B_{\rm HF})_{vv} \tag{7.101}$$

$$B^{(2)} = 2\sum_{nab}\frac{\tilde{g}_{abvn}\,b_{vnab}}{\epsilon_v+\epsilon_n-\epsilon_a-\epsilon_b} - 2\sum_{mnb}\frac{\tilde{g}_{vbmn}\,b_{mnvb}}{\epsilon_m+\epsilon_n-\epsilon_v-\epsilon_b} - \sum_{am}\frac{(B_{\rm HF})_{am}\tilde{g}_{vmva}}{\epsilon_m-\epsilon_a} - \sum_{am}\frac{\tilde{g}_{vavm}(B_{\rm HF})_{ma}}{\epsilon_m-\epsilon_a} \tag{7.102}$$

The second-order Breit energy after angular reduction is given by

$$B_v^{(2)} = \sum_k \frac{2}{[k][v]}\sum_{abn}\frac{Z_k(vnab)B_k(vnab)}{\epsilon_v+\epsilon_n-\epsilon_a-\epsilon_b} - \sum_k\frac{2}{[k][v]}\sum_{bmn}\frac{Z_k(mnvb)B_k(mnvb)}{\epsilon_m+\epsilon_n-\epsilon_v-\epsilon_b} + \sum_{am}\delta_{\kappa_a\kappa_m}\frac{(B_{\rm HF})_{am}Z_0(vmva)}{\epsilon_m-\epsilon_a} + \sum_{am}\delta_{\kappa_a\kappa_m}\frac{Z_0(vavm)(B_{\rm HF})_{ma}}{\epsilon_m-\epsilon_a}. \tag{7.103}$$

In Table 7.7, we list the contributions to the energies of $2s_{1/2}$, $2p_{1/2}$, and $2p_{3/2}$ levels of lithiumlike Ne VIII from Coulomb and Breit terms from Johnson et al. (1988b). The table also include reduced mass and mass polarization corrections. The Breit interaction, which is relatively small for this low-Z ion, influences the third digit of the energy. Since the resulting theoretical energies differ from measured energies in the fifth digit, it necessary to include contributions from the Breit interaction to understand energies to this level of precision. It should be mentioned that the residual differences between measurement and theory in this case arise primarily from the Lamb shift.

7.5 CI Calculations

An alternative to MBPT that has some advantages for simple atomic systems is the configuration-interaction (CI) method, which we here describe for the case of helium.

As a first step, we introduce the configuration state function

$$\Phi_{kl}(LS) = \eta_{kl} \sum_{\substack{m_k m_l \\ \mu_k \mu_l}} \quad [\text{diagram}] \quad a_k^\dagger a_l^\dagger \, |0\rangle, \tag{7.104}$$

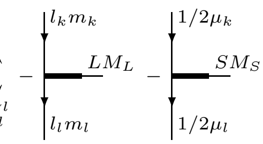

where η_{kl} is a symmetry factor defined by

$$\eta_{kl} = \begin{cases} 1/\sqrt{2}, & \text{for } k = l, \\ 1, & \text{for } k \neq l. \end{cases}$$

For the identical particle case $k = l$, the sum $L + S$ must be even. This function is an LS eigenstate of H_0 with energy $E_0 = \epsilon_k + \epsilon_l$. An LS eigenstate of the exact Hamiltonian $H_0 + V$ (the CI wave function) may be expressed as a linear combination of such configuration-state functions

$$\Psi(LS) = \sum_{k \leq l} C_{kl} \; \Phi_{kl}(LS), \tag{7.105}$$

where the expansion coefficients C_{kl} are to be determined. The normalization condition

$$\langle \Psi(LS) | \Psi(LS) \rangle = 1$$

reduces to

$$\sum_{k \leq l} C_{kl}^2 = 1.$$

We designate the interaction matrix $\langle \Phi_{vw}(LS) | V | \Phi_{xy}(LS) \rangle$ by $V_{vw,xy}$ and find

$$V_{vw,xy} = \eta_{vw} \eta_{xy} \sum_k \left[(-1)^{L+k+l_w+l_x} \left\{ \begin{array}{ccc} l_v & l_w & L \\ l_y & l_x & k \end{array} \right\} X_k(vwxy) \right.$$
$$\left. + (-1)^{S+k+l_w+l_x} \left\{ \begin{array}{ccc} l_v & l_w & L \\ l_x & l_y & k \end{array} \right\} X_k(vwyx) \right] . \tag{7.106}$$

The expectation value of the Hamiltonian obtained using the CI wave function becomes a quadratic function of the expansion coefficients

$$\langle \Psi(LS) | H | \Psi(LS) \rangle = \sum_{v \leq w, \, x \leq y} \Big[(\epsilon_v + \epsilon_w) \, \delta_{xv} \delta_{yw} + V_{vw,xy} \Big] C_{xy} C_{vw}.$$

To obtain the expansion coefficients, we minimize the expectation of the Hamiltonian subject to the normalization condition. This leads to the eigenvalue equation

$$\sum_{x \leq y} \Big[(\epsilon_v + \epsilon_w) \, \delta_{xv} \delta_{yw} + V_{vw,xy} \Big] C_{xy} = E \, C_{vw}. \tag{7.107}$$

Table 7.8: Contribution δE_l of $(nlml)$ configurations to the CI energy of the helium ground state. The dominant contributions are from the $l = 0$ $nsms$ configurations. Contributions of configurations with $l \geq 7$ are estimated by extrapolation.

l	$mlnl$	δE_l	E_l
0	msns	-2.8790278	-2.8790278
1	mpnp	-0.0214861	-2.9005139
2	mdnd	-0.0022505	-2.9027644
3	mfnf	-0.0005538	-2.9033182
4	mgng	-0.0001879	-2.9035061
5	mhnh	-0.0000811	-2.9035872
6	mjnj	-0.0000403	-2.9036275
$7 \cdots \infty$		-0.0000692	-2.9036967
Expt.			-2.9036778

Let us consider as a specific example the $^1\mathrm{S}_0$ ground state of helium. Angular momentum selection rules limit the possible configurations (vw) to those with $l_v = l_w$. Thus, we have contributions from states of the form $(msns)$, $(mpnp)$, $(mdnd)$, $\cdots$. In a basis with N basis functions, there are $N(N+1)/2$ pairs $(mlnl)$ with $m \leq n$. If we include, for example, 20 basis orbitals of type nl in our expansion, then we would have 210 expansion coefficients for each l.

In table Table 7.8, we show the results of a sequence of CI calculations of the helium ground-state energy including configurations with successively larger values of the orbital angular momentum. The major contributions are from $(msns)$ configurations, and contributions from higher-partial waves are seen to converge rapidly. The final extrapolated value of the CI energy differs from the experimental energy by 1 part in 10^6; the difference being due to omitted reduced-mass, relativistic and quantum-electrodynamic corrections.

7.5.1 Relativistic CI Calculations

To extend the CI calculations of two-electron ions to the relativistic case, we introduce the configuration state function

$$\Phi_{kl}(JM) = \eta_{kl} \sum_{m_k m_l} - \left| \begin{array}{c} j_k m_k \\ \\ JM \\ \\ j_l m_l \end{array} \right. \quad a_k^\dagger a_l^\dagger \, |0\rangle, \tag{7.108}$$

where, as in the nonrelativistic case, η_{kl} is a symmetry factor defined by

$$\eta_{kl} = \begin{cases} 1/\sqrt{2}, & \text{for } k = l, \\ 1, & \text{for } k \neq l. \end{cases}$$

For the identical particle case, $k = l$, the the total angular momentum J must be even. The parity of $\Phi_{kl}(JM)$ is $P = (-1)^{l_k+l_l}$. In the relativistic case, k and l are restricted to electron states only; k and l must not be negative-energy states.

The configuration state function is an eigenstate of H_0 with energy $E_0 = \epsilon_k + \epsilon_l$. The relativistic CI wave function is expressed as a linear combination (of specific parity P) of configuration-state functions

$$\Psi(JM) = \sum_{k \le l} C_{kl}\ \Phi_{kl}(JM). \tag{7.109}$$

As in the nonrelativistic case, we designate the interaction matrix $\langle \Phi_{vw}(JM)|V|\Phi_{xy}(JM)\rangle$ by $V_{vw,xy}$ and find

$$\begin{aligned} V_{vw,xy} = \eta_{vw}\eta_{xy} \sum_k \Bigg[&(-1)^{J+k+j_w+j_x} \begin{Bmatrix} j_v & j_w & J \\ j_y & j_x & k \end{Bmatrix} T_k(vwxy) \\ &+(-1)^{k+j_w+j_x} \begin{Bmatrix} j_v & j_w & J \\ j_x & j_y & k \end{Bmatrix} T_k(vwyx) \Bigg] . \end{aligned} \tag{7.110}$$

In the relativistic case, $T_k(vwxy) = X_k(vwxy) + B_k(vwxy)$ is the sum of Coulomb (7.38) and Breit (7.92) interaction matrix elements.

The expectation value of the Hamiltonian obtained using the CI wave function is a quadratic function of the expansion coefficients

$$\langle \Psi(LS)|H|\Psi(LS)\rangle = \sum_{v \le w,\, x \le y} \Big[(\epsilon_v + \epsilon_w)\, \delta_{xv}\delta_{yw} + V_{vw,xy} \Big] C_{xy} C_{vw}.$$

Minimizing the expectation of the Hamiltonian subject to the normalization condition leads to the eigenvalue equation

$$\sum_{x \le y} \Big[(\epsilon_v + \epsilon_w)\, \delta_{xv}\delta_{yw} + V_{vw,xy} \Big] C_{xy} = E\, C_{vw}. \tag{7.111}$$

In Table 7.9, we list energies of low-lying S, P, and D states of heliumlike iron obtained from a relativistic CI calculation. The Breit interaction is included in these calculations but SMS and QED corrections are omitted. The omitted QED corrections are primarily responsible for the differences between theory and observation seen in the table.

Table 7.9: Energies (a.u.) of S, P, and D states of heliumlike iron (FeXXV) obtained from a relativistic CI calculation compared with observed values (Obs.) from the NIST website.

Singlet States								
State	CI	Obs.	State	CI	Obs.	State	CI	Obs.
1^1S_0	-324.566	-324.425						
2^1S_0	-79.403	-79.379	2^1P_1	-78.195	-78.189			
3^1S_0	-35.159	-35.148	3^1P_1	-34.802	-34.798	3^1D_2	-34.753	-34.749
4^1S_0	-19.727	-19.720	4^1P_1	-19.577	-19.571	4^1D_2	-19.555	-19.551
5^1S_0	-12.604	-12.598	5^1P_1	-12.527	-12.522	5^1D_2	-12.515	
6^1S_0	-8.740		6^1P_1	-8.696		6^1D_2	-8.690	
Triplet States								
State	CI	Obs.	State	CI	Obs.	State	CI	Obs.
2^3S_1	-80.558	-80.534						
3^3S_1	-35.464	-35.454						
4^3S_1	-19.850	-19.848						
5^3S_1	-12.666	-12.663						
6^3S_1	-8.776							
2^3P_0	-79.474	-79.470	2^3P_1	-79.400	-79.396	2^3P_2	-78.859	-78.854
3^3P_0	-35.165	-35.161	3^3P_1	-35.144	-35.140	3^3P_2	-34.982	-34.978
4^3P_0	-19.727	-19.725	4^3P_1	-19.718	-19.716	4^3P_2	-19.650	-19.647
5^3P_0	-12.603	-12.602	5^3P_1	-12.599	-12.596	5^3P_2	-12.564	-12.560
6^3P_0	-8.740		6^3P_1	-8.738		6^3P_2	-8.718	
3^3D_1	-34.822	-34.821	3^3D_2	-34.825	-34.818	3^3D_3	-34.764	-34.759
4^3D_1	-19.584	-19.581	4^3D_2	-19.585	-19.580	4^3D_3	-19.560	-19.555
5^3D_1	-12.531		5^3D_2	-12.531		5^3D_3	-12.518	
6^3D_1	-8.699		6^3D_2	-8.699		6^3D_3	-8.692	

Chapter 8

MBPT for Matrix Elements

In Chapters 5 and 6, we carried out calculations of hyperfine constants, specific mass shift corrections, and transition matrix elements in the independent-particle approximation. We found that lowest-order calculations of such matrix elements were often in serious disagreement with experiment, especially for hyperfine constants and the specific mass shift. To understand and account for the disagreements, we consider second- and third-order correlation corrections to matrix elements in the present chapter.

8.1 Second-Order Corrections

Consider a general one-particle irreducible tensor operator

$$T = \sum_{ij} t_{ij} a_i^\dagger a_j = \sum_{ij} t_{ij} :a_i^\dagger a_j: + \sum_a t_{aa} \tag{8.1}$$

If T is an operator of rank $k > 0$, then the second term on the right above vanishes and the operator is normally ordered. For the special case of a scalar operator ($k = 0$), we must add the c-number $T_0 = \sum_a t_{aa}$ to the normally ordered operator.

Let us digress for a bit to discuss transition operators in greater detail. The electric dipole transition rate in an atom is determined by either the rank 1 "length-form" operator

$$R_\lambda = \sum_{ij} \langle i|r_\lambda|j\rangle \, :a_i^\dagger a_j:$$

or by the equivalent "velocity-form" operator

$$V_\lambda = \sum_{ij} \langle i|v_\lambda|j\rangle \, :a_i^\dagger a_j: \, .$$

Matrix elements of these two operators are related by

$$\langle F|V_\lambda|I\rangle = i\omega \langle F|R_\lambda|I\rangle \tag{8.2}$$

Table 8.1: First-order reduced matrix elements of the electric dipole operator in lithium and sodium in length L and velocity V forms.

Element	Transition	$L^{(1)}$	$V^{(1)}/\omega$
Li	$2p_{1/2} \to 2s_{1/2}$	3.3644	3.4301
	$2p_{3/2} \to 2s_{1/2}$	4.7580	4.8510
Na	$3p_{1/2} \to 3s_{1/2}$	3.6906	3.6516
	$3p_{3/2} \to 3s_{1/2}$	5.2188	5.1632

where $\omega = E_F - E_I$. In lowest-order calculations starting from a local potential, Eq.(8.2) is satisfied identically. However, for lowest-order calculations starting from the frozen-core HF potential, length-form and velocity-form matrix elements can differ substantially. This is an unfortunate circumstance, since, as pointed out in Chap. 6 length and velocity matrix elements are related by a gauge transformation; consequently, lowest-order calculations starting from a HF potential are gauge dependent! As correlation corrections to the matrix elements are included order by order, the difference between length-form and velocity-form matrix elements decreases. In exact calculations as well as certain approximate calculations, the difference vanishes completely. Keep in mind: gauge-independence is a necessary, but not sufficient, condition for accurate transition matrix elements, We will return to this point later when we consider the random-phase approximation (RPA).

The perturbation expansion for wave functions, leads automatically to a perturbation expansion for matrix elements. Thus, the matrix element of a operator T between states v and w in a one-electron atom may be expanded

$$T_{wv} = T_{wv}^{(1)} + T_{wv}^{(2)} + T_{wv}^{(3)} + \cdots ,$$

where

$$\begin{aligned}
T_{wv}^{(1)} &= \left\langle \psi_w^{(0)} \left| T \right| \psi_v^{(0)} \right\rangle \\
T_{wv}^{(2)} &= \left\langle \psi_w^{(0)} \left| T \right| \psi_v^{(1)} \right\rangle + \left\langle \psi_w^{(1)} \left| T \right| \psi_v^{(0)} \right\rangle \\
T_{wv}^{(3)} &= \left\langle \psi_w^{(0)} \left| T \right| \psi_v^{(2)} \right\rangle + \left\langle \psi_w^{(1)} \left| T \right| \psi_v^{(1)} \right\rangle + \left\langle \psi_w^{(2)} \left| T \right| \psi_v^{(0)} \right\rangle .
\end{aligned}$$

First Order In first order, we find

$$T_{wv}^{(1)} = \langle \Psi_w^{(0)} | T | \Psi_w^{(0)} \rangle = \langle 0_c | a_w T a_v^\dagger | 0_c \rangle = \langle w | t | v \rangle. \tag{8.3}$$

First-order reduced matrix elements of the electric-dipole transition operator in length L and velocity V forms are listed in Table 8.1 for $2p - 2s$ transitions in Li and $3p - 3s$ transitions in Na. The $L - V$ differences in lowest order are, as discussed above, a consequence of the HF starting potential.

Second Order To bring the second-order matrix element $T^{(2)}_{wv}$ into tractable form, we express the first-order wave function $\Psi^{(1)}_v$ in terms of the first-order correlation operator $\chi^{(1)}_v$ and find

$$T^{(2)}_{wv} = \langle 0_c|\, a_w T\, \chi^{(1)}_v\, a^\dagger_v|0_c\rangle + \langle 0_c|\, a_w \chi^\dagger_w T\, a^\dagger_v|0_c\rangle. \tag{8.4}$$

We note that only the second term in $\chi^{(1)}$ in Eq.(7.62) leads to nonvanishing contributions to $T^{(2)}$. With the aid of Wick's theorem, we find

$$T^{(2)}_{wv} = \sum_{am} \frac{t_{am}\tilde{g}_{wmva}}{\epsilon_a - \epsilon_m - \omega} + \sum_{am} \frac{\tilde{g}_{wavm}t_{ma}}{\epsilon_a - \epsilon_m + \omega} \tag{8.5}$$

where $\omega = \epsilon_w - \epsilon_v$. The sum over i in (8.5) runs over core and virtual states. In cases where the background potential is different from th HF potential, additional terms proportional to $(V_{\rm HF} - U)$ appear in the expression for the second-order matrix element.

8.1.1 Angular Reduction

Let's consider an irreducible tensor operator of rank k and examine the first-order matrix element from Eq.(8.3)

$$\left(T^k_q\right)^{(1)} = \langle wm_w|t^k_q|vm_v\rangle^{(1)} = -$$

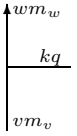

$$\times\, \langle w\|t^k\|v\rangle\,.$$

The second-order matrix element from Eq.(8.5) may be written in the precisely the same form:

$$\left(T^k_q\right)^{(2)} = -$$

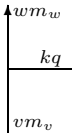

$$\times\, \langle w\|t^{(J)}\|v\rangle^{(2)}\,.$$

with

$$\langle w\|t^k\|v\rangle^{(2)} = \sum_{bn} \frac{(-1)^{b-n+k}}{[k]} \frac{\langle b\|t^k\|n\rangle Z_k(wnvb)}{\epsilon_b - \epsilon_n - \omega} + \sum_{bn} \frac{(-1)^{b-n+k}}{[k]} \frac{Z_k(wbvn)\langle n\|t^k\|b\rangle}{\epsilon_b - \epsilon_n + \omega}. \tag{8.6}$$

In the above equation, which is appropriate for relativistic calculations, the function $Z_k(abcd)$ is the anti-symmetrized Coulomb radial matrix element given in Eq.(7.42).

In Table 8.2, we give second-order reduced matrix elements of the dipole transition matrix in length and velocity forms determined from Eq.(8.6) for the transitions listed in Table 8.1. It can be seen by comparing the results in Table 8.2 with those in Table 8.1 that the length-velocity differences are substantially reduced when second-order corrections are included.

Table 8.2: Second-order reduced matrix elements and sums of first- and second-order reduced matrix elements for $E1$ transitions in lithium and sodium in length and velocity forms. RPA values given in the last column are identical in length and velocity form.

Element	Transition	$L^{(2)}$	$V^{(2)}/\omega$	$L^{(1+2)}$	$V^{(1+2)}/\omega$	$L^{\rm RPA} \equiv V^{\rm RPA}$
Li	$2p_{1/2} \to 2s_{1/2}$	-0.0116	-0.0588	3.3528	3.3714	3.3505
	$2p_{3/2} \to 2s_{1/2}$	-0.0164	-0.0831	4.7416	4.7679	4.7383
Na	$3p_{1/2} \to 3s_{1/2}$	-0.0385	-0.0024	3.6521	3.6492	3.6474
	$3p_{3/2} \to 3s_{1/2}$	-0.0544	-0.0029	5.1645	5.1603	5.1578

8.2 Random-Phase Approximation

We have established that the electric dipole matrix element to second order is given by the expression

$$t_{wv}^{(1+2)} = t_{wv} + \sum_{ma} \frac{t_{am}\tilde{g}_{wmva}}{\epsilon_a - \epsilon_m - \omega} + \sum_{ma} \frac{\tilde{g}_{wavm}t_{ma}}{\epsilon_a - \epsilon_m + \omega}, \tag{8.7}$$

assuming that we start our calculation in a HF potential. The matrix elements t_{am} and t_{ma} appearing in the numerators of the sums describe transitions between a closed-shell atom and a particle-hole excited state. Using the same analysis that led to Eq.(8.7) the first + second order particle-hole matrix elements are found to be

$$t_{am}^{(1+2)} = t_{am} + \sum_{bn} \frac{t_{bn}\tilde{g}_{anmb}}{\epsilon_b - \epsilon_n - \omega} + \sum_{bn} \frac{\tilde{g}_{abmn}t_{nb}}{\epsilon_b - \epsilon_n + \omega}\,,$$

$$t_{ma}^{(1+2)} = t_{ma} + \sum_{bn} \frac{t_{bn}\tilde{g}_{mnab}}{\epsilon_b - \epsilon_n - \omega} + \sum_{bn} \frac{\tilde{g}_{mban}t_{nb}}{\epsilon_b - \epsilon_n + \omega}\,.$$

Replacing the lowest-order matrix elements t_{bn} and t_{nb} in the sums on the right hand sides of the above by the corrected values $t_{bn}^{(1+2)}$ and $t_{nb}^{(1+2)}$, then relabeling the corrected matrix elements, we obtain the well-known equations of the random-phase approximation (RPA)

$$t_{am}^{\rm RPA} = t_{am} + \sum_{bn} \frac{t_{bn}^{\rm RPA}\tilde{g}_{anmb}}{\epsilon_b - \epsilon_n - \omega} + \sum_{bn} \frac{\tilde{g}_{abmn}t_{nb}^{\rm RPA}}{\epsilon_b - \epsilon_n + \omega}\,, \tag{8.8}$$

$$t_{ma}^{\rm RPA} = t_{ma} + \sum_{bn} \frac{t_{bn}^{\rm RPA}\tilde{g}_{mnab}}{\epsilon_b - \epsilon_n - \omega} + \sum_{bn} \frac{\tilde{g}_{mban}t_{nb}^{\rm RPA}}{\epsilon_b - \epsilon_n + \omega}\,. \tag{8.9}$$

Iterating these equations leads to the the first- and second-order matrix elements together with a subset of third-, fourth-, and higher-order corrections. The RPA

was originally introduced to treat Coulomb interactions in a degenerate electron gas by Bohm and Pines (1953) and has subsequently become an important mathematical tool in almost every branch of physics. Substituting the RPA matrix elements $t_{ma}^{\rm RPA}$ and $t_{am}^{\rm RPA}$ into the sums on the right hand side of Eq.(8.7) leads to the random-phase approximation to the matrix element t_{vw}.

$$t_{wv}^{\rm RPA} = t_{wv} + \sum_{ma} \frac{t_{am}^{\rm RPA}\tilde{g}_{wmva}}{\epsilon_a - \epsilon_m - \omega} + \sum_{ma} \frac{\tilde{g}_{wavm}t_{ma}^{\rm RPA}}{\epsilon_a - \epsilon_m + \omega}. \tag{8.10}$$

The RPA matrix element $t_{wv}^{\rm RPA}$ is evaluated by solving Eqs.(8.8-8.9) then substituting into Eq. (8.10). The resulting dipole matrix element is gauge independent. As will be shown below, L and V forms of the dipole matrix element are identical in the RPA. For this to be true in relativistic calculations, the virtual-orbital index m in the RPA equations must range over both positive- and negative-energy states. A discussion of the role of negative energy states in transition amplitudes for highly-charged ions can be found in Johnson et al. (1995), where it is shown that the length-form amplitudes for highly-charged ions are insensitive to negative-energy states.

The particle-hole RPA equations can be expressed in terms of reduced matrix elements through the equations

$$\begin{aligned}
\langle a||t^{\rm RPA}||m\rangle &= \langle a||t||m\rangle + \sum_{bn}(-1)^{b-n+k}\frac{1}{[k]}\frac{\langle b||t^{\rm RPA}||n\rangle Z_k(anmb)}{\epsilon_b - \epsilon_n - \omega} \\
&\quad + \sum_{bn}(-1)^{b-n+k}\frac{1}{[k]}\frac{Z_k(abmn)\langle n||t^{\rm RPA}||b\rangle}{\epsilon_b - \epsilon_n + \omega}\,, \qquad (8.11) \\
\langle m||t^{\rm RPA}||a\rangle &= \langle m||t||a\rangle + \sum_{bn}(-1)^{b-m+k}\frac{1}{[k]}\frac{\langle b||t^{\rm RPA}||m\rangle Z_k(mnab)}{\epsilon_b - \epsilon_n - \omega} \\
&\quad + \sum_{bn}(-1)^{b-n+k}\frac{1}{[k]}\frac{Z_k(mban)\langle n||t^{\rm RPA}||b\rangle}{\epsilon_b - \epsilon_n + \omega}, \qquad (8.12)
\end{aligned}$$

where $k = 1$ for the E1 case.

Numerical results for RPA reduced electric dipole matrix elements in Li and Na, which are identical in length and velocity form, are given in the last column of Table 8.2. Although we expect gauge invariance in exact many-body, the fact that RPA matrix element are independent of gauge certainly does not imply that there are no further higher-order corrections. Indeed, the third-order Brueckner corrections (discussed later) are in many cases *larger* than the RPA corrections. Nevertheless, since RPA is so similar to second-order perturbation theory, leads to gauge-independent transition matrix elements, and includes a class of many-body corrections to all orders, we will adopt RPA as a replacement for second-order perturbation theory in the sequel.

8.2.1 Gauge Independence of RPA

As discussed in Sec. 6.2.5, the change in the transition operator

$$t(\mathbf{r},\omega) = -c\alpha\cdot\mathbf{A}(\mathbf{r},\omega) + \phi(\mathbf{r},\omega), \tag{8.13}$$

induced by the gauge transformation

$$\mathbf{A}(\mathbf{r},\omega) \to \mathbf{A}(\mathbf{r},\omega) + \nabla\chi(\mathbf{r},\omega) \tag{8.14}$$

$$\phi(\mathbf{r},\omega) \to \phi(\mathbf{r},\omega) + i\omega\chi(\mathbf{r},\omega), \tag{8.15}$$

is given by

$$\Delta t = -c\alpha\nabla\chi(\mathbf{r},\omega) + i\omega\chi(\mathbf{r},\omega). \tag{8.16}$$

The unretarded velocity-form of the dipole operator is obtained by choosing $\mathbf{A}_v = -\hat{\epsilon}/c$ and $\phi_v = 0$, where $\hat{\epsilon}$ is the photon polarization vector. The corresponding length-form transition operator is obtained from potentials $\mathbf{A}_l = 0$ and $\phi_l = ik\,\hat{\epsilon}\cdot\mathbf{r}$, with $k = \omega/c$. The gauge function $\chi = -\hat{\epsilon}\cdot\mathbf{r}/c$ transforms the length-form dipole operator to velocity-form. The generalization to arbitrary multipoles including retardation was given in Sec. 6.3. Single-particle matrix elements of Δt can be expressed in terms of the gauge function $\chi(\mathbf{r},\omega)$ as

$$\Delta t_{ij}(\omega) = \langle i\,|\Delta t|\,j\rangle = -i(\epsilon_i - \epsilon_j - \omega)\chi_{ij} \qquad \text{(local potential)}, \tag{8.17}$$

provided the single-particle orbitals for states i and j are obtained in a local potential. For energy-conserving transitions ($\omega = \epsilon_i - \epsilon_j$), the change in t_{ij} induced by a gauge transformation vanishes, explaining why lowest-order matrix elements in a local potential are gauge independent. The identity (8.17) is the fundamental relation used by Savukov and Johnson (2000a) to establish the gauge-independence of second- and third-order MBPT calculations starting from a local-potential.

If transition matrix elements are calculated using DHF orbitals for states i and j, then the change induced by a gauge transformation is

$$\Delta t_{ij}(\omega) = -i(\epsilon_i - \epsilon_j - \omega)\chi_{ij} - i\sum_{ak}\left[g_{iaak}\,\chi_{kj} - \chi_{ik}\,g_{kaaj}\right] \quad \text{(DHF potential)}, \tag{8.18}$$

where g_{ijkl} are two-particle matrix elements of the electron-electron Coulomb interaction. The sum over a on the right hand side of Eq. (8.18) extends over occupied core orbitals and the sum over k extends over all possible (positive- and negative-energy) orbitals. The sum in Eq. (8.18) arises from the non-local exchange term in the DHF potential. It follows from Eq.(8.18) that DHF matrix elements are gauge-dependent even for energy-conserving transitions.

Now, let us verify that RPA amplitudes satisfy

$$\Delta t_{ij}^{\rm RPA} = -i(\epsilon_j - \epsilon_i - \omega)\,\chi_{ij}, \tag{8.19}$$

and consequently that RPA amplitudes are gauge independent for energy-conserving transitions. To establish this, we must show that Eq.(8.18) and

Eq.(8.19) satisfy the RPA equation identically. Substitute into the expression defining the RPA amplitude for a transition between states i and j, we find

$$(\Delta t^{\rm RPA})_{ij} = (\Delta t)_{ij} + \sum_{na} \frac{(\Delta t^{\rm RPA})_{an}\, \tilde{g}_{inja}}{\epsilon_a - \epsilon_n - \omega} + \sum_{na} \frac{\tilde{g}_{iajn}\, (\Delta t^{\rm RPA})_{na}}{\epsilon_a - \epsilon_n + \omega} \qquad (8.20)$$

With the aid of Eqs.(8.18) and (8.19), it is simple to verify that this expression reduces to

$$0 = \sum_{ak} [g_{iaak}\, \chi_{kj} - \chi_{ik}\, g_{kaaj}] + \sum_{na} [\chi_{an} g_{inja} - \chi_{an} g_{inaj} - g_{iajn} \chi_{na} + g_{ianj} \chi_{na}].$$

The sum over n can be extended to a sum over all states k by adding a sum over core states c

$$\sum_{ca} [\chi_{ac} g_{icja} - \chi_{ac} g_{icaj} - g_{iajc} \chi_{ca} + g_{iacj} \chi_{ca}].$$

On interchanging indices a and c in the last two terms above this additional term is easily seen to vanish. Thus, Eq.(8.20) becomes

$$0 = \sum_{ak} \left[g_{iaak}\, \chi_{kj} - \chi_{ik}\, g_{kaaj} + \chi_{ak} g_{ikja} - \chi_{ak} g_{ikaj} - g_{iajk} \chi_{ka} + g_{iakj} \chi_{ka} \right].$$

Carrying out the sum over k, one finds that the first and fourth, second and sixth, third and fifth terms on the right hand side of this expression cancel, verifying the identity and establishing the gauge independence of the RPA transition amplitude. The gauge independence of the RPA amplitude is crucial in establishing the gauge independence of third-order MBPT corrections that start from a HF potential (Savukov and Johnson, 2000b).

8.2.2 RPA for hyperfine constants

Before turning to higher-order calculations, it is of interest to compare RPA matrix elements of other tensor operators with their lowest-order values. As was pointed out in Chap. 5, Hartree-Fock calculations of hyperfine constants are in very poor agreement with experiment. It is, therefore, of more than passing interest to examine RPA corrections to hyperfine matrix elements.

The lowest-order expression for the hyperfine constant A_v of a state v in an atom with one valence electron given in Eq. (5.19) may be expressed in terms of a reduced matrix element of the dipole hyperfine operator t^1_λ by

$$A_v = \frac{\mu_I}{I} \sqrt{\frac{2j_v + 1}{j_v(j_v+1)}} \langle v \| t^1 \| v \rangle \times 13074.7\,{\rm MHz}\,. \qquad (8.21)$$

The reduced matrix element, in turn, is given by

$$\langle w \| t^1 \| v \rangle = (\kappa_v + \kappa_w)\, \langle -\kappa_w \| C^1 \| \kappa_v \rangle \left(\frac{1}{r^2} \right)_{wv}, \qquad (8.22)$$

Table 8.3: Comparison of HF and RPA calculations of hyperfine constants A(MHz) for states in Na ($\mu_I = 2.2176$, $I = 3/2$) with experimental data.

Term	$3s$	$3p_{1/2}$	$3p_{3/2}$	$4s$	$4p_{1/2}$	$3p_{3/2}$
$A^{\rm HF}$	623.64	63.43	12.60	150.48	20.99	4.17
ΔA	143.60	18.90	5.41	34.21	6.25	1.76
$A^{\rm RPA}$	767.24	82.33	18.01	184.70	27.24	5.93
Expt.	885.81	94.44	18.53	202	30.6	6.01

where $(1/r^2)_{wv}$ denotes the radial integral

$$\left(\frac{1}{r^2}\right)_{wv} = \int_0^\infty \frac{dr}{r^2}(P_{n_w\kappa_w}(r)Q_{n_v\kappa_v}(r) + Q_{n_w\kappa_w}(r)P_{n_v\kappa_v}(r))\,. \tag{8.23}$$

To evaluate A_v in the random-phase approximation, we simply replace $\langle v\|t^1\|v\rangle$ by the RPA matrix element in Eq.(8.12) with $\omega = 0$. Moreover, to determine the RPA matrix elements $t^{\rm RPA}_{bn}$ and $t^{\rm RPA}_{nb}$ on the RHS of Eq.(8.12), we must solve Eqs.(8.8) and (8.9) with $\omega = 0$.

In Table 8.3, we list lowest-order HF calculations of hyperfine constants for $n = 3$ and $n = 4$ states in Na, together with corrections ΔA obtained in the random-phase approximation and the resulting RPA values. (The value of $A^{\rm HF}$ for the $3s$ state differs from that in Table 5.1 because the later was evaluated in the nonrelativistic limit.) We see from this tabulation that RPA accounts for a sizable fraction of the difference between theory and experiment. It is also evident from the table that correlation corrections beyond the RPA are necessary for an understanding of hyperfine constants at the few percent level of accuracy.

8.3 Third-Order Matrix Elements

Explicit formulas for the third-order matrix elements are written out by Blundell et al. (1987) and evaluated for transitions in alkali-metal atoms and alkali-like ions by Johnson et al. (1996). The third-order matrix elements may be subdivided into classes according to

$$T^{(3)} = T^{\rm BO} + T^{\rm SR} + T^{\rm Norm} \tag{8.24}$$

There is, in addition, a third-order RPA term, which is omitted here since it can easily be included with the second-order matrix element as discussed in the previous section.

For matrix elements of transition operators such as the length-form dipole operator $i\omega\hat{\epsilon}\cdot\boldsymbol{r}$, it is also necessary to include a "derivative" term

$$T^{\rm deriv} = \frac{dT^{(1)}}{d\omega}\,\delta\omega^{(2)}. \tag{8.25}$$

to account for the fact that there is a second-order correction to transition energies in calculations that start from a HF potential. (For calculations starting from a local potential, derivative terms are also required in calculations of second-order matrix elements). To achieve gauge independence for transition matrix elements, it is necessary to replace all single-particle matrix elements t_{ij} in the expressions for the third-order terms by RPA amplitudes $t_{ij}^{\rm RPA}$. With these replacements, the Brueckner-orbital (BO) correction, which accounts for core polarization, becomes

$$T^{\rm BO} = \sum_{abmi}\left[\frac{g_{abmv}\,t_{wi}^{\rm RPA}\,\tilde{g}_{miba}}{(\epsilon_i-\epsilon_v)(\epsilon_v+\epsilon_m-\epsilon_a-\epsilon_b)}+{\rm c.c.}\right] \tag{8.26}$$

$$+ \sum_{amni}\left[\frac{\tilde{g}_{aimn}\,t_{wi}^{\rm RPA}\,g_{mnav}}{(\epsilon_i-\epsilon_v)(\epsilon_n+\epsilon_m-\epsilon_a-\epsilon_v)}+{\rm c.c.}\right]. \tag{8.27}$$

The structural-radiation (SR) correction, which accounts for radiation from virtual states, becomes

$$T^{\rm SR} = \sum_{abcn}\left[\frac{g_{bavc}\,t_{cn}^{\rm RPA}\,\tilde{g}_{wnba}}{(\epsilon_n-\epsilon_c+\epsilon_w-\epsilon_v)(\epsilon_n+\epsilon_w-\epsilon_a-\epsilon_b)}+{\rm c.c.}\right] \tag{8.28}$$

$$+ \sum_{abmn}\left[\frac{\tilde{g}_{nwab}\,t_{bm}^{\rm RPA}\,\tilde{g}_{amvn}}{(\epsilon_m-\epsilon_b+\epsilon_w-\epsilon_v)(\epsilon_n+\epsilon_w-\epsilon_a-\epsilon_b)}+{\rm c.c.}\right] \tag{8.29}$$

$$+ \sum_{amnr}\left[\frac{g_{wrnm}\,t_{ar}^{\rm RPA}\,\tilde{g}_{mnav}}{(\epsilon_r-\epsilon_a+\epsilon_w-\epsilon_v)(\epsilon_n+\epsilon_m-\epsilon_a-\epsilon_v)}+{\rm c.c.}\right] \tag{8.30}$$

$$+ \sum_{abmn}\left[\frac{\tilde{g}_{mnav}\,t_{bm}^{\rm RPA}\,\tilde{g}_{awnb}}{(\epsilon_m-\epsilon_b+\epsilon_w-\epsilon_v)(\epsilon_n+\epsilon_m-\epsilon_a-\epsilon_v)}+{\rm c.c.}\right] \tag{8.31}$$

$$+ \sum_{abmn}\frac{g_{abvn}\,t_{nm}^{\rm RPA}\,\tilde{g}_{mwab}}{(\epsilon_n+\epsilon_v-\epsilon_a-\epsilon_b)(\epsilon_m+\epsilon_w-\epsilon_a-\epsilon_b)} \tag{8.32}$$

$$+ \sum_{abcn}\frac{\tilde{g}_{wnab}\,t_{ac}^{\rm RPA}\,\tilde{g}_{bcnv}}{(\epsilon_n+\epsilon_v-\epsilon_b-\epsilon_c)(\epsilon_n+\epsilon_w-\epsilon_a-\epsilon_b)} \tag{8.33}$$

$$+ \sum_{abmn}\frac{g_{mnav}\,t_{ab}^{\rm RPA}\,\tilde{g}_{bwnm}}{(\epsilon_n+\epsilon_m-\epsilon_b-\epsilon_w)(\epsilon_n+\epsilon_m-\epsilon_a-\epsilon_v)} \tag{8.34}$$

$$+ \sum_{amnr}\frac{\tilde{g}_{wanr}\,t_{rm}^{\rm RPA}\,\tilde{g}_{mnav}}{(\epsilon_n+\epsilon_m-\epsilon_a-\epsilon_v)(\epsilon_r+\epsilon_n-\epsilon_a-\epsilon_w)}. \tag{8.35}$$

The normalization correction, which accounts for wave-function normalization and for "folded" diagrams (Lindgren and Morrison, 1985), becomes

$$T^{\rm Norm} = \frac{1}{2}t_{wv}^{\rm RPA}\left\{\sum_{amn}\frac{\tilde{g}_{vamn}g_{mnav}}{(\epsilon_m+\epsilon_n-\epsilon_a-\epsilon_v)^2} + \sum_{abn}\frac{\tilde{g}_{abnv}g_{nvba}}{(\epsilon_v+\epsilon_n-\epsilon_a-\epsilon_b)^2}+{\rm c.c.}\right\}. \tag{8.36}$$

Table 8.4: Contributions to the reduced matrix element of the electric dipole transition operator $\omega \boldsymbol{r}$ in length-form and in velocity form for the $3s - 3p_{1/2}$ transition in Na. Individual contributions to $T^{(3)}$ from Brueckner orbital (B.O.), structural radiation (S.R.), normalization (Norm.) and derivative terms (Deriv.) are given. ($\omega_0 = 0.072542$ a.u. and $\omega^{(2)} = 0.004077$ a.u.)

Term	L-form	V-form
$T^{(1)}$	-0.2677	-0.2649
$T^{\rm RPA}$	-0.2646	-0.2646
B.O.	0.0075	-0.0072
S.R.	-0.0002	-0.0006
Norm.	0.0004	0.0004
Deriv.	-0.0150	0.0000
$T^{(3)}$	-0.0074	-0.0074
$T^{(1..3)}$	-0.2720	-0.2720
$\lvert T^{(1..3)}/\omega \rvert$	3.550	3.550
Expt.	3.525(2)	

In Eqs. (8.26–8.36), the notation "c.c." designates complex conjugation together with interchange of indices v and w. No replacement is required in the derivative term, given by Eq. (8.25). Gauge-independence of the third-order matrix elements modified by replacing single-particle matrix elements t_{ij} by their RPA counterparts $t_{ij}^{\rm RPA}$ was established by Savukov and Johnson (2000a,b).

A detailed breakdown of contributions to the third-order matrix element of the dipole transition matrix element for the $3s - 3p_{1/2}$ transition in Na is given in Table 8.4. The first- plus second-order matrix element is replaced by the RPA matrix element $T^{\rm RPA}$. The importance of the derivative term in obtaining a gauge independent third-order contribution is obvious; in length form, it is a factor of two larger than the sum of the remaining contributions and of opposite sign. The resulting dipole matrix element differs from the precisely known experimental value by less than 1%.

In Table 8.5, we give the third-order corrections to the hyperfine constants for the $n = 3$ and $n = 4$ levels of Na. Comparing these third-order calculations with the second-order values given in Table 8.3, one sees that the agreement between theory and experiment improves dramatically. As in the case of transition matrix elements, the second-order hyperfine matrix elements are replaced by RPA matrix elements and the third-order corrections are dominated by Bruckner-orbital corrections.

Table 8.5: Third-Order MBPT calculation of hyperfine constants A(MHz) for states in Na ($\mu_I = 2.2176$, $I = 3/2$) compared with experimental data.

Term	$3s$	$3p_{1/2}$	$3p_{3/2}$	$4s$	$4p_{1/2}$	$3p_{3/2}$
$A^{(1)}$	623.64	63.43	12.60	150.48	20.99	4.17
$A^{(2)}$	143.60	18.90	5.41	34.21	6.25	1.76
$A^{(3)}$	100.04	10.19	0.75	17.21	2.84	0.12
A_{tot}	867.28	92.52	18.76	201.90	30.08	6.05
Expt.	885.81	94.44	18.53	202	30.6	6.01

8.4 Matrix Elements of Two-particle Operators

The perturbation expansion for off-diagonal matrix elements of two-particle operators follows the pattern discussed earlier for one-particle operators. Diagonal matrix elements are of greatest interest for operators such as the specific mass-shift operator $\boldsymbol{p}_1 \cdot \boldsymbol{p}_2$ or the Breit operator b_{12}. For diagonal matrix elements, one can make use of the existing perturbation expansion of the energy to obtain a perturbation expansion of the diagonal matrix element $\langle\Psi|T|\Psi\rangle$. Let us write the two-particle operator in its standard second-quantized form

$$T = \frac{1}{2}\sum_{ijkl} t_{ijkl} a_i^\dagger a_j^\dagger a_l a_k = \frac{1}{2}\sum_{ijkl} t_{ijkl} :a_i^\dagger a_j^\dagger a_l a: + \sum_{ij} t_{ij} :\, a_i^\dagger a_j :+ \frac{1}{2}\sum_a t_{aa}$$

where, for example, $t_{ijkl} = \langle ij|\boldsymbol{p}_1 \cdot \boldsymbol{p}_2|kl\rangle$ and $t_{ij} = \sum_b (t_{ibjb} - t_{ibbj})$ in the SMS case. Replacing g_{ijkl} by $g_{ijkl} + t_{ijkl}$ in Eq.(7.2), we find

$$E(T) = \langle\Psi|H_0|\Psi\rangle + \langle\Psi|V_I|\Psi\rangle + \langle\Psi|T|\Psi\rangle$$

Using the previously developed perturbation expansion for the energy and *linearizing* the result in powers of t_{ijkl}, we easily obtain the perturbation expansion for $\langle\Psi|T|\Psi\rangle$.

8.4.1 Two-Particle Operators: Closed-Shell Atoms

We suppose that the atom described in lowest-order in the HF approximation. The perturbation expansion for the energy then leads to

$$\langle 0|T|0\rangle^{(1)} = \frac{1}{2}\sum_a t_{aa} \tag{8.37}$$

$$\langle 0|T|0\rangle^{(2)} = \sum_{abmn} \frac{\tilde{g}_{abmn} t_{mnab}}{\epsilon_a + \epsilon_b - \epsilon_m - \epsilon_n}, \tag{8.38}$$

up to second order. As seen from Eq.(8.38), there is no contribution to the second-order matrix element from t_{ij}. Contributions from this term do occur,

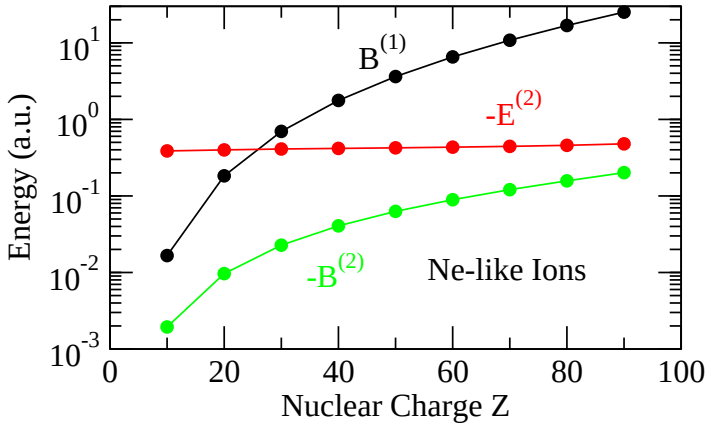

Figure 8.1: First- and second-order Breit corrections to the ground-stste energies of neonlike ions shown along with the second-order correlation energy. The first-order Breit energy $B^{(1)}$ grows roughly as Z^3, $B^{(2)}$ grows roughly as Z^2 and the second-order Coulomb energy $E^{(2)}$ is nearly constant.

however, in third- and higher order. Application of the above formulas to determine first- and second-order Breit corrections to the ground-state energies of Ne-like ions are shown in Fig. 8.1.

8.4.2 Two-Particle Operators: One Valence Electron Atoms

The diagonal matrix element of a two-particle operator T in the state v of a one-electron atom is, once again, easily obtained from the energy expansion. One finds,

$$\langle v|T|v\rangle^{(1)} = t_{vv} \tag{8.39}$$

$$\langle v|T|v\rangle^{(2)} = -\sum_{bmn} \frac{\tilde{g}_{vbmn}t_{mnvb}}{\epsilon_m + \epsilon_n - \epsilon_v - \epsilon_b} + \sum_{abn} \frac{\tilde{g}_{abvn}t_{vnab}}{\epsilon_v + \epsilon_n - \epsilon_a - \epsilon_b} + \sum_{am} \frac{t_{am}\tilde{g}_{vavm}}{\epsilon_a - \epsilon_m} + \sum_{am} \frac{\tilde{g}_{vmva}t_{ma}}{\epsilon_a - \epsilon_m} \tag{8.40}$$

Terms on the second line of Eq.(8.40) are second-order corrections to the "effective" one-particle operator $\sum_{ij} t_{ij} :a_i^\dagger a_j:$. This term often dominates the second-order correlation corrections. In such cases, one replaces the term by its RPA counterpart.

Breit interaction in Cu

As an example, we present a breakdown of the Breit corrections to energies of $4s$ and $4p$ states of copper in Table 8.6. The terms $B_s^{(2)}$ and $B_d^{(2)}$ refer to

Table 8.6: Matrix elements of two-particle operators Breit operator for $4s$ and $4p$ states in copper (Z=29) Numbers in brackets represent powers of 10; $a[-b] \equiv a \times 10^{-b}$

Term	$4s$	$4p_{1/2}$	$4p_{3/2}$
$B^{(1)}$	1.880[-04]	7.015[-05]	5.140[-05]
$B_s^{(2)}$	4.288[-06]	1.623[-06]	1.431[-06]
$B_d^{(2)}$	-1.250[-05]	-3.675[-06]	-3.518[-06]
$B_e^{(2)}$	-4.290[-04]	-1.222[-04]	-1.167[-04]
$B_{\rm RPA}$	-6.993[-04]	-2.020[-04]	-1.310[-04]
$B^{(3)}$	6.400[-05]	3.212[-05]	2.319[-05]
$B_{\rm tot}$	-4.555[-04]	-1.018[-04]	-5.853[-05]

the sums over single and double excited states, respectively, on the first line of Eq.(8.40). These terms are seen to be relatively small corrections to the lowest-order Breit interaction $B^{(1)}$. The term $B_e^{(2)}$ is the contribution from the effective single-particle operator on second line of Eq.(8.40). This term is the dominant second-order correction; indeed, it is larger than the first-order correction and has opposite sign. Iterating this term leads to the term $B_{\rm RPA}$. The RPA correction is seen to be substantially different from $B_e^{(2)}$ for each of the three states listed in the table. We replace $B_e^{(2)}$ by $B_{\rm RPA}$ in the sum $B_{\rm tot}$. The relatively small term $B^{(3)}$ is the Brueckner-orbital correction associated with the effective single-particle operator and is expected to dominate the residual third-order corrections. The extreme example given in Table 8.6 illustrates the importance of correlation corrections to two-particle operators; the correlated matrix elements are larger in magnitude and differ in sign from the lowest-order values!

Isotope Shift in Na

As a further example, let us consider correlation corrections to the isotope shift in sodium. As discussed in Chap. 5, the isotope shift consists or three parts, the normal mass shift NMS, the specific mass shift SMS and the field shift F. We separate the SMS matrix element for states of Na, designated by P, into two-parts, $P = S+T$; S being the contribution from the effective single-particle operator and T being the normally-ordered two-particle contribution. Second- and third-order correlation corrections $S^{(2)}$ and $S^{(3)}$ are calculated following the procedure discussed earlier for the hyperfine operator. The second-order two-particle contribution $T^{(2)}$ is obtained from the first line of Eq.(8.40) while $T^{(3)}$ is obtained by linearizing the expression for the third-order energy. A complete discussion of the evaluation of $T^{(3)}$, which is an imposing task, is given by Safronova and Johnson (2001). The relative importance of the third-order contributions to SMS constants is illustrated in Table 8.7. It follows from

Table 8.7: Contributions to specific-mass isotope shift constants (GHz amu) for $3s$ and $3p$ states of Na.

Term	$3s$	$3p_{1/2}$	$3p_{3/2}$
$P^{(1)}$	-222.00	-115.55	-115.46
$S^{(2)}$	167.93	48.35	48.28
$S^{(3)}$	28.11	1.20	1.20
$S^{(2)}+S^{(3)}$	196.04	49.55	49.48
$T^{(2)}$	95.04	28.16	28.11
$T^{(3)}$	-24.37	-7.54	-7.52
$T^{(2)}+T^{(3)}$	70.68	20.62	20.59
$P_{\rm tot}$	44.72	-45.38	-45.39

Table 8.8: Contributions to field-shifts constants F (MHz/fm^2) for $3s$ and $3p$ states in Na.

Term	ns	$np_{1/2}$	$np_{3/2}$
$F^{(1)}$	-29.70	-0.01	0.00
$F^{(2)}$	-1.88	1.65	1.65
$F^{(3)}$	-5.25	-0.04	-0.04
$F_{\rm tot}$	-36.83	1.60	1.60

the table that the correlation correction is largest for the $3s$ state; the lowest-order value $P^{(1)}$ for the $3s$ state has the same order of magnitude as $S^{(2)}$ but has an opposite sign. The contribution $S^{(3)}$ for the $3s$ state is 17% of $S^{(2)}$. Two-particle contributions $T^{(2)}+T^{(3)}$ are two to three times smaller than one-particle contributions $S^{(2)}+S^{(3)}$ for the three states listed.

Values of the MBPT contributions to the field shift operator F for $3s$ and $3p$ states in Na are given in Table 8.8. Since the field-shift operator is a single-particle operator, we follow the procedure discussed previously for hyperfine constants to evaluate the first-, second- and third-order contributions.

Finally, Table 8.9, we compare values for the isotope shifts $\delta\nu^{22,23}$ of n=3 states in Na with experimental data Huber et al. (1978) The sum of the third-order MBPT values for the SMS and the NMS are listed in the second column of the table. In converting the calculated field shift constants to MHz units, we use the value $\delta\langle r^2\rangle^{22,23}$=-0.205(3) fm^2 obtained from Eq. (3.157). Our data for the isotope shift for $3p-3s$ transitions agrees with experiment at the 5% level.

Table 8.9: Isotope shifts $\delta\nu^{22,23}$ (MHz) for $3s$ and $3p$ states of Na.

	NMS+SMS$^{(3)}$	FS	Total IS	Expt.
$3s$	1430.6	-7.5	1423.1	
$3p_{1/2}$	704.0	0.3	704.3	
$3p_{3/2}$	703.4	0.3	703.7	
$3p_{3/2} - 3s$	-727.2	7.8	-719.4	-757(2)

8.5 CI Calculations for Two-Electron Atoms

As pointed out in Chapter 7, configuration interaction calculations lead to precise theoretical energies for two electron atoms and ions. Precise theoretical values for matrix elements between two-electron states may also be calculated using CI wave functions.

To this end, consider the matrix element of an irreducible tensor operator T^k_q between an initial state

$$|I\rangle = \sum_{u\le v} \eta_{uv} C_{uv} - \left|\begin{array}{c} j_v m_v \\ \hline J_I M_I \\ \hline j_w m_w \end{array}\right. \quad a^\dagger_v a^\dagger_w |0\rangle$$

and a final state

$$|F\rangle = \sum_{x\le y} \eta_{xy} C_{xy} - \left|\begin{array}{c} j_x m_x \\ \hline J_F M_F \\ \hline j_y m_y \end{array}\right. \quad a^\dagger_x a^\dagger_y |0\rangle.$$

The matrix element $\langle F|T^k_q|I\rangle$ is given by

$$\langle F|T^k_q|I\rangle = \sum_{v\le w\ x\le y} \eta_{vw}\eta_{xy} C_{vw} C_{xy} - \left|\begin{array}{c} j_x m_x \\ \hline J_F M_F \\ \hline j_y m_y \end{array}\right. - \left|\begin{array}{c} j_v m_v \\ \hline J_I M_I \\ \hline j_w m_w \end{array}\right.$$
$$\left[\langle x|t^k_q|v\rangle\delta_{yw} - \langle x|t^k_q|w\rangle\delta_{yv} - \langle y|t^k_q|v\rangle\delta_{xw} + \langle y|t^k_q|w\rangle\delta_{xv}\right] \quad (8.41)$$

Carrying out the sums over (m_v, m_w, m_x, m_y) the matrix element can be rewritten as

$$\langle F|T^k_q|I\rangle = - \left|\begin{array}{c} J_F M_F \\ \hline kq \\ \hline J_I M_I \end{array}\right. \times \langle F\|T^k\|I\rangle,$$

where the reduced matrix element $\langle F\|T^k\|I\rangle$ is given in terms of single-particle

reduced matrix elements $\langle x\|t^k\|v\rangle$ between final-state orbitals ϕ_x and initial-state orbitals ϕ_v as

$$\begin{aligned}\langle F\|T^k\|I\rangle = (-1)^k\sqrt{[J_I][J_F]}\sum_{v\le w\ x\le y}\eta_{vw}\eta_{xy}C_{vw}C_{xy}\\ \Bigg[(-1)^{j_w+j_x+J_I}\begin{Bmatrix} J_F & J_I & k\\ j_v & j_x & j_w\end{Bmatrix}\langle x\|t^k\|v\rangle\delta_{yw}\\ +(-1)^{j_w+j_x}\begin{Bmatrix} J_F & J_I & k\\ j_w & j_x & j_v\end{Bmatrix}\langle x\|t^k\|w\rangle\delta_{yv}\\ +(-1)^{J_I+J_F+1}\begin{Bmatrix} J_F & J_I & k\\ j_v & j_y & j_w\end{Bmatrix}\langle y\|t^k\|v\rangle\delta_{xw}\\ +(-1)^{j_w+j_v+J_F}\begin{Bmatrix} J_F & J_I & k\\ j_w & j_y & j_v\end{Bmatrix}\langle y\|t^k\|v\rangle\delta_{xv}\Bigg]. \quad (8.42)\end{aligned}$$

8.5.1 E1 Transitions in He

As a specific example, let us consider electric dipole transitions between the 2P states and 2S states in helium. Wavelengths and oscillator strengths for transitions between nP and mS states for heliumlike ions were evaluated in the nonrelativistic independent-particle model and tabulated in Section 6.2.8.

Recall that the spontaneous decay rate $A(\mathrm{s}^{-1})$ in the relativistic case is given by

$$A = \frac{2.02613\times 10^{18}}{\lambda^3}\frac{S}{[J_I]}\,s^{-1}, \quad (8.43)$$

where the line strength $S = |\langle F\|Q_1^{(1)}\|I\rangle|^2$. The operator $Q_{JM}^{(1)}$ above is the relativistic electric dipole operator defined in Eq. (6.134). In Table 8.10, we list wavelengths λ, transition rates A, oscillator strengths f, and line strengths S for singlet-singlet, triplet-triplet and intercombination transitions between 2P and 2S states in helium.

Several comments should be made concerning these transitions: Firstly, the relativistic CI calculations automatically account for the splitting of the 2^3P level into fine-structure components $J = 0$, 1, 2. Secondly, the theoretical wavelengths predicted by the relativistic CI calculations are in precise agreement with observed energies; the largest difference in Table 8.10 is 0.02%. By contrast the differences between theoretical and experimental wavelengths in the nonrelativistic CI calculations range from 2% to 25%. Since oscillator strengths are proportional to the square of the respective transition energies, we find substantial differences between nonrelativistic independent-particle predictions and relativistic CI predictions. Thirdly, since the dipole transition operator is spin independent, E1 transitions between singlet and triplet states (intercombination transitions) are forbidden nonrelativistically. Such transitions, however, have nonvanishing rates in the relativistic theory. The $2^3\mathrm{P}_1$ - $1^1\mathrm{S}_0$ transition is the only possible E1 transition from the triplet state. The $2^3\mathrm{P}_0$ - $1^1\mathrm{S}_0$ transition is strictly forbidden by angular momentum conservation, while the $2^3\mathrm{P}_2$ - $1^1\mathrm{S}_0$

Table 8.10: Relativistic CI calculations of wavelengths λ(Å), transition rates $A(\mathrm{s}^{-1})$, oscillator strengths f, and line strengths S(a.u.) for 2P $\rightarrow$ 1S & 2S states in helium. Numbers in brackets represent powers of 10.

	λ(Å)	$A(\mathrm{s}^{-1})$	f	S(a.u.)
2^1P_1 - 1^1S_0	584.25	1.799[9]	0.2761	0.5311
2^1P_1 - 2^1S_0	20584.	1.976[9]	0.1255	25.52
2^3P_0 - 2^3S_1	10831.	1.022[7]	0.0599	6.408
2^3P_1 - 2^3S_1	10832.	1.022[7]	0.1797	19.22
2^3P_2 - 2^3S_1	10832.	1.022[7]	0.2995	32.04
2^1P_1 - 2^3S_1	8864.8	1.552[0]	1.828[-8]	1.601[-6]
2^3P_1 - 1^1S_0	591.33	1.787[2]	2.810[-8]	5.470[-8]

transition is an allowed M2 transition with transition rate $A = 0.3271(\mathrm{s}^{-1})$. A complete study of 2-1 and 2-2 transitions in heliumlike ions is presented in Johnson et al. (1995).

Appendix A

Exercises

A.1 Chapter 1

1. Derive the relations

$$\begin{aligned} J^2 &= J_+ J_- + J_z^2 - J_z \,, \\ J^2 &= J_- J_+ + J_z^2 + J_z \,. \end{aligned}$$

2. Show that the normalization factor c in the equation $\Theta_{l,-l}(\theta) = c\ \sin^l \theta$ is

$$c = \frac{1}{2^l l!} \sqrt{\frac{(2l+1)!}{2}},$$

and thereby verify that Eq. (1.30) is correct.

3. Write a MAPLE or MATHEMATICA program to obtain the first 10 Legendre polynomials using Rodrigues' formula.

4. Legendre polynomials satisfy the recurrence relation

$$l P_l(x) = (2l-1) x P_{l-1}(x) - (l-1) P_{l-2}(x).$$

Write a MAPLE or MATHEMATICA program to determine $P_2(x), P_3(x), \cdots, P_{10}(x)$ (starting with $P_0(x) = 1$ and $P_1(x) = x$) using the above recurrence relation.

5. Write a MAPLE or MATHEMATICA program to generate the associated Legendre functions and $P_l^m(x)$. Determine all $P_l^m(x)$ with $l \leq 4$ and $1 \leq m \leq l$.

6. The first two spherical Bessel functions are

$$\begin{aligned} j_0(x) &= \frac{\sin x}{x} \\ j_1(x) &= \frac{\sin x}{x^2} - \frac{\cos x}{x}. \end{aligned}$$

Spherical Bessel functions satisfy the recurrence relation

$$j_{n+1}(x) + j_{n-1}(x) = \frac{(2n+1)}{x}\, j_n(x).$$

Use MAPLE or MATHEMATICA to obtain an expression for $j_6(x)$.

7. Show by direct calculation, using Eqs.(1.20-1.24), that

$$L_+L_- + L_z^2 - L_z = L^2$$
$$L_-L_+ + L_z^2 + L_z = L^2$$

Hint: To avoid excessive pain in carrying out the differentiations, use MATHEMATICA or MAPLE and print out the MAPLE worksheet or MATHEMATICA notebook.

8. Write a MAPLE or MATHEMATICA routine to obtain formulas for $\Theta_{l,m}(\theta)$ for $l = 4$ and $m \leq l$ using Eq.(1.36). With the aid of your results, give explicit formulas for $Y_{4,m}(\theta, \phi)$, $m = -4 \cdots 4$. Verify by direct calculation that $Y_{4,m}(\theta, \phi)$ are properly normalized.

9. Use the MAPLE routine CGC.MAP or built in MATHEMATICA routine to evaluate $C(1, 3/2, J; m_1, m_2, M)$ for all possible values of (m_1, m_2, J, M). Show that the resulting values satisfy the two orthogonality relations.

10. Determine numerical values of $C(j_1\, j_2\, J;\, m_1\, m_2\, M)$ for

$$j_1 = 2 \quad j_2 = 1/2 \quad J = 3/2$$

and all possible values of m_1, m_2, and M.

11. Prove

$$\langle l_1||C^k||l_2\rangle = (-1)^{l_1-l_2}\langle l_2||C^k||l_1\rangle,$$

where C^k_q is the tensor operator

$$C^k_q \stackrel{\text{def}}{=} \sqrt{\frac{4\pi}{2k+1}}\; Y_{kq}(\theta, \phi).$$

12. Prove

$$[J^2, \boldsymbol{\sigma}\cdot\boldsymbol{r}] = 0\,,$$
$$[J_z, \boldsymbol{\sigma}\cdot\boldsymbol{r}] = 0\,,$$

where $\boldsymbol{J} = \boldsymbol{L} + \frac{\mathbf{1}}{\mathbf{2}}\boldsymbol{\sigma}$

13. Prove

$$Y_{JJM}(\hat{r}) = \frac{\mathbf{L}}{\sqrt{J(J+1)}} Y_{JM}(\hat{r})$$

14. Show that the spherical harmonics $Y_{kq}(\theta, \phi)$, $q = -k, -k+1, \cdots, k$ are components of a spherical tensor operator of rank k.

15. Prove [Varshalovich, Sec. 5.9.1, Eq.(5)]

$$\int_0^{2\pi} d\phi \int_0^{\pi} d\theta \sin\theta \; Y_{l_1,m_1}(\theta,\phi)\, Y_{l_2 m_2}(\theta,\phi)\, Y_{l_3 m_3}(\theta,\phi)$$
$$= \sqrt{\frac{(2l_1+1)(2l_2+1)(2l_3+1)}{4\pi}} \begin{pmatrix} l_1 & l_2 & l_3 \\ 0 & 0 & 0 \end{pmatrix} \begin{pmatrix} l_1 & l_2 & l_3 \\ m_1 & m_2 & m_3 \end{pmatrix}$$

16. Derive the identity

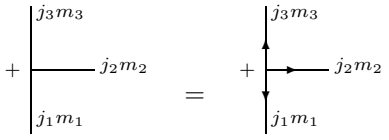

17. Derive the graphical identity

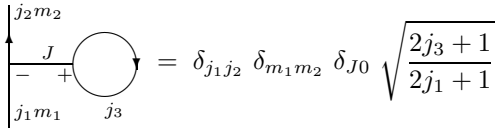

$$= \delta_{j_1 j_2}\; \delta_{m_1 m_2}\; \delta_{J0}\; \sqrt{\frac{2j_3+1}{2j_1+1}}$$

A.2 Chapter 2

1. Write a MAPLE or MATHEMATICA procedure to generate the formula for the radial Coulomb wave function $P_{nl}(r)$.

   (a) Plot the radial functions $P_{nl}(r)$ for $n = 4$ and all possible values of l.

   (b) Show by direct calculation that the $l = 1$ radial functions $P_{nl}(r)$ satisfy

   $$\int_0^{\infty} dr P_{nl}(r) P_{n'l}(r) = \delta_{nn'}$$

   for $2 \le n,\, n' \le 4$.

2. Use MAPLE or MATHEMATICA to obtain an expression for the expectation value

   $$\left\langle \frac{1}{r^2} \right\rangle$$

   in the $3d$ state of a hydrogenlike ion with nuclear charge Z. What is the numerical value of this quantity for a hydrogenlike lithium ($Z = 3$)?

3. The Coulomb field of the nucleus is modified at short distances by the finite size of the nuclear charge distribution.

   (a) Assuming that the nuclear charge density is constant, show that the potential inside the nucleus is

   $$V = -\frac{Z}{R}\left[\frac{3}{2} - \frac{1}{2}\left(\frac{r}{R}\right)^2\right], \quad r \le R$$

(b) Show by explicit calculation for n from 2 to 5 that the leading term in powers of R of the finite size shift in energy is

$$\begin{aligned} \Delta E_{n,0} &= \frac{2Z^2}{15n^3}(ZR)^2 \quad \text{for } l = 0 \\ \Delta E_{n,1} &= \frac{2(n^2-1)Z^2}{105n^5}(ZR)^4 \quad \text{for } l = 1 \end{aligned}$$

4. Find the shift in energy of the $1s$ state of a hydrogenlike ion assuming that the charge of the nucleus is distributed uniformly over the *surface* of a sphere of radius $R << a_0/Z$. Estimate the order of magnitude of the shift for hydrogen. Use your answer to show that the $1s$ Lamb shift in hydrogen (≈ 8000 MHz) is not caused by nuclear finite size.

5. The ground state of hydrogen is a $1s$ state (orbital angular momentum eigenvalue $l = 0$). The total angular momentum (orbital + spin) of this state is $j = 1/2$ with two degenerate substates $m = \pm 1/2$. The angular wave functions of the two degenerate states are

$$|j, m\rangle = Y_{00}(\theta, \phi)\ \chi_m \equiv \sqrt{\frac{1}{4\pi}}\chi_m.$$

Determine the values of total angular momentum of a $2p$ state (orbital angular momentum $l = 1$) of hydrogen and write out the angular wave functions for each of the 6 possible substates.

6. Use the FORTRAN program MOD_POT.F to determine the value of b in the parametric potential

$$V(r) = -\frac{Z}{r} + \frac{Z-1}{r}(1 - e^{-br}),$$

that gives the best least-squares fit to the $4s, 5s, 6s, 4p, 5p, 3d$ and $4d$ levels in potassium. Use the resulting potential to predict the value of the $1s$ binding energy in potassium. How does your prediction compare with experiment? The data for the energy levels are found in C.E. Moore, NSRDS-NBS 35, Vol. 1. You should average over the fine structure of the p and d levels.

- The routine GOLDEN from the NUMERICAL RECIPES library is used to minimize the sum of squares of energy differences.
- The linear algebra routines used in OUTSCH.F are to from the LINPACK library.

7. The lowest eight states of the sodiumlike ion Al^{+2} ($Z = 13$) are

n	l	$E_{nl}(cm^{-1})$
3	0	0.0
3	1	53800
3	2	115956
4	0	126163
4	1	143672
4	2	165786
4	3	167612
5	0	170636

The ionization threshold is 229454 cm^{-1}. Determine the parameter p in the potential

$$V(r,p) = -\frac{Z}{r} + (Z-3)\frac{1}{p+r}$$

that gives a best least-squares fit to these levels.

(Answer: $p \approx 0.088$)

8. Use the FORTRAN program THOMAS.F to determine the Thomas-Fermi potential for potassium, Z=19.
   (a) Find the K^+ core radius R.
   (b) Plot the effective charge $Z_{\rm eff}(r)$, defined by the relation:

$$V(r) = -\frac{Z_{\rm eff}(r)}{r} = -\frac{Z-N}{R} - \frac{Z\phi(r)}{r}$$

9. Sodium atom with a TF core.
   (a) Download and compile the routines thomas.f and nrelMP.f
   (b) Use the routine *thomas* to determine $\phi(r)$, $N(r)$, and $Z_{\rm eff}(r)$ for Na (Z=11). Submit a plot of the data.
   (c) Edit the output data set "thomas.dat" from the above step to make a two column file: r vs. zeff. Name the resulting data set "zeff.dat". This data set will be used as input to *nrelMP*.
   (d) Create an input file "mod.in" (standard input unit 5) in the form:

```
 Z
 n1   l1   e1
 n2   l2   e2
 n3   l3   e3
etc.
```

   where Z=11 for Na, where n1, l1 are quantum numbers of energy levels of Na and e1 is an estimate of the energy. For example, the row
   (3, 0, -0.2)
   would correspond to a 3s state with a guess of -0.2 au for the energy. Use the routine *nrelMP* to evaluate energies of the seven lowest levels of Na.

(e) Compare your calculated energy levels with spectroscopic data. this data is available from http://physics.nist.gov under the heading Physical Reference Data, subheading Atomic Spectroscopy Database [Version 3.0] The energies in this database are relative to the atomic ground state. The theoretical energies are relative to the ionization limit. To compare the measured energies with calculations, you must subtract the ionization limit from the measured values and convert to atomic units!

10. Prove that $\boldsymbol{J} = \boldsymbol{L} + \boldsymbol{S}$ commutes with the Dirac Hamiltonian.

11. Show that Eqs. (2.129-2.130) reduce to Eqs. (2.140-2.141) in a Coulomb potential.

12. Let $\phi_a(\vec{r})$ and $\phi_b(\vec{r})$ be solutions to the Dirac equation. Prove that

$$c\langle\phi_b|\,\vec{\alpha}\,|\phi_a\rangle = i\omega\ \langle\phi_b|\,\vec{r}\,|\phi_a\rangle,$$

where $\omega = (E_b - E_a)/\hbar$.

13. What is the Pauli approximation? Use the Pauli approximation to evaluate the integral $I_{n\kappa} = \int_0^\infty P_{n\kappa}(r)Q_{n\kappa}(r)rdr$. Compare your answer with the exact value of the integral for the $1s$ state of a hydrogenic ion with charge Z.

14. Write out specific formulas for the radial Dirac functions $P_{n\kappa}(r)$ and $Q_{n\kappa}(r)$ of the $n = 2$ states of a hydrogenlike ion with nuclear charge Z. You may use MAPLE if you wish, however, you may find it simpler to expand the hypergeometric functions by hand.

15. Verify that the $n = 2$ radial functions determined in the previous problem are properly normalized for each of the three states.

16. Plot the radial density function $P_{n\kappa}(r)^2 + Q_{n\kappa}(r)^2$ for each of the $n = 2$ states assuming $Z = 20$.

17. Give formulas for $\langle r\rangle$ and $\langle 1/r\rangle$ for each state in (c) above. Verify that the relativistic formulas approach the proper nonrelativistic limits.

18. Suppose the nucleus is represented by a uniformly charged ball of radius R:

(a) Show that the nuclear potential (in atomic units) is given by

$$V_{\rm nuc}(r) = \begin{cases} -\frac{Z}{R}\left(\frac{3}{2} - \frac{r^2}{2R^2}\right), & r < R, \\ -\frac{Z}{r}, & r \geq R. \end{cases}$$

(b) Determine the nuclear finite-size correction to the $n = 1$ and $n = 2$ Dirac energy levels using first-order perturbation theory. How large are these corrections for hydrogen? (Assume $R = 1.04$ fm for H and give your answer in cm^{-1}.) How large are they for hydrogenlike uranium? (Assume $R = 7.25$ fm for U and give your answer in eV.)

A.3 Chapter 3

1. Consider the 12-fold degenerate set of product wave functions:

$$\psi_{2p,m,\sigma}(\boldsymbol{r}_1)\psi_{1s,\mu}(\boldsymbol{r}_2) = \frac{1}{r_1 r_2} P_{2p}(r_1)P_{1s}(r_2)Y_{1m}(\hat{r}_1)Y_{00}(\hat{r}_2)\chi_\sigma(1)\chi_\mu(2).$$

   (a) Combine these wave functions to give eigenstates of L^2, L_z, S^2, S_z, where $\boldsymbol{L} = \boldsymbol{L}_1 + \boldsymbol{L}_2$ and $\boldsymbol{S} = \boldsymbol{S}_1 + \boldsymbol{S}_2$.

   (b) With the aid of the above result, write down all possible *antisymmetric* angular momentum eigenstates describing $1s2p$ levels of helium. What is the number of such states?

2. Write out explicitly the radial Hartree-Fock equations for neon.

3. Show that the ionization energy of an atom with one valence electron is $-\epsilon_v$ in the "frozen-core" Hartree-Fock approximation. (Here, ϵ_v is the eigenvalue of the valence electron Hartree-Fock equation.)

A.4 Chapter 4

1. Which of the following products are normally ordered?

   (a) $a_m^\dagger a_a$ (d) $a_m^\dagger a_a a_n^\dagger a_b$
   (b) $a_a a_m^\dagger$ (e) $a_c^\dagger a_d^\dagger a_a a_b$
   (c) $a_a a_b^\dagger$ (f) $a_c^\dagger a_b a_d^\dagger a_c$

   Determine the expectation of each of the above products in the core state.

2. Prove that all doubly-excited states of helium are in the continuum above the first ionization threshold.

3. Low-lying states of Mg are linear combinations of product states formed from $3s$, $3p$ and $3d$ orbitals. In jj coupling the orbitals $(nl_j\, n'l'_{j'})$ are coupled to form states of angular momentum J such as $(3s_{1/2}3p_{3/2})[1]$ while in LS coupling, the orbitals $(nl\sigma\, n'l'\sigma')$ are coupled to form states such as $(3p)^2\ {}^3P$. Give the spectroscopic designation of all possible low-lying *even parity* states in the jj and LS coupling schemes. Show that the total number of jj and LS states (including magnetic substates) is identical.

4. Low energy states of B are linear combinations of product states formed from $2s$ and $2p$ orbitals. In the LS scheme, orbitals $2s$ and $2p$ can be coupled to form states such as $(2s2s2p)\ {}^2P$ or $(2p)^3\ {}^4P$, while in the jj scheme, these orbitals can be coupled to form states such as $(2s_{1/2}2p_{1/2}2p_{1/2})[1/2]$. Give the spectroscopic designation of all possible *even parity* states in B obtained by coupling $2s$ and $2p$ orbitals in both jj and LS coupling schemes. Show that the total number of magnetic substates is identical in the two coupling schemes.

5. Show that the exchange contribution to the interaction energy for the state $|ab, LS\rangle$ is

$$\eta^2 \sum_k (-1)^{l_a+l_b+S+k} \left\{ \begin{array}{ccc} l_a & l_b & L \\ l_a & l_b & k \end{array} \right\} X_k(abba)\,.$$

6. Show in detail that Eq.(4.50) follows from Eq.(4.47).

7. LS to jj transformation matrix:

   (a) Each nonrelativistic LS-coupled state belonging to a given J,

   $$|\,[(l_1 l_2)L, (s_1 s_2)S]J\rangle\,,$$

   can be expanded as a linear combination of the nonrelativistic jj-coupled states

   $$|\,[(l_1 s_1)j_1, (l_2 s_2)j_2]J\rangle\,,$$

   belonging to the same J. Write the matrix of expansion coefficients in terms of six-j symbols. (The expansion coefficients are related to 9-j symbols.)

   (b) Prove that this transformation matrix is symmetric.

   (c) Give numerical values for the elements of the 2×2 matrix that gives the two (sp) states $^1P_1$ and $^3P_1$ in terms of the two states $(s_{1/2}p_{1/2})_1$ and $(s_{1/2}p_{3/2})_1$.

   (d) Give numerical values for the elements of the 3×3 matrix that gives the three (pd) states $^1P_1$, $^3P_1$ and $^3D_1$ in terms of the three states $(p_{1/2}d_{3/2})_1$, $(p_{3/2}d_{3/2})_1$ and $(p_{3/2}d_{5/2})_1$.

8. For an atom with two valence electrons above a closed core, determine the number of states in the configuration $(nsn'l)$ and give LS and jj designations of the states. Determine the number of states in an $(nd)^2$ configuration and give LS and jj designations of the states.

9. In the Auger process, an initial state $|I\rangle = a_a|O_c\rangle$ with a hole in state a makes a transition to a final state $|F\rangle$ with holes in states b and c and an excited electron in state m. The transition probability is proportional to the square of the matrix element $\langle F|V_I|I\rangle$. Express this matrix element in terms of the two-particle Coulomb integrals g_{ijkl}.

10. In the relativistic case, show that the energy in the relativistic particle-hole state obtained by coupling states $|(-1)^{j_a-m_a} a_v^\dagger a_a|O_c\rangle$ to angular momentum JM is

$$E^{(1)}((j_v j_a)J) = \frac{(-1)^{J+j_v-j_a}}{[J]} \left[X_J(vaav) + [J] \sum_k \left\{ \begin{array}{ccc} j_v & j_a & J \\ j_a & j_v & k \end{array} \right\} X_k(vava) \right]$$

provided the orbitals are evaluated in a V^{N-1} HF potential. Express this matrix element in terms of Slater integrals for the case: $a = 2p_{1/2}$, $v = 3s_{1/2}$, and $J = 0$. What is the LS designation of this state?

A.5 Chapter 5

1. Let $|(ls)j\rangle$ be a state formed by coupling orbital angular momentum l and spin angular momentum $s = 1/2$ to total angular momentum j. Given that the tensor operator T^k_ν is independent of spin, express $\langle (l_a s)j_a||T^k||(l_b s)j_b\rangle$ in terms of $\langle l_a||T^k||l_b\rangle$.

2. Hyperfine Structure:

   (a) Determine the number of ground-state hyperfine levels of the hydrogen-like ion $^{209}Bi^{+82}$. Find the eigenvalue f of total angular momentum $\boldsymbol{F} = \boldsymbol{I} + \boldsymbol{J}$ for each level and give its degeneracy. Look up the nuclear spin of ^{209}Bi on the web.

   (b) Calculate the energy separation between hyperfine levels using a relativistic $1s$ wave functions for the atomic state.

   (c) Compare your theoretical calculations with experiment.

3. The nuclear spin of ^{7}Li is $I = 3/2$ and $g_I = 3.256$. Approximate the $2s$ wave function using a $2s$ hydrogenic wave function with $Z_{\rm eff} = 1.5$ and calculate the $2s$ hyperfine splitting $\delta\nu$. How does your value compare with the observed splitting $\delta\nu = 803.5$ MHz?

4. Zeeman effect: The vector potential for a uniform magnetic $\boldsymbol{B}$ can be written

$$\boldsymbol{A} = \frac{1}{2}[\boldsymbol{B} \times \boldsymbol{r}]$$

   (a) Show that the interaction Hamiltonian of an electron with this field is

$$h_{\rm int}(r) = \frac{iec}{2} B\sqrt{2}\, r \left(\boldsymbol{\alpha} \cdot \boldsymbol{C}^{(0)}_{10}\right),$$

   assuming that the field is oriented along the z axis.

   (b) Show that the expectation value of the *many-electron* Hamiltonian $H_{\rm int} = \sum_i h_{\rm int}(r_i)$ for a one-valence electron atom in state v reduces to

$$\langle v m_v|H_{\rm int}|v m_v\rangle = -ecB\kappa\, \langle -\kappa_v m_m|C^1_0|\kappa_v m_v\rangle\, (r)_{vv}$$

   in the independent-particle approximation. Here,

$$(r)_{vv} = 2\int_0^\infty dr\, r\, P_v(r)\, Q_v(r)$$

(c) Evaluate $(r)_{vv}$ in the Pauli approximation and show that the interaction energy can be written

$$W = -\mu_B B g_v m_v$$

where the Landé g-factor is given by

$$g_v = \frac{\kappa_v(\kappa_v - 1/2)}{j_v(j_v+1)}.$$

This factor has the value 2, 2/3, 4/3, 4/5, 6/5, for $s_{1/2}$, $p_{1/2}$, $p_{3/2}$, $d_{3/2}$, $d_{5/2}$ states, respectively. In the above, $\mu_B = e/2m$ is the Bohr magneton. Its value is $e/2$ in atomic units.

5. Isotope Shift in Li

(a) Using experimental energies from the NIST data base, evaluate the normal mass shift correction to energies of the $2s$ and $2p$ states of the isotopes ^{6}Li and ^{7}Li.

(b) Assuming that the $1s$ wave function of Li is a Coulomb wave function in a field with $Z = 3 - 5/16$ and that the $2s$ and $2p$ wave functions are Coulomb wave functions in a field $Z = 1 + 1/8$, determine the specific mass shift for $2s$ and $2p$ states of ^{6}Li and ^{7}Li.

(c) Combine the above calculations to determine the difference between $2s$ energies in the two isotopes. Repeat the calculation for $2p$ levels. What shift (cm^{-1}) is expected in the $2s-2p$ transition energy? What shift (MHz) is expected in the transition frequency? What shift (Å) is expected in the transition wavelength?

A.6 Chapter 6

1. Verify the relation:

$$\langle b||\nabla||a\rangle = \langle l_b||C_1||l_a\rangle \begin{cases} \int_0^\infty dr P_b \left(\frac{d}{dr} + \frac{l_a}{r}\right) P_a, & \text{for } l_b = l_a - 1, \\ \int_0^\infty dr P_b \left(\frac{d}{dr} - \frac{l_a+1}{r}\right) P_a, & \text{for } l_b = l_a + 1. \end{cases}$$

Hint: Use vector spherical harmonics. at the first step.

2. Verify

$$\sum_n \bar{f}_{ks\to np} = 1$$

and

$$\begin{aligned} \sum_n \bar{f}_{kl\to nl-1} &= -\frac{l(2l-1)}{3(2l+1)}, \\ \sum_n \bar{f}_{kl\to nl+1} &= \frac{(l+1)(2l+3)}{3(2l+1)}. \end{aligned}$$

Hint: Use the completeness relation for radial functions $P_{nl}(r)$ and formulas for the radial matrix elements of r and v.

3. Determine the lifetime of the $3p_{3/2}$ excited state in Al. Hint: This state decays to the ground state by an M1 transition. The transition energy is found in the spectroscopic tables.

4. Heliumlike Ne ($Z = 10$)

   (a) Determine the wavelength (Å) of the transition $(1s3p)\ ^3P \rightarrow (1s2s)\ ^3S$ in heliumlike Ne ($Z = 10$). Assume that the $1s$ orbital is described by a Coulomb wave function in the unscreened nuclear field Z and that the excited $2s$ and $2p$ orbitals are described by Coulomb wave functions in a screened Coulomb field $Z - 1$. Compare your result with the NIST database.

   (b) Calculate the spontaneous decay rate (s^{-1}) for the $(1s3p)\ ^3P \rightarrow (1s2s)\ ^3S$ transition.

5. Heliumlike boron ($Z = 5$)

   (a) Evaluate the *excitation* energies of the $(1s2p)^1P$ and $(1s2p)^3P$ states of heliumlike boron ($Z = 5$). Assume that the $1s$ and $2p$ states are described by Coulomb wave functions with $Z_{\rm eff} = (Z - 5/16)$ and $Z - 1$, respectively. Compare your calculated energies with values from the NIST website.

   (b) Determine the lifetime of the $(1s2p)^1P$ state of heliumlike boron and NIST wavelengths (Experimental lifetime: 2.69×10^{-12} s.)

6. Determine the dominant decay mode (E1, M1, E2), the decay channels ($I \rightarrow F$), and the wavelengths in Å of transitions from each of the following initial states I.

7. The lowest 4 states of sodium are

State	Energy cm^{-1}
$3s$	0
$3p$	16964
$4s$	25740
$3d$	29173

   (a) Determine the *lifetime* of the $3p$ state of sodium. The experimental $3p - 3s$ wavelength is $\lambda \approx 5895$Å.

   (b) The $3p$ state is actually a doublet. The $3p_{3/2}$ state is higher in energy and has a transition wavelength $\lambda_{3/2} = 5891.58$ Å, while the lower energy $3p_{1/2}$ state and has a wavelength $\lambda_{1/2} = 5897.55$ Å. Find the *line strength* and initial state *degeneracy* for each of the two transitions and compare the individual *transition rates* to the ground state.

(c) Determine the *reduced oscillator strength* for each of the two transitions in the example above.

(d) The $4s$ state can decay to the $3p$ state by an $E1$ transition or to the $3s$ state by an $M1$ transition. Determine the corresponding *decay rates*.

(e) Describe all possible radiative decay channels for the $3d$ state and calculate the *decay rate for each channel*. What is the *lifetime* of the $3d$ state?

Use the NRHF program to obtain the radial wave functions, and evaluate the necessary radial integrals numerically using the subroutine RINT.

8. Energies (cm^{-1}) of the five lowest levels in one-valence-electron ion La^{+2} are given in the little table below. Determine the multipolarity (E1, M1, ...) of the dominant one-photon decay mode for each of the four excited levels and give the corresponding photon wavelength.

$5d_{3/2}$	0.00
$5d_{5/2}$	1603.23
$4f_{5/2}$	7195.14
$4f_{7/2}$	8695.41
$6s_{1/2}$	13591.14

9. Determine the single-photon decay modes permitted by angular momentum and parity selection rules for the each of the three sublevels $J = (0, 1, 2)$ of the $(2s2p)\ ^3P$ level in Be. Use your analysis to prove that the $(2s2p)\ ^3P$ level is stable against single-photon decay nonrelativistically.

(a) H $3p$ state

(b) Al^{2+} $3p$ (Na-like) state

(c) Al $3p_{3/2}$ state

(d) Ba^{+} $5d_{3/2}$ state

You can determine wavelengths from the NIST database or from the tables *Atomic Energy Levels NSRDS-NBS 35*.

10. Prove that following states are stable against single-photon decay in the non-relativistic approximation: H $2s$ state, He $(1s2s)\ ^1S_0$ state, He $(1s2s)\ ^3S_1$ state.

A.7 Chapter 7

1. Prove:

   (a)
   $$\left\langle 0_c \left| \sum_{ij} (\Delta V)_{ij} \, :a_i^\dagger a_j :: a_m^\dagger a_a : \right| 0_c \right\rangle = (\Delta V)_{am}$$

   (b)
   $$\left\langle 0_c \left| \frac{1}{2} \sum_{ijkl} g_{ijkl} \, :a_i^\dagger a_j^\dagger a_l a_k :: a_m^\dagger a_n^\dagger a_b a_a : \right| 0_c \right\rangle = \tilde{g}_{abmn}$$

2. Prove:

   (a)
   $$\sum_{\substack{m_a m_b m_m m_n \\ \sigma_a \sigma_b \sigma_m \sigma_n}} g_{abnm} \; g_{mnab} = 2 \sum_{l,k} \left\{ \begin{array}{ccc} l_a & l_m & l \\ l_b & l_n & k \end{array} \right\} X_k(nmab) X_l(mnab)$$

   (b)
   $$\sum_{\substack{m_a m_b m_m m_n \\ \sigma_a \sigma_b \sigma_m \sigma_n}} g_{abmn} \; g_{mnab} = 4 \sum_{l} \frac{1}{[l]} X_l(mnab) X_l(mnab)$$

3. The right-hand side of the equation $(H_0 - E_0)\Psi^{(1)} = (E^{(1)} - V_I)\Psi_0$ is
   $$- \left[\sum_{na} (\Delta V)_{na} a_n^\dagger a_a + \frac{1}{2} \sum_{mnab} g_{mnab} a_m^\dagger a_n^\dagger a_b a_a \right] \Psi_0$$
   for a closed-shell atom. What is the corresponding expression for an atom with one electron beyond closed shells?

4. In a classical picture, the valence electron in Li induces a dipole moment $\boldsymbol{p} = \alpha \boldsymbol{E}$ in the heliumlike core, where $\boldsymbol{E}$ is the electric field produced by the valence electron at the origin, and α is the core polarizability ($\alpha = 0.189 a_0^3$ for Li^+).

   (a) Show that the classical interaction energy of the valence electron with the induced dipole field is
   $$\delta W = -\frac{1}{2} \frac{\alpha}{r^4}$$

   (b) Determine numerically the energy correction $\langle v|\delta W|v\rangle$ for $3d$ and $4f$ states of Li using wave functions in a screened Coulomb potential ($Z_{1s} = 3 - 5/16$ and $Z_{3d,4f} = 1$). Compare your answers with the following results from second-order MBPT:
   $$E_{3d}^{(2)} = -4.07 \times 10^{-5} \text{a.u.} \qquad E_{4f}^{(2)} = -2.93 \times 10^{-6} \text{a.u.}$$

5. Suppose we choose to describe an atom in lowest order using a potential $U(r)$ other than the HF potential.

   (a) Show that the correction to the first-order energy from the single-particle part of the potential (V_1) for a one electron atom in a state v is
   $$E_v^{(1)} = \Delta_{vv},$$
   where $\Delta = V_{\rm HF} - U$.

   (b) Show that the following additional terms appear in the second-order valence energy:
   $$E_v^{(2)} = -\sum_{na} \frac{\Delta_{na}\tilde{g}_{avnv} + \tilde{g}_{avnv}\Delta_{an}}{\epsilon_n - \epsilon_a} - \sum_{i\neq v} \frac{\Delta_{vi}\Delta_{iv}}{\epsilon_i - \epsilon_v}.$$
   Here, i runs over all states.

6. Breit Interaction:

   (a) Show that for a heliumlike ion
   $$B^{(1)} = \frac{8}{3}\int_0^\infty dr_1 P_{1s}(r_1)Q_{1s}(r_1)\int_0^\infty dr_2\, \frac{r_<}{r_>^2}\, P_{1s}(r_2)Q_{1s}(r_2),$$
   where $P_{1s}(r)$ and and $Q_{1s}(r)$ are radial Dirac wave functions.

   (b) Set $Z = 10$ and assume that the $1s$ wave functions for a heliumlike ion can be approximated by Dirac Coulomb wave functions with $Z \to Z - 5/16$. Evaluate $B^{(1)}$ numerically and compare with the value given in the notes.

A.8 Chapter 8

1. The r.m.s. radius of an atom is $R_{\rm rms} = \sqrt{\langle \boldsymbol{R}^2\rangle}$ where
   $$\boldsymbol{R} = \sum_i \boldsymbol{r}_i.$$

   (a) Write out the expression for $\boldsymbol{R}^2$ in second quantized form. (Take care! This operator is a combination of one- and two-particle operators.)

   (b) Express each part of the $\boldsymbol{R}^2$ operator in normal order with respect to a closed core.

   (c) Write down explicit formulas for the first-order matrix element of $\langle v|\boldsymbol{R}^2|v\rangle$ in an atom with one valence electron. (Keep in mind the fact that $\boldsymbol{R}^2$ is an irreducible tensor operator of rank 0.)

   (d) Evaluate $R_{\rm rms}$ to first-order for the $2p$ state of Li using screened Coulomb wave functions for the core and valence electrons: $Z_{1s} = 3 - 5/16$ and $Z_{2p} = 1.25$.

2. Consider an atom with one valence electron that is described in lowest order by a local potential $U(r) \neq V_{\rm HF}$.

   (a) Write out the expressions for first- and second-order matrix elements $\langle \Psi_w | T | \Psi_v \rangle$ of the dipole transition operator $T(\omega)$, being careful to account for $\Delta = V_{\rm HF} - U$ and to include terms arising from the energy dependence of T.

   (b) Show that both first- and second-order matrix elements of T are gauge-independent.

Bibliography

M. Abramowitz and I. A. Stegun, editors. *Handbook of Mathematical Functions*. Applied Mathematics Series 55. U. S. Government Printing Office, Washington D. C., 1964.

A. I. Akhiezer and V. B. Berestetskii. *Quantum Electrodynamics*. U. S. Atomic Energy Commission, Technical Information Service Extension, Oak Ridge, 1953.

E. Anderson, Z. Bai, C. Bischof, S. Blackford, J. Demmel, J. Dongarra, J. Du Croz, A. Greenbaum, S. Hammarling, A. McKenney, and D. Sorensen. *LAPACK User's Guide*. SIAM, Philadelphia, 1999.

J. A. Bearden and A. F. Burr. Reevaluation of x-ray atomic energy levels. *Rev. Mod. Phys.*, 39:125–142, 1967.

H. A. Bethe and E. E. Salpeter. *Quantum Mechanics of One- and Two-Electron Atoms*. Academic Press, New York, 1957.

L. C. Biedenharn. *J. Math. and Phys.*, 31:287, 1953.

S. A. Blundell, D. S. Guo, W. R. Johnson, and J. Sapirstein. *At. Data and Nucl. Data Tables*, 37:103, 1987.

D. Bohm and D. Pines. A collective description of electron interactions:III. Coulomb interactions in a degenerate electron gas. *Phys. Rev.*, 92, 1953.

G. Breit. *Phys. Rev.*, 34:553, 1929.

G. Breit. *Phys. Rev.*, 36:383, 1930.

G. Breit. *Phys. Rev.*, 39:616, 1932.

G. E. Brown and D. G. Ravenhall. *Proc. Roy. Soc. A*, 208:552, 1951.

A. Chodos, R. L. Jaffee, K. Johnson, C. B. Thorn, and V. W. Weisskopf. New extended model of hadrons. *Phys. Rev. D*, 9, 1974.

G. Dahlberg and Å. Björck. *Numerical Methods*. Prentice Hall, New York, 1974.

C. deBoor. *A Practical Guide to Splines*. Springer, New York, 1978.

C. Eckart. The application of group theory to the quantum dynamics of monatomic systems. *Rev. Mod. Phys.*, 2:305–380, 1930.

A. R. Edmonds. *Angular Momentum in Quantum Mechanics*. Princeton University Press, Princeton, New Jersey, 1974.

J. P. Elliott. *Proc. Roy. Soc. A*, 218:345, 1953.

J. A. Gaunt. *Proc. Roy. Soc. (London)*, A122:513, 1929.

A. E. S. Green, D. L. Sellin, and A. S. Zachor. *Phys. Rev.*, 184:1, 1969.

D. R. Hartree. *The Calculation of Atomic Structures*. J. Wiley, New York, 1957.

G. Huber, F. Touchard, S. Büttgenbach, C. Thibault, R. Klapisch, H. T. Duong, S. Liberman, J. Pinard, J. L. Vialle, P. Juncar, and P. Jacquinot. Spins, magnetic moments, and isotope shifts of $^{21-31}$na by high resolution laser spectroscopy the atomic d_1 line. *Phys. Rev. C*, 18:2342–2354, 1978.

W. R. Johnson, S. A. Blundell, and J. Sapirstein. Finite basis sets for the dirac equation constructed from b-splines. *Phys. Rev. A*, 37, 1988a.

W. R. Johnson, S. A. Blundell, and J. Sapirstein. Many-body perturbation-theory calculations of energy levels along the lithium isoelectronic sequence. *Phys. Rev. A*, 37:2764–2777, 1988b.

W. R. Johnson, Z. W. Liu, and J. Sapirstein. *At. Data and Nucl. Data Tables*, 64:279, 1996.

W. R. Johnson, D. R. Plante, and J. Sapirstein. Relativistic calculations of transition amplitudes in the helium isoelectronic sequence. *Advances in Atomic, Molecular and Optical Physics*, 35, 1995.

W. R. Johnson and G. Soff. Lamb shift in high z atoms. *Atomic Data and Nuclear Data Tables*, 33, 1985.

A. Jucys, Y. Levinson, and V. Vanagas. *Mathematical Apparatus of the Theory of Angular Momentum*. Israel Program for Scientific Translations, Jerusalem, 1964.

B. R. Judd. *Operator Techniques in Atomic Spectroscopy*. McGraw-Hill, New York, 1963.

I. Lindgren and J. Morrison. *Atomic Many-Body Theory*. Springer-Verlag, Berlin, 2nd edition, 1985.

W. Magnus and F. Oberhettinger. *Formulas and Theorems for the Functions of Mathematical Physics*. Chelsea, New York, 1949.

J. B. Mann and W. R. Johnson. Breit interaction in multielectron atoms. *Phys. Rev. A*, 4, 1971.

A. M. Mårtensson and S. Salomonson. *J. Phys. B*, 15, 1982.

A. Messiah. *Quantum Mechanics II*. North Holland, Amsterdam, 1961.

M. H. Mittleman. Structure of heavy atoms: Three-body potentials. *Phys. Rev. A*, 4:893–900, 1971.

M. H. Mittleman. Configuration-space hamiltonian for heavy atoms and correction to the breit interaction. *Phys. Rev. A*, 5:2395–2401, 1972.

M. H. Mittleman. Theory of relativistic effects on atoms: Configuration-space hamiltonian. *Phys. Rev. A*, 24:1167–1175, 1981.

C. E. Moore. *Atomic Energy Levels*, volume I-III of *Nat. Stand. Ref. Ser., Nat. Bur. Stand. (U.S.), 35*. U. S. Government Printing Office, Washington D.C., 1957.

G. Racah. Theory of complex spectra. ii. *Phys. Rev.*, 62:438–462, 1942.

M. E. Rose. *Elementary Theory of Angular Momentum*. Wiley, New York, 1957.

M. S. Safronova and W. R. Johnson. Third-order isotope-shift constants for alkali-metal atoms and ions. *Phys. Rev. A*, 64:052501, 2001.

J. J. Sakuri. *Advanced Quantum Mechanics*. Addison-Wesley, Reading, MA, 1967.

I. M. Savukov and W. R. Johnson. Equality of length-form and velocity-form transition amplitudes in relativistic many-body perturbation theory. *Phys. Rev. A*, 62:052506, 2000a.

I. M. Savukov and W. R. Johnson. Form-independent third-order transition amplitudes for atoms with one valence electron. *Phys. Rev. A*, 62:052506, 2000b.

M. Scheer, C. A. Brodie, R. C. Bilodeau, and H. K. Haugen. Laser spectroscopic measurements of binding energies and fine-structure splittings of co-, ni-, rh-, and pd-. *Phys. Rev. A*, 58, 1998.

Charles Schwartz. Theory of hyperfine structure. *Phys. Rev.*, 97, 1955.

J. Sucher. Foundations of the relativistic theory of many-electron atoms. *Phys. Rev. A*, 22:348,362, 1980.

T. Tietz. *J. Chem. Phys.*, 22:2094, 1954.

D. A. Varshalovich, A.N. Moskalev, and V.K. Khersonski. *Quantum Theory of Angular Momentum*. World Scientific, Singapore, 1988.

E. P. Wigner. *Gruppentheorie*. Friedrich Vieweg und Sohn, Braunschweig, 1931.